High-Pressure Photooxygenation of Olefins in Flow: Mechanism, Reactivity and Reactor Design

Dissertation

zur Erlangung des Doktorgrades der Naturwissenschaften
Dr. rer. nat.
an der Fakultät für Chemie und Pharmazie
der Universität Regensburg

vorgelegt von

Patrick Bayer

aus Rotthalmünster

Regensburg 2020

The experimental part of this work was carried out between November 2016 and February 2018 at the University of Regensburg, Institute of Organic Chemistry, and between March 2018 and February 2020 at the University of Hamburg, Institute of Inorganic and Applied Chemistry.

Doctoral application submitted on 12 May 2020.

The dissertation was supervised by Prof. Dr. Axel Jacobi von Wangelin.

Board of examiners:

Apl. Prof. Dr. Rainer Müller	(Chairman)
Prof. Dr. Axel Jacobi von Wangelin	(1st Referee)
Prof. Dr. Burkhard König	(2nd Referee)
Prof. Dr. Frank-Michael Matysik	(Examiner)

Table of Contents

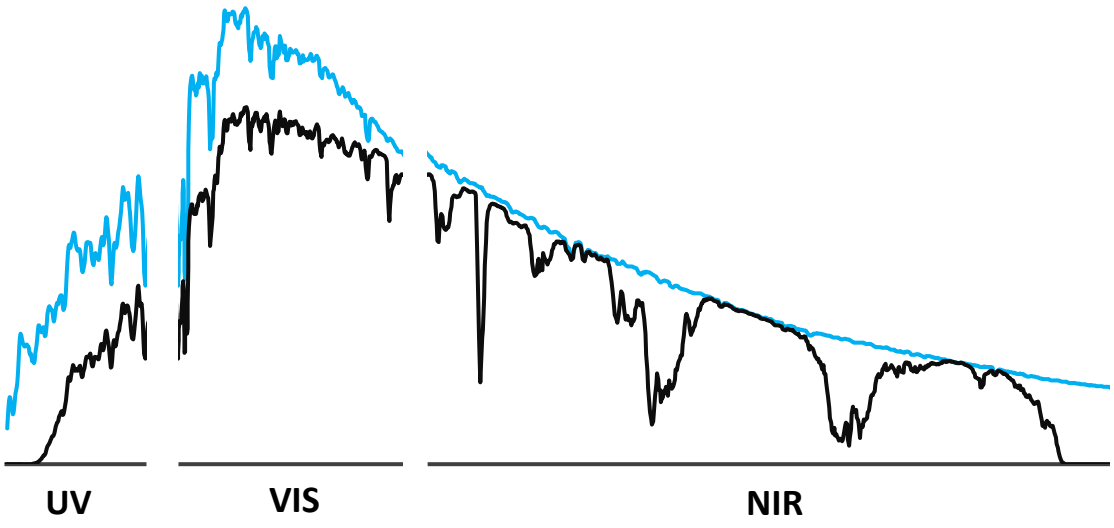
UV
VIS
NIR

I Introduction

1 Chemistry with Oxygen and Light

Molecular dioxygen O_2 (hereafter also referred to as *oxygen*) is integral to many chemical processes on earth, besides its key role in the maintenance of life and destruction of materials. Unlike the vast majority of molecules we know, the electronic ground state of O_2 is a spin triplet (called "triplet oxygen" and denoted $^3O_2$) and thus, reactions are governed by radical-like behavior.[1] In contrast, the lowest-energy excited electronic state of oxygen is a spin singlet (commonly called "singlet oxygen" and denoted $^1O_2$) featuring a significantly different but no less rich chemistry which is characterized by much more selective transformations.[2]

Light-induced reactions are the topic of the well-established area of photochemistry. The majority of organic molecules only absorb ultraviolet radiation of a wavelength $\lambda < 300$ nm, and UV radiation is scarcely available for reactions on the surface of the earth where the short wavelength part of the spectrum of the sun is luckily blocked by an ozone layer (Figure 1). To convert gases, or molecules not absorbing below 300 nm, by the help of visible light ($380 < \lambda < 720$ nm) which constitutes the highest intensity of electromagnetic radiation in the solar spectrum, a photosensitizer or photocatalyst is required.

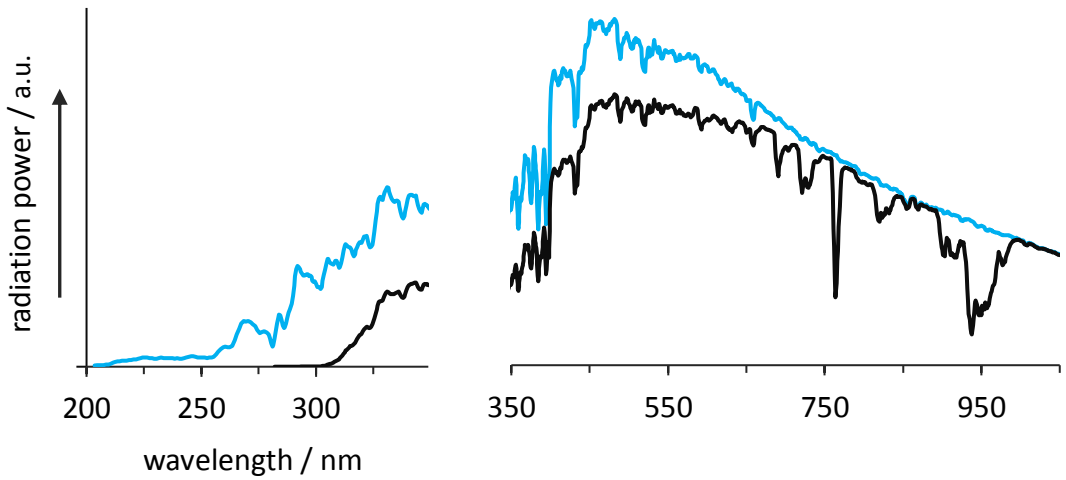

Figure 1. Solar radiation power – measured extraterrestrial (blue) and on earth (black).[3]

Singlet oxygen can be produced in a variety of ways which include electronic energy transfer from an excited state of another molecule to triplet oxygen, a prime example for photosensitization. As excited electronic states can be readily produced by irradiation with UV or visible light, and since we live in a world that provides us with plenty of visible light, oxygen, and molecules which are efficient sensitizers, this is the most convenient and widely applied method for $^1O_2$ generation.[2] However, low solubility of oxygen and limited penetration depth of light in solution represent a major challenge of this process.

Since 1895, oxygen is readily available in pressurized cylinders after Carl von Linde and William Hampson independently developed the first commercially viable process for liquefying gases.[4] High-brightness LEDs in any RGB primary color are available as an ideal source of light with defined intensity and wavelength range since the early 1990s,[5] allowing for simple and affordable irradiation independent from the sun and substituting incandescent light bulbs as well as mercury containing CFLs. In combination with continuous-flow photo-microreactor technology, reported in detail in 2005 by Booker-Milburn and Berry,[6] a set of technical simple, effective, customizable, and affordable tools for applying highly pressurized singlet oxygen in chemical reactions is available. Substrates far less reactive than α-terpinene (Figure 2) can nowadays be photo-oxygenated within minutes or seconds, allowing for a broad range of applications in exploratory, synthetic, and biological chemistry combined with steady research interest.[7,8]

Figure 2. Günther Otto Schenck (1913-2003) at his pilot plant for sensitized photooxygenation of α-terpinene by sunlight in his garden in Heidelberg (1950).[9]

2 Oxygen: Beyond a Kinetically Persistent Biradical

Molecular oxygen O_2, described as chemical element in 1774 and given the name *oxygène* (from Greek *oxys*: "acid producer") in 1777 by Antoine Lavoisier, is the only abundant paramagnetic molecule we know with a spin triplet ground state. Despite its simple structure, typically drawn O=O, it exhibits rather unusual properties regarding its magnetic behavior, energy-transfer processes, and chemical reactivity. The ground state ($^3\Sigma_g^-$) features two unpaired electrons which typically encourages other radicals or biradicals to stabilize themselves by forming bonds to each other, and to neighboring oxygen or hydrogen atoms (Figure 3).[1]

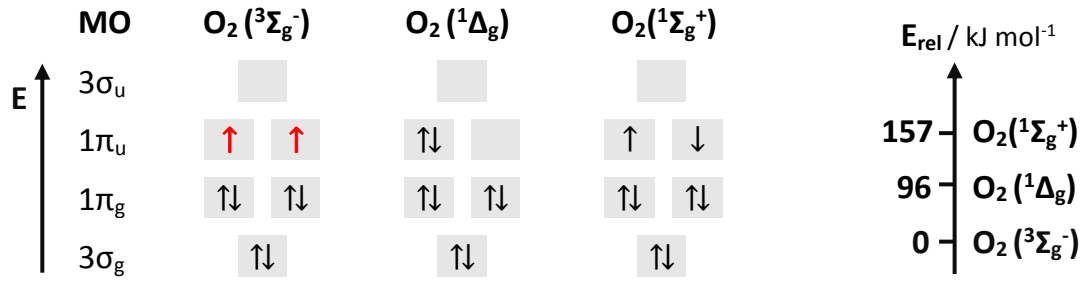

Figure 3. Molecular orbital occupation of ground and excited states of O_2. MOs are sorted by energy in ascending order (bottom to top), $(1\sigma_g)^2(1\sigma_u)^2(2\sigma_g)^2(2\sigma_u)^2$ omitted for simplicity.

Sixteen electrons are filled into the molecular orbitals according to Aufbau principle (orbitals are filled starting at the lowest possible energy levels), the Pauli exclusion principle (no two electrons can have the same set of quantum numbers), and Hund's rule which states energy is lowest when degenerate orbitals are occupied by two electrons singly and with the same spin before, for the second-lowest energetic state, they are filled in one orbital as a pair. Three electronic configurations of oxygen are depicted in figure 3: the biradical triplet ground state $^3\Sigma_g^-$, the first excited state $^1\Delta_g$ (commonly called "singlet oxygen" and abbreviated $^1O_2$), and the second excited singlet state $^1\Sigma_g^+$. A distinct but rich chemistry is known for $^3O_2$, the allotrope O_3, and $^1O_2$ (Scheme 1).[8] Species such as the second excited singlet oxygen (which is usually not formed from triplet oxygen applying sensitizers with comparatively low triplet energies such as methylene blue) and allotropes like the oxygen atom, O_4, or O_8 which are only stable for a very short lifetime or under special conditions.

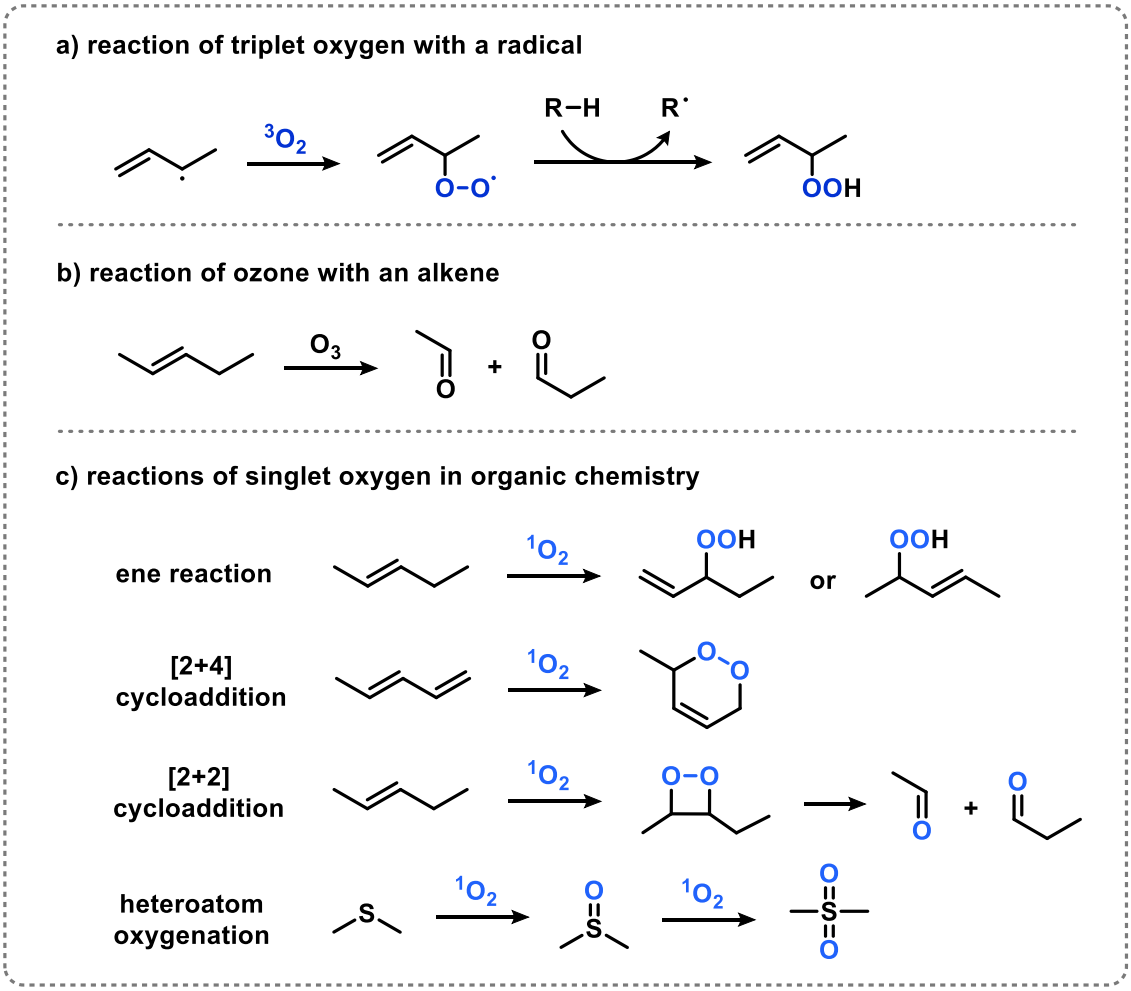

Scheme 1. Reactivity of triplet oxygen (a), ozone (b), and singlet oxygen (c).[8]

Triplet oxygen is especially reactive in contact with other radicals while it is kinetically persistent towards reaction with almost any other compound. It is important to note that $^3O_2$, however, reacts exothermically with any compound or element but gold. In that sense, it is an energy-rich molecule – featuring a high activation barrier. The hydrogen balloon exploding in a chemistry class does not go off until activation energy in form of a spark enters the scene and paper does not ignite until it reaches a temperature of roughly 230 °C. Triplet oxygen does not abstract hydrogen atoms to form HOO$^\bullet$ under reaction conditions where peroxyl radicals ROO$^\bullet$ are easily able to (Scheme 1a), due to the very large resonance stabilization energy of $^3O_2$ resulting in a strong π-bonding which can be explained by VB and MO theory.[1]

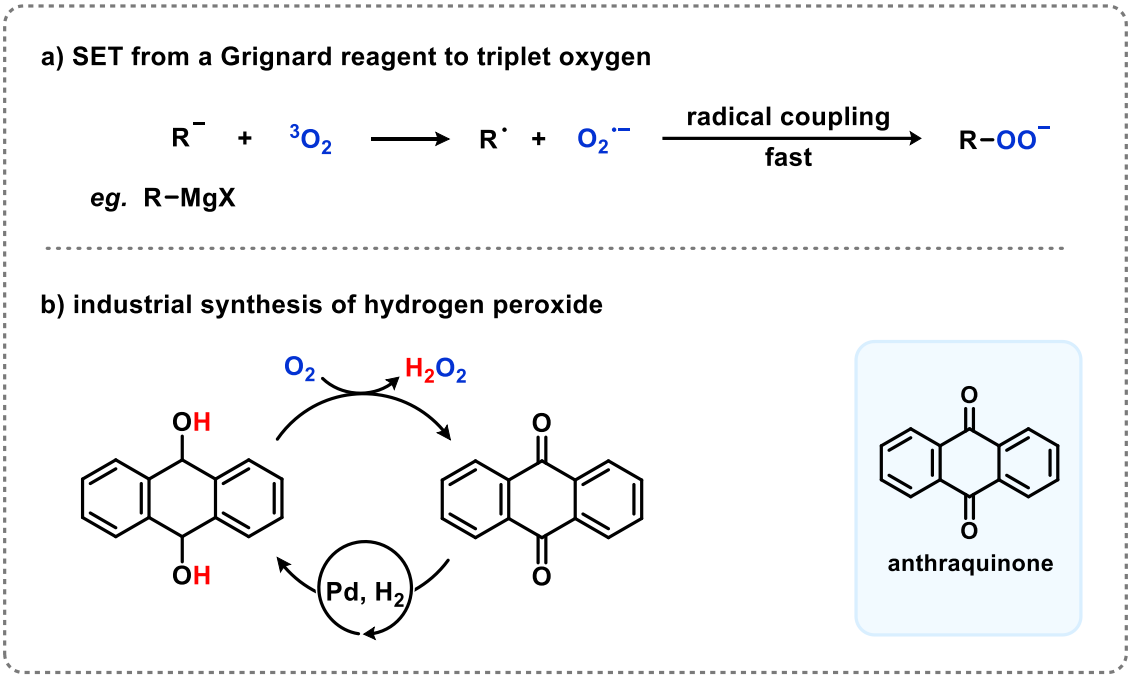

Scheme 2. Grignard oxidation (a) and anthraquinone process for H_2O_2 synthesis (b).

Besides its important role in food (*e.g.* oil) spoilage,[10] triplet oxygen is of synthetic and industrial value for example during Grignard oxidation (by a single electron transfer mechanism)[11] or H_2O_2 production in the anthraquinone process[12] (Scheme 2).

Ozone, the triatomic form of oxygen, is less stable than triplet oxygen but also much more reactive towards olefins and alkynes.[13] The molecular structure resembles a bent dipolar molecule (Scheme 3).

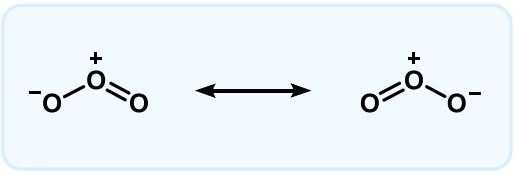

Scheme 3. Resonance structures of ozone.

O_3 is typically generated from diatomic oxygen which is exposed to an electrical field or UV light; due to a half-life of about one day, ozone can be and is typically generated spatially separated from the reaction mixture in an ozone generator.[14] Alkene C=C double bonds are readily cleaved by ozone (Scheme 4). Ozonolysis of olefins typically features a mechanism with a primary and secondary ozonide formed *via* a Criegee intermediate (which can be written as

biradical like in scheme 4b or as zwitterion). The reaction needs to be terminated with a redox reaction which breaks the weak oxygen-oxygen single bond of the primary oxidation products.[15]

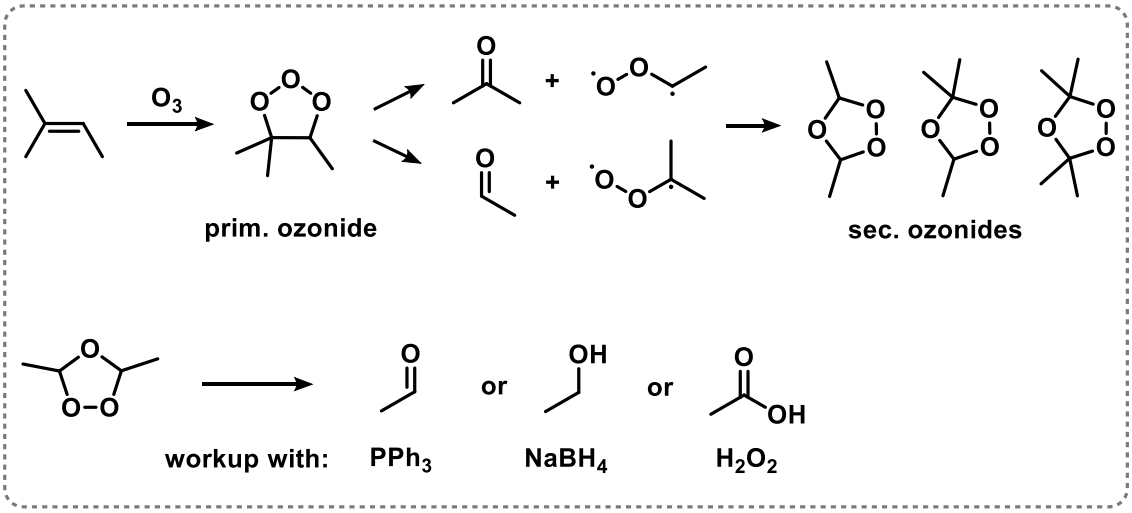

Scheme 4. Mechanism: ozonolysis of an alkene and subsequent workup.

Although the primarily formed ozonides are instable and potentially explosive, ozonolyses are applied in analytical chemistry as well as synthetic and pharmaceutical applications.[16]

In contrast to triplet oxygen undergoing unselective radical reactions or ozone cleaving π and σ-bonds subsequently and with multiple formed products, reactions with singlet oxygen are known for comparatively high selectivity, mild reaction conditions, and narrow product distribution.

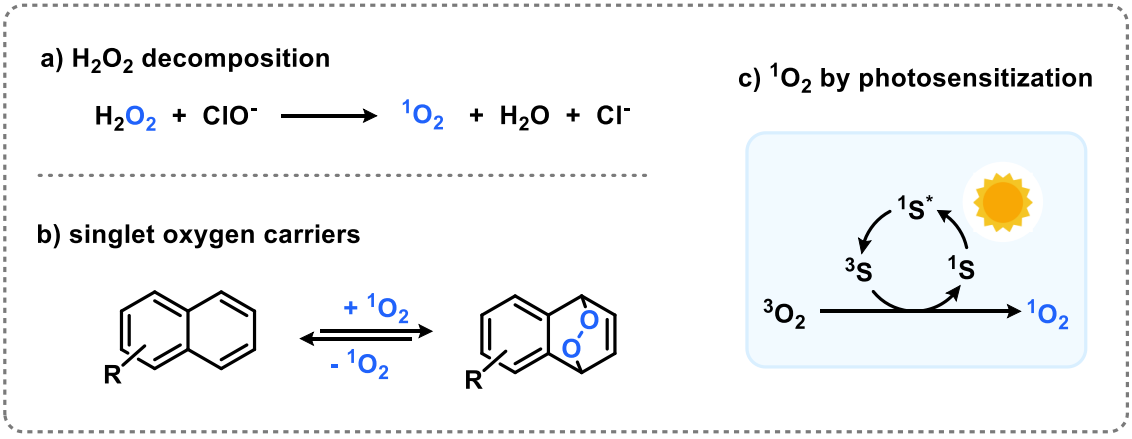

Scheme 5. Common methods to generate $^1O_2$. S=Sensitizer, for example methylene blue.

Due to the very limited lifetime of $^1O_2$ (τ_Δ: 10^{-1} s in CCl_4, 10^{-4} s in DCM, 10^{-5} s in MeOH, 10^{-6} s in H_2O; values rounded), it must be generated close to its reaction partner. Besides generation of singlet oxygen from triplet oxygen by direct absorption of light (not effective due to low c and ε),[17] by catalyzed hydrogen peroxide decomposition,[18] or release from oxygenated carriers like anthracenes, photsensitized production from $^3O_2$ by the help of visible light is well investigated and applied (Scheme 5c).[8,19] Photosensitizers like methylene blue or tetraphenylporphyrin featuring high extinction coefficients (up to 500,000 L mol^{-1} cm^{-1}) and quantum yields (>0.5) for singlet oxygen generation are well described in literature and readily available.[20] Due to its high reactivity especially towards double bonds (see scheme 1c), the reactive oxygen species is used for photodynamic therapy during cancer treatment and water decontamination besides its role in synthetic chemistry.[21,22] Besides cycloaddition and heteroatom oxidation reactions, the singlet oxygen ene reaction (also called Schenck ene reaction) constitutes a valuable oxygenation reaction in organic synthesis; it was discovered in 1943 by Günther Otto Schenck.[23,24] While the reactivity of a substrate towards $^1O_2$ oxygenation can be predicted rather well,[25] product selectivity, especially in case of complex substrates, is heavily dependent on geometric and electronic aspects (Scheme 6).

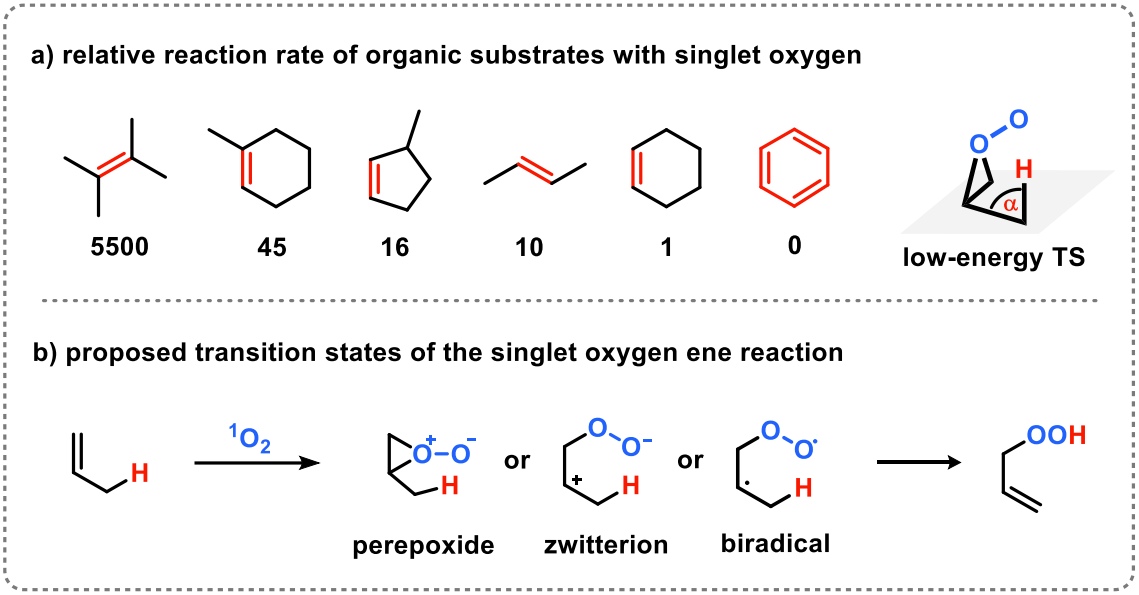

Scheme 6. Substrate reactivity and proposed transition states of the $^1O_2$ ene reaction.

The reaction rate is heavily dependent on the substitution pattern of the alkene and whether the double bond is present in a cycle or not. If the bond angle α (Scheme 6a) of the abstracted allylic hydrogen atom is near to 90 degrees, a low transition state energy and thus high reactivity can be predicted. Tetramethylethylene is thus known for its role as singlet oxygen quencher (by reactive quenching, in contrast to physical deactivation by solvents). Reactions with singlet oxygen are generally very rapid, with an activation enthalpy below 5 kcal/mol,[26] and thus the bond-making and bond-breaking steps of the mechanism are hard to address with experimental tests. For different classes of substrates, numerous investigations and studies showed different transition states to be more likely.[27] Many investigated reactions involve substrates with specialized physical or chemical properties which does not allow for generalization of the results and thus, prediction of product selectivity is yet hardly possible without substantial uncertainties.

Applications of $^1O_2$ in industrial scale are scarce, not only because the outcome after oxygenation of complex molecules is hard to predict: studies on efficient process design for this gas-liquid-light reaction are still ongoing. The three distinct phases are hardly miscible and, in addition, singlet oxygen has a long lifetime in especially harmful and expensive solvents such as $CDCl_3$ or CCl_4.[8,19]

3 Reactor Systems for Gas-Liquid-Light Reactions

The group of Kevin Booker-Milburn reported on the first continuous flow reactor for organic photochemistry in 2005.[6] Traditionally, The reactor consisted of an HPLC pump providing the substrate(s) and solvent with a constant flow rate, and a thin synthetic capillary wrapped around a glass cylinder. A (UV) lamp was installed inside the cylinder, and the lamp as well as the capillary containing the reaction mixture could be cooled (Figure 4).

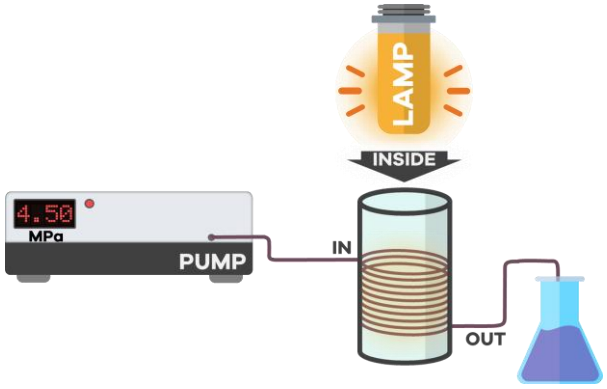

Figure 4. Schematic representation of the first continuous flow photochemistry reactor.

Steady delivery of the reaction mixture and a thin capillary ensured high reproducibility and efficiency of the irradiation. Due to the Lambert-Beer law, light penetration into solution follows a logarithmic dependency and thus, the thin (1/32 inch, or 0.79 mm inner diameter) commercial FEP (Scheme 7) and PFA (more expensive but rated for higher pressures/temperatures) capillaries allow for effective irradiation and high throughput.[28]

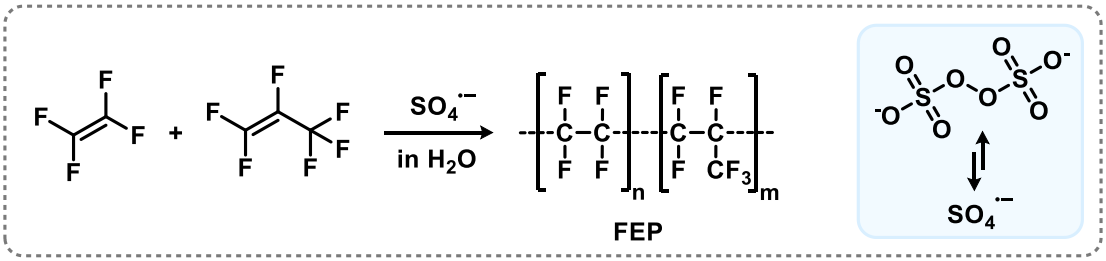

Scheme 7. Common synthesis pathway of fluorinated ethylene propylene (FEP).[29]

In 2016, two reports on the adaption and assembly of such a flow reactor system for gas-liquid reactions were published independently by the groups of A. Jacobi von Wangelin and T. Noël.[28,30] The implementation of a thermal

mass-flow controller for gases and a back-pressure regulator allow for a constant delivery of a variety of gases at elevated pressures of up to 80 bar. The elevated pressure however makes an HPLC pump – which does not allow for any particles like present in a suspension – mandatory, whereas for ambient pressure applications, a cheap syringe pump or a peristaltic pump can be used (Figure 5).

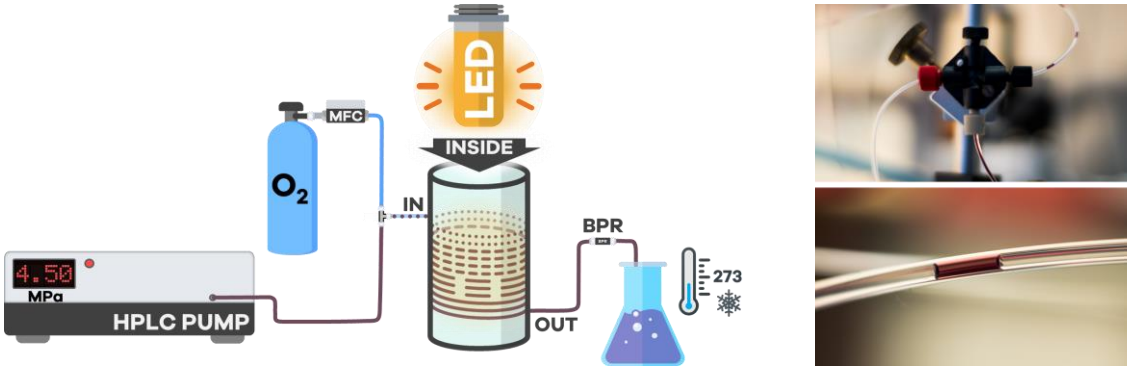

Figure 5. Modular gas-liquid-light process setup reported by the AJvW and Noël groups.

By the use of a T-mixing valve (figure 5 top right), gas and liquid phase are mixed, generating a so-called slug flow pattern which can be adjusted by controlling the distinct flow rates. The amount of gas in solution and thus reaction speed is highly dependent on the pressure: in acetonitrile, the concentration of O_2 was determined as 2.5 mM at ambient pressure, 35 mM at 9 bar, and 350 mM at 50 bar.[31] The modular system allows for broad applicability, using a variety of gases, light sources (UV/Vis), mixing and quenching events (using multiple pumps), temperature control, and is the ideal base for quick adaption of batch reactions to micro-flow in a laboratory environment. For information on the reactor setup used for reactions in this thesis, see Ref.[28] and illustration/explanation p. 142.

Besides this modular micro-flow setup, investigations on gas-liquid-light reactor technology are still ongoing: in 2009, a photooxidation process was reported using singlet oxygen in the alternative solvent sc-CO_2 at very high pressures up to 180 bar;[32] in 2016, the group of Burkhard König investigated the solvent-free oxidation of benzylic alcohols by air in a rod mill reactor under elevated temperatures;[33] photoxidations by a pneumatically generated aerosol in a nebulizer-based continuous flow reactor were reported in 2017;[34] in the same year, a reactor system to perform singlet oxygen oxygenations using a gas–liquid membrane reactor was developed.[35]

4 Photosensitization, Photocatalysis and Photooxygenation

Photosensitization and photocatalysis have very similar definitions; basically, each term is used in a different scientific community. The common accepted IUPAC definitions

Photochemistry

"The branch of chemistry concerned with the chemical effects of light (far UV to IR)."

Photocatalysis

"Change in the rate of a chemical reaction or its initiation under the action of ultraviolet, visible or infrared radiation in the presence of a substance – the photocatalyst – that absorbs light and is involved in the chemical transformation of the reaction partners."

Photosensitization

"The process by which a photochemical or photophysical alteration occurs in one molecular entity as a result of initial absorption of radiation by another molecular entity called a photosensitizer. In mechanistic photochemistry the term is limited to cases in which the photosensitizer is not consumed in the reaction."

Photooxygenation

"The incorporation of molecular oxygen into a molecular entity. There are three common mechanisms. Type I: the reaction of triplet molecular oxygen with radicals formed photochemically. Type II: the reaction of photochemically produced singlet molecular oxygen with molecular entities to give rise to oxygen containing molecular entities. The third mechanism proceeds by electron transfer producing superoxide anion as the reactive species."

leave enough space for interpretation and thus, researchers proceed to classify their research topics and choose a definition they think fits best in their current scientific community.[36] Thus, the term *photooxygenation* used in this thesis refers to a IUPAC photooxygenation Type II. In this context, *photosensitizer* and the terms *photosensitization* or *photooxygenation* are used instead of the related

terms *photocatalyst* and *photocatalysis*. The latter are often associated with a more intense involvement of the catalyst to the chemical transformation of the reaction partners beyond an energy transfer, like an electron transfer in photoredox catalysis (Scheme 8).[37]

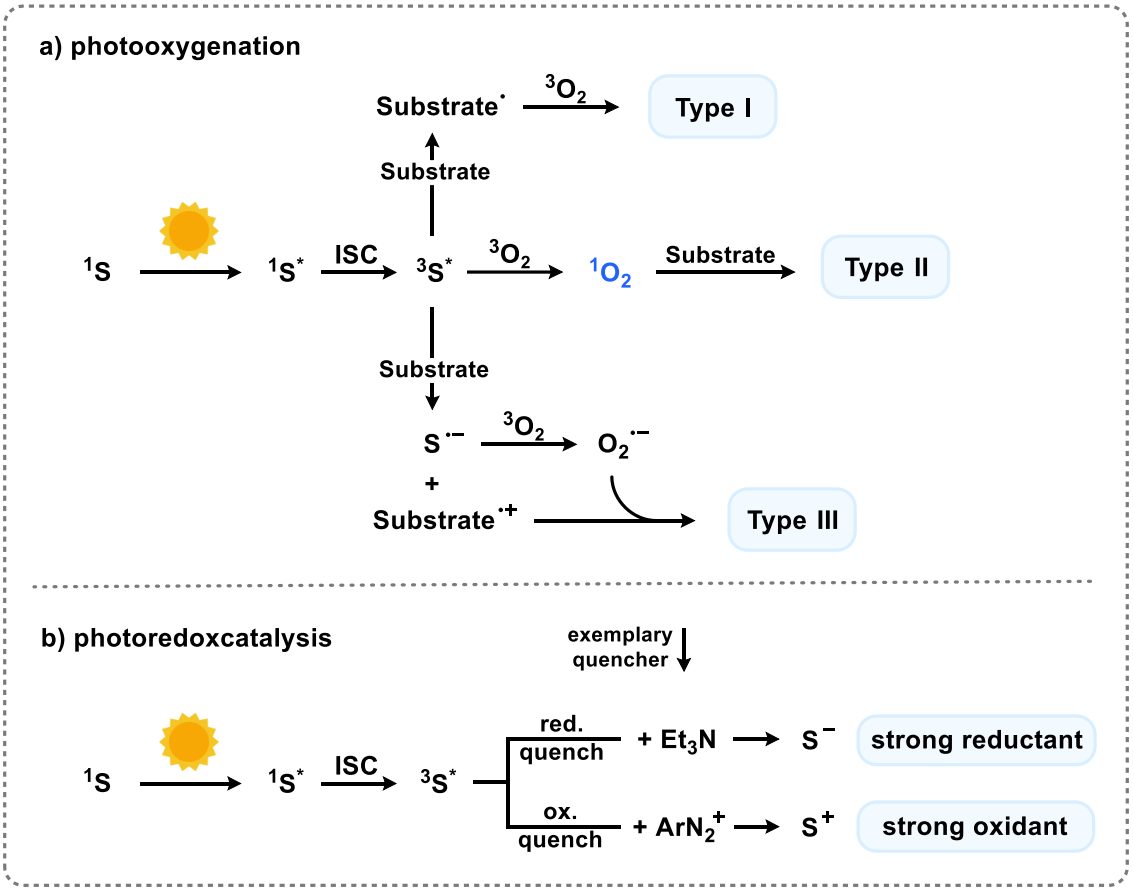

Scheme 8. Types of photooxygenations (a; the third mechanism is sometimes called Type III) and examples for photoredox catalysis (b).

It is apparent that these (excerpts of) mechanisms are identical in the irradiation of the catalyst/sensitizer and even overlap: a photooxygenation type III could also be called photo-redox reaction featuring reductive quenching. The singlet ground state absorbs light and a short-lived (3.5×10^{-10} s; ^{1}MB* in H_2O) singlet excited state is formed (^{1}S*). Through a quantum chemical process called intersystem crossing, the important and comparatively long-lived (4.5×10^{-5} s; ^{3}MB* in H_2O) triplet excited state (^{3}S*) forms. This triplet state is, in case of aerated solvent and MB, quenched by molecular oxygen with a bimolecular rate constant of about 10^9 M^{-1} s^{-1}; singlet oxygen is formed by this process. The lifetime of ^{3}MB* is lowered to about 3×10^{-6} s in case air-equilibrated water is used.[38]

The aim of photoredoxcatalysis is to generate strong oxidants/reductants for subsequent bond dissociation/forming reactions. One reason for the use of a sensitizer instead of direct excitation of the substrates by light to trigger bond dissociation is the low VIS and near-UV light absorbance of most substrates (as they are usually colorless/white). Far-UV radiation could be used for direct excitation; however, the energy content of such photons is too high (and they are seldomly employed aside the use of ultraviolet radiation for radical chain processes). In most cases, irradiation by Far-UV light results in an unseletive decomposition of the reaction mixture.

5 Green Chemistry: Principles and Practice

.. is the title of a renowned high impact (>1000 citations) article from Paul Anatas from 2009 covering the concepts of design and the scientific philosophy of sustainable chemistry. The aim of Green Chemistry is to reduce hazards across the life-cycle stages of a chemical process, whereby a hazard is defined as the ability to cause negative consequences to humans or the environment. Luckily, hazard reduction has often been shown to be economically profitable.[39]

Of the 12 principles explained in detail, numbers 5, 6, and 7 cover the topics solvent use, energy efficiency, and renewable materials. Solvents are, according to the authors, "*perhaps the most active area of Green Chemistry research*". Large quantities of solvents per mass of the final product are used in fine-chemical and pharmaceutical production; in addition to the need for solvent recycling or disposal, the product must be separated in a first step – *e.g.* in an energy intense distillation or by crystallization.

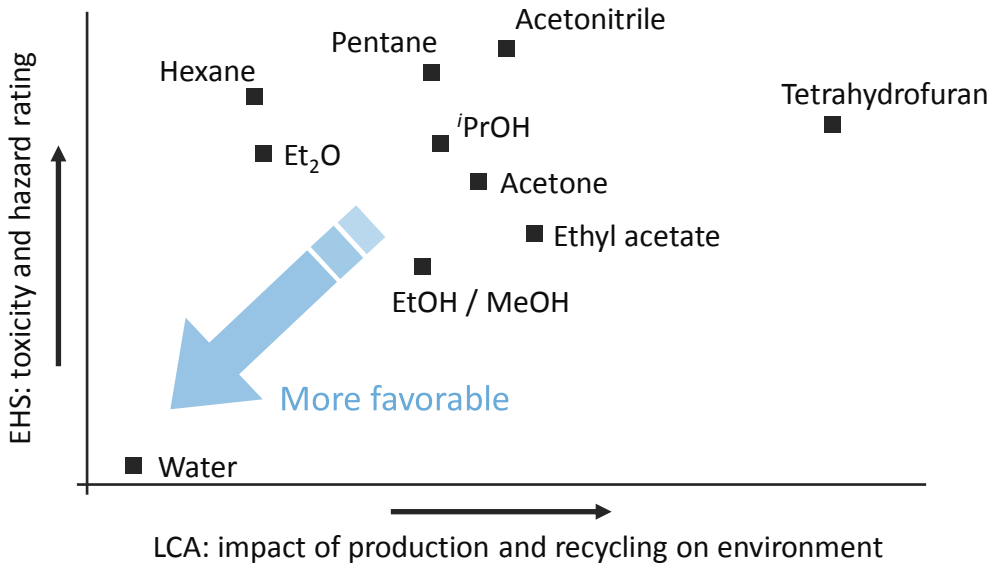

Figure 6. Environment and hazard assessment of common organic solvents.[40]

General purpose solvent selection guides are available in literature (Figure 6). Halogenated solvents like chloroform or DCM are often not included as their impact is disproportionally high. Although selection guides like the one above represent a quick method to compare, for example, production and recycling impact of two solvents on the environment, these tools are still unable to

specifically guide solvent selection for particular applications. Thus, reaction specific solvent selection guides like for chromatography applications are reported.[41] Besides water as a well-known solvent with very low impact, the field of organic synthesis without conventional solvents (*e.g.* by using sc-CO_2 or ionic liquids) or without any solvent at all ("neat" reactions) is intensely studied.[42]

Aside of the development of reactor setups to reduce solvent waste, the impact of the production of substrates can be reduced using renewable materials, or waste products from an already existing process. The vast majority of substrates are derived from petroleum feedstock or natural gas while these are finite sources with limited recycling options. Renewable materials range from cellulose and other wood compounds to lactic acid, chitin, starch, glycerol, and vegetable oils such as cardanol (Scheme 9).

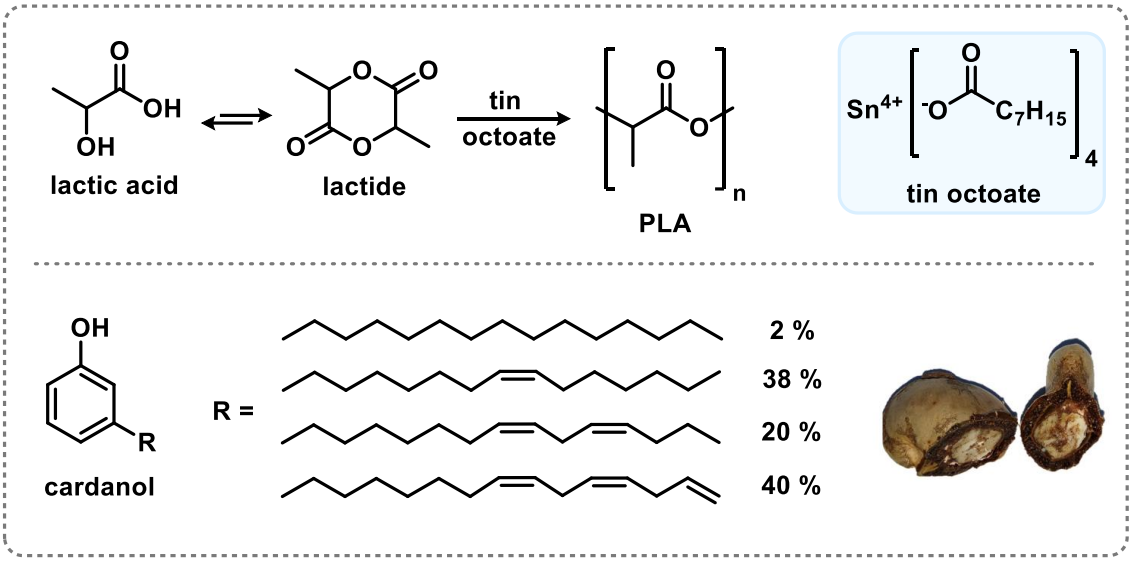

Scheme 9. Exemplary renewable substrates: lactic acid and cardanol.

While substrates like glycerol and lactic acid are obtained in high purity and can be applied even for fine chemical synthesis, others such as cardanol arise as a mixture of compounds. Due to the very similar physical properties of the cardanol compounds, they can not be separated in large scale and thus, the mixture is typically used in polymerization reactions. Cardanol arises as technical waste product during cashew nut processing and is commercially available below 500 $ per ton with an annual production of 10^6 tons (raw oil, for comparison: 4,000 x 10^6 t/a).[43]

6 References

[1] W. T. Borden, R. Hoffmann, T. Stuyver, B. Chen, *J. Am. Chem. Soc.* **2017**, *139*, 9010–9018.
[2] P. R. Ogilby, *Chem. Soc. Rev.* **2010**, *39*, 3181–3209.
[3] C. A. Gueymard, D. Myers, K. Emery, *Sol. Energy* **2002**, *73*, 443–467.
[4] W. Hampson, Patent GB189510165, **1895**, Title: Improvements Relating to the Progressive Refrigeration of Gases.
[5] D. Feezell, S. Nakamura, *C. R. Phys.* **2018**, *19*, 113–133.
[6] B. D. A. Hook, W. Dohle, P. R. Hirst, M. Pickworth, M. B. Berry, K. I. Booker-Milburn, *J. Org. Chem.* **2005**, *70*, 7558–7564.
[7] A. A. Ghogare, A. Greer, *Chem. Rev.* **2016**, *116*, 9994–10034.
[8] S. Nonell, C. Flors, *Singlet Oxygen: Applications in Biosciences and Nanosciences (Volume 1)*, Royal Society Of Chemistry, Cambridge, **2016**.
[9] K. Schaffner, *Angew. Chem.* **2003**, *115*, 3038–3039.
[10] D. B. Min, J. M. Boff, *Compr. Rev. Food Sci. Food Saf.* **2002**, *1*, 58–72.
[11] C. Walling, S. A. Buckler, *J. Am. Chem. Soc.* **1955**, *77*, 6032–6038.
[12] T. Nishimi, T. Kamachi, K. Kato, T. Kato, K. Yoshizawa, *Eur. J. Org. Chem.* **2011**, 4113–4120.
[13] P. S. Bailey, in *Ozonation in Organic Chemistry*, Academic Press Inc., London, **1982**, pp. 1–2.
[14] J. D. McClurkin, D. E. Maier, *Julius-Kühn-Archiv* **2010**, 381.
[15] R. Brückner, *Organic Mechanisms*, Springer, Berlin/Heidelberg, **2010**.
[16] S. G. Van Ornum, R. M. Champeau, R. Pariza, *Chem. Rev.* **2006**, *106*, 2990–3001.
[17] C. Long, D. R. Kearns, *J. Chem. Phys.* **1973**, *59*, 5729–5736.
[18] H. H. Seliger, *Anal. Biochem.* **1960**, *1*, 60–65.
[19] T. Noël, M. Escriba Gelonch, K. Huvaere, in *Photochemical Processes in Continuous-Flow Reactors*, World Scientific Publishing Europe Ltd., London, **2017**, pp. 245–267.
[20] M. DeRosa, R. J. Crutchley, *Coord. Chem. Rev.* **2002**, *233–234*, 351–371.
[21] R. Saini, N. Lee, K. Liu, C. Poh, *Cancers* **2016**, *8*, 83.
[22] L. Villén, F. Manjón, D. García-Fresnadillo, G. Orellana, *Appl. Catal. B Environ.* **2006**, *69*, 1–9.
[23] G. O. Schenck, Patent DE933925C, **1943**, Title: Verfahren Zur Herstellung von Pinocarveylhydroperoxyd.
[24] M. Prein, W. Adam, *Angew. Chem. Int. Ed.* **1996**, *35*, 477–494.
[25] K. R. Kopecky, H. J. Reich, *Can. J. Chem.* **1965**, *43*, 2265–2270.
[26] L. M. Stephenson, M. J. Grdina, M. Orfanopoulos, *Acc. Chem. Res.* **1980**, *13*, 419–425.
[27] A. A. Frimer, *Chem. Rev.* **1979**, *79*, 359–387.
[28] J. Schachtner, P. Bayer, A. Jacobi von Wangelin, *Beilstein J. Org. Chem.* **2016**, *12*, 1798–1811.
[29] K. Hintzer, T. Zipplies, D. P. Carlson, W. Schmiegel, in *Ullmann's Encyclopedia of Industrial Chemistry*, Wiley-VCH, Weinheim, **2014**, pp. 1–55.
[30] N. J. W. Straathof, Y. Su, V. Hessel, T. Noël, *Nat. Protoc.* **2016**, *11*, 10–21.
[31] P. Bayer, A. Jacobi von Wangelin. Unpublished results.
[32] R. A. Bourne, X. Han, M. Poliakoff, M. W. George, *Angew. Chem. Int. Ed.* **2009**, *48*, 5322–5325.
[33] M. Obst, B. König, *Beilstein J. Org. Chem.* **2016**, *12*, 2358–2363.

[34] G. I. Ioannou, T. Montagnon, D. Kalaitzakis, S. A. Pergantis, G. Vassilikogiannakis, *ChemPhotoChem* **2017**, *1*, 173–177.
[35] A. Kouridaki, K. Huvaere, *React. Chem. Eng.* **2017**, *2*, 590–597.
[36] M. Nič, J. Jirát, B. Košata, A. Jenkins, A. McNaught, *IUPAC Compendium of Chemical Terminology*, IUPAC, Research Triagle Park, NC, **2009**.
[37] B. König, *Chemical Photocatalysis*, De Gruyter, Berlin/Boston, **2013**.
[38] S. J. M. Nassar, C. Wills, A. Harriman, *ChemPhotoChem* **2019**, *3*, 1042–1049.
[39] P. Anastas, N. Eghbali, *Chem. Soc. Rev.* **2010**, *39*, 301–312.
[40] C. Capello, U. Fischer, K. Hungerbühler, *Green Chem.* **2007**, *9*, 927–934.
[41] F. P. Byrne, S. Jin, G. Paggiola, T. H. M. Petchey, J. H. Clark, T. J. Farmer, A. J. Hunt, C. Robert McElroy, J. Sherwood, *Sustain. Chem. Process.* **2016**, *4*, 7.
[42] M. Obst, B. König, *Eur. J. Org. Chem.* **2018**, 4213–4232.
[43] P. Anilkumar, *Cashew Nut Shell Liquid*, Springer International Publishing, Cham, **2017**.

7 Thesis Structure and Outline

The main part of this thesis is divided into four chapters. Chapter II comprises a review over stereoselective photooxygenations by the singlet oxygen ene reaction with an introduction into photosensitized $^1O_2$ generation and reaction selectivity (published in *ChemPhotoChem*). Mechanistic investigations on the photooxygenation of 1-aryl-1-cyclohexenes in a home-built photo-flow reactor follow in chapter III, accompanied by results on synthesis and analysis of the peroxide-containing primary products (published in *Org Chem Front*).

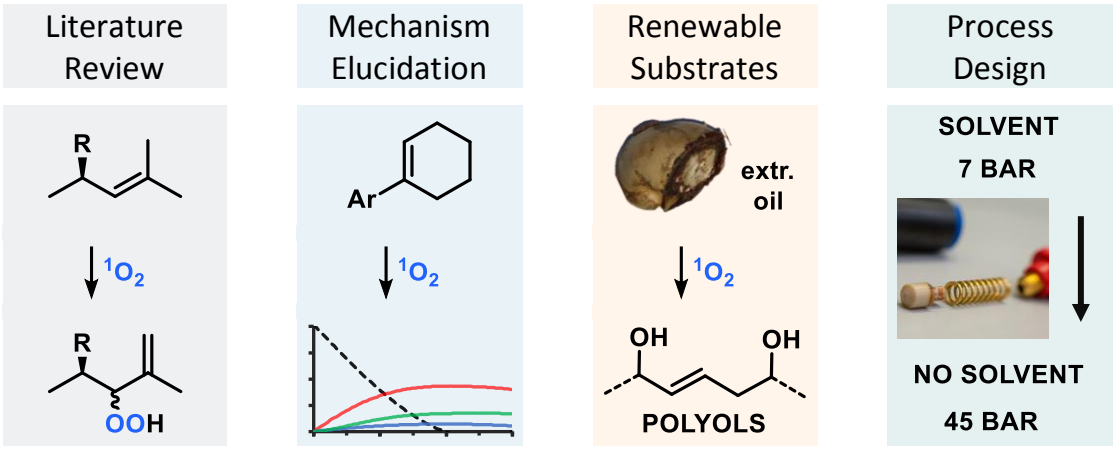

Chapter II	Chapter III	Chapter IV	Chapter V
pp. 29-57	pp. 59-98	pp. 99-128	pp. 129-149

Results on the oxygenation of the renewable feedstock cardanol (extracted oil from the cashew nut shell) accompanied by modification and optimization of the flow reactor are summarized in chapter IV, with a close look onto NMR analysis. The main section is concluded after chapter V in which the possibilities and limits of a novel process for entirely solvent-free photooxygenation of olefins under continuous-flow conditions applying highly pressurized oxygen (published in *Green Chem*) are presented.

Chapters feature progressive numbering of tables, schemes and figures while citation numbers and compound labels are kept separate. In case of already published results, the experimental part is appended in a condensed form and contains selected information and details.

II Review: Stereoselective Photooxygenations

published with minor modifications as

"Stereoselective Photooxidations by the Schenck Ene Reaction"

in *ChemPhotoChem* **2018**, *2*, 559-570.

Author contributions:

Patrick Bayer wrote the manuscript and performed literature review.
Raúl Pérez-Ruiz assisted in literature review and early-stage manuscript.
The work was supervised by Prof. Dr. Axel Jacobi von Wangelin.

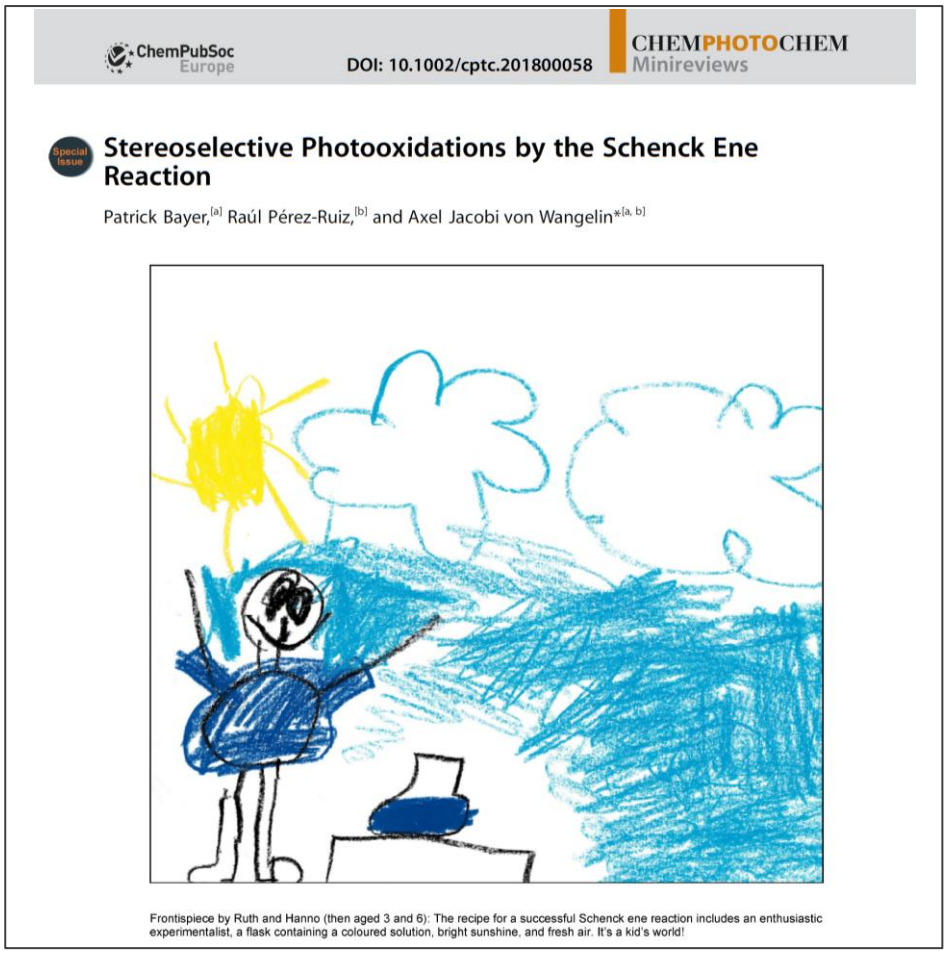

ChemPubSoc Europe
DOI: 10.1002/cptc.201800058
CHEMPHOTOCHEM Minireviews

Special Issue

Stereoselective Photooxidations by the Schenck Ene Reaction

Patrick Bayer,[a] Raúl Pérez-Ruiz,[b] and Axel Jacobi von Wangelin*[a, b]

Frontispiece by Ruth and Hanno (then aged 3 and 6): The recipe for a successful Schenck ene reaction includes an enthusiastic experimentalist, a flask containing a coloured solution, bright sunshine, and fresh air. It's a kid's world!

1 Introduction

The appreciation of modern sustainability criteria in chemical transformations has stimulated the use of abundant, cheap, and environmentally benign reagents and energy sources for the valorization of chemicals. Prime examples of such processes, among others, are oxidations with atmospheric oxygen and visible light-driven processes. An especially powerful yet under-utilized combination of these two ubiquitous entities with easily available hydrocarbons is the Schenck ene reaction.[1,2] Unbiased alkenes and atmospheric oxygen react under visible light irradiation in the presence of a suitable catalytic photosensitizer to give allylhydro-peroxides. This reaction displays perfect atom economy and high functional group tolerance and enables the access to versatile allyl alcohol derivatives which are key precursors to functionalized C_3 units and can undergo facile rearrangements (Scheme 10).

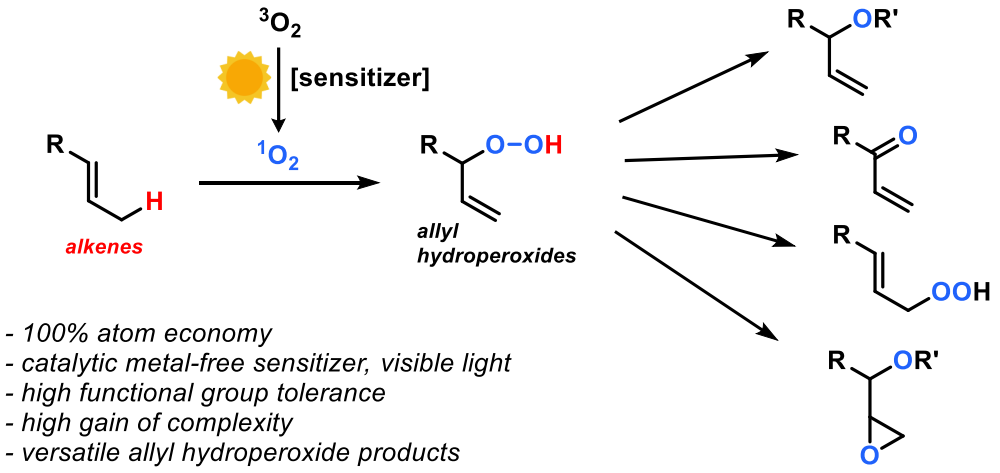

Scheme 10. Photooxygenation of hydrocarbons by the (Schenck) singlet oxygen ene reaction.

The mechanism of this hydrocarbon oxidation involving 1,3-allylic transposition and olefin dioxygenation have been intensively studied.[3–8] The reaction generally relies upon the effective generation of singlet oxygen ($^1O_2$), the first excited state of dioxygen 95 kJ mol^{-1} above the triplet ground state. In contrast to chemical methods of producing singlet oxygen, the use of light in combination with a catalytic photo-sensitizer constitutes an environmentally benign approach.[9,10] Upon irradiation with visible light, the photo-sensitizer populates

its triplet excited state via intersystem crossing. Energy transfer with the natural triplet oxygen ($^3O_2$) results in the formation of singlet oxygen which has a lifetime of a few microseconds in various solvents like ethanol, acetone, and acetonitrile (Scheme 11a).[11] The use of less polar and deuterated solvents enhances the stability of singlet oxygen up to lifetimes of a few ms ($CDCl_3$, CD_3CN) to more than 50 ms (perhalo compounds such as CCl_4).[12] The stereoselectivity of the reactions are not affected by the $^1O_2$ lifetime.

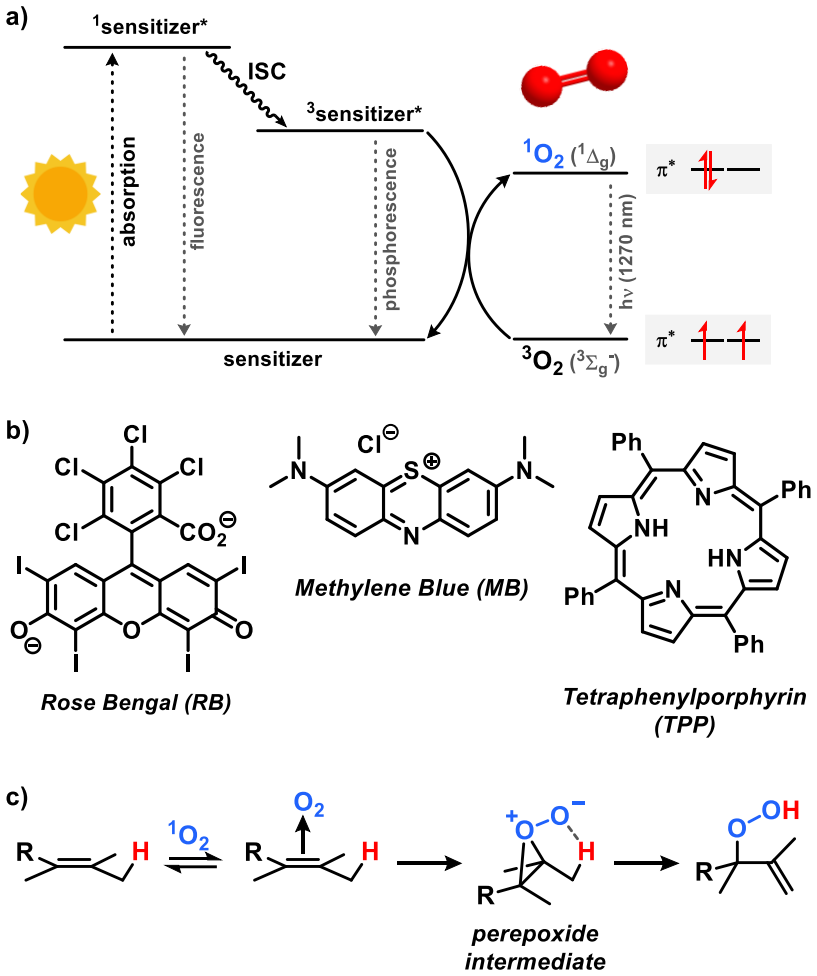

Scheme 11. a) Photo-sensitized formation of $^1O_2$; b) common photo-sensitizers; c) postulated mechanism and intermediate of the $^1O_2$-ene reaction.

The most common photo-sensitizers are the metal-free dyes methylene blue, (dianionic) rose bengal and tetraphenylporphyrin which reach quantum yields of >0.5 for the $^1O_2$ formation (Scheme 11b).[13,14] The alkene oxidation is a supra-facial process that involves a 1,3-allylic transposition and most likely proceeds *via* a perepoxide intermediate (Scheme 11c).[8] The overall reaction rate is strongly

dependent on the electron density of the alkene (tetra-methylethylene is one of the most reactive substrate in this context), the conformation of an accessible allylic hydrogen atom (shown in red; ideally perpendicular to the plane of the alkene), and various substituent effects.

Today, 150 years after the first report of an organic reaction with singlet oxygen ($^1O_2$)[15] and 70 years after the seminal discovery of dye-sensitized photo-oxidations of terpenes by Schenck,[2] $^1O_2$-ene reactions have been developed to maturity. The renaissance of the Schenck reaction is also fueled by the high sustainability of this atom-economic oxidation of easily available hydrocarbons with air or oxygen in the presence of a metal-free catalyst and visible light. The low requirement of an alkene bearing a γ-hydrogen atom, which can easily be fulfilled by many substrate families (biomass chemicals, petrochemical building blocks, fine chemicals, pharmaceuticals, agrochemicals, natural products, materials), and the low costs of the reaction (room temp., air/oxygen, cheap dye) allows for wide applications of this technology to chemical valorization strategies.[3,16,17] Importantly, the general reaction bears a close conceptual relationship to naturally occurring hydrocarbon oxidations that utilize similar substrates, form similar products but operate by different mechanisms (Scheme 12).

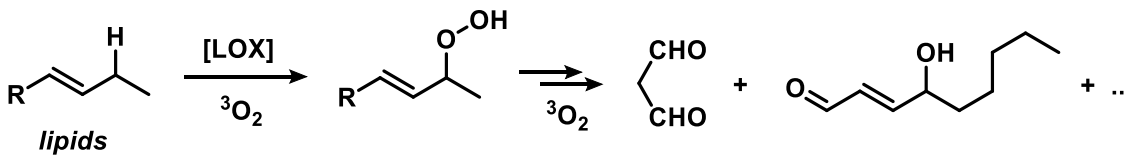

Scheme 12. Biological allylic dioxygenation with triplet oxygen: oxidative degradation of lipids.

The aerobic oxidation of fatty alkenes occurs also in the dark and involves radical H atom abstraction and reaction of the resultant allyl radical intermediate with the naturally occurring triplet dioxygen $^3O_2$. Prominent examples are dioxygenations of various lipids by enzyme catalysts such as lipoxygenase (LOX) or cyclooxygenase (COX). These reactions are key steps in the oxidative degradation of fat molecules,[18,19] the biosynthesis of prostaglandins, leukotrienes and lipoxins via hydroperoxyeicosa-tetraenoic acids[14,20–22].

Despite the use of the biradicaloid triplet oxygen in biological dioxygenations, extremely high levels of stereoselectivity are achieved by the enzyme catalysts. The lack of similarly complex chiral environments in lab-scale Schenck ene reactions with singlet oxygen generally leads to low stereoselectivities with simple alkene substrates. However, this limitation has recently been overcome by the identification of significant substituent effects and implementation into complex molecule syntheses. These observations have enabled the development of Schenck reactions with high levels of chemo-, regio-, and stereocontrol. High selectivities can even be induced by stereoelectronic effects despite the presence of several chemically similar allylic CH bonds:[23] The *cis*-effect leads to preferential H atom abstraction at the more congested half of the alkene due to better stabilization of the negative charge of the perepoxide intermediate by H-bonding motifs.[24] Regioselectivity governed by the *gem*-effect is induced by hyperconjugation between the n(O) and σ*(C-EWG) orbitals.[25,26] Electronic perturbation by heteroatom-substituents[27] and intramolecular H bonding motifs[28] were also reported to induce high selectivities. Furthermore, stereocenters in close proximity to the alkene can induce high diastereoselectivities. Various combinations of several of these intensively studied steering effects have enabled highly chemo-, regio-, and stereoselective Schenck reactions with suitably decorated alkenes.

Generally, diastereoselectivity is mostly induced by proximal (mostly allylic) stereocenters of chiral substrates and stereoelectronic effects of heteroatom-based substituents or chiral auxiliaries.[7] This minireview is intended to provide the reader with a timely review of the major concepts of stereoselective singlet oxygen ene reactions and their applications to modern complex molecule synthesis. The multi-faceted roles of proximal substituents and chiral auxiliaries and their underlying mechanisms of stereo-induction will be discussed.

2 Stereoselectivity in Singlet Oxygen Ene Reactions

▪ Alkenes

Unlike in biological enzyme-catalyzed dioxygenations, the stereo-control of Schenck ene oxidations of unbiased acyclic hydrocarbons is generally only moderate. There are no reports of effective enantioselective Schenck ene reactions.[29–33] However, the careful analysis of reactions with chiral alkenes laid the mechanistic foundations that have enabled the design of effective diastereoselective reactions. The first significant work was reported by Orfanopoulos and Stephenson in 1980.[34] It manifested the postulate of suprafacial singlet-dioxygen attack and H-atom transfer (Scheme 13A). Consequently, the enantio-merically pure deuteroalkene exclusively afforded an equimolar mixture of the (*E*)-allylhydroperoxides in overall 82% yield. These results suggested the operation of a suprafacial mechanism via the most stable conformer. The absence of a significant primary kinetic H/D-isotope effect in this reaction ruled out a concerted reaction pathway. In similar fashion, a deuterated enantiopure C_2-symmetric substrate cleanly reacted *via* a suprafacial mechanism exclusively affording *E*-alkenes (Scheme 13B).[35]

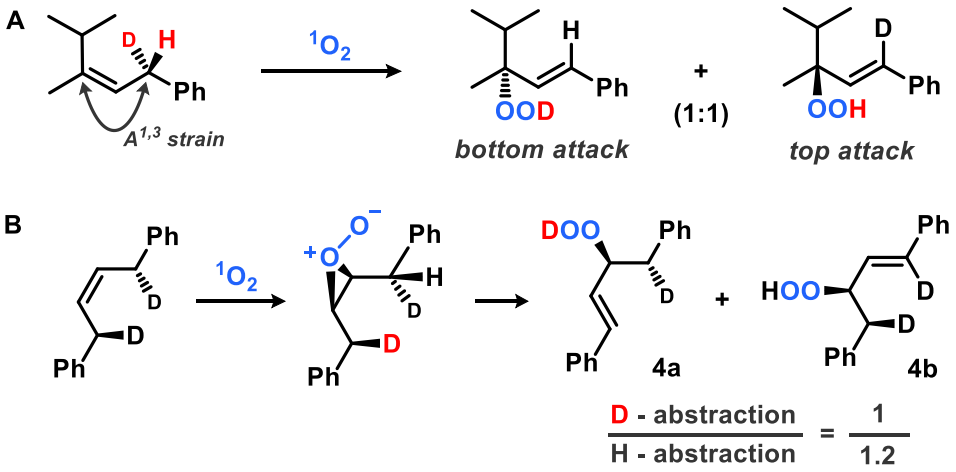

Scheme 13. Dioxygenation of enantiopure alkenes as a proof of the suprafacial mode of $^1O_2$ attack and H-abstraction.

Identical products and ratios were obtained in dichloromethane, acetone, acetonitrile, and methanol which supports the notion of an H-bonded perepoxide intermediate that is independent on solvent polarity.

According to the IUPAC, an ene reaction is defined as *the addition of a compound with a double bond having an allylic hydrogen (the 'ene') to a compound with a multiple bond (the 'enophile') with transfer of the allylic hydrogen and a concomitant reorganization of the bonding*.[36] The stereoselective photooxidation of tryptophan investigated by Nakagawa in 1981 is not strictly a Schenck ene reaction but despite the presence of an amine-based H atom donor bears a close conceptual analogy (Scheme 14).[37] The mechanism of the photo-oxidation is not entirely understood, however, the intermediacy of a labile hydroperoxide is widely accepted but could not be isolated due to rapid rearrangement upon contact with acids or silica.[38] The electron-rich enamine motif of such substituted tryptamines undergoes much more rapid β-oxidation than the conventional $^1O_2$ ene reaction in allylic position. In case of tryptophan, the final product was obtained as a 60:40 mixture with its diastereomer and could easily be isolated directly or crystallized after reduction to the corresponding alcohol. Although the diastereoselectivity is not remarkably high in this example, the underlying reaction path has later been applied to many natural product syntheses with good diastereocontrol (up to 85:15).[39,40]

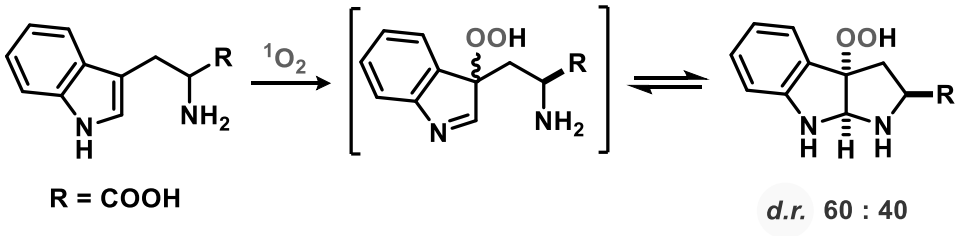

Scheme 14. Tryptophan oxidation with singlet oxygen and subsequent rearrangement.

1,3-Dienes easily undergo formal [4+2]-cycloadditions with singlet oxygen when an s-*cis* conformer can be accessed. Dienes also display equally high reactivities as simple alkenes in Schenck ene reactions, whereby the reaction pathways differ between conjugated, cumulated, and isolated dienes. With suitable substituents, conjugated dienes can adopt twisted conformations that contain a suitably positioned allylic hydrogen atom. For example, allenes were prepared in

moderate yields from stereo-selective $^1O_2$ ene reactions of hexadienols (Scheme 15). The photooxygenation of allenes yet is very sensitive to substituent effects and affords complex mixtures in many cases.[41–45]

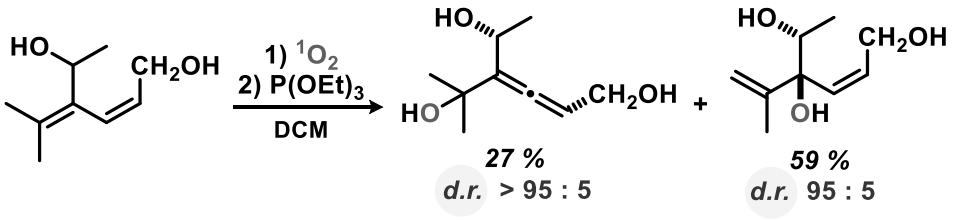

Scheme 15. Allene formation by the $^1O_2$ ene reaction.

Conformational control and the exploitation of (weak) diene-benzene interactions have enabled the stereoselective oxygenation of isolated skipped (*Z*)-dienes as simplified models of fatty acid dienes. However, there are few comparable literature examples.[46] Similar π-interactions facilitated an asymmetric dioxygenation of (prochiral) enoates featuring a naphthalene-containing chiral auxiliary.[47]

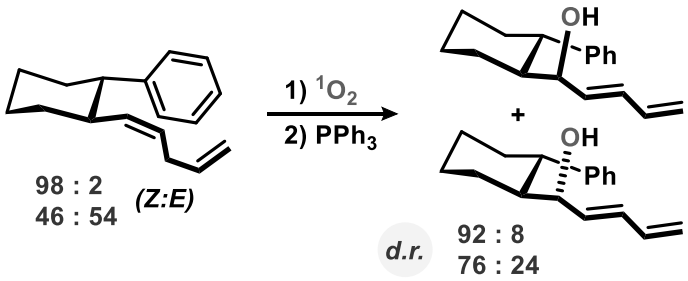

Scheme 16. Stereoinduction by π-face blockage in a chiral skipped diene.

In contrast to the various examples of intramolecular stereo-induction by substrate conformation, chiral centers, and auxiliaries, the use of solid matrices such as polymer supports and zeolite confinement of substrates also enabled remarkable diastereoselectivity of Schenck ene reactions.[48,49]

▪ Alkenes with allylic heteroatom substituents

While alkyl groups in allylic position only moderately affect the stereoselectivity,[50] heteroatomic substituents induce substantial electrostatic and orbital interactions and remarkable diastereo-control. The ease of synthetic

access to the starting materials and the great utility of the resultant dioxygenation products have prompted intensive investigations into the stereodirecting effects of alkenes bearing allylic heteroatom-substituents (O, N, S, halides). Allyl alcohols undergo especially facile Schenck ene reactions with high regiocontrol in favour of the 1,2-diols (rather than 1,3-diols). The occurrence of H-bonding motifs between the hydroxyl function and the perepoxide terminus can result in high *cis*-regioselectivity (regarding the methyl group in the shown alkene substrate) and *syn*-stereoselectivity (regarding the 1,2-diol product) (Scheme 17). The high regio- and stereocontrol observed in reactions of many easily accessible chiral allyl alcohols makes their photooxidation an especially attractive strategy. The resultant 1-butene-3,4-diol derivatives constitute highly versatile building blocks in complex molecule syntheses.[51,52]

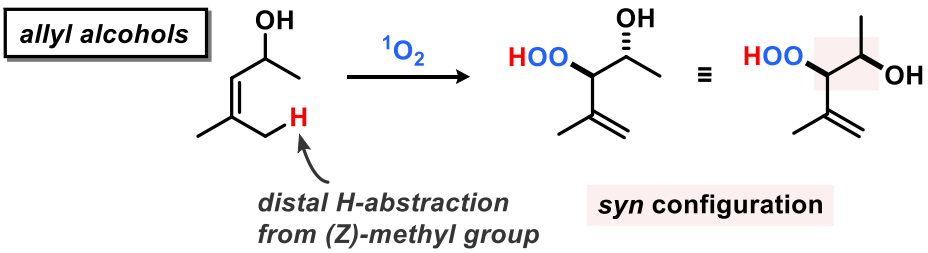

Scheme 17. Regio- and stereocontrol of Schenck ene reactions of allyl alcohols.

Deuterium-labelling experiments provided deeper insight into the origin of diastereoselectivities in Schenck ene reactions of allyl alcohols.[53–55] The employment of deuterated dimethylpentenol documented a significant solvent dependence of the *syn*/*anti*-selectivity of the methyl substituent (Scheme 18). Non-polar solvents (benzene, CCl_4) favoured attack of the *Z*-methyl group, while a hydrogen atom from the *E*-methyl group was abstracted in polar solvents like methanol or acetonitrile. This regioselectivity is a consequence of the postulated hydrogen bonding between the hydroxyl group and the perepoxide terminus in the rate-determining step of the reaction.

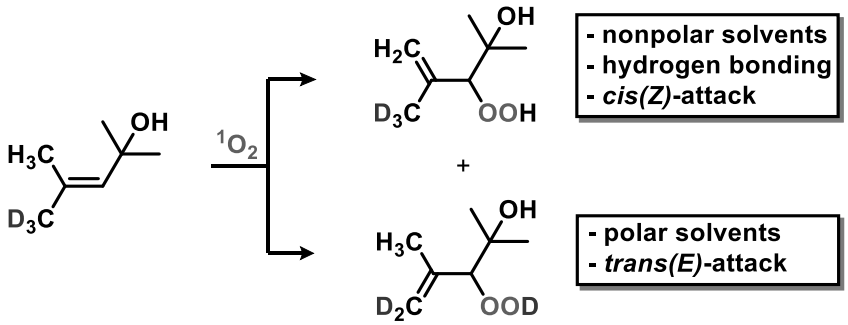

Scheme 18. Effect of solvent polarity on side selectivity and hydrogen bonding.

A detailed mechanism of photooxygenations of various chiral allylamine derivatives was provided by Adam.[28] The formation of diastereomeric perepoxide intermediates and exciplexes during the oxyfunctionalization step was proposed. The high selectivities were rationalized based on attractive or repulsive interactions between the incipient, negatively charged O atom and the respective allylic substituent. Here, stabilizing hydrogen bonding is especially important with accessible donor moieties such as OH and NH_2 (Scheme 19).

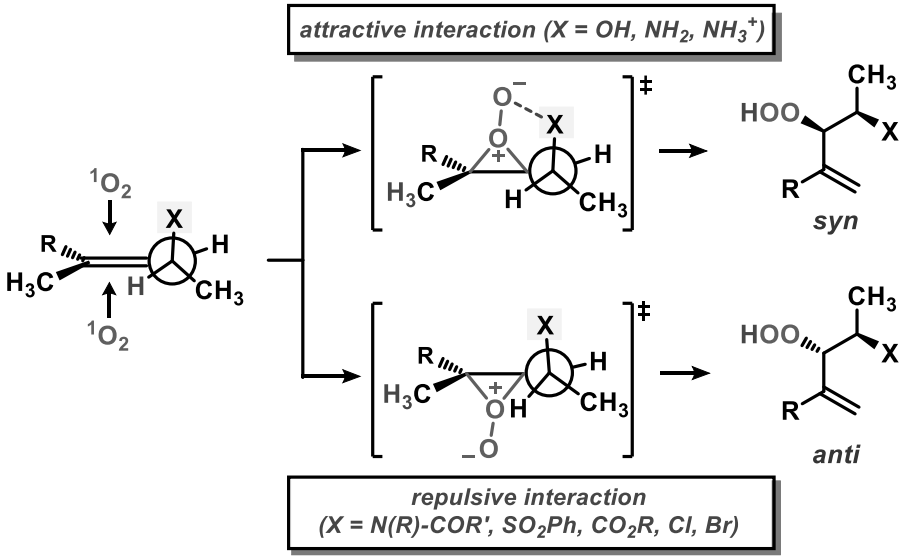

Scheme 19. Conformational bias in the diastereoselective oxidation of prenyl-X derivatives. H bonding motifs (top) afford *syn*-products; electronic repulsion of the incipient O_2 by the substituent X (bottom) leads to *anti*-hydroperoxides.

The efficacy of H bonding motifs and their solvent dependence were further studied in reactions of allylic alcohols in methanol and methanol-d_4 (Scheme 20).[56] The differences in diastereo-selectivity were not related to the rates of O_2-uptake (higher $^1O_2$ lifetimes in deuterated solvents!). In CD_3OD, the

diastereomeric ratio was lower than in methanol. This observation was rationalized by the solvent-induced deactivation of H-bonding between the allyl alcohol and $^1O_2$. The more effective OD (vs. OH) bonding provided an experimental evidence of the importance of the hydroxyl-directing effect in the perepoxide transition state.

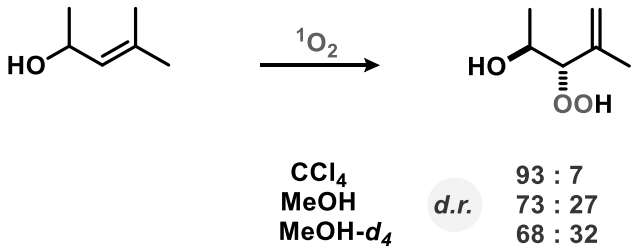

Scheme 20. Effect of polarity and solvent deuteration on stereoselectivity.

In continuation of these studies of allylalcohol oxidations, a highly useful follow-up reaction was developed. The resultant allylhydro-peroxides can be subjected to diastereoselective Ti(O^iPr)$_4$-catalyzed self-epoxidations in the absence of added peroxide reagents. This atom-economic intermolecular oxygen transfer effectively utilizes both functionalities within the product, the alkene and hydroperoxide, and constitutes a synthetically useful access route to 1,2,3,4-tetraoxy-functionalized hydrocarbon building blocks (Scheme 21).[57,58] H-bonding in the transition state was postulated to constitute the key factor that governs the observed diastereoselectivities.[59] Adam and co-workers reported the full data on the synthetic and mechanistic aspects of this useful diastereoselective $^1O_2$-ene reaction.

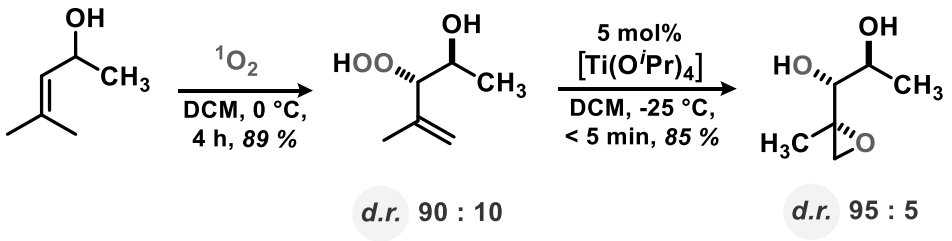

Scheme 21. Stereoselective photooxidation and intermolecular self-epoxidation.

Primary amines are effective physical quenchers of the singlet oxygen state with rates in the range of 10^{-5} M^{-1} s^{-1},[60] which is only slightly slower than the rate of $^1O_2$-ene reactions with tri-substituted alkenes (~10^{-6} M^{-1} s^{-1}).[61] The potential

competing reaction pathways of $^1O_2$ quenching and Schenck ene reactions with allylamine derivatives were firstly investigated by Adam et al. Successful photooxygenations of chiral racemic allylamines were realized in CCl_4 or CD_3OD (where $^1O_2$ lifetimes are long) with higher stereoselectivity in CCl_4 solution due to low interaction with intramolecular H bonds. Due to solubility issues, tetraphenyl-porphine (in CCl_4) and Rose Bengal (MeOH-d_4) were used as photosensitizers.[28] High diastereoselectivity in favour of the *syn*-hydroperoxide product was observed for the primary amine (Scheme 22). This stereocontrol was most likely a consequence of an unprecedented steering effect of the nucleophilic NH_2 by H-bonding with the electrophilic $^1O_2$. This is accompanied by a minimization of 1,3-allylic strain between the allylic and (*Z*)-alkenyl methyl groups. The reverse diastereoselectivity was obtained from reactions of the *N*-acetyl and *N*-phthaloyl derivatives under similar conditions. The bulky phthalimide moiety exerted steric repulsion and forced the $^1O_2$ attack to the opposite face of the alkene. These results enabled the controlled preparation of the *threo* (*syn*) or *erythro* (*anti*) diastereomers of allylic α-amino alcohols based on the *N*-substitution of the substrates.

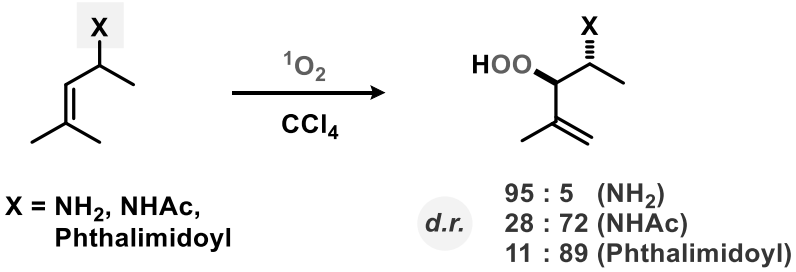

Scheme 22. Amine-directed stereoselective synthesis of allyl aminoalcohols.

▪ Chiral auxiliaries: Catalytic enamine formation

Significant efforts have been devoted to the control of diastereo-selectivities using chiral auxiliaries in $^1O_2$ ene reactions due to the fact that substrates void of allylic H-bonding donors such as hydroxyl or amino groups may not steer the incoming singlet oxygen in a diastereoselective way. Most of the reported examples involve pre-installed chiral auxiliaries, one example of a catalytic strategy via reversibly formed chiral enamine intermediates has been reported to enable the diastereoselective α-hydroxylation of carbonyl derivatives. This

reaction is of high importance as enantioselective oxidations could be achieved using amino acid derivatives (i.e. prolinol). Reductive work-up with $NaBH_4$ resulted in the formation of 1,2-diols (Scheme 23). Excellent stereoelectivities were observed with *d.r.* values of >95:5 in the photo-oxidation and *e.e.* up to 98% after work-up.[62,63]

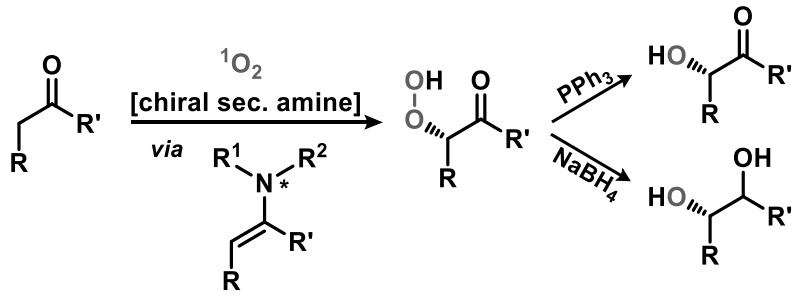

Scheme 23. Catalytic formation of enamines for selective $^1O_2$ oxidations.

▪ Chiral auxiliaries: *N*-Functionalized 2-alkenyl-oxazolidines

While auxiliaries like 2-alkenyl-*N*-acyloxazolidines gave low diastereoselectivity, the corresponding *N*-ureyloxazolidines resulted in very good diastereocontrol with *d.r.* values above 95:5 (Scheme 24).[64] These results provided compelling evidence for transition state stabilization by an attractive hydrogen bonding between the approaching $^1O_2$ enophile and the NH group of the urea function.

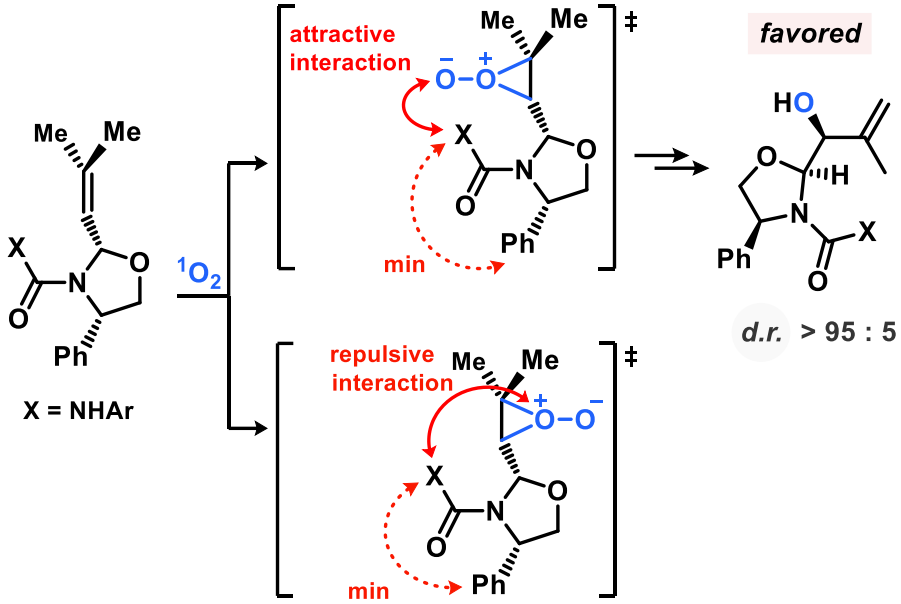

Scheme 24. Use of oxazolidines as chiral auxiliaries and favored transition geometry.

▪ Chiral auxiliaries: Oxazolidinones

The capacity of oxazolidines to act as chiral auxiliaries in Schenck ene reactions has prompted further work toward the utilization of amine-based directing groups. Adam and coworkers reported photooxygenations of ene carbamates that are equipped with a chiral oxazolidinone auxiliary. The desired ene reaction resulted in good diastereoselectivites but was accompanied by highly stereoselective [2+2] and minor [4+2] cycloadditions.[65–68] Photooxygenation of the (*E*)-styryl carbamates led preferably to the allylic hydroperoxides; the (*Z*)-isomers gave mainly the dioxetane in high diastereoselectivities. This chemoselectivity was explained by an orbital-directing effect of the ene carbamate moiety. DFT calculations showed high electron density at the vinylic N atom in the HOMO of the ene carbamate. Interaction with the LUMO of the incoming $^1O_2$ directs the attack. If no allylic H atom is present on this side of the alkene, competing [2+2] cycloaddition occurs (Scheme 25). Here, a general issue of many diastereoselective $^1O_2$-ene reactions became evident: the competition by several other (photo)oxidation pathways under the reaction conditions that lower the overall chemoselectivity.

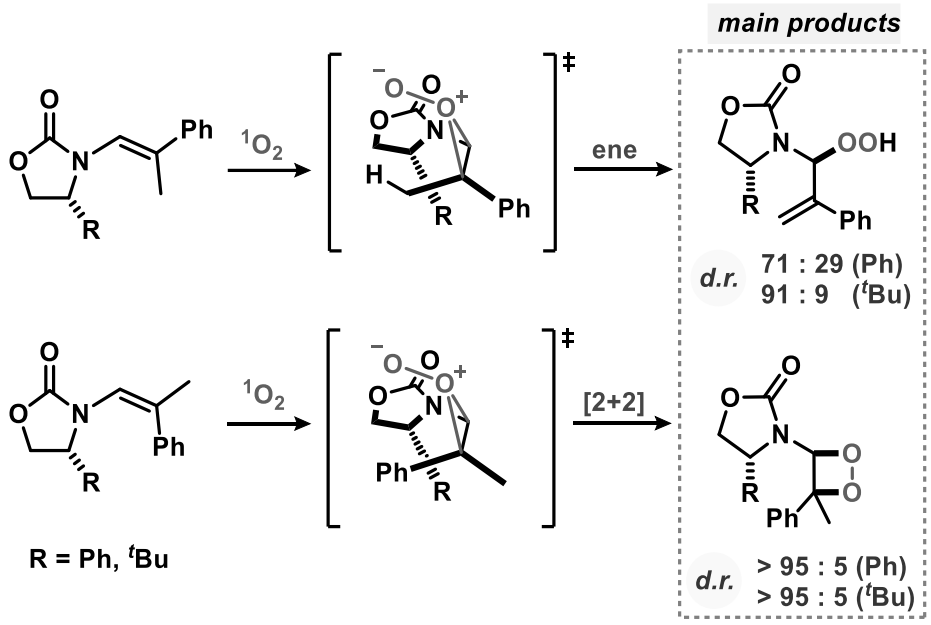

Scheme 25. Chemoselectivity through favorable orbital interactions.

Theoretical studies have provided a rationale for the origin of regioselectivity and stereoselectivity in $^1O_2$ additions to enecarba-mates.[69] The computed Gibbs free energy profiles for the reactions of (*E*) and (*Z*)-isomers showed distinct differences in the stereoelectronic properties of the diastereotopic $^1O_2$ attack. The (*E*)-enecarbamate displayed a lower-energy ene pathway (vs. dioxetane formation). The observed high stereoselectivity was a direct consequence of diastereotopic face differentiation in the rate-determining $^1O_2$ attack.

▪ Chiral auxiliaries: Oppolzer sultams

The Oppolzer bornane sultam[70,71] has been successfully implemented in diastereoselective reactions of tiglic amide derivatives.[72,73] Steric bulk at the β-acryl position led to a stronger stereochemical bias of the ground state conformer (Scheme 26), but the yield slightly eroded from 90 % (R=Me) to 78 % (R=^{i}Pr).

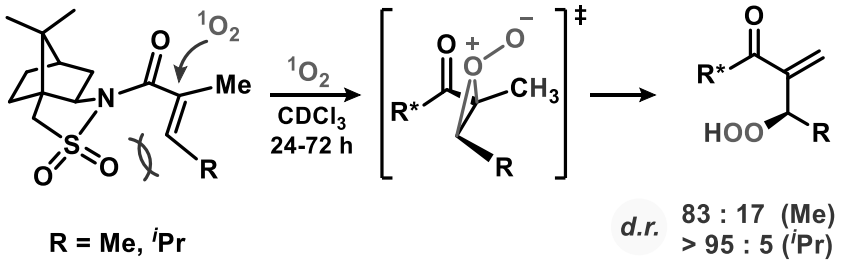

Scheme 26. Oppolzer auxiliary and favoured transition state geometry.

▪ Cycloalkenes

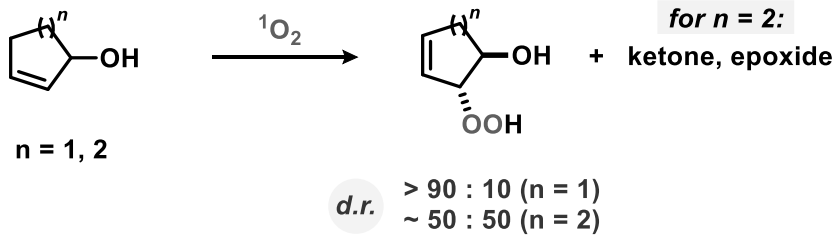

Scheme 27. Diastereoselectivity and chemoselectivity of cycloalkenol reactions.

The $^1O_2$ ene reaction constitutes a powerful oxidation method of alkenes that involves dioxygenation and allylic transposition. The reaction mechanism is highly sensitive to the steric environment of the alkene as co-planar arrangement of the alkene π-orbitals and an allylic H atom is required. The conformational bias induced by rigid cycloalkenes can enhance the population of such reactive conformers and thereby accelerate $^1O_2$ ene reactions significantly. Further key parameters that dictate reactivity and selectivity are cycloalkene ring size and substitution patterns (Scheme 27).[3]

Linker and Fröhlich studied the diastereoselectivity of photooxygenations of chiral 1,4-cyclohexadiene-3-carboxylates (Scheme 28).[74] Small 3-substituents such as methyl favoured the formation of the *trans*-product (acyl vs. OOH). This stereo-selectivity was further increased by deprotonation of the carboxylic acid which produced a repulsive interaction between the carboxylate anion and the negatively polarized O_2 terminus in the transition state. With sterically demanding alkyl substituents in 3-position, the *cis*-products were selectively formed. Modification of the carboxylic acid into an ester afforded a similar stereochemical outcome, while reduction to an alcohol moiety resulted in the

formation of the *cis*-configured products in all cases, most presumably due to H-bonding interactions with the O_2-terminus.[75] Similarly, homochiral cyclohexene ketals were stereoselectively photooxidized in good yields and high regioselectivities by the help of chiral auxiliaries.[76]

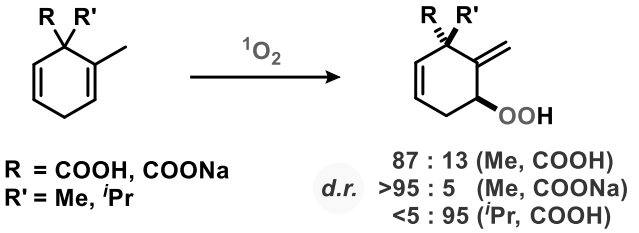

Scheme 28. Diastereoselective photooxygenations of chiral cyclohexadienes.

The chemoselectivity and stereoselectivity of 1,3-cyclohexa-dienes toward ene-type photooxygenation or [4+2]-cyclo-addition[77] with singlet oxygen was studied with a set of chiral alcohol derivatives (Scheme 29).[78] The 1-substituent at the diene had a great impact on the reaction mode. Phenyl and alkyl groups afforded mixtures of allyl hydroperoxides and cycloadducts. With the trimethylsilyl group, ene-type reactivity was exclusively operative, presumably due to steric repulsion.[79] However, the very similar diastereoselectivity observed for both reaction modes is indicative of common perepoxide intermediates that undergo either C-H bond (ene) or C=C bond attack (cycloaddition).

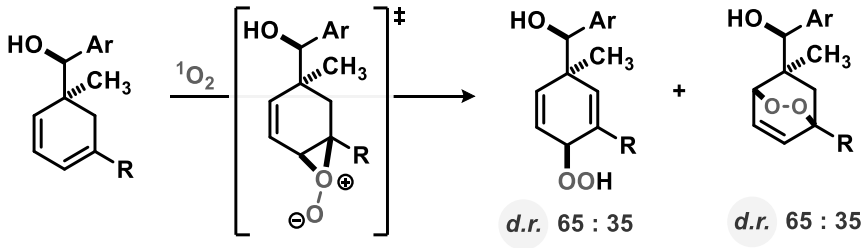

Scheme 29. Reaction modes and stereoselectivity of cyclic 1,3-dienes.

The α-cyclogeranyl skeleton (a chiral cyclohexene) was found to be a competent substrate for ene reaction with $^1O_2$.[80] Photooxygenation of several α-cyclogeranyl derivatives afforded the exocyclic allylic hydroperoxides in very high regioselectivity and moderate to good diastereoselectivity in favour of the *cis*-isomer (Scheme 30). The stereocontrol induced by the allylic substituent X was interpreted as direct consequences of conformational bias and attractive or repulsive interactions in the transition states. Conformer **A** exhibits low steric

repulsion between X and the vinyl-Me group. The remarkable product selectivity is mainly caused by the $^1O_2$ attack occurring from the less hindered face of **A** and by favorable electronic interactions of X with the perepoxide in case of X being CH_2OH or CH_2Br.

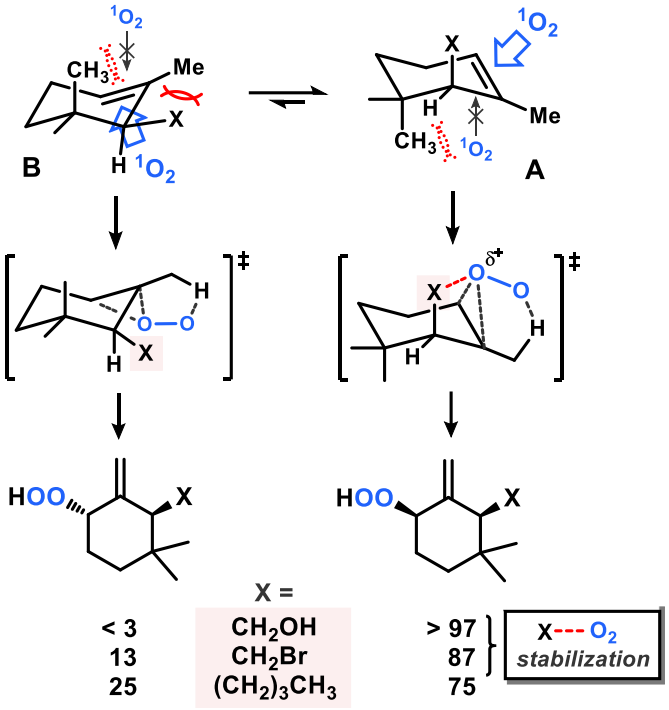

Scheme 30. Conformational control and attractive substituent interactions favour diastereoselective oxidations of cyclogeranyl derivatives.

▪ Bicyclic and polycyclic alkenes

The rigidity of oligocyclic alkenes can lead to accelerated Schenck ene reactions. The carbocyclic skeleton itself can adopt a reactive conformation with orthogonal relation between the alkene and an allylic C-H bond or it can exist in an unreactive conformation and thus prevent any reaction from the carboskeleton and instead enable CH abstraction from a peripheral alkyl substituent. α-Pinene, a methylene bridged cyclohexene, is a very competent trap of $^1O_2$. Highly regio- and stereoselective singlet oxygen ene reaction was observed by Schenck *et al.* already in 1953[81] which was further investigated by Jefford and co-workers twenty years later (Scheme 31).[82] Various stereoisomeric mixtures of α-pinene were oxidized by abstraction of an exocyclic H atom and O_2-attack *trans* to the dimethylmethylene bridge. The formation of non-ene

byproducts could be prevented by reactions in confined spaces such as vesicles ("micro-reactors") or mesoporous molecular sieves ("nano-reactors").[83,84]

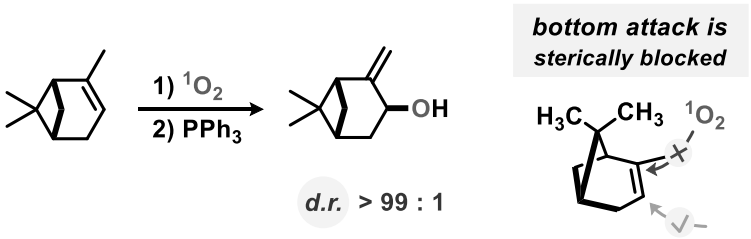

Scheme 31. Photo-oxidation of α-pinene investigated by Schenck et al.

Tricyclic propellane derivatives bearing an anhydride or imide ring cleanly afforded the corresponding *syn*-hydroperoxides (Scheme 32).[85] Secondary orbital interactions between the HOMO of $^1O_2$ (π*) and the LUMO of the carbonyls (π*) were postulated to induce the observed high stereoselectivities. Analogues void of the carbonyl groups gave equimolar *syn*/*anti* product mixtures.

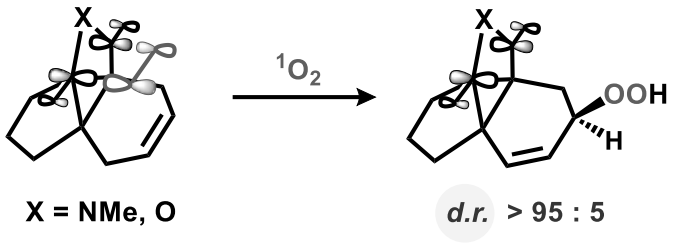

Scheme 32. Secondary π*-π* orbital interactions in $^1O_2$ oxidations of tricyclic carbonyl derivatives.

A related example of orbital-controlled stereoselectivity is the photooxygenation of alkylidene norbornenes. Houk et al. reported a synthetic and theoretical study of electrostatic effects and the interaction of point charges with the π system (Scheme 33).[86] Despite its oxidizing ability, singlet oxygen carries a high electron density on its surface due to the lone electron pairs. This results in a somewhat nucleophilic property which renders additions to alkenes to occur preferentially from the less electron-rich π-face. $^1O_2$ is therefore also called a *nucleophilic electrophile* or *transvestial electrophile*.[87] This effect is observed in the favourable *syn*-addition to the tetrafluorobenzo-anellated bicycle.[86]

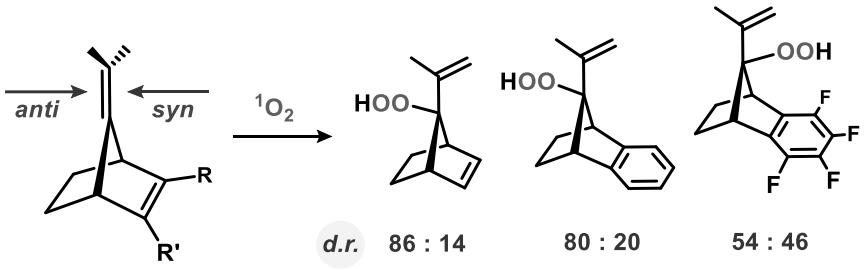

Scheme 33. *Syn* and *anti*-directing effects caused by orbital interactions.

The group of Jacobi von Wangelin has recently studied the photooxygenations of simple bicyclics obtained from Diels-Alder cycloadditions of easily available precursors. Very rapid and highly stereoselective reactions were observed under flow conditions to give access to highly versatile cyclohexene derivatives bearing 1,2-aminoalcohol, dicarbonyl, and ethylene functions (Scheme 34).[88] A concise study and computational calculations of this general reaction documented the strong conformational bias of such bicycloalkenes for endocyclic H atom abstraction which enabled full conversion within a few minutes at room temperature.

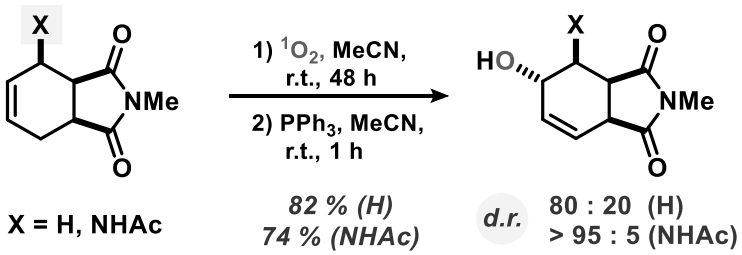

Scheme 34. Highly stereoselective photo-oxidation of tetrahydrophthalimides under flow conditions.

3 Synthesis of Natural Products and Drugs

The advent of effective protocols and the mechanistic understanding of Schenck ene reactions have prompted several applications to the synthesis of natural products and drugs.[16] The adaptation of (micro)flow conditions has enabled special selectivities and precise control of overoxidation and side product formation.[89,90] Over the past 20 years, a steadily increasing number of natural products have been synthesized including the photosensitized $^1O_2$-ene reaction as a key strategic step. The first examples include the synthesis of clavukerin C in 1991,[91] a key intermediate toward the cytotoxic clavularin A, and the naturally occurring β-aminoalcohol merucathin from 1995.[92] These early examples illustrate two general concepts of stereoinduction of such reactions. Unexpectedly high selectivity and yield was obtained in the synthesis of clavukerin C by the defined rigid geometry of the bicyclic substrate (Scheme 35A). For the synthesis of merucathin, a bulky amide function was exploited to direct the selectivity in favour of the desired diastereomer by *anti*-H abstraction (Scheme 35B). The newly formed double bond of merucathin was exclusively *E*-configured.

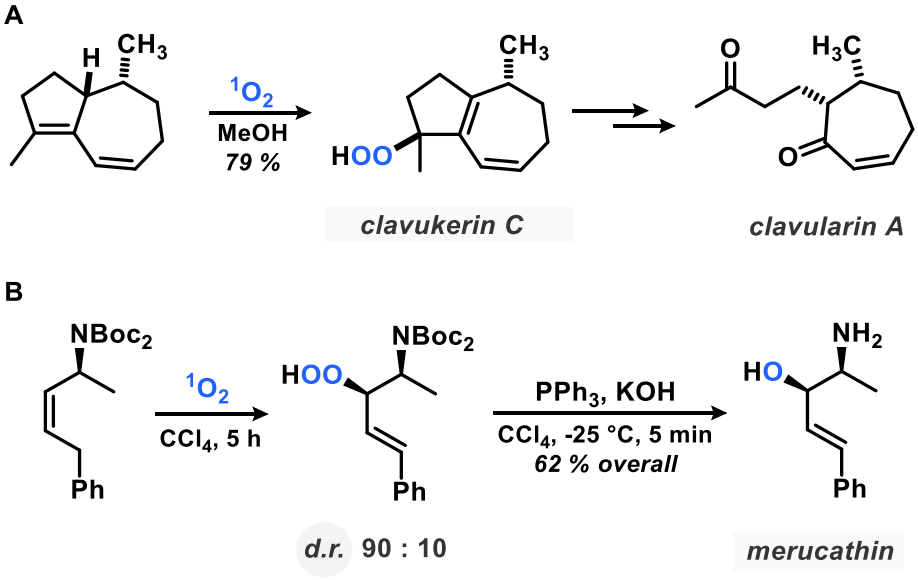

Scheme 35. Early applications of stereoselective singlet oxygen ene reactions to the synthesis of clavukerin C and merucathin.

The highly diastereoselective photooxidation of allyl alcohols by $^1O_2$ was applied to the stereoselective preparation of perketals. The mechanism involved a radical-induced 1,3-transposition of a hydroperoxyl group with stereo-retention (Scheme 36).[93]

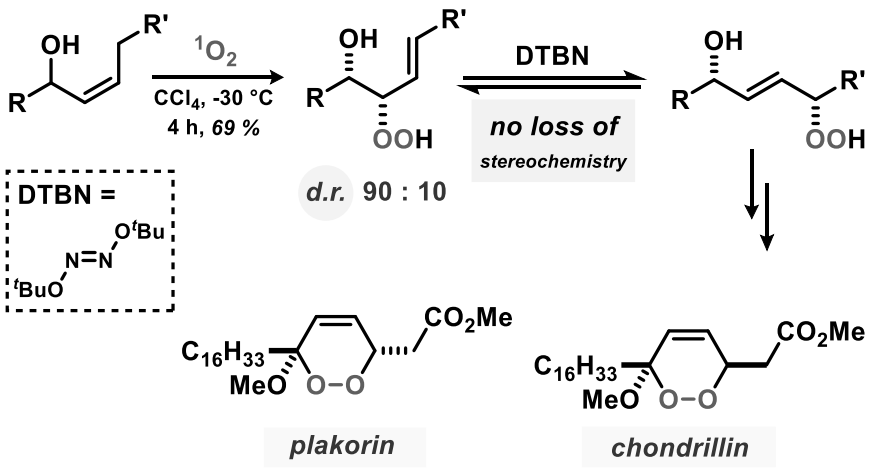

Scheme 36. Radical-induced hydroperoxide shift with stereoretention.

In 2001, Nakano *et al.* exploited the special reactivity of a twisted 1,3-diene (see scheme 15) for an oxidative synthesis of allene subunits of a large family of natural carotenoids (Scheme 37A). The diastereoselectivity of these reactions could not be precisely determined.[94] Cointeaux *et al.* prepared antimalarial peroxides starting from functionalized terpenoid substrates bearing the strongly stereo-inducing pinene motif (for this concept see scheme 31).[95] Interestingly, the photooxidation reactions involved the transfer of a trimethylsilyl group rather than an H atom as in the conventional Schenck ene reaction (Scheme 37B), a concept first reported in 1972.[96,97] A stereoselective synthesis of the biologically active heptacyclic alkaloid okaramine N enabled by singlet oxygen-mediated ring closure (see scheme 14) was reported to be operating through the facile oxidation of the indole moiety (Scheme 37C).[40]

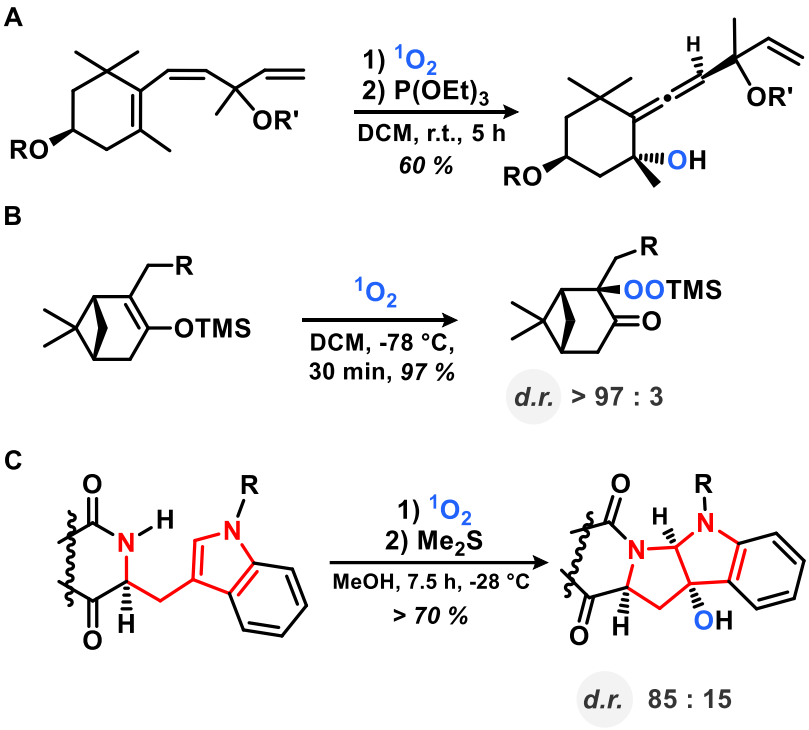

Scheme 37. Complex molecule synthesis by stereoselective $^1O_2$-mediated oxidations.

Further examples of highly effective stereoselective Schenck ene reactions in the context of complex molecule syntheses include the photo-oxidation of a cholesterol analogue toward the neuro-pharmaceutic drug withanolide A,[98] the combination of various oxidation protocols with the highly stereo-selective photo-oxidation of substituted cyclohexenes en route to carbasugars,[99] and the synthesis of the antiviral steroid glaucogenin D[100] (examples not shown). Griesbeck and coworkers investigated the synthesis of peroxo-glutathione transferase inhibitors by *syn*-selective formation of β-hydroxy-hydroperoxides with *d.r.* of 90:10 (for the underlying concept, see scheme 19).[101] The arguably most prominent and commercially most relevant application of a stereoselective $^1O_2$-ene photooxidation is the flow-assisted preparation of the antimalaria drug artemisinin which was reported by Seeberger and Levesque in 2012. The diastereo-selective Schenck ene reaction is the first step of this multi-step process and introduces a tertiary hydroperoxide motif via an *exo*-selective attack of $^1O_2$ onto the *cis*-decalin skeleton of an artemisinic acid derivative (Figure 7).[102] Further oxidative transformations include a Hock cleavage/rearrangement and enol oxidation by dioxygen.[103] The overall flow process includes five steps (with three operations each) and a variety of reaction conditions starting from the

technical product dihydroartemisinic acid and features an overall synthetic yield of 40%. This route challenges a commercialized photochemical batch production of artemisinin by Sanofi-Aventis from 2011. Utilizing a specially designed flow reactor (10,000 USD), Seeberger *et al.* calculated artemisinin to be available in improved space/time yields for roughly 20 $/kg which is less than one tenth of its market price.[104]

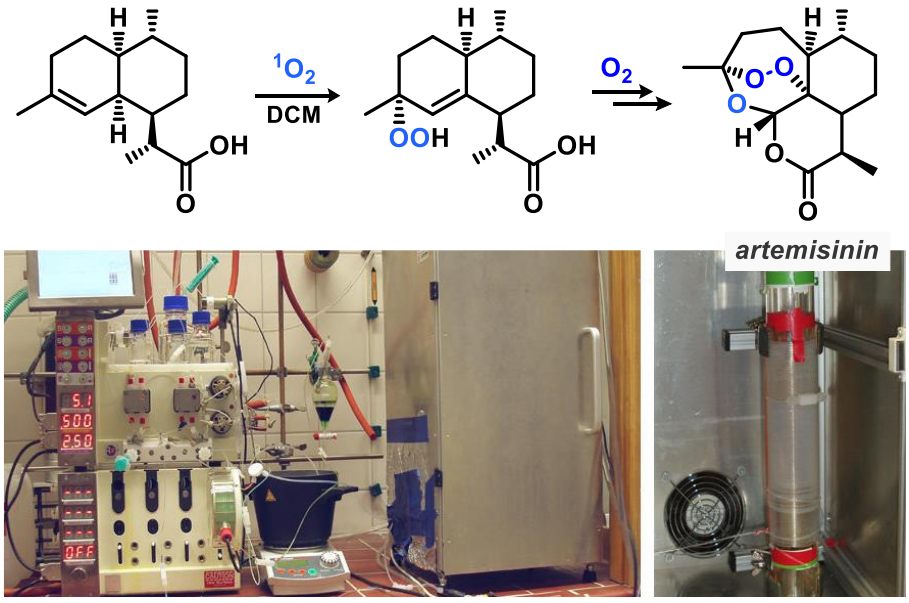

Figure 7. Flow-assisted synthesis of the antimalaria drug artemisinin.

4 Conclusion

150 years after the first report of an organic reaction with $^1O_2$ and 70 years after the discovery of the $^1O_2$-ene reaction, this allylic photooxidation has matured to a powerful transformation that enabled the straight-forward access to allyl alcohol derivatives. With several substrate classes, good levels of chemo, regio, and stereocontrol were observed and various applications to the synthesis of fine chemical building blocks and biologically active molecules were reported. Stereoselective oxygen-ene reactions were especially successful with 3-functionalized alkenes, rigid cycloalkenes, and bulky chiral auxiliaries. However, there are still some challenges to be solved. Many of the reported protocols involve the formation of several byproducts ($^1O_2$ cycloadditions, overoxidations, oxidative degradation, heteroatom oxidations) which complicate workup and isolation. The reactions mostly require expensive and toxic solvents (CCl_4, $CDCl_3$) and proceed at slow reaction rates in batch conditions. It is also important to note that many of the protocols reported herein are model studies that involve determinations of diastereoselectivities at low conversions and therefore do not mirror the conditions of synthetic setups that aim for larger scales and high yields. Conceptually, the $^1O_2$-ene reaction is a process of utmost utility in the context of sustainable synthesis: It requires some of the most abundant and inexpensive starting materials, alkenes and oxygen. An organic dye is used as a photosensitizer under irradiation by visible light. The application of flow reactors to the Schenck ene reaction has been demonstrated to dramatically enhance the efficacy of such reactions. The obvious economic and environmental benefits of visible light mediated oxidations of hydrocarbons with air or oxygen will certainly gain further momentum and ultimately lead to many applications in the bulk chemical manufacture and lab-scale syntheses of functional molecules.

5 References

[1] G. O. Schenck, Patent DE933925C, **1943**, Title: Verfahren Zur Herstellung von Pinocarveylhydroperoxyd.
[2] G. O. Schenck, *Die Naturwissenschaften* **1948**, *35*, 28–29.
[3] M. Prein, W. Adam, *Angew. Chem. Int. Ed.* **1996**, *35*, 477–494.
[4] W. Adam, K. Peters, E.-M. Peters, S. B. Schambony, *J. Am. Chem. Soc.* **2000**, *122*, 7610–7611.
[5] H. S. Dang, A. G. Davies, I. G. E. Davison, C. H. Schiesser, *J. Org. Chem.* **1990**, *55*, 1432–1438.
[6] I. A. Yaremenko, V. A. Vil', D. V. Demchuk, A. O. Terent'ev, *Beilstein J. Org. Chem.* **2016**, *12*, 1647–1748.
[7] M. Alberti, M. Orfanopoulos, *Synlett* **2010**, *2010*, 999–1026.
[8] L. M. Stephenson, M. J. Grdina, M. Orfanopoulos, *Acc. Chem. Res.* **1980**, *13*, 419–425.
[9] A. Greer, *Acc. Chem. Res.* **2006**, *39*, 797–804.
[10] S. Nonell, C. Flors, *Singlet Oxygen: Applications in Biosciences and Nanosciences (Volume 1)*, Royal Society Of Chemistry, Cambridge, **2016**.
[11] T. A. Jenny, N. J. Turro, *Tetrahedron Lett.* **1982**, *23*, 2923–2926.
[12] M. Bregnhøj, M. Westberg, F. Jensen, P. R. Ogilby, *Phys. Chem. Chem. Phys.* **2016**, *18*, 22946–22961.
[13] M. DeRosa, R. J. Crutchley, *Coord. Chem. Rev.* **2002**, *233–234*, 351–371.
[14] R. W. Redmond, J. N. Gamlin, *Photochem. Photobiol.* **1999**, *70*, 391–475.
[15] M. Fritzsche, *Comptes Rendus l'Académie des Sci. - Ser. IIC - Chem.* **1867**, *64*, 1035–1037.
[16] A. A. Ghogare, A. Greer, *Chem. Rev.* **2016**, *116*, 9994–10034.
[17] T. Montagnon, D. Kalaitzakis, M. Sofiadis, G. Vassilikogiannakis, *Org. Biomol. Chem.* **2016**, *14*, 8636–8640.
[18] L. J. Marnett, *Mutat. Res. Mol. Mech. Mutagen.* **1999**, *424*, 83–95.
[19] F. L. Muller, M. S. Lustgarten, Y. Jang, A. Richardson, H. Van Remmen, *Free Radic. Biol. Med.* **2007**, *43*, 477–503.
[20] W. A. van der Donk, A.-L. Tsai, R. J. Kulmacz, *Biochemistry* **2002**, *41*, 15451–15458.
[21] S. W. Rowlinson, B. C. Crews, C. A. Lanzo, L. J. Marnett, *J. Biol. Chem.* **1999**, *274*, 23305–23310.
[22] L. J. Marnett, S. W. Rowlinson, D. C. Goodwin, A. S. Kalgutkar, C. A. Lanzo, *J. Biol. Chem.* **1999**, *274*, 22903–22906.
[23] W. M. Horspool, F. Lenci, *CRC Handbook of Organic Photochemistry and Photobiology (Volumes 1 & 2)*, CRC Press, Boca Raton, **2003**.
[24] K. N. Houk, J. C. Williams, P. A. Mitchell, K. Yamaguchi, *J. Am. Chem. Soc.* **1981**, *103*, 949–951.
[25] M. Orfanopoulos, C. S. Foote, *Tetrahedron Lett.* **1985**, *26*, 5991–5994.
[26] E. L. Clennan, X. Chen, J. J. Koola, *J. Am. Chem. Soc.* **1990**, *112*, 5193–5199.
[27] E. L. Clennan, X. Chen, *J. Org. Chem.* **1988**, *53*, 3124–3125.
[28] W. Adam, H. G. Brünker, *J. Am. Chem. Soc.* **1993**, *115*, 3008–3009.
[29] For example, the Schenck ene reaction of prenylbenzene in the presence of (+)-pseudoephedrine inside a zeolite was reported to give up to 15% enantiomeric excess. In addition, cyclodextrin sandwiched porphyrin oxidation of linoleic acid resulted in 22% enantiomeric excess. See the following four citations for more information.
[30] Y. Kuroda, T. Sera, H. Ogoshi, *J. Am. Chem. Soc.* **1991**, *113*, 2793–2794.

[31] J. Sivaguru, T. Poon, R. Franz, S. Jockusch, W. Adam, N. J. Turro, *J. Am. Chem. Soc.* **2004**, *126*, 10816–10817.
[32] A. Joy, R. J. Robbins, K. Pitchumani, V. Ramamurthy, *Tetrahedron Lett.* **1997**, *38*, 8825–8828.
[33] A. G. Griesbeck, M. a Miranda, J. Uhlig, *Photochem. Photobiol. Sci.* **2011**, *10*, 1431–1435.
[34] M. Orfanopoulos, L. M. Stephenson, *J. Am. Chem. Soc.* **1980**, *102*, 1417–1418.
[35] M. N. Alberti, G. Vassilikogiannakis, M. Orfanopoulos, *Org. Lett.* **2008**, *10*, 3997–4000.
[36] M. Nič, J. Jirát, B. Košata, A. Jenkins, A. McNaught, in *IUPAC Compendium of Chemical Terminology*, IUPAC, Research Triagle Park, NC, **2014**, p. 2099.
[37] M. Nakagawa, S. Kato, S. Kataoka, S. Kodato, H. Watanabe, H. Okajima, T. Hino, *Chem. Pharm. Bull.* **1981**, *29*, 1013–1026.
[38] M. Nakagawa, S. Kato, H. Fukazawa, Y. Hasegawa, J. Miyazawa, T. Hino, *Tetrahedron Lett.* **1985**, *26*, 5871–5874.
[39] C. Didier, D. J. Critcher, N. D. Walshe, Y. Kojima, Y. Yamauchi, A. G. M. Barrett, *J. Org. Chem.* **2004**, *69*, 7875–7879.
[40] P. S. Baran, C. A. Guerrero, E. J. Corey, *J. Am. Chem. Soc.* **2003**, *125*, 5628–5629.
[41] H. Mori, T. Matsuo, K. Yamashita, S. Katsumura, *Tetrahedron Lett.* **1999**, *40*, 6461–6464.
[42] K. Gollnick, A. Schnatterer, *Tetrahedron Lett.* **1985**, *26*, 5029–5032.
[43] K. Gollnick, A. Griesbeck, *Tetrahedron* **1984**, *40*, 3235–3250.
[44] I. Erden, T. R. Martinez, *Tetrahedron Lett.* **1991**, *32*, 1859–1862.
[45] H. Mori, K. Ikoma, Y. Masui, S. Isoe, K. Kitaura, S. Katsumura, *Tetrahedron Lett.* **1996**, *37*, 7771–7774.
[46] P. H. Dussault, M. R. Hayden, *Tetrahedron Lett.* **1992**, *33*, 443–446.
[47] P. H. Dussault, K. R. Woller, M. C. Hillier, *Tetrahedron* **1994**, *50*, 8929–8940.
[48] M. Stratakis, D. Kalaitzakis, D. Stavroulakis, G. Kosmas, C. Tsangarakis, *Org. Lett.* **2003**, *5*, 3471–3474.
[49] A. G. Griesbeck, A. Bartoschek, J. Neudörfl, C. Miara, *Photochem. Photobiol.* **2006**, *82*, 1233.
[50] H.-G. Brünker, W. Adam, *J. Am. Chem. Soc.* **1995**, *117*, 3976–3982.
[51] W. Adam, B. Nestler, *J. Am. Chem. Soc.* **1992**, *114*, 6549–6550.
[52] S. Clayden, in *Houben-Weyl Methods of Molecular Transformations (Vol. 36)*, Thieme, Stuttgart/New York, **2008**, p. 757.
[53] W. Adam, N. Bottke, O. Krebs, I. Lykakis, M. Orfanopoulos, M. Stratakis, *J. Am. Chem. Soc.* **2002**, *124*, 14403–14409.
[54] G. Vassilikogiannakis, M. Stratakis, M. Orfanopoulos, C. S. Foote, *J. Org. Chem.* **1999**, *64*, 4130–4139.
[55] M. Stratakis, M. Orfanopoulos, C. S. Foote, *Tetrahedron Lett.* **1996**, *37*, 7159–7162.
[56] A. G. Griesbeck, W. Adam, A. Bartoschek, T. T. El-Idreesy, *Photochem. Photobiol. Sci.* **2003**, *2*, 877–881.
[57] W. Adam, B. Nestler, *Angew. Chem.* **1993**, *105*, 767–769.
[58] E. M. Elgendy, S. A. Khayyat, *Russ. J. Org. Chem.* **2008**, *44*, 823–829.
[59] W. Adam, H.-G. G. Brünker, S. Kumar, E.-M. Peters, K. Peters, U. Schneider, H. G. von Schnering, *J. Am. Chem. Soc.* **1996**, *118*, 1899–1905.
[60] D. G. James N. Pitts, George S. Hammond, Klaus Gollnick, in *Advances in Photochemistry (Volume 11)*, John Wiley & Sons, New York/Chichester/Brisbane/Toronto, **1979**, pp. 105–205.
[61] A. A. Frimer, in *Singlet O2*, CRC Press, Boca Raton, **1985**, p. 203.
[62] I. Ibrahem, G.-L. Zhao, H. Sundén, A. Córdova, *Tetrahedron Lett.* **2006**, *47*, 4659–4663.

[63] H. Sundén, M. Engqvist, J. Casas, I. Ibrahem, A. Córdova, *Angew. Chem.* **2004**, *116*, 6694–6697.
[64] W. Adam, K. Peters, E.-M. Peters, S. B. Schambony, *J. Am. Chem. Soc.* **2001**, *123*, 7228–7232.
[65] W. Adam, S. G. Bosio, N. J. Turro, *J. Am. Chem. Soc.* **2002**, *124*, 8814–8815.
[66] W. Adam, S. G. Bosio, N. J. Turro, *J. Am. Chem. Soc.* **2002**, *124*, 14004–14005.
[67] W. Adam, S. G. Bosio, N. J. Turro, B. T. Wolff, *J. Org. Chem.* **2004**, *69*, 1704–1715.
[68] J. Sivaguru, M. R. Solomon, T. Poon, S. Jockusch, S. G. Bosio, W. Adam, N. J. Turro, *Acc. Chem. Res.* **2008**, *41*, 387–400.
[69] R. Rajeev, R. B. Sunoj, *J. Org. Chem.* **2012**, *77*, 2474–2485.
[70] W. Oppolzer, G. Poli, A. J. Kingma, C. Starkemann, G. Bernardinelli, *Helv. Chim. Acta* **1987**, *70*, 2201–2214.
[71] W. Oppolzer, *Angew. Chem.* **1984**, *96*, 840–854.
[72] W. Adam, H.-G. Degen, O. Krebs, C. R. Saha-Möller, *J. Am. Chem. Soc.* **2002**, *124*, 12938–12939.
[73] W. Adam, S. G. Bosio, H. Degen, O. Krebs, D. Stalke, D. Schumacher, *Eur. J. Org. Chem.* **2002**, *2002*, 3944–3953.
[74] T. Linker, L. Fröhlich, *Angew. Chem. Int. Ed.* **1994**, *33*, 1971–1972.
[75] T. Linker, L. Fröhlich, *J. Am. Chem. Soc.* **1995**, *117*, 2694–2697.
[76] W. Fudickar, K. Vorndran, T. Linker, *Tetrahedron* **2006**, *62*, 10639–10646.
[77] W. M. Horspool, in *CRC Handbook of Organic Photochemistry and Photobiology*, CRC Press, Boca Raton, **1995**, p. 311.
[78] T. Linker, T. Krüger, W. Hess, G. Hilt, *Arkivoc* **2007**, 85–96.
[79] M. Stratakis, M. Orfanopoulos, *Tetrahedron* **2000**, *56*, 1595–1615.
[80] C. Tsangarakis, I.-P. Zaravinos, M. Stratakis, *Synlett* **2005**, 1857–1860.
[81] G. O. Schenck, H. Eggert, W. Denk, *Justus Liebigs Ann. der Chemie* **1953**, *584*, 177–198.
[82] C. W. Jefford, A. F. Boschung, R. M. Moriarty, C. G. Rimbault, M. H. Laffer, *Helv. Chim. Acta* **1973**, *56*, 2649–2659.
[83] E. L. Clennan, A. Pace, *Tetrahedron* **2005**, *61*, 6665–6691.
[84] D. V Avila, A. G. Davies, I. G. E. Davison, *J. Chem. Soc. Perkin Trans. 2* **1988**, 1847–1852.
[85] I. Landheer, D. Ginsburg, *Tetrahedron* **1981**, *37*, 143–150.
[86] Y. D. Wu, Y. Li, J. Na, K. N. Houk, *J. Org. Chem.* **1993**, *58*, 4625–4628.
[87] A. R. Chamberlin, R. L. Mulholland, S. D. Kahn, W. J. Hehre, *J. Am. Chem. Soc.* **1987**, *109*, 672–677.
[88] J. Schachtner, M. Majek, R. Fichtler, R. Perez-Ruiz, J. Regensburger, M. Wegmann, W. Bäumler, T. Bach, A. Jacobi von Wangelin, *unpublished results* **2016**.
[89] B. D. A. Hook, W. Dohle, P. R. Hirst, M. Pickworth, M. B. Berry, K. I. Booker-Milburn, *J. Org. Chem.* **2005**, *70*, 7558–7564.
[90] J. Schachtner, P. Bayer, A. Jacobi von Wangelin, *Beilstein J. Org. Chem.* **2016**, *12*, 1798–1811.
[91] S. K. Kim, C. S. Pak, *J. Org. Chem.* **1991**, *56*, 6829–6832.
[92] W. Adam, H. G. Brünker, *Synthesis* **1995**, *1995*, 1066–1068.
[93] P. H. Dussault, C. T. Eary, K. R. Woller, *J. Org. Chem.* **1999**, *64*, 1789–1797.
[94] M. Nakano, N. Furuichi, H. Mori, S. Katsumura, *Tetrahedron Lett.* **2001**, *42*, 7307–7310.
[95] L. Cointeaux, J.-F. Berrien, J. Mahuteau, M. . Trân Huu-Dâu, L. Cicéron, M. Danis, J. Mayrargue, *Bioorg. Med. Chem.* **2003**, *11*, 3791–3794.
[96] G. M. Rubottom, M. I. Lopez Nieves, *Tetrahedron Lett.* **1972**, *13*, 2423–2425.
[97] E. Friedrich, W. Lutz, *Chem. Ber.* **1980**, *113*, 1245–1263.
[98] C. K. Jana, J. Hoecker, T. M. Woods, H. J. Jessen, M. Neuburger, K. Gademann, *Angew. Chem. Int. Ed.* **2011**, *50*, 8407–8411.

[99] N. Horasan Kishali, D. Doğan, E. Şahin, A. Gunel, Y. Kara, M. Balci, *Tetrahedron* **2011**, *67*, 1193–1200.
[100] J. Gui, H. Tian, W. Tian, *Org. Lett.* **2013**, *15*, 4802–4805.
[101] A. G. Griesbeck, A. Maaßen, M. Bräutigam, M. Pietsch, *Eur. J. Org. Chem.* **2015**, *2015*, 4349–4352.
[102] F. Lévesque, P. H. Seeberger, *Angew. Chem. Int. Ed.* **2012**, *51*, 1706–1709.
[103] L.-K. Sy, G. D. Brown, *Tetrahedron* **2002**, *58*, 897–908.
[104] D. Kopetzki, F. Lévesque, P. H. Seeberger, *Chem. - A Eur. J.* **2013**, *19*, 5450–5456.

III Mechanism of Arylcyclohexene Oxygenation

published with minor modifications as

"Visible Light-Mediated Photo-Oxygenation of Arylcyclohexenes"

in *Org. Chem. Front.* **2019**, *6*, 2877–2883.

50% of the experimental results (esp. Table 1, Figure 8) are part of the Master Thesis "Investigations into the Photooxygenation of 1-Phenyl-1-Cyclohexenes under Continuous Flow Conditions" by Patrick Bayer.

Author contributions:

Patrick Bayer wrote the final manuscript and performed most reactions.
Josef Schachtner assisted in early-stage manuscript and reactions.
Michal Májek performed the quantum-chemical calculations.
The work was supervised by Prof. Dr. Axel Jacobi von Wangelin.

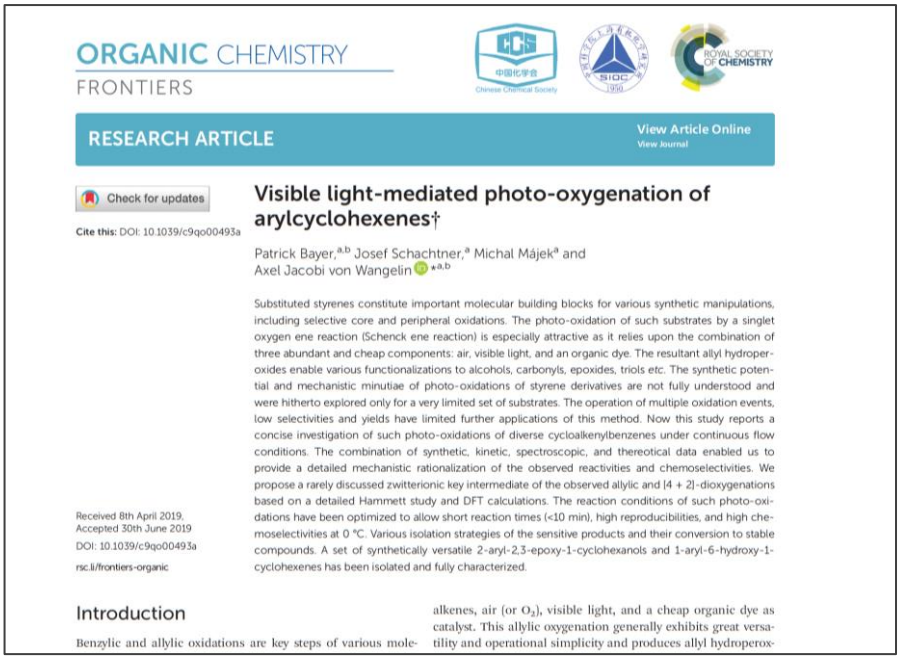

ORGANIC CHEMISTRY FRONTIERS

RESEARCH ARTICLE

View Article Online
View Journal

Check for updates

Cite this: DOI: 10.1039/c9qo00493a

Visible light-mediated photo-oxygenation of arylcyclohexenes†

Patrick Bayer,[a,b] Josef Schachtner,[a] Michal Májek[a] and Axel Jacobi von Wangelin[a,b]*

Substituted styrenes constitute important molecular building blocks for various synthetic manipulations, including selective core and peripheral oxidations. The photo-oxidation of such substrates by a singlet oxygen ene reaction (Schenck ene reaction) is especially attractive as it relies upon the combination of three abundant and cheap components: air, visible light, and an organic dye. The resultant allyl hydroperoxides enable various functionalizations to alcohols, carbonyls, epoxides, triols *etc.* The synthetic potential and mechanistic minutiae of photo-oxidations of styrene derivatives are not fully understood and were hitherto explored only for a very limited set of substrates. The operation of multiple oxidation events, low selectivities and yields have limited further applications of this method. Now this study reports a concise investigation of such photo-oxidations of diverse cycloalkenylbenzenes under continuous flow conditions. The combination of synthetic, kinetic, spectroscopic, and thereotical data enabled us to provide a detailed mechanistic rationalization of the observed reactivities and chemoselectivities. We propose a rarely discussed zwitterionic key intermediate of the observed allylic and [4 + 2]-dioxygenations based on a detailed Hammett study and DFT calculations. The reaction conditions of such photo-oxidations have been optimized to allow short reaction times (<10 min), high reproducibilities, and high chemoselectivities at 0 °C. Various isolation strategies of the sensitive products and their conversion to stable compounds. A set of synthetically versatile 2-aryl-2,3-epoxy-1-cyclohexanols and 1-aryl-6-hydroxy-1-cyclohexenes has been isolated and fully characterized.

Received 8th April 2019,
Accepted 30th June 2019
DOI: 10.1039/c9qo00493a
rsc.li/frontiers-organic

Introduction

Benzylic and allylic oxidations are key steps of various molecules, air (or O_2), visible light, and a cheap organic dye as catalyst. This allylic oxygenation generally exhibits great versatility and operational simplicity and produces allyl hydroperox-

Reproduced with permission from the Chinese Chemical Society (CCS), Shanghai Institute of Organic Chemistry (SIOC), and the Royal Society of Chemistry.

1 Introduction

Substituted styrenes constitute important molecular building blocks for various synthetic manipulations including selective core and peripheral oxidations. The photooxygenation of such substrates by a singlet oxygen ene reaction is especially attractive as it relies upon the combination of three abundant and cheap components: air, visible light, and an organic dye. The resultant allyl hydroperoxides enable various functionalizations to alcohols, carbonyls, epoxides, triols etc. This study reports a concise investigation of such photo-oxidations of diverse cycloalkenylbenzenes under continuous flow conditions. We propose a rarely discussed zwitterionic key intermediate of the observed allylic and [4+2]-dioxygenations based on a detailed Hammett study and DFT calculations.

Benzylic and allylic oxidations are key steps of various molecular functionalizations, valorizations, and degradations in industrial and biological processes.[1–3] The majority of available synthetic methods involve metal complexes and/or special stoichiometric oxidants (peracids, H_2O_2).[4–6] Contrary to that, the use of the most abundant oxidant air (or dioxygen O_2) in combination with a metal-free sensitizer and visible light constitutes an especially desirable inexpensive and sustainable way of performing hydrocarbon oxidations.[7] Unlike biological oxidations with triplet oxygen $^3O_2$, such photo-oxidations involve the generation of singlet oxygen $^1O_2$, operate via closed-shell intermediates, and often exhibit high levels of regiocontrol. The Schenck-ene reaction is a prime example of a sustainable CH-oxidation method that relies on the combination of highly abundant components: simple unbiased alkenes, air (or O_2), visible light, and a cheap organic dye as catalyst. This allylic oxygenation generally exhibits great versatility and operational simplicity and produces allyl hydroperoxides as highly reactive building block molecules. Reaction rates and selectivities (chemo, regio, stereo) are highly dependent on substitution patterns and conformations of the hydrocarbon substrates. In the past decades, most research activities have been devoted to photo-oxidations of electron-rich acyclic alkenes that often bear hetero-atomic functional groups or directing groups. Interestingly, the abundantly available cyclohexene derivatives are an especially unreactive class of

substrates for CH-oxidations, which is mostly a direct consequence of unfavourable chair-like conformations in the transition states (Scheme 38).[8]

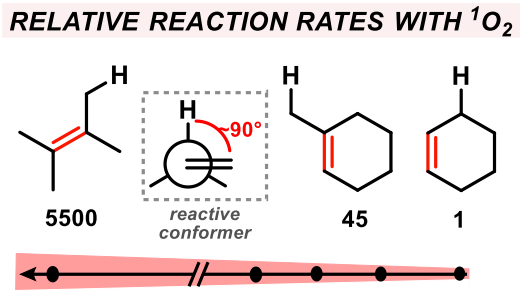

Scheme 38. Relative reaction rates of $^1O_2$ with various alkenes.

We report the first concise study of the photo-oxidation of arylcyclohexenes with a series of 14 functionalized 1-aryl-1-cyclohexenes under optimized Schenck-ene conditions. The products were isolated and characterized and a concise mechanistic study (by-products, kinetics, NMR, DFT) was performed (Scheme 39).

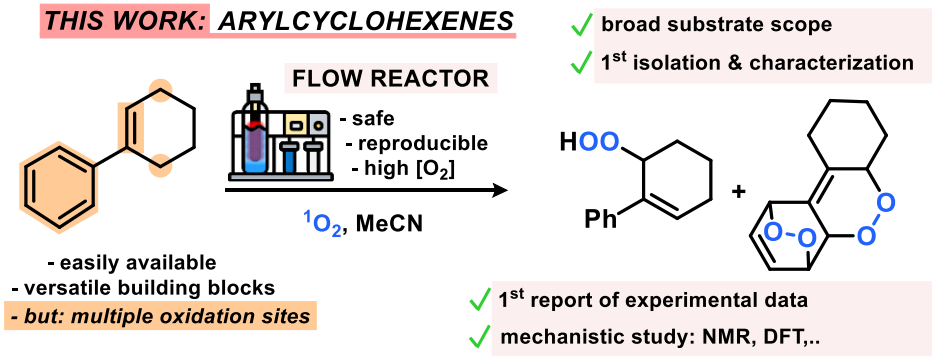

Scheme 39. Novel investigations on arylcyclohexenes covered in the subsequent sections.

2 Results and Discussion

The mechanism of the Schenck ene reaction is strongly depending on the stereoelectronic properties of the substrate, directing group effects, solvent polarity and proticity. For most reactions, a per-epoxide intermediate has been postulated as key intermediate which converts to a transition state that adopts an orthogonal orientation of the abstracting allylic H-atom and the evolving alkene plane.[9–12] Our group has recently investigated the use of strained bicyclic alkenes for enhanced Schenck ene reactions,[13] others have exploited confinement effects to access reactive conformations.[14] We surmised that introduction of an aryl substituent in 1-position of cyclohexenes would result in a considerable stereoelectronic modulation of the ground state and transition state conformations which ultimately affect the rate of photo-oxidation. On the other hand, the presence of aryl substituents in cyclohexenes may enable competitive arene, alkene, and CH-oxidations under similar conditions and thereby result in the formation of complex reaction mixtures.[15]

We initially probed the reactivity of the model substrate 1-phenyl-1-cyclohexene (**1**) under the photo-oxidation conditions of the Schenck ene reaction in acetonitrile with 1 mol% methylene blue as sensitizer and pressurized O_2.[16] We have applied and optimized a self-made continuous-flow microreactor.[13] Such reactor setups exhibit several advantages over batch reactions which enabled highly reproducible reactions,[7] such as effective temperature control, excellent absorbance characteristics and energy efficiency using high power LEDs,[17] a thin capillary for short reaction times, and high operational safety with regard to the formation of hazardous peroxides.[18]

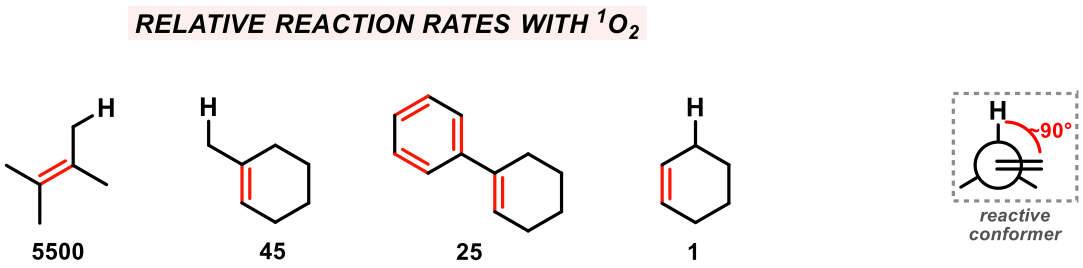

Scheme 40. Determined relative reaction rate for 1-phenyl-1-cyclohexene in our MR.

We observed a strong rate enhancement of the reaction of 1-phenyl-1-cyclohexene (**1**) vs. cyclohexene (Scheme 40) which is in full accord with our hypothesis that introduction of the phenyl moiety (in conjugated position, resulting in (slight) steric repulsion from the *ortho*-CH) directly affects the transition state conformations.[19] However, arylcyclohexenes such as **1** are a highly challenging class of substrates due to the presence of multiple oxidation-sensitive sites which can lead to various oxidation products in reactions with $^1O_2$. Besides allylic oxidation to allyl hydroperoxides, the same conditions could induce [4+2]-cycloaddition to endoperoxides or [2+2]-cycloaddition with following 1,6-dicarbonyl formation.[20,21] With our standard conditions (50 sec irradiation in flow reactor, red LEDs, 30 bar O_2, 0 °C, 0.1 M **1** in MeCN, 1 mol% methylene blue), we observed the formation of two main products: the major O_2-ene product 6-hydroperoxy-1-phenyl-1-cyclohexene (**2**) and the double [4+2]-cycloadduct (**3**). Three minor products were isolated: 6-oxo-6-phenylhexanal (**4**), the other $^1O_2$-ene regioisomer **5**, and after reductive workup with triphenylphosphine (PPh_3) the 1,2-diol derivative **6** (*anti*/*syn* = 4/1). In contrast to the few reported photooxygenations of open-chain styrenes,[21–23] reactions of arylcycloalkenes in this study did not form isolable mono-[4+2]-cycloadducts (Scheme 41).[24]

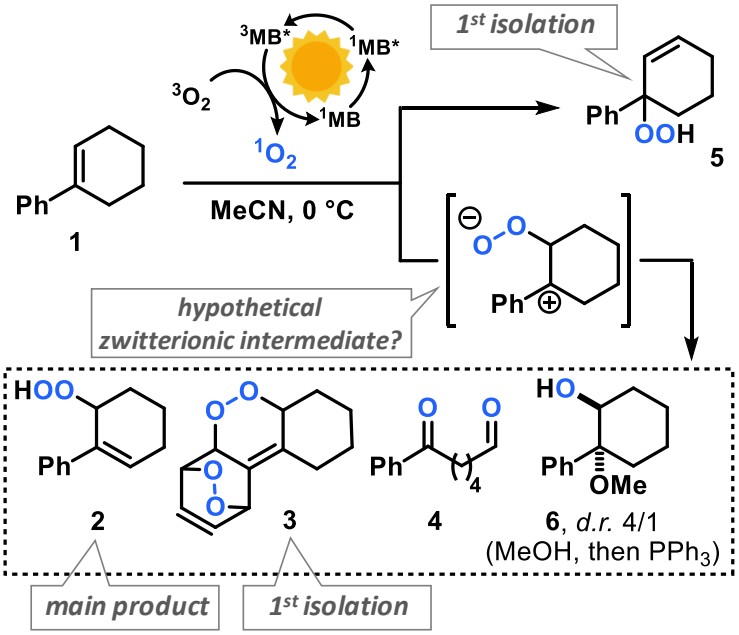

Scheme 41. Isolated products of the photooxygenation of phenylcyclohexene **1**.

Our observations are remarkable in that they significantly expand the knowledge of photooxygenation pathways and product distributions of this family of easily available and synthetically versatile arylcyclohexenes. The desired allyl hydroperoxide **2** indeed was the major product under our photo-oxidation conditions. This is in stark contrast to earlier work by Foote et al. who observed only trace amounts of O_2-ene products from the related styrene derivative *trans*-anethole using tetra-phenylporphyrin (TPP) as sensitizer and a high-power Xe lamp.[21] Furthermore, the formation of the second O_2-ene regioisomer, the tertiary allyl hydroperoxide **5**, has yet not been reported.[25] The postulated intermediacy of a peroxy zwitterion would suggest a strong dependence on the proticity of the solvent and the interception of the carbocation by competent nucleophiles.[21,26,27] Both hypotheses were experimentally substantiated: The change from acetonitrile to methanol resulted in the increased formation of desired allyl hydroperoxide **2** at total conversion (MeCN: **2**/**3** = 2.1; MeOH: **2**/**3** = 5.0; *vide infra*). The formation of the 1,2-dioxy derivative **6** in MeOH is indicative of a carbocation intermediate which underwent nucleophilic attack by MeOH followed by reduction with PPh_3.[26–28]

We then set out to explore the substrate scope of this photooxygenation and establish structure-activity relationships. The variation of the aryl substitution pattern in a Hammett study would directly address the nature of the reactive intermediate of the photooxygenation reaction. The postulated zwitterion bearing a carbocation in benzylic position would be subject to effective charge stabilization by donor substituents at the arene.[29]

▪ Mechanistic studies

A preliminary mechanistic discussion of the photooxygenation of *trans*-anethole by Foote and coworkers involved the potential intermediacy of a zwitterion containing a benzyl cation. Peroxy-anion addition to the electrophilic *ortho*-arene position could account for the observed endoperoxide formation which was largely suppressed in the presence of protic solvents or acidic additives.[21] In an effort to explore the mechanistic minutiae of the photooxygenation of 1-aryl-1-cyclohexenes, we performed a concise Hammett

study that generally considers electric field effects, polarizabilities, inductive and resonance contributions within the characteristic substituent constants σ.[30–33] We prepared a set of 14 *meta*- and *para*-substituted 1-aryl-1-cyclohexenes and subjected them to photooxygenation under standard conditions (Table 1, Figure 8). Consistent with our hypotheses, the overall reaction rates exhibited a strong linear correlation with the electronic properties of the aryl substituents (σ_{meta}, σ_{para}).

Table 1. Hammett data of photo-oxidations of *m*- and *p*-substituted arylcyclohexenes.

Entry	Substituent	σ_m	σ_p	Conversion [%] [a]	AHP/EPO [b]
1	- CN		0.66	18	8.3
2	- CN	0.56		34	*n.d.*
3	- CF_3		0.54	16	6.4
4	- Br	0.39		45	*n.d.*
5	- OCF_3		0.35	34	4.8
6	- Cl		0.23	55	3.3
7	- OMe	0.12		52	*n.d.*
8	- F		0.06	47	2.5
9	- H		0.00	57	2.2
10	- Ph [c]		- 0.01	48	2.3
11	- Me		- 0.17	61	2.2
12	- ^{t}Bu		- 0.20	65	2.1
13	- OMe		- 0.27	72	2.7
14	- NMe_2		- 0.83	*0*	*n.d.*

Hammett constants are given for *meta*-(σ_m) and *para*-substituents (σ_p).[31] Conditions: 50 sec irradiation in the flow reactor with red LEDs, O_2 (~30 bar), 0 °C, c(MB) = 1 mM, c(substrate) = 0.1 M. [a] Conversion was determined by GC-FID. [b] Ratio of allyl hydroperoxide (AHP) / endoperoxide (EPO) was determined by ^{1}H-NMR of the crude reactions. Product ratios could not be determined (*n.d.*) for *meta*-substituted substrates. [c] MeCN/toluene (1:1) was used for solubility issues.

Electron donors gave faster conversions, with the 4-methoxy derivative reaching 72% conversion within 50 sec irradiation in the flow reactor (entry 13). 1-(4-

Trifluoromethylphenyl)-1-cyclohexene was the least reactive substrate (16% conversion, entry 3). These observations argue in favour of the formation of an intermediate benzyl cation as rate-determining step. The experimental results were complemented with theoretical studies (PCM solvation model, MeCN; B3LYP 6-311++G(2d,p)) which clearly documented the stabilization of the postulated zwitterion by 3.3 kcal/mol for the 4-methoxy derivative (vs. the parent substrate **1**) and destabilization by 2.2 kcal/mol for the 4-trifluoromethyl derivative (vs. **1**). Photooxygenation of the 4-(*N*,*N*-dimethylamino) derivative resulted in complete inhibition, most likely as a consequence of effective physical quenching of $^1O_2$ by the amine (entry 14).[34]

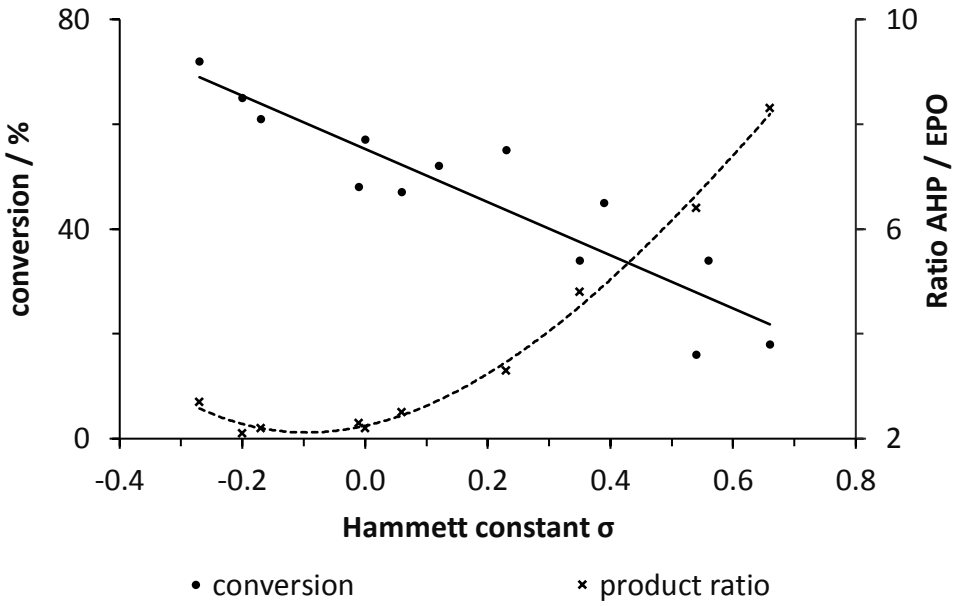

Figure 8. Relation between alkene conversion, product ratios (allyl hydroperoxide, AHP; endoperoxide, EPO), and Hammett substituent constants σ. See Table 1.

The trend line of conversion vs. σ inhabited the (pseudo)halogen substituents F, Cl, Br, CN as outliers (see half-black dots in Figure 8) which are known to often deviate from standard Hammett trends.[35–37] The R^2 value of trend line accuracy improves from 0.84 to 0.96 when eliminating the data points of *m*-Br, *p*-Cl, *p*-F, and *m*-CN. The chemoselectivity of the reaction was also strongly depending on the aryl substituents (Table 1, Figure 8). The ratios of the two main primary oxidation products, the allyl hydroperoxide (AHP) and the endoperoxide (EPO), AHP/EPO increased with strongly electron-withdrawing *para*-substituents (large

σ_p values, *e.g.* CN, CF_3, OCF_3). The formation of different regioisomers and stereoisomers of the endoperoxides from *meta*-substituted aryl-cyclohexenes prohibited a reliable product analysis so that no product ratios are given. The Hammett plot minimum for weakly electron-donating substituents without mesomeric stabilization (H, Me, *t*Bu; entries 9, 11, 12 in Table 1) might indicate a change of reaction mechanism (Figure 8).[33]

Based on few literature precedents and our experimental and theoretical studies,[22-24] we propose a reaction mechanism that involves a charge-separated zwitterion with benzyl cation character as key intermediate (Scheme 42). The Mulliken charges and stabilities of three zwitterions with different *para*-aryl substituents (OMe, H, CF_3) were calculated by DFT (B3LYP, 6-311+G(d,p), Scheme 42, top).

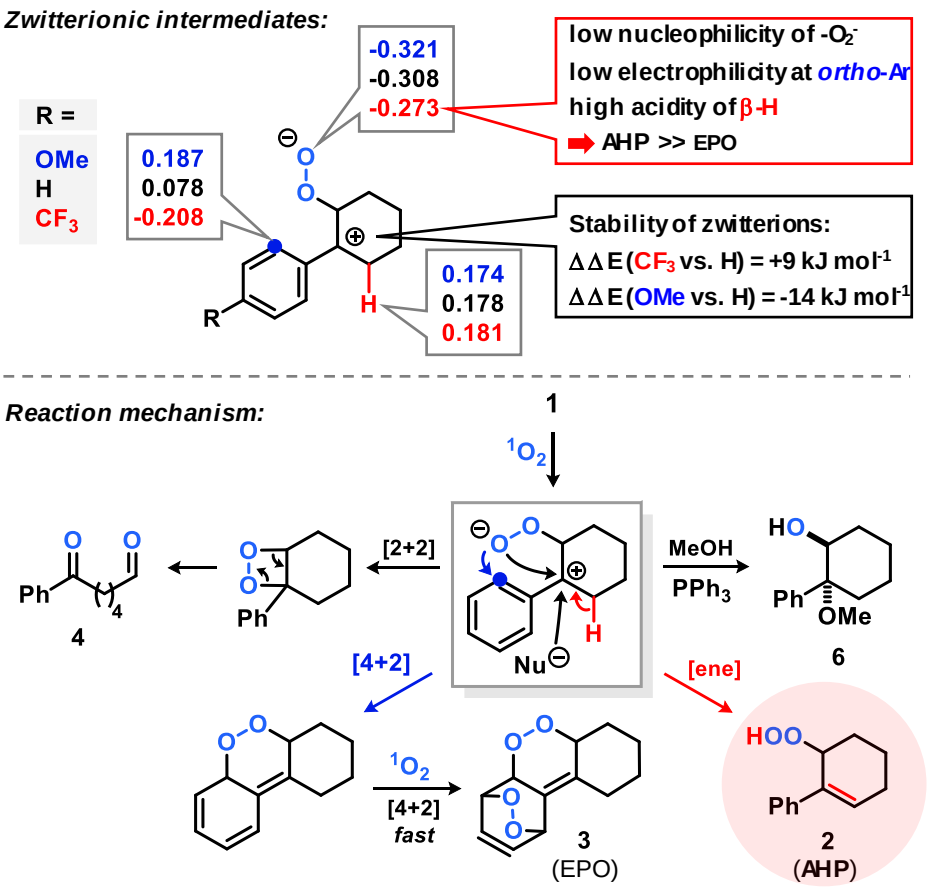

Scheme 42. Top: Proposed zwitterionic intermediate with calculated Mulliken charges at reactive O, C, and H-sites and thermodynamic stabilities. Bottom: Postulated mechanism of the photooxygenation of arylcyclohexenes.

These theoretical data support the notion of competing allyl hydroperoxide (AHP) and endoperoxide (EPO) formation. The introduction of a 4-methoxy substituent results in strong stabilization of the zwitterion (-14 kJ/mol vs. 4-H-substitution), lower acidity of the β-proton, higher nucleophilicity of the peroxy anion, and higher electrophilicity of the *ortho*-aryl position. These conditions should enhance the formation of the endoperoxide which is in full accord with the experiments (AHP/EPO 2.7, Table 1). With the 4-trifluoro-methyl group, allyl hydroperoxide formation is much more favoured due to the destabilization of the intermediate benzyl cation (+9 kJ/mol vs. 4-H), higher acidity of the β-H, lower nucleophilicity of the peroxy anion, and lower electrophilicity at the *ortho*-aryl position (experiment: AHP/EPO 6.4, Table 1). As the zwitterion formation is the rate-determining step, the conversions of electron-deficient arylcyclohexenes are low (Table 1, Figure 8).

▪ Synthesis, isolation and conversion of primary products

The optimization of the continuous-flow photo-oxidation revealed that reactions at 0°C provided the best compromise between reaction time and selectivity toward the allyl hydroperoxide (AHP), whereas the temperature did not have a significant impact on the ratio AHP/EPO. However, the sensitizer methylene blue could undergo oxidative decomposition if reaction times are long.[38] The ratio of the two $^1O_2$-ene regioisomers (from phenylcyclohexene: **2** and **5**, see Scheme 42) was 7/1 and nearly constant over the whole set of different *meta*- and *para*-substituted substrates and different conditions. Importantly, the regioselectivity of the $^1O_2$-ene reactions was much higher with *ortho*-substituted arylcyclo-hexenes as <3% of the *tert*-hydro-peroxide isomers formed. This cannot be explained by electronic effects whereas steric hindrance around the benzylic carbon prevents $^1O_2$ attack. On preparative scales, the formation of further oxidation products in minor quantities (such as **4** and **5**) hamper the isolation of pure compounds. NMR monitoring studies with (1-(4-chlorophenyl)-1-cyclohexene documented the generally low reaction selectivity by formation of further oxidation products beside the major products **AHP** (and regioisomer) and **EPO** (Figure 10).

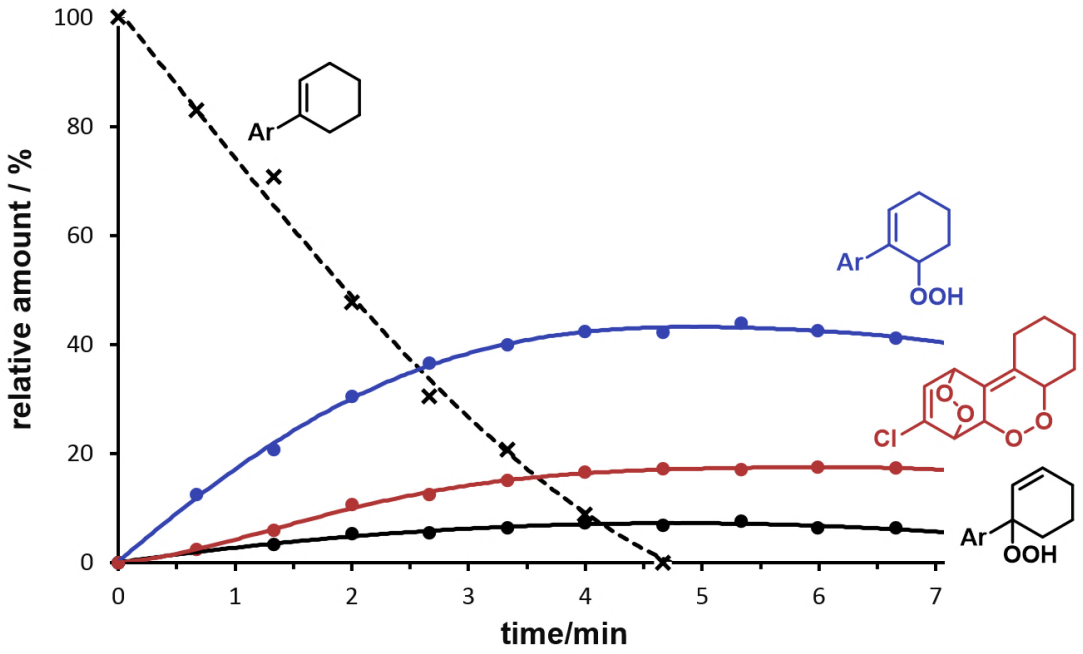

Figure 9. Conversion and major products of the photooxygenation of 4-chloro-1-phenyl-1-cyclohexene from ^{1}H NMR monitoring (Ar = 4-chlorophenyl).

^{1}H resonances at 10-12 ppm might stem from further double bond oxidation, hydroperoxide degradation or polymerization. It is important to note that – unlike earlier reports – the endoperoxide appeared to be stable under the reaction conditions.[39] We probed various isolation and derivatization strategies for preparative scales reactions. The rather non-polar starting materials could be easily separated from the products by SiO_2 gel flash chromatography. However, the several oxidation products were difficult to separate from each other. SiO_2 chromatography resulted in significant losses of materials to give only moderate to low isolated yields of reactions that exhibited good NMR yields. The bulkier *ortho*-substituted arylcyclohexenes underwent more selective photooxygenations and resulted in more stable products so that chromatographic isolations were effective.

Most isolated allyl hydroperoxides and endoperoxides could be stored for days to months in a freezer and only slowly decomposed due to the low dissociation energy of the O-O bond.[40,41] An alternative strategy to the isolation of the labile peroxo products is their derivatization to more stable secondary products. We have mostly applied reductions of the allyl hydroperoxides with by triphenylphosphine to give the corresponding allylic alcohols.[42] PPh_3 is also known to reduce endoperoxides to highly polar polyols[43] which can easily be

separated. Table 2 displays a selection of isolated allyl hydroperoxides and their reduced allyl alcohol derivatives:

Table 2. Photooxygenation products and their subsequent reduction with PPh_3.

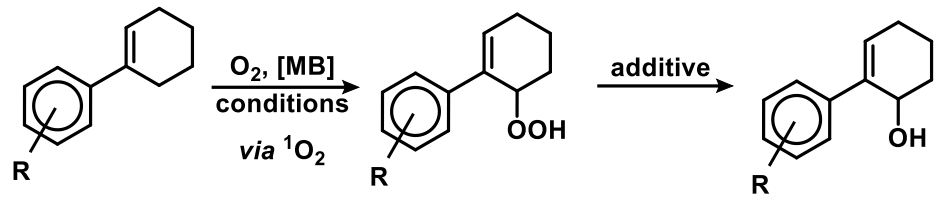

Entry	R	Conversion [%]	Yield [%]	Additive[a]	Yield [%]
1	-	100	39[b]	PPh_3	33[d]
2	2-Ph	100	63[c]	-	
3	4-Cl	100	n.d.	PPh_3	31[d]
4	2-Me	90	31	-	
5	4-CN	90	n.d.	PPh_3	39

Conditions: 8 min irradiation in the flow reactor with red LEDs, O_2 (30 bar), MeCN, 0 °C, 1 mol% methylene blue (MB). [a] Addition of 1 equiv. PPh_3 without prior work-up. [b] Determined by ^{1}H-NMR. [c] 12 min of irradiation; 85% conversion, 48% yield. [d] 5% of the regioisomeric O_2-ene-derived allyl alcohol was formed.

We have then applied the general photooxygenation conditions to the ring size homologues 1-phenyl-1-cyclopentene (**7**) and 1-phenyl-1-cyclo-heptene (**8**). Both substrates showed much higher conversions than **1** and near-perfect AHP selectivities in combination with clean NMR spectra showing little side product formation (Figure 10). After 50 s in the flow reactor, quantitative conversions were observed and the exclusive formation of the desired Schenck-ene products (with isolated yields of 43% and 65%, respectively). These results manifest the facile thermal accessibility of reactive conformations of cyclopentenes and cycloheptenes bearing orthogonal orientation of the allylic CH bond to the plane of the alkene.[44]

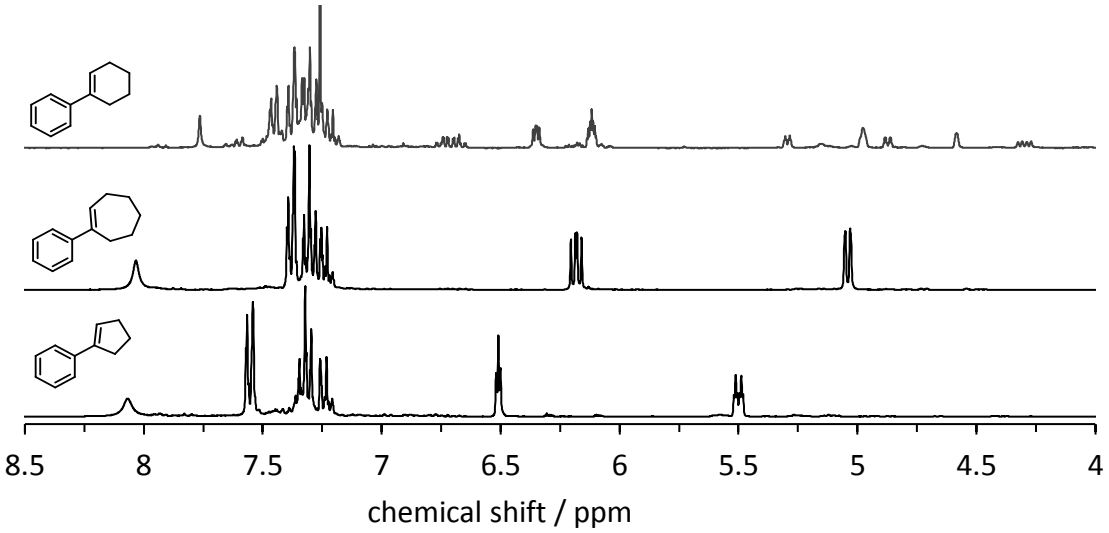

Figure 10. Comparison of crude ^{1}H-NMR spectra after photooxygenation of 1-aryl-1-cycloalkenes (see Table 1 for conditions).

Subsequently, we explored the scope of the photooxygenation with further substrates (Scheme 43). 6-Hydroxy-1-phenyl-1-cyclohexene, the PPh_3-reduced product of the photooxygenation of **1**, itself is a good substrate for another photooxygenation.[45,46] Doubled reaction time (compared to the standard substrate **1**) led to full conversion.[47]

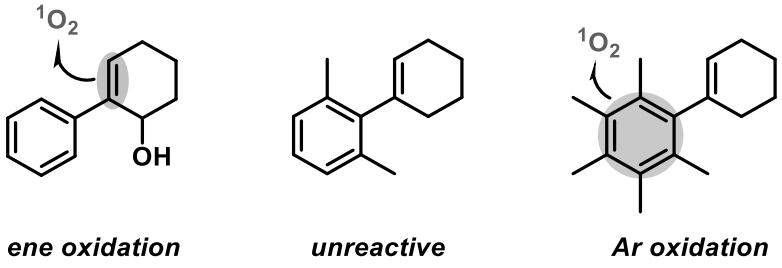

Scheme 43. Chemoselective conversions of substituted arylcyclohexenes.

Two sterically congested arylcyclohexenes with *ortho*,*ortho*-aryl substitution were also tested. 1-(2',6'-Dimethyl-phenyl)-1-cyclohexene was unreactive towards oxidation even under prolonged irradiation times. DFT calculations showed that the alkene and arene planes are twisted out of conjugation so that the $^1O_2$ attack is sterically hindered. 1-(Pentamethylphenyl)-1-cyclohexene gave full conversion but formed complex mixtures of arene oxidation products.[47]

The photooxygenation products derived from reactions of aryl-cyclohexenes with $^1O_2$ are versatile building blocks of great synthetic utility. Reduction of the the

peroxy functions (by PPh_3 or Na_2SO_3) gives the corresponding alcohols. Base-mediated acetylation with pyridine/Ac_2O has been used to prepare α,β-unsaturated carbonyls.[8]

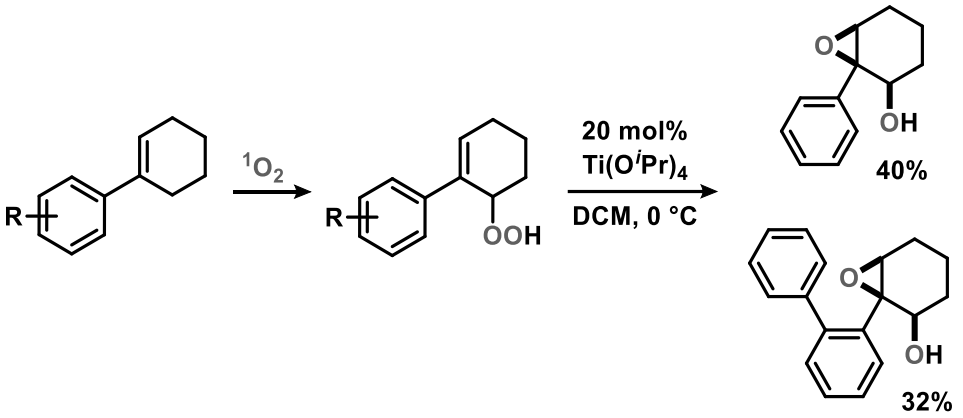

Scheme 44. Sequential photooxygenation and Ti-catalyzed "self"-epoxidation results in full incorporation of both O-atoms from O_2 into α,β-epoxy alcohols. Flash chromatographic separation of hydroperoxide prior to Ti(O^{i}Pr)$_4$ addition (20 mol%) at 0 °C in dichloromethane (DCM). Photo-oxidation conditions in Table 2.

Another interesting follow-up reaction is the titanium-catalyzed "self"-epoxidation. 2,3-Epoxy alcohols can be prepared from allyl hydroperoxides in high diastereoselectivity by a Sharpless epoxidation protocol in the absence of any further oxidant.[48,49] The presence of the alkene and hydroperoxide groups within the same molecule enables an intramolecular expoxidation at the Ti(IV) catalyst to give the *syn*-epoxy alcohol (*d.r.* 99%) in good yields over two steps (Scheme 44).

3 Conclusion

The development of oxidations of unbiased hydrocarbons with oxygen/air as the stoichiometric oxidant is a prime objective in the quest for sustainable chemical reactions. Cyclohexenes are notoriously unreactive substrates for photooxygenations with singlet oxygen. This concise synthetic and mechanistic study has established that easily available 1-aryl-1-cyclohexenes are a highly competent class of substrates that display enhanced reactivity. For the first time, optimized conditions in a custom-made photo flow reactor have enabled photooxygenations of a diverse set of arylcycloalkenes bearing various substitution patterns and ring sizes. The major products are the desired allyl hydroperoxides ($^1O_2$-ene products). Minor oxidation products include endoperoxides which appeared to be rather stable and could be isolated and characterized for the first time. Detailed mechanistic investigations including a Hammett study, reaction profile analyses, the isolation of various by-products, and DFT calculations have been performed. We postulate a reaction mechanism that involves a zwitterionic intermediate that undergoes rapid allyl hydroperoxide formation under protic conditions, with electron-deficient aryl substituents, or with (slight) steric hindrance by *ortho*-aryl substituents. The major allyl hydro-peroxides were isolated, fully characterized, and converted to stable allyl alcohol derivatives (by reduction) or to α,β-epoxy alcohols (by intramolecular oxygen-transfer). The photooxygenation tolerated various functional groups (F, Cl, Br, CN. CF_3, OCF_3, OMe, OH).

4 Experimental Part

Commercial chemicals (≥ 98 % purity), especially phenylcyclohexene (95 % purity), were used as obtained without further purification. Oxygen gas (GA 201) was obtained by a 50 L pressure cylinder. Methylene blue hydrate (CAS 122965-43-9) was obtained from *Alfa Aesar* (high purity biological stain, >98 % purity). TLC was performed using commercial silica gel coated aluminum plates (DC Kieselgel 60 F_{254}, *Merck*); visualization was done using UV light. Staining was realized with a solution of phosphomolybdic acid in ethanol (7 wt%). Product yields were determined from isolated materials after normal or flash column chromatography on silica gel (mesh 230-400) or for optimization and screening purposes by quantitative GC-FID measurements, with dodecanenitrile as internal standard on an *Agilent* 7820A GC-System with N_2 as carrier gas. HPLC separation was conducted on a *Bischoff* HPLC system in combination with the DAD-4L UV-Vis detector. Infrared spectra were recorded on an *Agilent* Cary 630 FTIR spectrometer equipped with an ATR unit; abbreviations: s – strong, m – medium, w – weak. Purity and structure were confirmed by ^{1}H-NMR, ^{13}C-NMR, and MS. Low-resolution mass spectrometry (LRMS) was carried out on an *Agilent* 6890N GC-System coupled to a 5975 MSD unit and H_2 as carrier gas. High resolution mass spectrometry (HRMS) was carried out by the Central Analytics at the department of chemistry, University of Regensburg, on various machines. Abbreviations used in MS spectra: M – molar mass of target compound, r.I. – relative intensity, EI – electron impact, ESI – electrospray ionization. NMR spectral data were collected on a *Bruker* Avance 300 (300 MHz for ^{1}H; 75 MHz for ^{13}C) and a *Bruker* Avance 400 (400 MHz for ^{1}H; 100 MHz for ^{13}C) spectrometer at 25 °C. Solvent residual peaks or TMS from TMS-containing deuterated solvents were used as internal standard for NMR measurements. The quantification of ^{1}H cores was obtained by integration of resonance signals. Abbreviations used in ^{13}C-NMR spectra: C_p – primary carbon, C_s – secondary carbon, C_t – tertiary carbon, C_q – quaternary carbon, C_{sp2} – sp^2 hybridization at this atom, C_{sp3} – sp^3 hybridization at this atom. Abbreviations used in ^{1}H-NMR spectra: s – singlet, bs – broad singlet, d – doublet, t – triplet, q – quartet, m – multiplet, R – organic rest, not hydrogen.

In case of literature-known compounds, at least one source of available spectroscopic data is cited. For literature-known syntheses, the source for preparation is cited in conjunction to the compound name.

▪ Synthesis of starting materials

1-phenyl-1-cyclohexene

This starting material which was used as obtained and contained about 5 % further oxidized / unsaturated (like biphenyl) compounds which are hard to separate, however they do not interfere in the oxidation process.

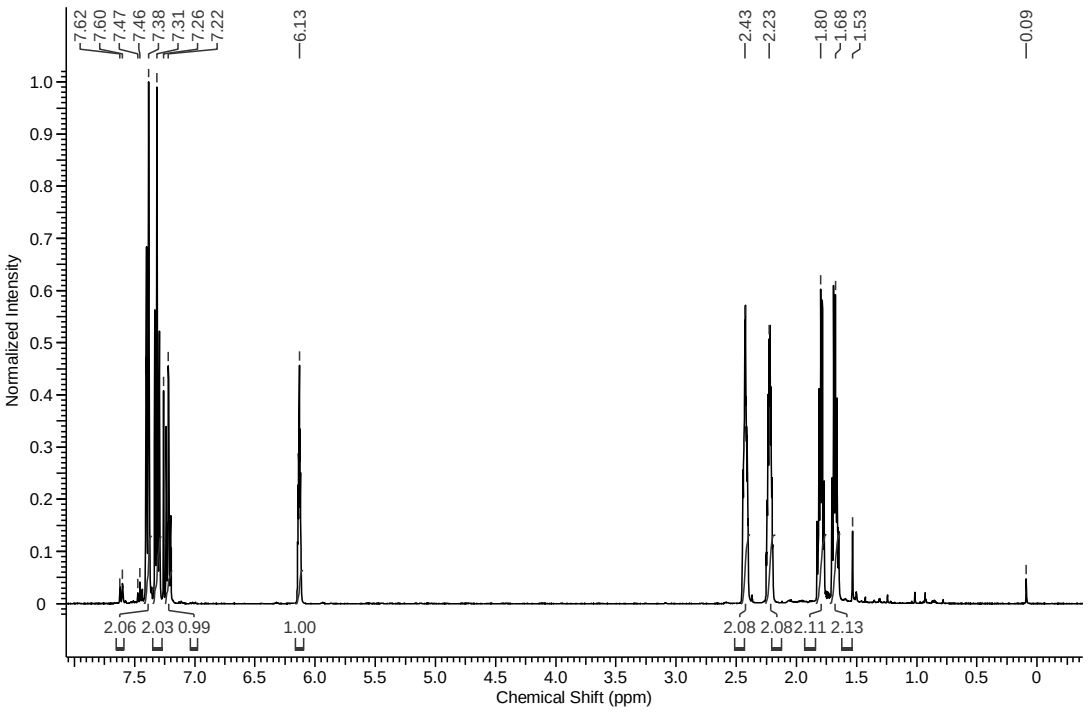

4'-chloro-2,3,4,5-tetrahydro-1,1'-biphenyl [50]

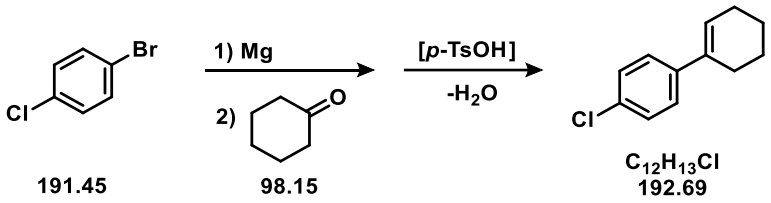

First, the Grignard was synthesized by addition of 1-bromo-4-chlorobenzene (6.1 g, 31.9 mmol, 1.8 equiv.) to a mixture of Mg turnings (0.88 g, 36.2 mmol, 2.1 equiv.) in dry diethylether (20 mL) at room temperature, with slight cooling when boiling. After 12 h of stirring, the Grignard reagent solution was added to a solution of cyclohexanone (1.70 g, 1.79 mL, 17.3 mmol, 1.0 equiv.) in diethylether (40 mL) at 0 °C. After stirring for 20 more hours, the reaction mixture was quenched on ice. Hydrochloric acid (ca. 30 mL)

was added until a homogeneous aqueous layer was obtained. The aqueous layer was separated, extracted twice with ether (20 mL each), and washed with sodium bicarbonate (aq. sat., 20 mL) and brine (sat., 20 mL). After removal of solvents in vacuo, an orange oil (4.97 g) was afforded. The resulting oil was dissolved in toluene (60 mL) and heated to reflux under Dean Stark conditions together with p-toluenesulfonic acid (0.1 g) for 3 h. The solvent was removed in vacuo to yield a brown mixture (3.85 g). The crude product was purified by column chromatography with pure PE to give the product (2.33 g, 69.9 %) as white crystals.

R_f (PE) = 0.62. ^{1}H-NMR (400 MHz, $CDCl_3$): δ [ppm] = 7.33 – 7.26 (m, 4H), 6.13 – 6.07 (m, 1H), 2.40 – 2.32 (m, 1H), 2.23 – 2.15 (m, 2H), 1.82 – 1.73 (m, 2H), 1.69 – 1.60 (m, 2H). ^{13}C-NMR (100 MHz, $CDCl_3$): δ [ppm] = 141.1 (C), 135.6 (C), 132.2 (C), 128.3 (CH), 126.2 (CH), 125.4 (CH), 27.3 (CH_2), 25.9 (CH_2), 23.0 (CH_2), 22.0 (CH_2). LRMS (EI): m/z (r.I.) = 192 (46) $[M]^+$, 129 (100), 115 (42), 157 (34). Spectral data were consistent with literature.[50]

2,3,4,5-tetrahydro-1,1':2',1''-terphenyl

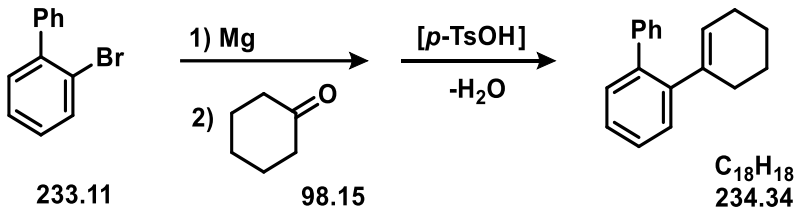

The Grignard reagent was synthesized by addition of 2-bromobiphenyl (4.65 g, 3.42 mL, 20.0 mmol, 1.0 equiv.) to a mixture of Mg turnings (0.58 g, 24.4 mmol, 1.2 equiv.) in dry THF (20 mL) at room temperature with slight cooling when necessary / boiling. After 15 h of stirring, a solution of cyclohexanone (1.96 g, 2.07 mL, 20.0 mmol, 1.0 equiv.) in THF (20 mL) was added to the slurry Grignard solution at 0 °C. After stirring for 4 more hours, the reaction mixture was quenched on ice. Hydrochloric acid (conc. aq.) was added until a homogeneous aqueous layer was obtained. The aqueous layer was separated, extracted with ether (2 x 20 mL), and the combined organic phases were washed with sodium bicarbonate (20 mL, sat. aq.) and brine (20 mL, sat.). After removal of solvents in vacuo, a brown oil was obtained.

The resulting oil was dissolved in toluene (80 mL) and heated to reflux under Dean Stark conditions together with p-toluenesulfonic acid (0.15 g) for 24 h. The solvent of the mixture was again removed in vacuo, ethyl acetate was added, and the organic phase was washed with water, the aqueous phase was separated and extracted with EtOAc two times, the organic layers were combined and dried with brine (sat.) and over $MgSO_4$ to yield a brown mixture. After distillation under reduced pressure (12 mbar), the low-boiling side products like biphenyl were separated and distilled off at a boiling point of

up to 170 °C. The residual crude product was purified via column chromatography with pure pentane to yield the desired compound (1.02 g, 22 %) as colorless oil.

R_f (pentane) = 0.60. 1H-NMR (400 MHz, $CDCl_3$): δ [ppm] = 7.47 – 7.22 (m, 9H), 5.71 – 5.65 (m, 1H), 2.14 – 2.04 (m, 2H), 1.87 – 1.78 (m, 2H), 1.58 – 1.42 (m, 4H). ^{13}C-NMR (100 MHz, $CDCl_3$): δ [ppm] = 143.7 (C), 142.3 (C), 139.7 (C), 139.4 (C), 130.0 (CH), 129.3 (CH), 129.0 (CH), 127.9 (CH), 127.6 (CH), 127.2 (CH), 126.8 (CH), 126.7 (CH), 29.5 (CH_2), 25.8 (CH_2), 23.0 (CH_2), 22.0(CH_2). HRMS (EI): m/z = 234.1409 $[M]^+$, calc.: 234.1403.

2',3',4',5',6'-pentamethyl-2,3,4,5-tetrahydro-1,1'-biphenyl

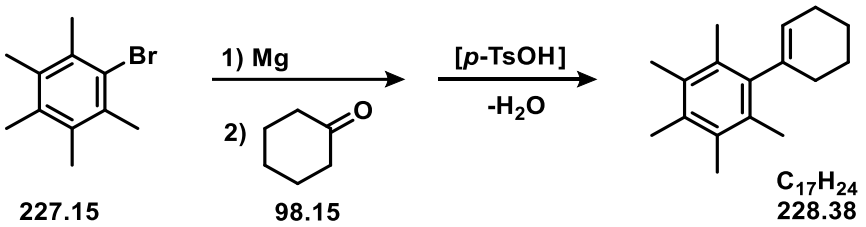

The Grignard reagent was synthesized by addition of pentamethylphenylbromide (10 g, 44 mmol, 1.0 equiv.) to a mixture of Mg (chips; 1.28 g, 53 mmol, 1.2 equiv.) in dry THF (80 mL) in a dry 100 mL Schlenk flask under nitrogen and cooling if necessary. The synthesis of the Grignard started after addition of ca. 500 mg iodine, followed by stirring for 24 h. Cyclohexanone (4.1 mL, 3.88 g, 39.6 mmol, 0.9 equiv.) was added. After 48 h of stirring at room temperature, the mixture was quenched on ice, EtOAc and 12M HCl were added until two distinct phases were visible, the organic phase was separated, and the aqueous phase was extracted twice with EtOAc. The combined organic phases were washed with $NaHCO_3$ (aq. sat.) & brine (sat.) to yield the crude alcohol after solvent removal *in vacuo* and column chromatography of the crude mixture with EA/pentane as eluent (5 to 15 % EA).

The resulting oil was dissolved in toluene (150 mL) and refluxed under Dean Stark conditions together with *p*-toluenesulfonic acid (0.3 g) for 48 h. The solvent of the mixture was removed *in vacuo*. The crude product was purified *via* column chromatography with pentane and recrystallization from ethanol to yield colorless plates (470 mg, 2.06 mmol, 5 %).

1H-NMR (300 MHz, $CDCl_3$): δ [ppm] = 5.46-5.38 (m, 1H), 2.25-2.22 (s, 6H), 2.22-2.15 (s, 6H), 2.08-1.99 (m, 2H), 1.81-1.65 (m, 4H). ^{13}C-NMR (100 MHz, $CDCl_3$): δ [ppm] = 141.6, 139.2, 133.1, 132.3, 130.1, 125.3, 30.4, 25.5, 23.2, 22.3, 17.4, 16.7, 16.6. HRMS (EI): m/z = 228.1873 $[M]^+$, calc.: 228.1873.

▪ Photo-oxidation reactions in flow and batch

Typically, reactions were conducted in our home-built photo-flow microreactor setup which is explained in detail in a preceding publication.[13] Usual reactions feature acetonitrile as solvent, irradiation with 24 water-cooled red high-power LEDs (Cree XP-E2 red, I = 700 mA, U = 2.43 V, P = 1.7 W; per lamp), a temperature of 0 °C, a reaction time of approximately 7 minutes, a 12 bar backpressure regulator, and oxygen gas at an inlet pressure of 30 bar (435 psi).

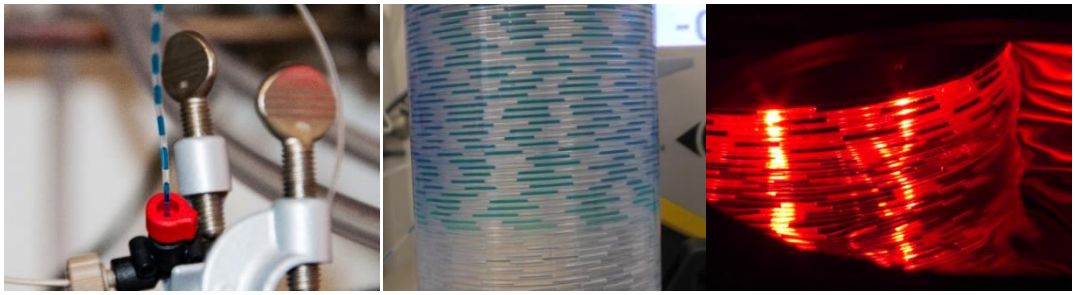

Batch reactions were conducted in u-tubes made from glass with a built-in frit, irradiated by six water-cooled white high-power LEDs (Cree MK-R warm white; I = 700 mA, U = 11.6 V, P = 8.1 W; per lamp) at room temperature. Pure oxygen was bubbled through the solution during the irradiation, with near to atmospheric pressure.

Because of a maximum efficiency of the power adapters of 95 %, a minimum of 106 % of the given power (wattage) is consumed.

▪ Oxidation of phenylcyclohexene in acetonitrile

When oxidizing phenylcyclohexene in the flow reactor[13] (8 min, 0 °C, MeCN, 0.1 M substrate, 1mM MB), a variety of products was obtained and detected *via* ^{1}H-NMR spectroscopy. In the following, the crude spectrum after solvent removal *in vacuo* is shown:

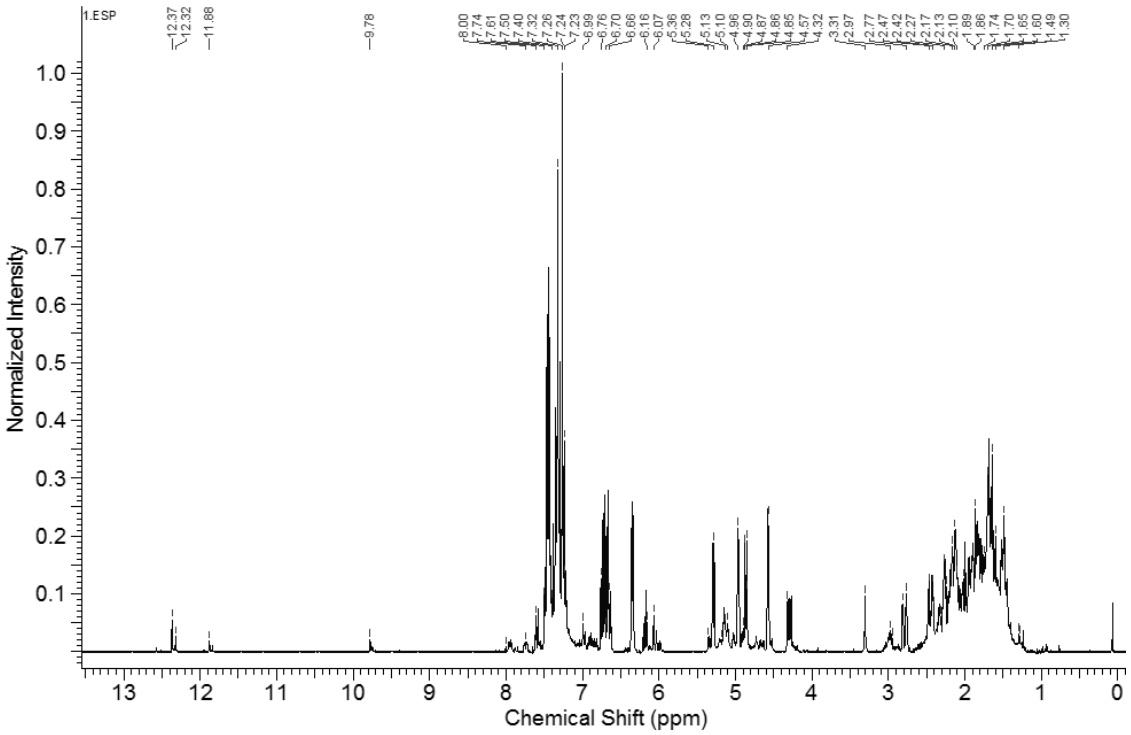

The spectroscopic data on first stage products after oxidation of 1-phenyl-1-cyclohexene in the flow reactor is not obtained by pure and isolated compounds, but by mixtures of isomers with other / degradation products; the signals were decisively assignable to the respective compound after one or two silica-based column chromatography separation attempts.

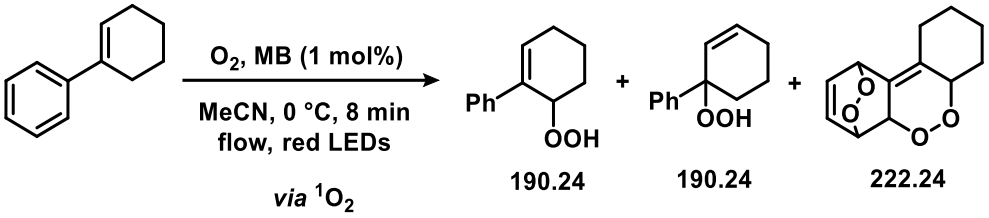

6-hydroperoxy-1-phenyl-1-cyclohexene

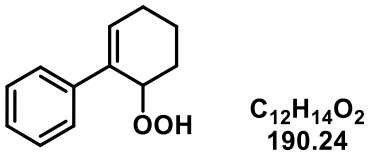

R_f (pentane/EA 4/1) = 0.70. ^{1}H-NMR (400 MHz, $CDCl_3$): δ [ppm] = 7.82-7.71 (m, 1H, OOH), 7.48-7.43 (m, 2H), 7.37-7.27 (m, 3H), 6.39-6.31 (m, 1H, C), 5.01-4.95 (m, 1H), 2.48-2.40 (m, 1H), 2.35-2.10 (m, 2H), 1.88-1.76 (m, 1H), 1.72-1.62 (m, 1H). ^{13}C-NMR (100 MHz, $CDCl_3$): δ [ppm] = 140.5, 133.9, 133.2 (CH), 128.4 (CH), 127.1 (CH), 125.8 (CH), 79.3 (COOH), 26.4 (CH_2), 26.2 (CH_2), 16.8 (CH_2). HRMS (ESI): *m/z* = 191.1067 $[M+H]^+$, calc.: 191.1067.

▪ Conversion and Product formation kinetics of 4-chloro-1-phenyl-1-cyclohexene

Standard added: dimethylsulfone, ca. 1 equiv. with respect to substrate, before reaction.

Kinetic experiment in microreactor: the reactor tubing was filled with reaction mixture (0.1 M substrate in MeCN together w/ 0.1 M dimethylsulfone and 0.001 M methylene blue) and oxygen, just as in a usual run. When the reactor was continuously running with this mixture, the red light-source (which was switched on already before the reaction but outside the vessel for reproducible LED irradiation) was added to the reactor setup for irradiation, and samples were taken at the outlet of the reactor after certain times (see timescale) which directly correspond to irradiation and reaction time.

▪ Microreactor productivity and performance

We could determine the ideal conditions for the photooxygenation of the model substrate phenylcyclohexene in the photo-flow reactor varying a broad palette of reaction parameters. Applying an oxygen inlet pressure of 30 bar, a back-pressure regulator of 7 bar, red LEDs (24 × Cree XP-E 2), and acetonitrile at 0 °C, very good results regarding productivity and energy efficiency were achieved without exhausting the upper pressure limits of the reactor tubing. The sensitizer loading could be reduced to a minimum of 0.05 mol%. The production capacity of the flow system clearly stands out comparing batch and flow reaction, and especially the energy saving potential of up to more than 99.8 % with respect to the according batch reaction is a huge advantage comparing the best results of both systems:

Table. Productivity and power consumption of the model photooxygenation of 1-phenyl-1-cyclohexene.

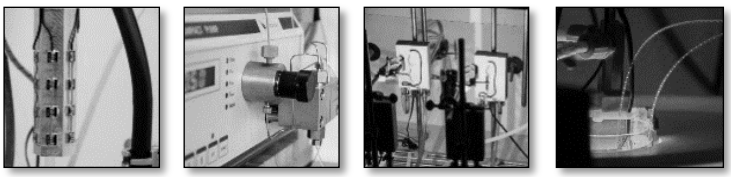

Reactor	c[a]	LEDs	Time[b]	Power[c]	Productivity[d]
batch	0.1	white	8 h	819	0.25
batch	1	white	> 48 h	491	< 0.42
flow	0.1	white	1.0 min	22.7	9
flow	0.1	red	4.3 min	9.6	4.5
flow	**1**	**red**	**8.5 min**	**1.43**	**30**

[a]Concentration in mmol/L. [b]Time required for complete conversion of phenylcyclohexene. [c]Consumed power in Wh $mmol^{-1}$. [d]Productivity in mmol h^{-1}.

▪ Isolated and clean products

The clean products were obtained by oxidation in the micro flow reactor and, in some cases, addition of an additive with a possible intermediate isolation of the hydroperoxide.

General procedure GP-2:

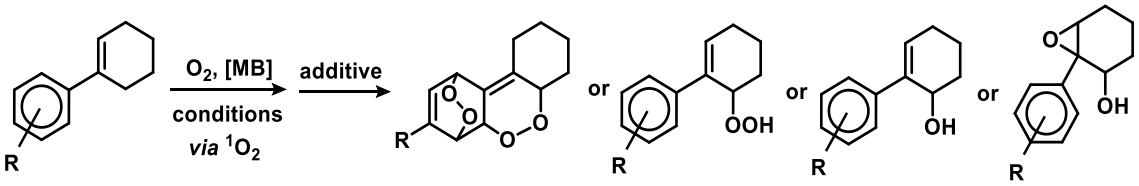

The starting material was dissolved in a solution of methylene blue (1 mM, in MeCN) in acetonitrile to give a 0.1 molar solution of the substrate (1 mol% of MB sensitizer with respect to the substrate), whereby ultrasonication was used to assure a homogeneous and particle-free solution. The solution was then injected to our micro flow reactor at 0 °C, and irradiated for 8 min with 24 red LEDs in an approximately 13 m long 1/16 inch (0.79 mm) inner diameter FEP[51] tubing, together with oxygen at a pressure of roughly 30 bar. The crude mixture was further treated as explained in the respective experimental details.

2-hydroperoxy-2'-methoxy-2,3,4,5-tetrahydro-1,1'-biphenyl

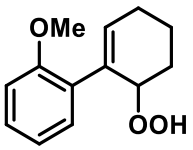

$C_{13}H_{16}O_3$
220.27

The compound was synthesized according to GP-2 with 1-(*o*-methoxyphenyl)-1-cyclohexene (94.1 mg, 0.5 mmol) in 5 mL sensitizer solution. After oxidation, the solvent of the crude mixture was removed *in vacuo* and the crude product was purified via column chromatography with EA in pentane (15 to 30 % EA) as eluent to give the title compound (34.0 mg, 31 %) as white solid.

R_f (pentane/EA 4/1) = 0.61. ^{1}H-NMR (400 MHz, $CDCl_3$): δ [ppm] = 8.00 (s, 1H), 7.28-7.23 (m, 1H), 7.14 (dd, *J* = 7.4 Hz, *J* = 1.7 Hz, 1H), 6.94 (td, *J* = 7.4 Hz, *J* = 0.9 Hz, 1H), 6.89 (d, *J* = 8.1 Hz, 1H), 6.0 (t, *J* = 3.8 Hz, 1H), 4.94 (t, *J* = 3.7 Hz, 1H), 3.83 (s, 3H), 2.35-2.15 (m, 3H), 1.94-1.80 (m, 2H), 1.75-1.64 (m, 1H). ^{13}C-NMR (100 MHz, $CDCl_3$): δ [ppm] = 156.8

(COMe), 134.7 (C), 134.2 (CH), 130.9 (C), 130.6 (CH), 128.5 (CH), 120.9 (CH), 110.8 (H), 80.4 (COOH), 55.6 (CH_3), 26.8 (CH_2), 25.8 (CH_2), 18.2 (CH_2). IR (ATR): $\tilde{\nu}$ [cm^{-1}] = 3381 (m), 2934 (m), 2837 (w), 1598 (w), 1489 (m), 1240 (s). HRMS (EI): *m/z* = 221.1172 $[M+H]^+$, calc.: 221.1172.

2-hydroperoxy-2,3,4,5-tetrahydro-1,1':2',1''-terphenyl

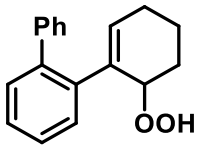

$C_{18}H_{18}O_2$
266.34

The compound was synthesized according to GP-2 with 1-(*o*-biphenyl)-1-cyclohexene (93.7 mg, 0.4 mmol) in 4 mL sensitizer solution. After oxidation, the solvent of the crude mixture was removed *in vacuo* and the crude product was purified via column chromatography with EA in pentane (10 to 20 % EA) as eluent to give the title compound (51 mg, 48 %) as colorless oil.

R_f (pentane/EA 7/1) = 0.46. ^{1}H-NMR (400 MHz, $CDCl_3$): δ [ppm] = 7.53 (s, 1H), 7.44-7.27 (9H), 5.99 (t, *J* = 3.7 Hz, 1H), 4.1 (t, *J* = 3.4 Hz, 1H), 2.17-1.99 (m, 3H), 1.81-1.64 (m, 1H), 1.61-1.47 (m, 1H), 1.43-1.25 (m, 1H). ^{13}C-NMR (100 MHz, $CDCl_3$): δ [ppm] = 141.9 (C), 140.5 (C), 140.0 (C), 136.1 (C), 135.9 (CH), 130.1 (CH), 130.0 (CH), 129.3 (CH), 128.0 (CH), 127.5 (CH), 127.4 (CH), 126.8 (CH), 80.3 (CO), 26.1 (CH_2), 26.0 (CH_2), 17.0(CH_2). IR (ATR): $\tilde{\nu}$ [cm^{-1}] = 3400 (broad, m), 2934 (m), 1478 (m), 1437 (m), 909 (s). HRMS (EI): *m/z* = 267.1365 $[M+H]^+$, calc.: 267.1380.

2'-hydroxy-2',3',4',5'-tetrahydro-[1,1'-biphenyl]-4-carbonitrile

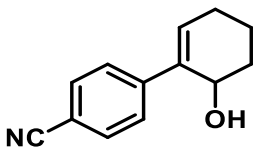

$C_{13}H_{13}NO$
199.25

The compound was synthesized according to GP-2 with 1-(*p*-cyanophenyl)-1-cyclohexene (73.3 mg, 0.4 mmol, 1.0 equiv.) in 4 mL sensitizer solution. When leaving the microreactor, the crude mixture was directly dropping into a solution of PPh_3 (105 mg, 0.4 mmol, 1.0 equiv.) in MeCN (5.0 mL). Ten minutes after the irradiation, the solvent was removed under reduced pressure, and the crude product was purified via column chromatography with EA in pentane (18 to 25 % EA) as eluent to yield the desired compound (34.7 mg, 44 %) as slightly green oil.

R_f (pentane/EA 4/1) = 0.25. ^{1}H-NMR (400 MHz, $CDCl_3$): δ [ppm] = 7.64-7.54 (m, 4H), 6.32 (dd, *J* = 4.6 Hz, *J* = 3.4 Hz, 1H), 4.67 (t, *J* = 3.8 Hz, 1H), 2.38-2.27 (m, 1H), 2.26-2.15 (m, 1H), 2.01-1.93 (m, 1H), 1.91-1.67 (m, 3H). ^{13}C-NMR (100 MHz, $CDCl_3$): δ [ppm] = 145.1 (C), 137.7 (C), 132.2 (CH), 132.0 (CH), 126.5 (CH), 119.1 (C), 110.2 (C), 65.2 (CO), 31.8 (CH_2), 26.1 (CH_2), 17.0 (CH_2). HRMS (EI): *m/z* = 199.0996 $[M]^+$, calc.: 199.0992.

Cis 1-([1,1'-biphenyl]-2-yl)-7-oxabicyclo[4.1.0]heptan-2-ol + determination of diastereomeric ratio

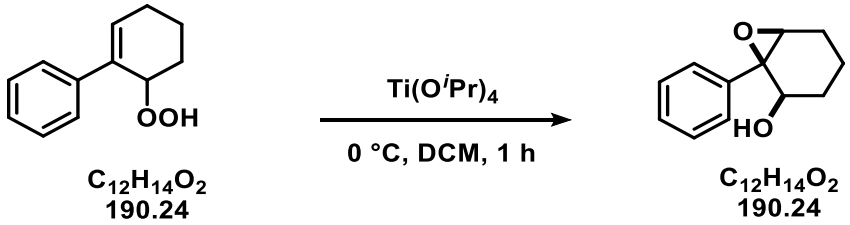

$C_{12}H_{14}O_2$
190.24

$C_{12}H_{14}O_2$
190.24

The compound was synthesized according to GP-2 with phenylcyclohexene (79.1 mg, 0.5 mmol) in 5 mL sensitizer solution. After oxidation, the solvent was removed under reduced pressure, and the crude product was purified via column chromatography with 15 % EA in pentane as eluent to yield the hydroperoxide (35 mg, 37 %) (together with approximately 13 % regioisomer featuring the hydroperoxyl group at the tertiary carbon) as slightly yellow oil. 110 mg of hydroperoxide synthesized this way (0.58 mmol, 1 equiv.) was added to a solution of Ti(O^{i}Pr)$_4$ (30 µL, 28 mg, 0.1 mmol, 20 mol%) in DCM (5 mL) at 0 °C, and stirred for 1 h. The reaction was quenched with water (0.5 mL). The organic phase was extracted with DCM twice. The organic phases were dried over sodium sulfate. The solvent was removed under reduced pressure, and the crude product (containing amongst other substances 0.3 % of the trans diastereomer) was purified via column chromatography with 20 % EA in PE to yield the title compound (95 mg, 32 % overall yield) as white solid. For the detection of *d.r.*, the same reaction was conducted, while dibromomethane (DBM; 111.4 mg) was added before addition of the crude product mixture (without applying the final column chromatography) to the NMR tube.

R_f (PE/EA 4/1) = 0.26. ^{1}H-NMR (400 MHz, $CDCl_3$): δ [ppm] = 7.45-7.40 (m, 2H), 7.39-7.33 (m, 2H), 7.32-7.27 (m, 1H), 4.53-4.44 (m, 1H), 3.25 (d, *J* = 3.1 Hz, 1H), 2.03-1.86 (m, 3H), 1.81-1.60 (m, 3H). ^{13}C-NMR (100 MHz, $CDCl_3$): δ [ppm] = 139.3 (C), 128.5 (CH), 127.7 (CH), 125.8 (CH), 69.0 (CO), 65.2 (CO), 63.3 (CO), 29.6 (CH_2), 24.0 (CH_2), 17.8 (CH_2). LRMS (EI): *m/z* = 190 (6) $[M]^+$, 105 (100), 77 (100), 133 (77), 91 (64). Spectral data were consistent with literature.[52]

The byproduct 2-phenyl-7-oxabicyclo[4.1.0]heptan-2-ol (6 mg, 2 % overall yield) was isolated as white solid.

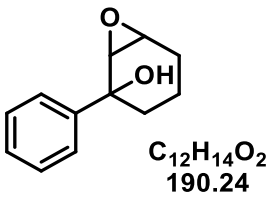

R_f (PE/EA 4/1) = 0.30. ^{1}H-NMR (300 MHz, $CDCl_3$): δ [ppm] = 7.53-7.47 (m, 2H), 7.42-7.35 (m, 2H), 7.33-7.26 (m, 1H), 3.60-2.55 (m, 1H), 3.34 (d, *J* = 3.9 Hz, 1H), 2.96-2.53 (bs, 1H), 2.20-2.01 (m, 1H), 1.97-1.71 (m, 2H), 1.63-1.56 (m, 1H), 1.43-1.18 (m, 2H). ^{13}C-NMR (75 MHz, $CDCl_3$): δ [ppm] = 145.3 (C), 128.3 (CH), 127.2 (CH), 125.1 (CH), 71.6 (CO), 59.0 (CO), 56.2 (CO), 37.8 (CH_2), 23.5 (CH_2), 15.8 (CH_2). LRMS (EI): *m/z* = 190 (6) $[M]^+$, 105 (100), 77 (72), 121 (32). Spectral data were consistent with literature.[53]

▪ Hammett study

For the product ratios regarding the Hammett study, signals of clearly assignable protons of the two products in ^{1}H-NMR of the crude mixture after solvent removal were integrated. The crude NMR after the oxidation of phenylcyclohexenes shows a clear pattern of signals which makes an assignment possible without the necessity of isolating all products: the signals of the starting materials are known because of their synthesis, the hydroperoxide features a non-aromatic sp^2-proton slightly low-field shifted with respect to the starting material and one allylic proton in the middle of the signals of the endoperoxide. The shifts of the protons of the endoperoxide at carbon atoms attached to oxygen can be clearly assigned by four signals with equal integrals being high-field shifted with respect to the starting material; one more proton signal is a low-field shifted multiplet with integral 2, or 1 in the case of substitution in *para* position, which again arises because of one or two non-aromatic sp^2-proton(s).

In many cases, endoperoxide and hydroperoxide product could be identified via ^{1}H-NMR in a precedent oxidation of the starting material and subsequent column chromatography (whereby they are not isolable in most cases).

The following two spectra show how integration was performed. The typical, empirically determined error is in the region of approximately 8 % or an uncertainty of about ± 0.3 regarding the ratio. As relaxation times at the used NMR machines were set to 2 min in all experiments, the signal of the hydrogen atom attached to the carbon featuring the hydroperoxy group has the tendency to show an integral being too low.[54]

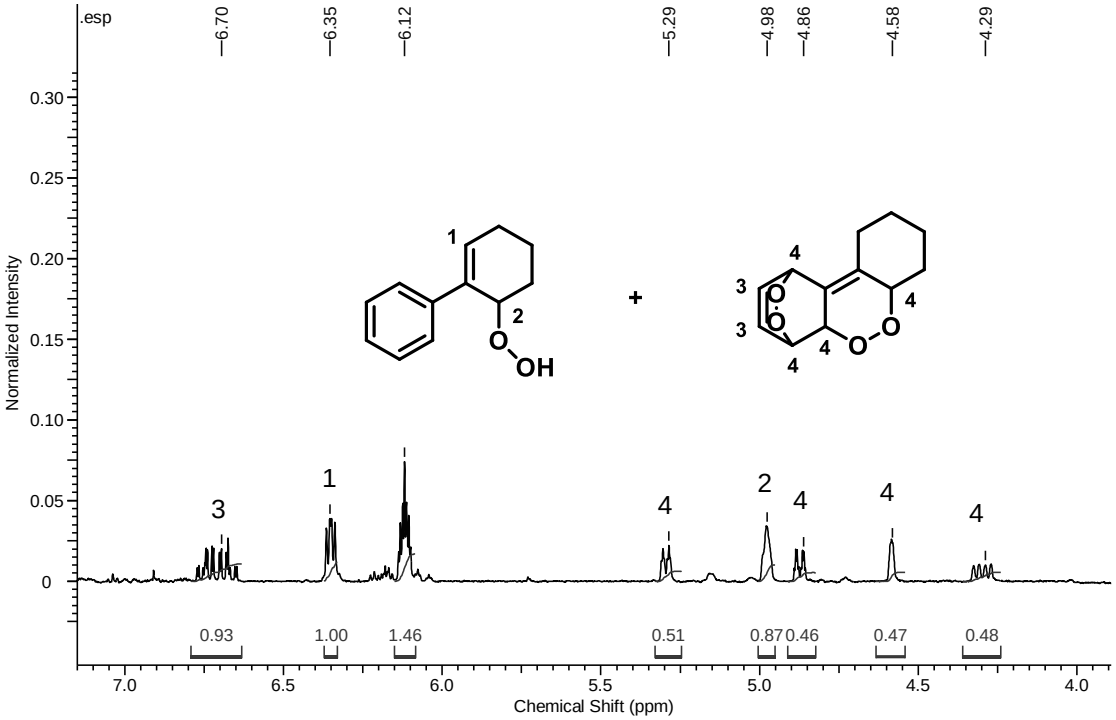
.esp
6.70
6.35
6.12
5.29
4.98
4.86
4.58
4.29
Normalized Intensity
0.30
0.25
0.20
0.15
0.10
0.05
0
1
2
OH
+
4
3
O
O
4
O
O
4
3
1
1
2
4
4
4
4
0.93
1.00
1.46
0.51
0.87
0.46
0.47
0.48
7.0
6.5
6.0
5.5
5.0
4.5
4.0
Chemical Shift (ppm)

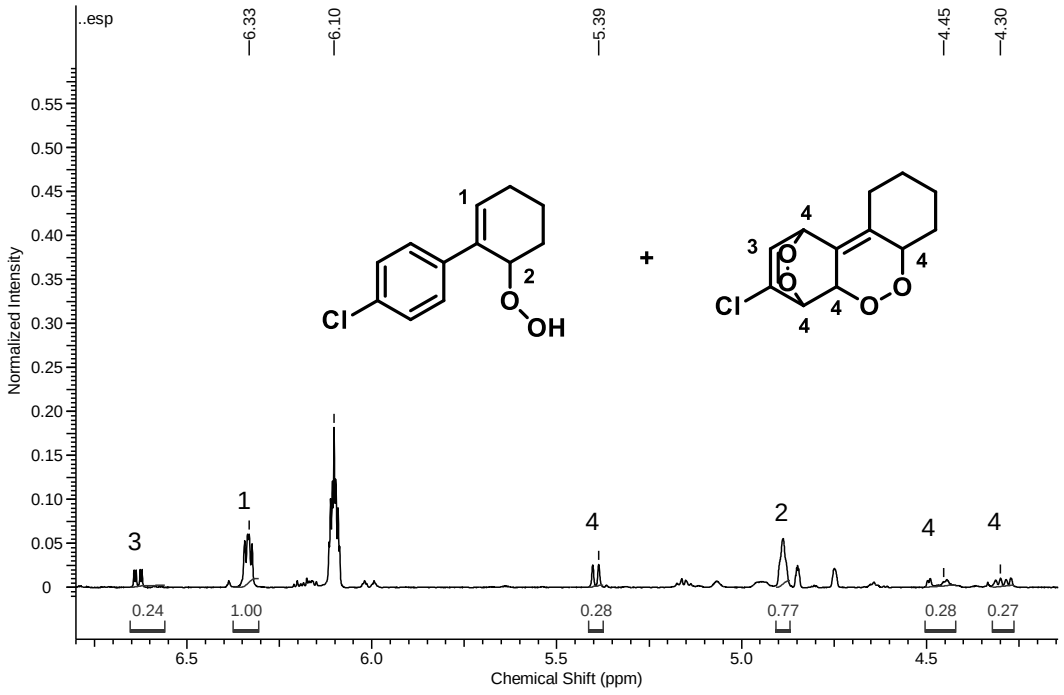
..esp
6.33
6.10
5.39
4.45
4.30
Normalized Intensity
0.55
0.50
0.45
0.40
0.35
0.30
0.25
0.20
0.15
0.10
0.05
0
1
2
OH
Cl
+
4
3
O
O
4
O
O
4
Cl
4
3
1
1
4
2
4
4
0.24
1.00
0.28
0.77
0.28
0.27
6.5
6.0
5.5
5.0
4.5
Chemical Shift (ppm)

- **Relative Rate Comparison: phenylcyclohexene**

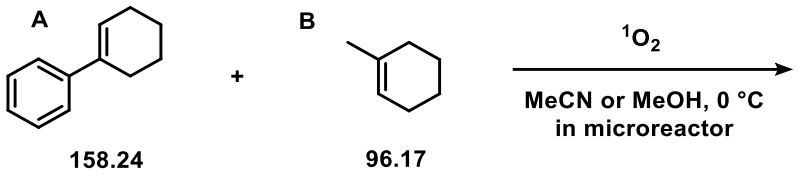

Reaction in microreactor environment, determination of relative reaction rate by one-pot oxidation of two substrates where one is literature-known.[15,55,56] Relative amounts were measured via GC-FID against the internal standard dodecanenitrile.

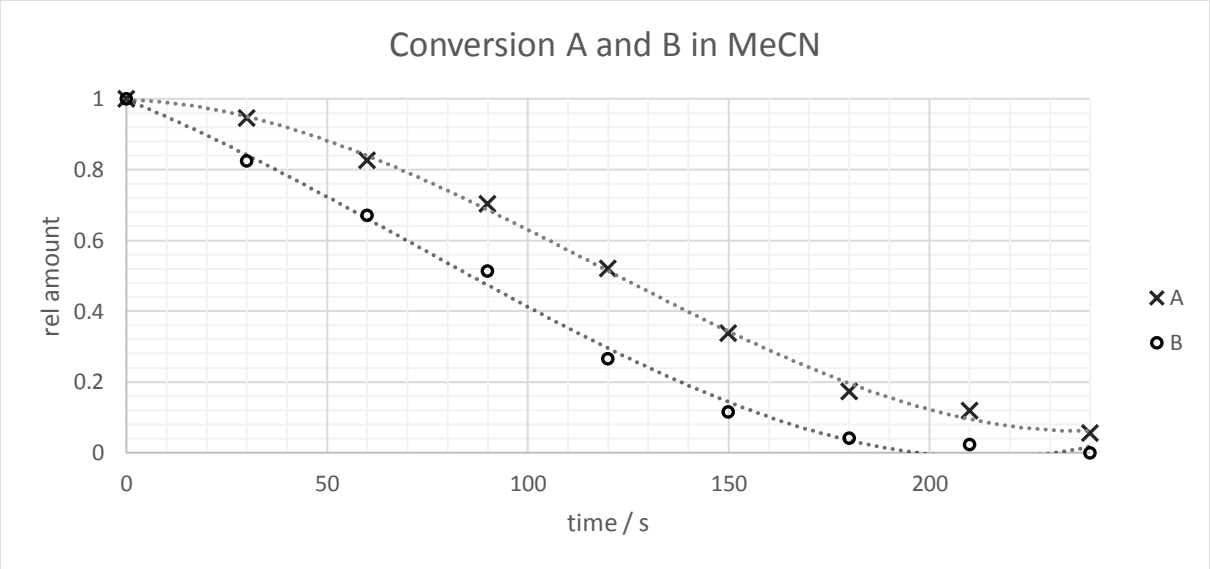

Conditions:

red LED, 40 bar, 13 m reactor length, solvent MeCN, dye MB, standard dodecanenitrile, flow rate oxygen 300, flow rate solution 0.5 mL/min, irradiation time 7 min, concentration starting material 0.1 mol/L, concentration dye 1 mmol/L.

k_A/k_B (MeCN) = 0.5476

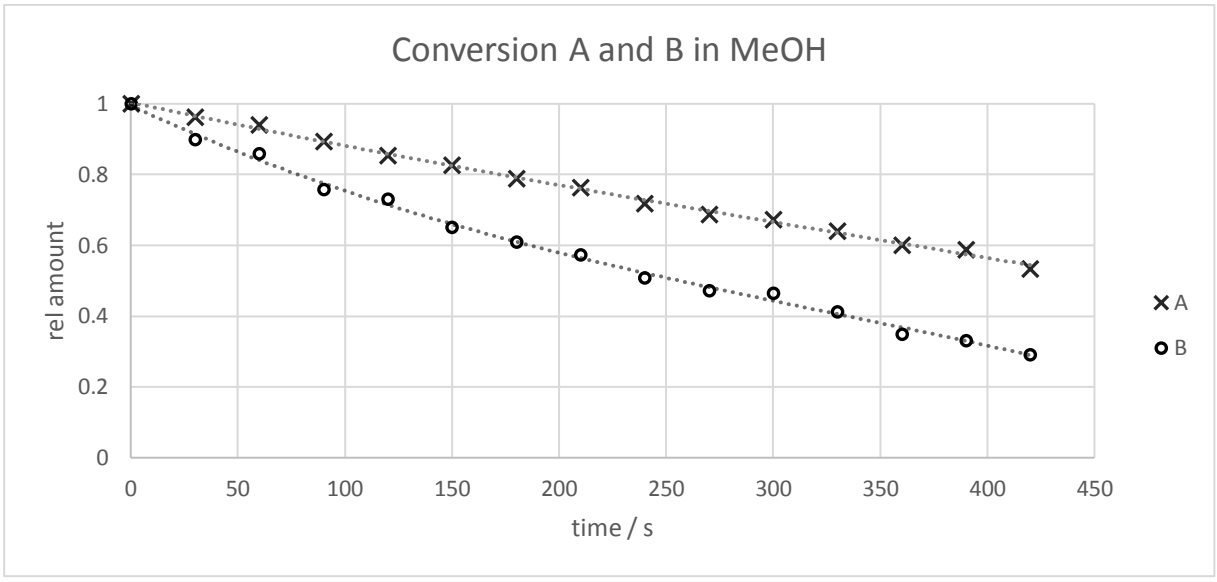

Conditions analogue to the reaction conducted in MeCN. Reactivity of the substrates is much lower in methanol, likely due to singlet oxygen quenching by MeOH. The curve fitting for relative rate determination is very good:

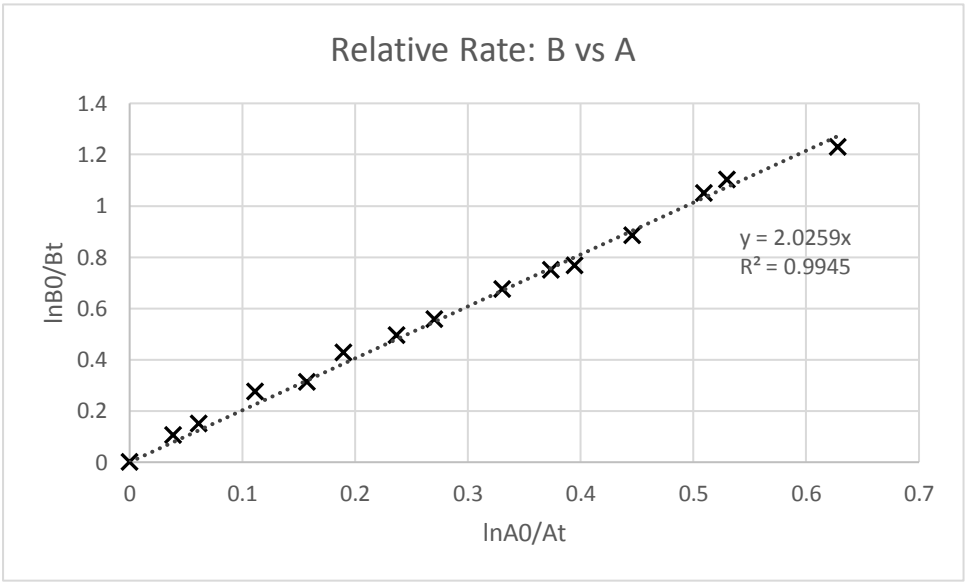

k_A/k_B (MeOH) = 0.4936

▪ Computational part

DFT and MP2 calculations were performed with the Gaussian G09 software package.[57] Vibrational analyses were performed on all optimized geometries to ascertain the types of minima obtained. Energies E are total electronic energies and usually given in Hartree, zero-point energy calculations are included. Three-dimensional molecular graphics were obtained using the Avogadro molecular visualization software, v 1.1.1.[58]

Calculations were usually performed on the Athene HPC-Cluster at the University of Regensburg.

Stabilization / destabilization of zwitterionic intermediates

Optimization of geometries and single point calculations were performed using the PCM solvation model (in acetonitrile) using the DFT method with B3LYP functional and 6-311++G(2d,p) basis set.

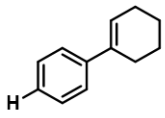

Structure A1

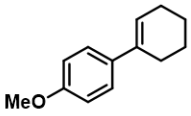

Structure A2

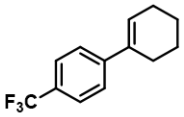

Structure A3

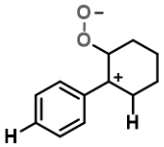

Structure B1

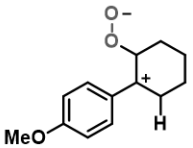

Structure B2

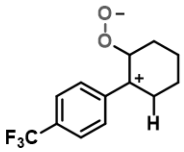

Structure B3

Structure A1 optimized geometry

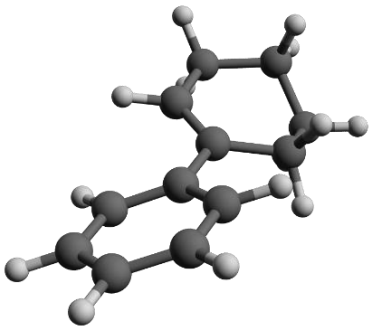

The relative stabilization energy was calculated by comparison of difference of substrate energy vs reaction intermediate energy.

Structure	E	ZPE	E+ZPE	ΔE	ΔΔE	ΔΔE / kcal mol^{-1}
A1	-465.8400	0.2264	-465.6136	-150.3318	0	0
B1	-616.1790	0.2336	-615.9454			
A2	-580.4010	0.2585	-580.1425	-150.3371	-0.0053	-3.33 (stab.)
B2	-730.7455	0.2659	-730.4796			
A3	-803.0001	0.2305	-802.7696	-150.3283	+0.0035	+2.20 (destab.)
B3	-953.3355	0.2376	-953.0979			

▪ DFT-calculated charges

Optimization of geometries was performed using the DFT method with B3LYP functional and 6-311+G(d,p) basis set. The indicated numbers are computed Mulliken charges.

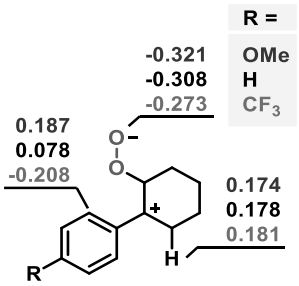

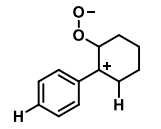

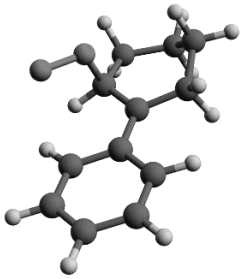

▪ Epoxy alcohol diastereoisomers

The compounds showed to be too complex for evaluation of NMR coupling constants or NOE effects for structure determination. The gained NMR data set showed to be too complex for reasonable interpretation.

The following graphics show one enantiomer per diastereomer as the discussed physical properties of the respective enantiomers are equal.

Optimization of geometries and single point calculations were performed using the MP2 method with 6-311++G(2d,p) basis set combined with the PCM solvation model (in chloroform). Higher energy conformers were also computed using the same method. NMR shielding was computed by the GIAO method against the magnetic shielding of TMS as reference using the PCM solvation model (in chloroform), the MP2 method which is reported to be superior to HF or DFT calculations of NMR shieldings,[59] and 6-311++G(2d,p) basis set.

Calculations using the DFT method (not explicitly listed) list analogue results pointing towards the shown structure correlation. The shifts calculated *via* DFT model are, as assumed, less precise than MP2 results. The higher energy conformers show equal shifts.

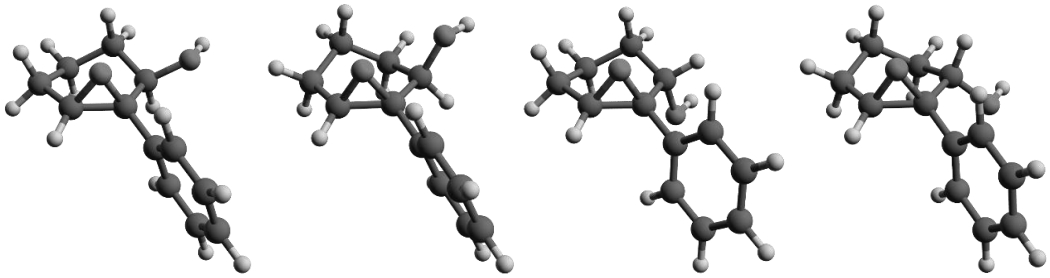

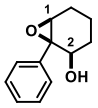

cis isomer
conformer A
structure ST-1

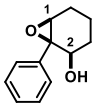

cis isomer
conformer B
structure ST-2

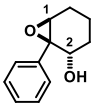

trans isomer
conformer A
structure ST-3

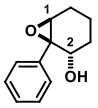

trans isomer
conformer B
structure ST-4

Structure	E	ZPE	E+ZPE	δ_{exp} | δ_{calc} (1-H)	δ_{exp} | δ_{calc} (2-H)	Dipole / D
ST-1	-614.6420	0.2365	-614.4055	3.24 | 3.02	4.48 | 4.65	4.36
ST-2	-614.6399	0.2367	-614.4032	3.24 | 3.03	4.48 | 4.78	4.38
ST-3	-614.6408	0.2365	-614.4043	3.40 | 3.38	4.28 | 4.38	2.46
ST-4	-614.6393	0.2363	-614.4030	3.40 | 3.30	4.28 | 4.04	3.28

- **Selected spectra**

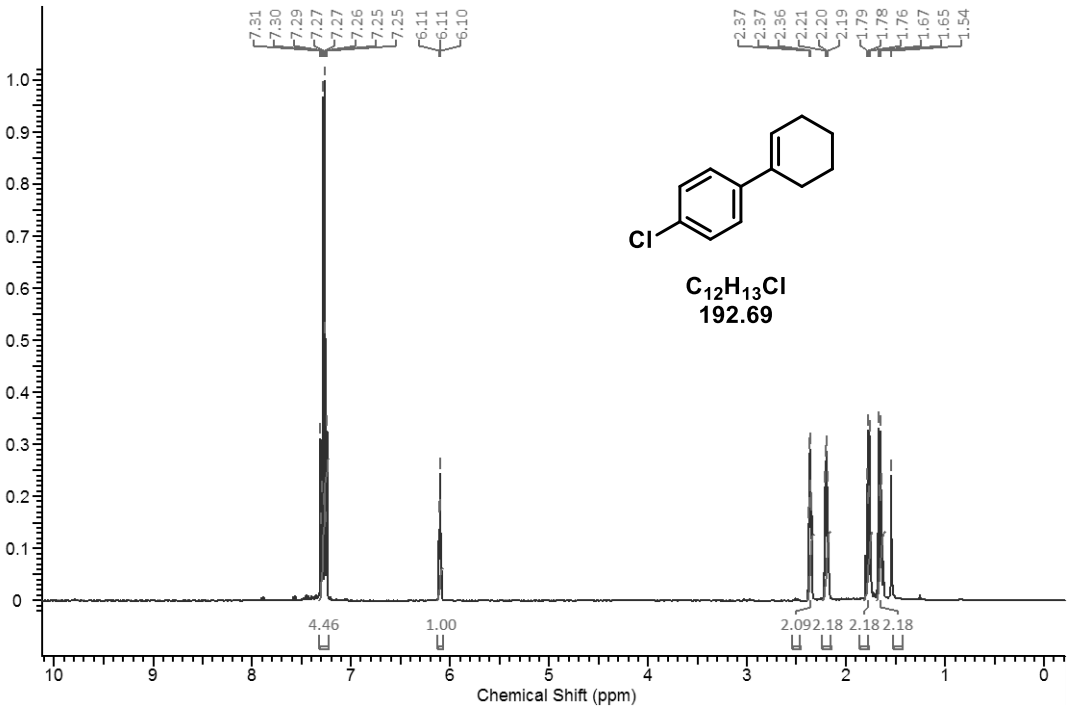

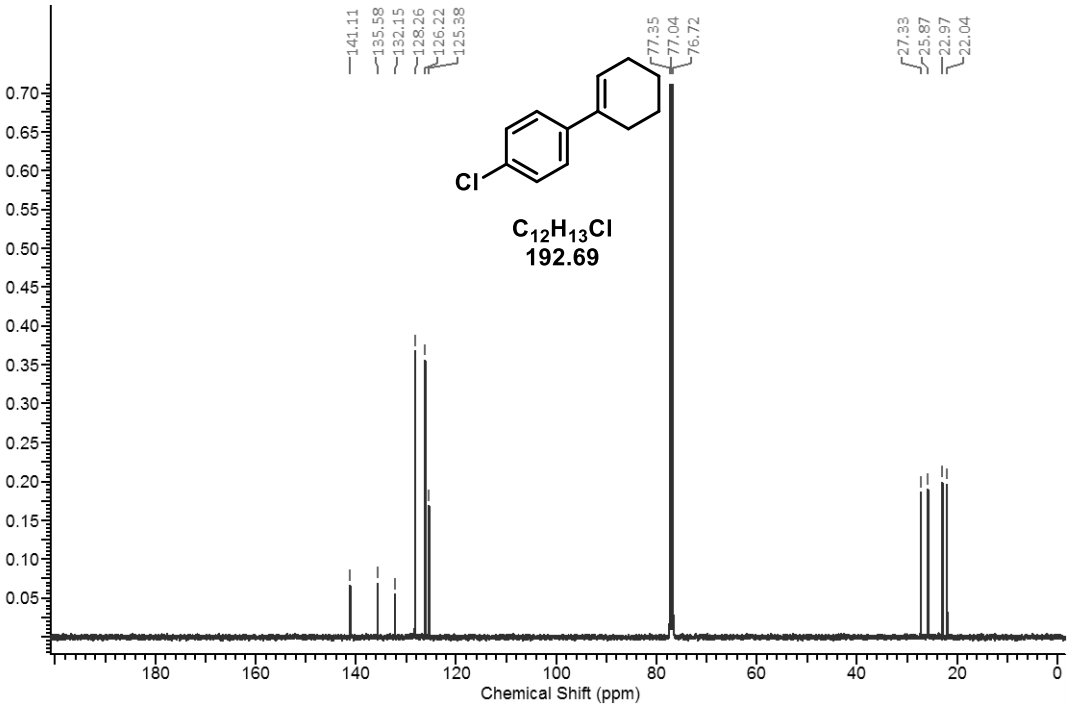

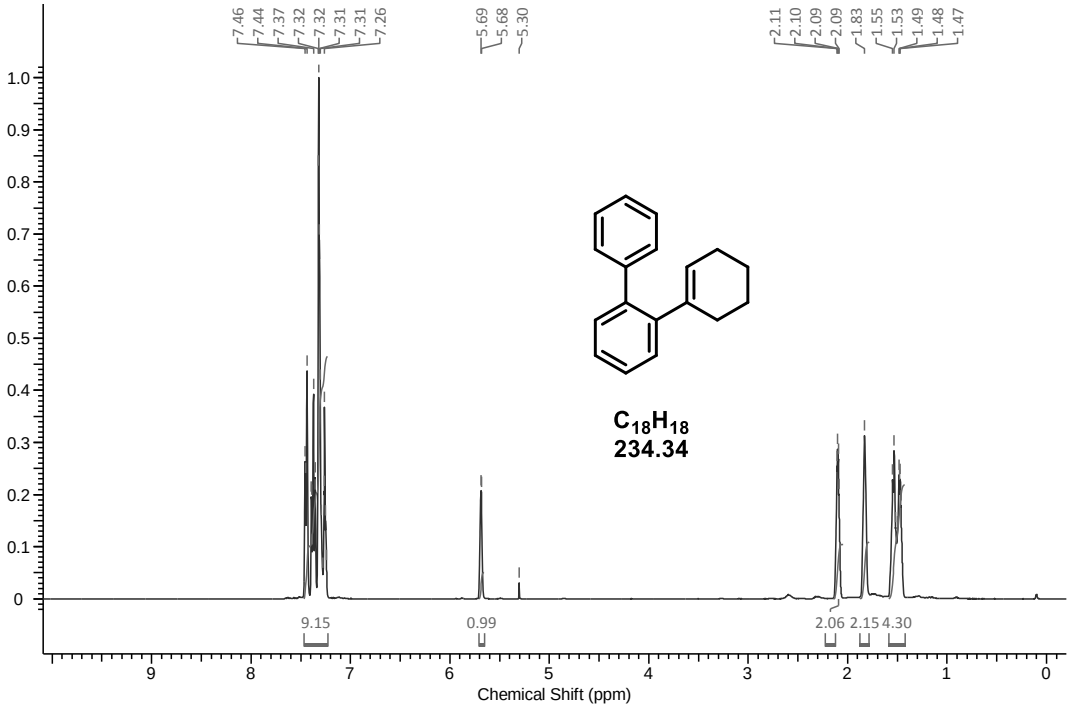
7.46
7.44
7.37
7.32
7.32
7.31
7.31
7.26
5.69
5.68
5.30
2.11
2.10
2.09
2.09
1.83
1.55
1.53
1.49
1.48
1.47
C18H18
234.34
9.15
0.99
2.06
2.15
4.30
Chemical Shift (ppm)

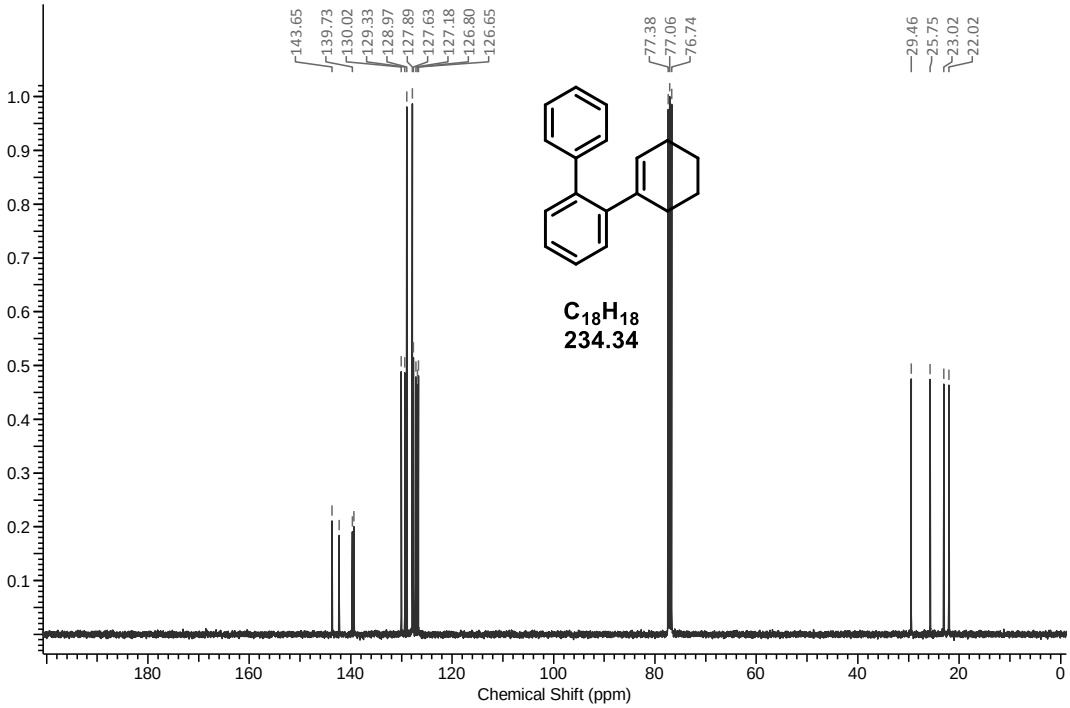
143.65
139.73
130.02
129.33
128.97
127.89
127.63
127.18
126.80
126.65
77.38
77.06
76.74
29.46
25.75
23.02
22.02
C18H18
234.34
Chemical Shift (ppm)

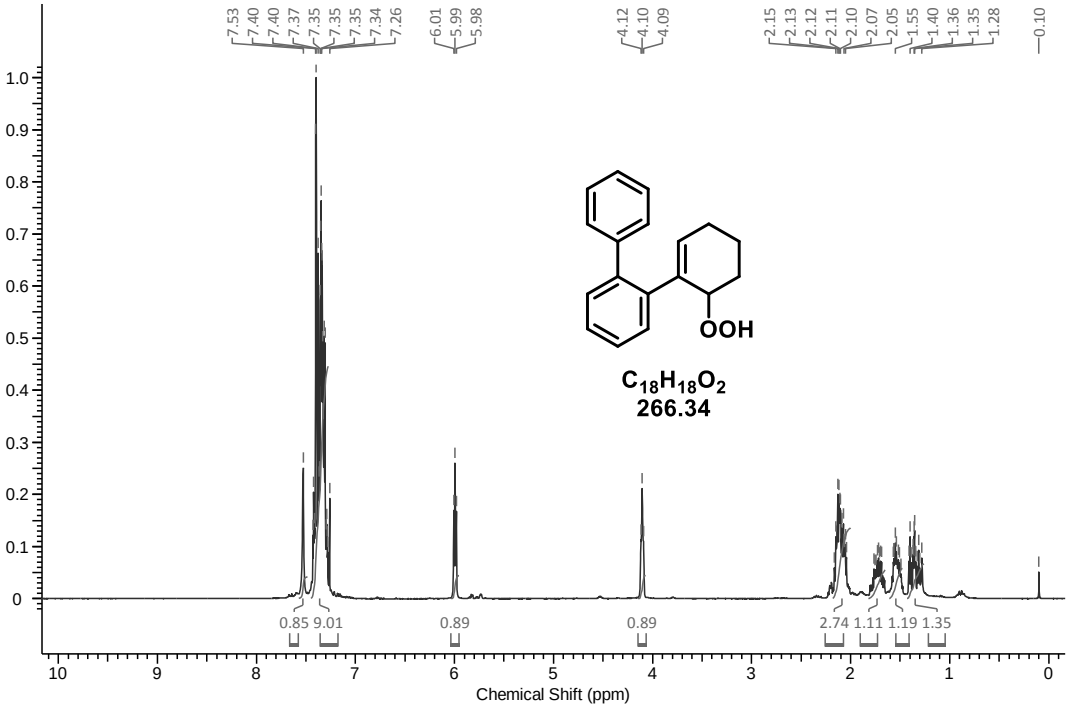
7.53
7.40
7.40
7.37
7.35
7.35
7.35
7.34
7.26
6.01
5.99
5.98
4.12
4.10
4.09
2.15
2.13
2.12
2.11
2.10
2.07
2.05
1.55
1.40
1.36
1.35
1.28
0.10
OOH
C18H18O2
266.34
0.85 9.01 0.89 0.89 2.74 1.11 1.19 1.35
Chemical Shift (ppm)

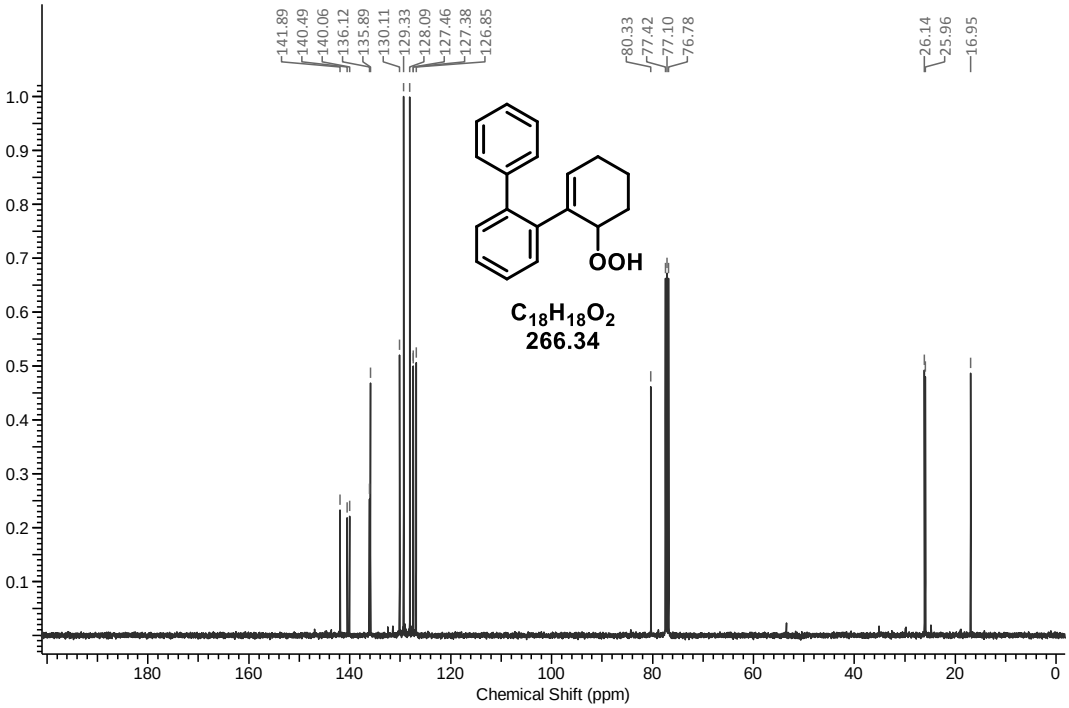
141.89
140.49
140.06
136.12
135.89
130.11
129.33
128.09
127.46
127.38
126.85
80.33
77.42
77.10
76.78
26.14
25.96
16.95
OOH
C18H18O2
266.34
Chemical Shift (ppm)

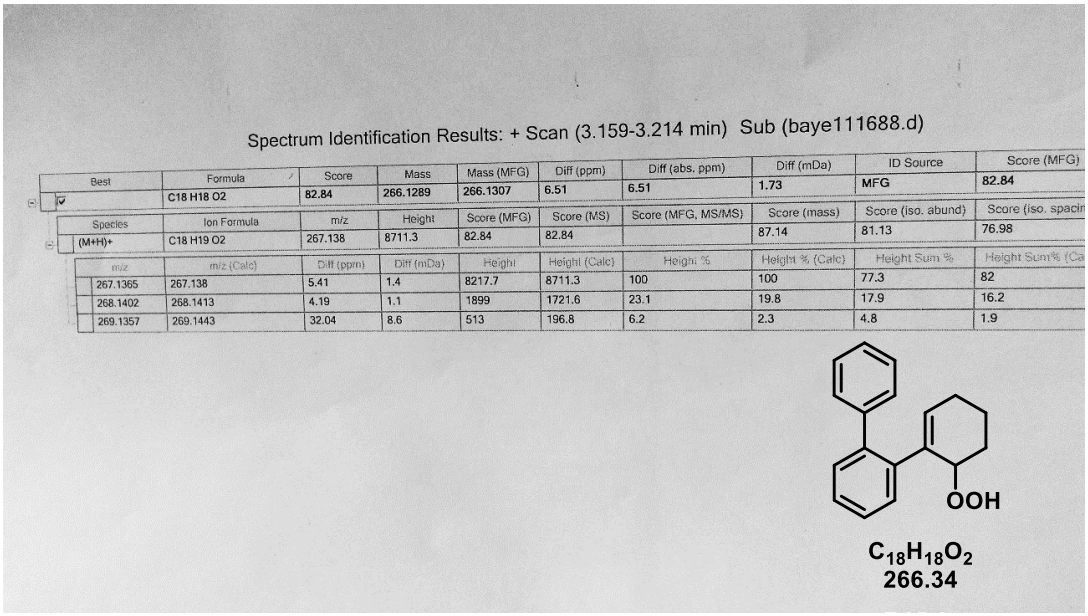

Best	Formula	Score	Mass	Mass (MFG)	Diff (ppm)	Diff (abs. ppm)	Diff (mDa)	ID Source	Score (MFG)
☑	C18 H18 O2	82.84	266.1289	266.1307	6.51	6.51	1.73	MFG	82.84

Species	Ion Formula	m/z	Height	Score (MFG)	Score (MS)	Score (MFG, MS/MS)	Score (mass)	Score (iso. abund)	Score (iso. spacin
(M+H)+	C18 H19 O2	267.138	8711.3	82.84	82.84		87.14	81.13	76.98

m/z	m/z (Calc)	Diff (ppm)	Diff (mDa)	Height	Height (Calc)	Height %	Height % (Calc)	Height Sum %	Height Sum% (Ca
267.1365	267.138	5.41	1.4	8217.7	8711.3	100	100	77.3	82
268.1402	268.1413	4.19	1.1	1899	1721.6	23.1	19.8	17.9	16.2
269.1357	269.1443	32.04	8.6	513	196.8	6.2	2.3	4.8	1.9

HRMS photograph

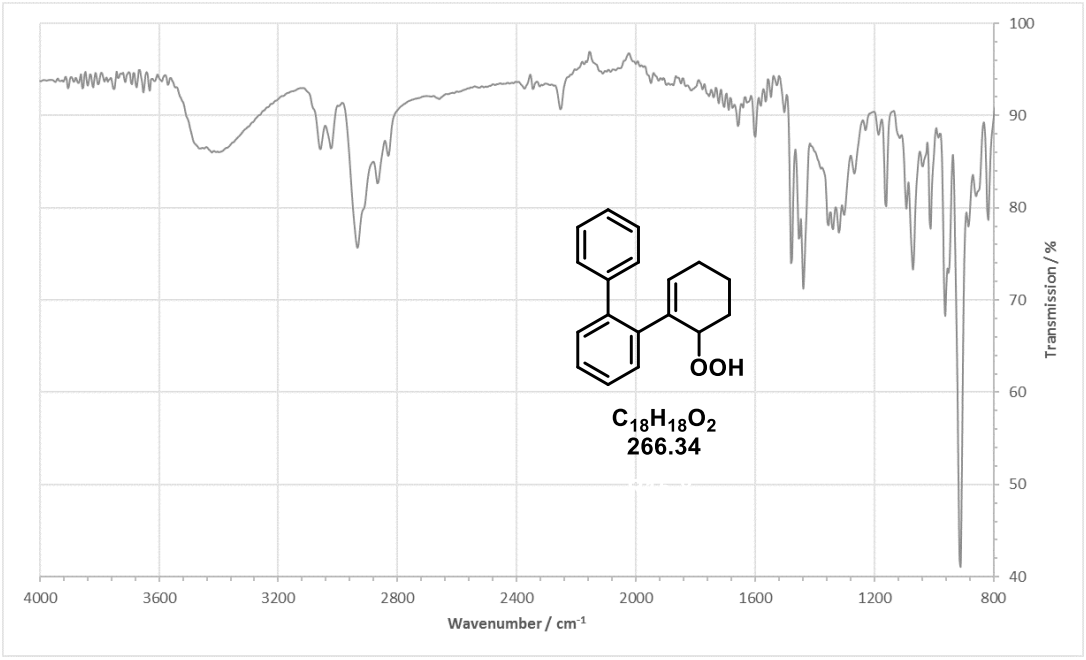

Infrared spectrum.

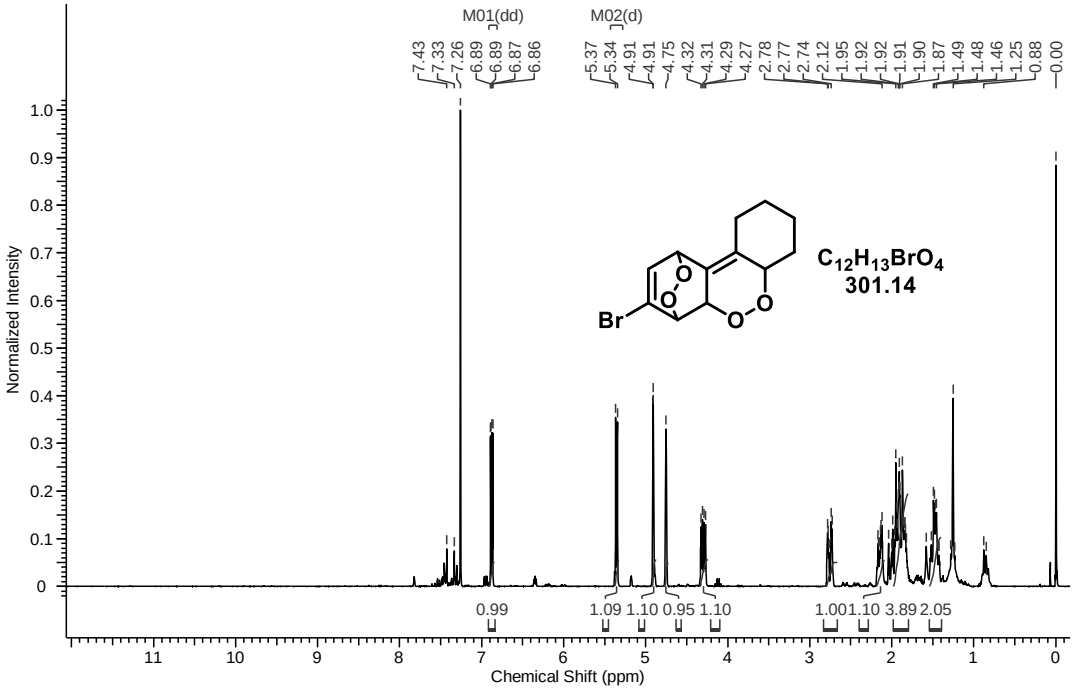
M01(dd)
M02(d)
7.43
7.33
7.26
6.89
6.89
6.87
6.86
5.37
5.34
4.91
4.91
4.75
4.32
4.31
4.29
4.27
2.78
2.77
2.74
2.12
1.95
1.92
1.92
1.91
1.90
1.87
1.49
1.48
1.46
1.25
0.88
0.00
Br
O
O
O
O
C12H13BrO4
301.14
Normalized Intensity
0.99
1.09
1.10
0.95
1.10
1.00
1.10
3.89
2.05
Chemical Shift (ppm)

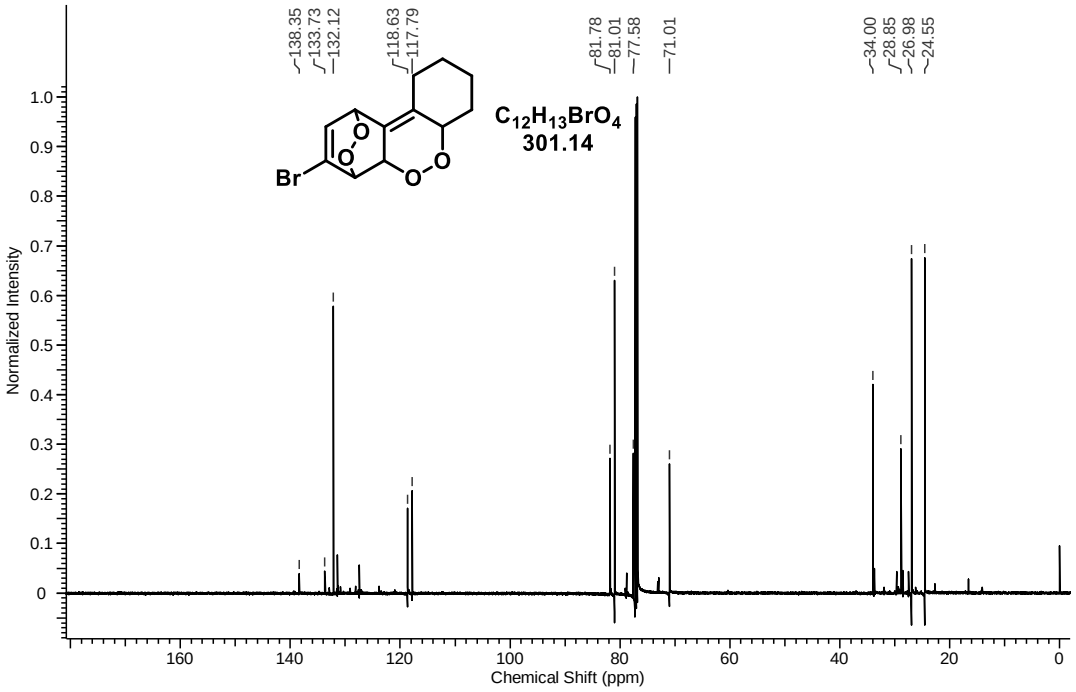
138.35
133.73
132.12
118.63
117.79
81.78
81.01
77.58
71.01
34.00
28.85
26.98
24.55
Br
O
O
O
O
C12H13BrO4
301.14
Normalized Intensity
Chemical Shift (ppm)

5 References

[1] R. A. Sheldon, H. van Bekkum, in *Fine Chemicals through Heterogeneous Catalysis*, Wiley-VCH, Weinheim, **2000**, pp. 473–551.
[2] G. Zheng, H. Liu, M. Wang, *Chin. J. Chem.* **2016**, *34*, 519–523.
[3] J. L. Jeffrey, E. S. Bartlett, R. Sarpong, *Angew. Chem. Int. Ed.* **2013**, *52*, 2194–2197.
[4] R. D. Bach, C. Canepa, J. E. Winter, P. E. Blanchette, *J. Org. Chem.* **1997**, *62*, 5191–5197.
[5] A. Goti, F. Cardona, in *Green Chemical Reactions*, Springer, Dordrecht, **2006**, pp. 191–212.
[6] Z. Shi, C. Zhang, C. Tang, N. Jiao, *Chem. Soc. Rev.* **2012**, *41*, 3381.
[7] D. Cambié, C. Bottecchia, N. J. W. Straathof, V. Hessel, T. Noël, *Chem. Rev.* **2016**, *116*, 10276–10341.
[8] M. Prein, W. Adam, *Angew. Chem. Int. Ed.* **1996**, *35*, 477–494.
[9] A. A. Frimer, *Chem. Rev.* **1979**, *79*, 359–387.
[10] M. Orfanopoulos, I. Smonou, C. S. Foote, *J. Am. Chem. Soc.* **1990**, *112*, 3607–3614.
[11] A. A. Gorman, I. R. Gould, I. Hamblett, *J. Am. Chem. Soc.* **1982**, *104*, 7098–7104.
[12] J. R. Hurst, S. L. Wilson, G. B. Schuster, *Tetrahedron* **1985**, *41*, 2191–2197.
[13] J. Schachtner, P. Bayer, A. Jacobi von Wangelin, *Beilstein J. Org. Chem.* **2016**, *12*, 1798–1811.
[14] M. Stratakis, M. Orfanopoulos, *Tetrahedron* **2000**, *56*, 1595–1615.
[15] K. R. Kopecky, H. J. Reich, *Can. J. Chem.* **1965**, *43*, 2265–2270.
[16] The organic dye and common singlet oxygen sensitizer MB in MeCN was preferred over porphyrin systems in DCM for reasons of solubility of substrates and environmental care.
[17] See the supporting information for microreactor productivity and performance.
[18] H. Klenk, P. H. Götz, R. Siegmeier, W. Mayr, in *Ullmann's Encyclopedia of Industrial Chemistry*, Wiley-VCH, Weinheim, **2000**.
[19] J. P. Finley, J. R. Cable, *J. Phys. Chem.* **1993**, *97*, 4595–4600.
[20] M. DeRosa, R. J. Crutchley, *Coord. Chem. Rev.* **2002**, *233–234*, 351–371.
[21] A. Greer, G. Vassilikogiannakis, K.-C. Lee, T. S. Koffas, K. Nahm, C. S. Foote, *J. Org. Chem.* **2000**, *65*, 6876–6878.
[22] D. Lerdal, C. S. Foote, *Tetrahedron Lett.* **1978**, *19*, 3227–3230.
[23] C. S. Foote, S. Mazur, P. A. Burns, D. Lerdal, *J. Am. Chem. Soc.* **1973**, *95*, 586–588.
[24] Different products and product distributions were observed with (radical) decatungstate-sensitized or charge-transfer induced oxidations: a) I. N. Lykakis, M. Orfanopoulos, Synlett 2004, 12, 2131-2134; b) K. Masanobu, S. Hirochika, T. Katsumi, Bull. Chem. Soc. Jpn. 1987, 60, 3331-3336.
[25] C. W. Jefford, C. G. Rimbault, *Tetrahedron Lett.* **1976**, *17*, 2479–2482.
[26] C. W. Jefford, A. F. Boschung, C. G. Rimbault, *Helv. Chim. Acta* **1976**, *59*, 2542–2550.
[27] C. W. Jefford, *Chem. Soc. Rev.* **1993**, *22*, 59.
[28] The diastereomers and disatereomeric ratios were identified with the help of authentic samples on GC-MS and H-NMR.
[29] I.-H. Um, H.-J. Han, J.-A. Ahn, S. Kang, E. Buncel, *J. Org. Chem.* **2002**, *67*, 8475–8480.
[30] I. Fernández, G. Frenking, *J. Org. Chem.* **2006**, *71*, 2251–2256.
[31] C. Hansch, A. Leo, R. W. Taft, *Chem. Rev.* **1991**, *91*, 165–195.
[32] L. P. Hammett, *J. Am. Chem. Soc.* **1937**, *59*, 96–103.
[33] E. V. Anslyn, D. A. Dougherty, *Modern Physical Organic Chemistry*, University Science Books, Dulles, **2006**.

[34] A. Farmilo, F. Wilkinson, *Photochem. Photobiol.* **1973**, *18*, 447–450.
[35] J. E. Heffner, C. T. Wigal, O. A. Moe, *Electroanalysis* **1997**, *9*, 629–632.
[36] A. Hedström, U. Bollmann, J. Bravidor, P.-O. Norrby, *Chem. - A Eur. J.* **2011**, *17*, 11991–11993.
[37] D. A. Culkin, J. F. Hartwig, *Organometallics* **2004**, *23*, 3398–3416.
[38] A. Xu, X. Li, S. Ye, G. Yin, Q. Zeng, *Appl. Catal. B Environ.* **2011**, *102*, 37–43.
[39] 4-Chloro-1-phenyl-1-cyclohexene was used for kinetic studies because it reacts more slowly as phenylcyclohexene.
[40] P. R. Ogilby, *Chem. Soc. Rev.* **2010**, *39*, 3181–3209.
[41] The allyl hydroperoxides are very stable in a metal and solvent-free environment at low temperatures (-30 °C in our case) and can even be stored for multiple months without visible (NMR) decomposition. Endoperoxides feature a more short-time stability.
[42] R. Hiatt, R. J. Smythe, C. McColeman, *Can. J. Chem.* **1971**, *49*, 1707–1711.
[43] W. Adam, S. Weinkötz, *Tetrahedron Lett.* **1995**, *36*, 7431–7432.
[44] T. Matsuura, A. Horinaka, R. Nakashima, *Chem. Lett.* **1973**, *2*, 887–890.
[45] A. G. Griesbeck, W. Adam, A. Bartoschek, T. T. El-Idreesy, *Photochem. Photobiol. Sci.* **2003**, *2*, 877–881.
[46] E. L. Clennan, D. Zhang, J. Singleton, *Photochem. Photobiol.* **2006**, *82*, 1226.
[47] As we expected, spectroscopical data suggests the formation of a broad range of products. Several attempts to isolate, purify, and characterize single compounds failed.
[48] W. Adam, A. Griesbeck, E. Staab, *Angew. Chem. Int. Ed.* **1986**, *25*, 269–270.
[49] E. M. Elgendy, S. A. Khayyat, *Russ. J. Org. Chem.* **2008**, *44*, 823–829.
[50] Y. Nakamura, S. Takeuchi, Y. Ohgo, M. Yamaoka, A. Yoshida, K. Mikami, *Tetrahedron* **1999**, *55*, 4595–4620.
[51] S. Ebnesajjad, P. R. Khaladkar, *Fluoropolymers Applications in Chemical Processing Industries*, William Andrew, Inc., Norwich, **2005**.
[52] H. Jackman, S. P. Marsden, P. Shapland, S. Barrett, *Org. Lett.* **2007**, *9*, 5179–5182.
[53] J. Siewert, R. Sandmann, P. von Zezschwitz, *Angew. Chem. Int. Ed.* **2007**, *46*, 7122–7124.
[54] D. J. Wink, *J. Chem. Educ.* **1989**, *66*, 810.
[55] R. Atkinson, *Chem. Rev.* **1986**, *86*, 69–201.
[56] F. Wilkinson, W. P. Helman, A. B. Ross, *J. Phys. Chem. Ref. Data* **1995**, *24*, 663–677.
[57] M. J. Frisch, G. W. Trucks, H. B. Schlegel, G. E. Scuseria, M. A. Robb, J. R. Cheeseman, G. Scalmani, V. Barone, B. Mennucci, G. A. Petersson, H. Nakatsuji, M. Caricato, X. Li, H. P. Hratchian, A. F. Izmaylov, J. Bloino, G. Zheng, J. L. Sonnenberg, M. Hada, M. Ehara, K. Toyota, R. Fukuda, J. Hasegawa, M. Ishida, T. Nakajima, Y. Honda, O. Kitao, H. Nakai, T. Vreven, J. A. J. Montgomery, J. E. Peralta, F. Ogliaro, M. Bearpark, J. J. Heyd, E. Brothers, K. N. Kudin, V. N. Staroverov, T. Keith, R. Kobayashi, J. Normand, K. Raghavachari, A. Rendell, J. C. Burant, S. S. Iyengar, J. Tomasi, M. Cossi, N. Rega, J. M. Millam, M. Klene, J. E. Knox, J. B. Cross, V. Bakken, C. Adamo, J. Jaramillo, R. Gomperts, R. E. Stratmann, O. Yazyev, A. J. Austin, R. Cammi, C. Pomelli, J. W. Ochterski, R. L. Martin, K. Morokuma, V. G. Zakrzewski, G. A. Voth, P. Salvador, J. J. Dannenberg, S. Dapprich, A. D. Daniels, O. Farkas, J. B. Foresman, J. V. Ortiz, J. Cioslowski, D. J. Fox, *Gaussian 09 Revision E.01*, Gaussian Inc., Wallingford, **2013**.
[58] M. D. Hanwell, D. E. Curtis, D. C. Lonie, T. Vandermeersch, E. Zurek, G. R. Hutchison, *J. Cheminformatics* **2012**, *4*, 17.
[59] J. R. Cheeseman, G. W. Trucks, T. A. Keith, M. J. Frisch, *J. Chem. Phys.* **1996**, *104*, 5497–5509.

the project is currently investigated and planned to be published.

Author contributions:

Patrick Bayer wrote the manuscript and performed reactions.
Robin Stuhr assisted in the manuscript and performed reactions.
The work was supervised by Prof. Dr. Axel Jacobi von Wangelin.

1 Introduction

Plant oils such as cardanol or castor oil are produced in annual multiton scale (5×10^5 and 3×10^5 t/a, respectively) and thus provide and ideal base for investigations on the synthetic use of renewable feedstock. Cardanol, a technical oil resulting as waste from the so-called hot oil process during cashew nut processing, consists of three major phenolic compounds with a various degree of unsaturation. Castor oil, in contrast, mainly contains the triglyceride of ricinoleic acid, a mono-unsaturated fatty acid (Scheme 45).[1,2] While the price per kilogram is below 500 $ per ton for both liquids, castor oil does not arise as waste material as the oil is obtained from the nut, contrary to the cashew nut shell liquid (CNSL).

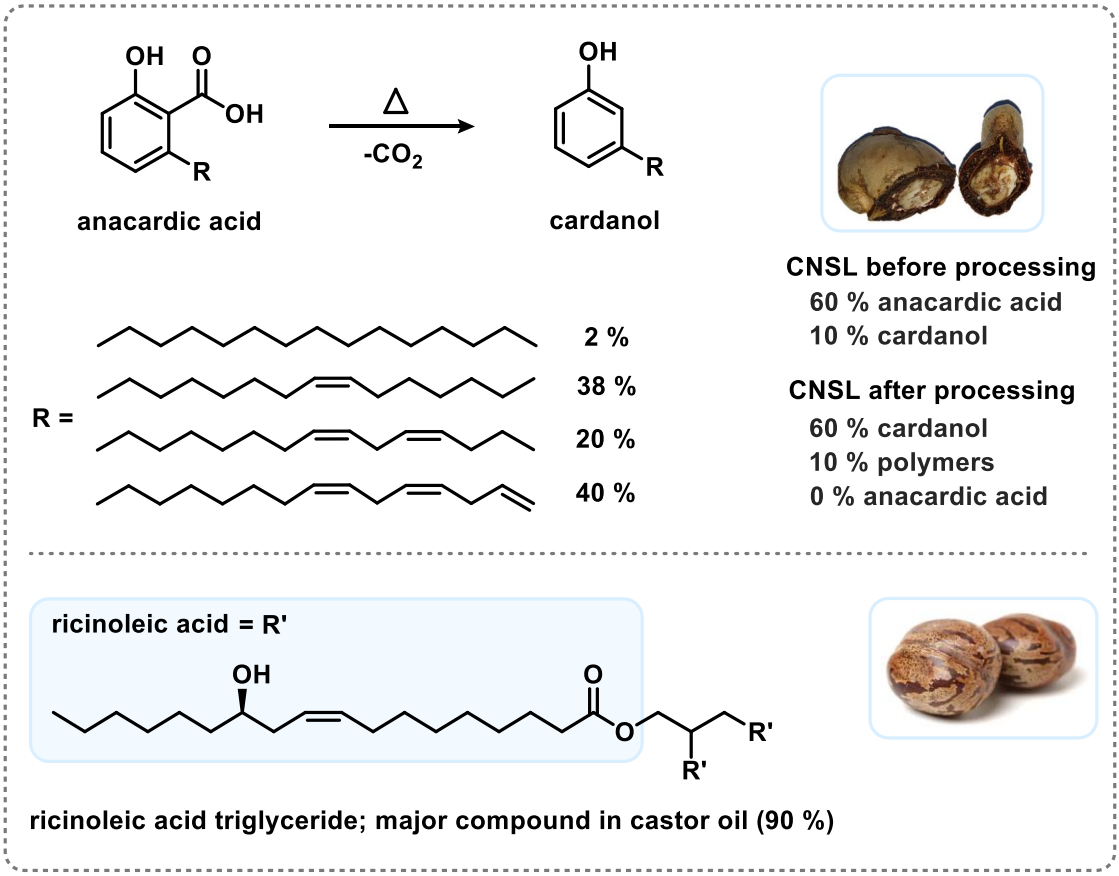

Scheme 45. Cardanol and major component of castor oil.

Levels of cardanol and anacardic acid in CNSL are highly dependent on the extraction method. In the hot oil process, raw nuts are passed through a hot CNSL bath (200 °C) releasing the cashew nut shell liquid; all of the anacardic acid is decarboxylated (Scheme 45). The roasting method used charred shells and

applies a very high pressure which forces the liquid out of the shell. By the screw press method, raw shells are screwed by a hydraulic press and an anacardic-rich CNSL is obtained. A cardanol-rich CNSL is typically obtained by a subsequent distillation.[3]

The synthesis of polyols from these olefins, which may be applied in polyurethane or polyester resin synthesis (see scheme 50, p. 112), is feasible by a variety of synthetic pathways such as ozonolysis, epoxidation/ring opening, or epoxidation with subsequent hydrogenation. An ene-type photooxygenation with singlet oxygen constitutes a 100 % atom-economic synthesis of allyl alcohols or, in a one-step procedure combined with catalytic amounts of $Ti(O^iPr)_4$,[4] α-hydroxy epoxides which can undergo a subsequent ring-opening with nucleophiles like alcohols. The group of Michael A. R. Meier investigated the photosensitized oxygenatio of oleic acid triglyceride, a plant oil similar to ricinoleic acid triglyceride without a hydroxyl group, and the subsequent transformation of primary products to polyols (Scheme 46).

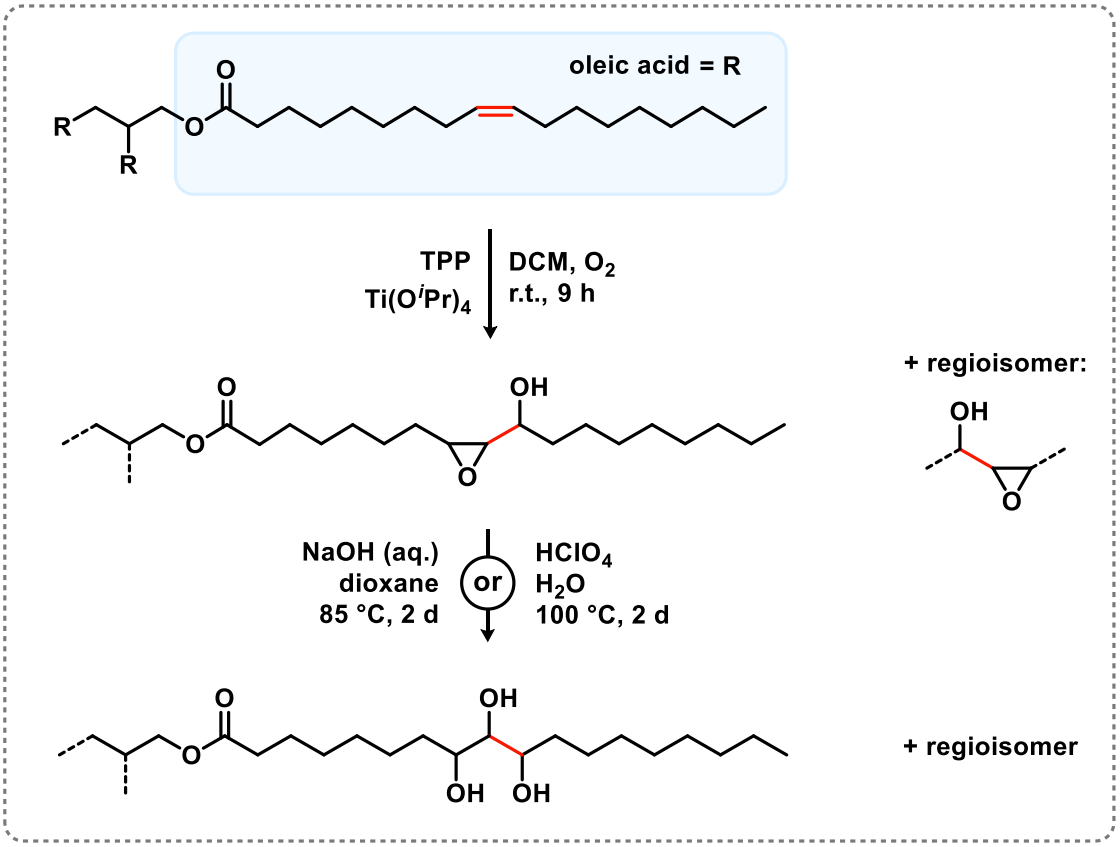

Scheme 46. Investigations on the photooxygenation of oleic acid triglyceride from 2018.[5]

Tetraphenylporphyrin (0.01 mol%) in DCM was applied as photosensitizer, together with titanium(IV) isopropoxide (3 mol%). After 9 h in a photochemical reactor, the α-hydroxy epoxides were obtained without further workup. While yields of 65 % are reported for the subsequent triol formation applying $HClO_4/H_2O$ or NaOH/dioxane, no yield is stated for the preliminary photooxygenation reaction; the article has a focus on conversion of the plant oil derived α-hydroxy epoxides and thorough analysis of the resulting products. The use of large quantities of the halogenated solvent dichloromethane (39 equivalents with respect to to the substrate) and nonexistent information on space-time yields mark a drawback towards a potential industrial use.[5]

Cardanol is technically available as a mixture of four or more compounds and features a phenol moiety. Reactivity and possibilities for further transformations cannot be easily predicted from the reactivity of the similar triglycerides. Titanium(IV) isopropoxide, for example, can bind to the hydroxyl group of a phenol and inhibit an efficient self-epoxidation of the primarily formed hydroperoxides.

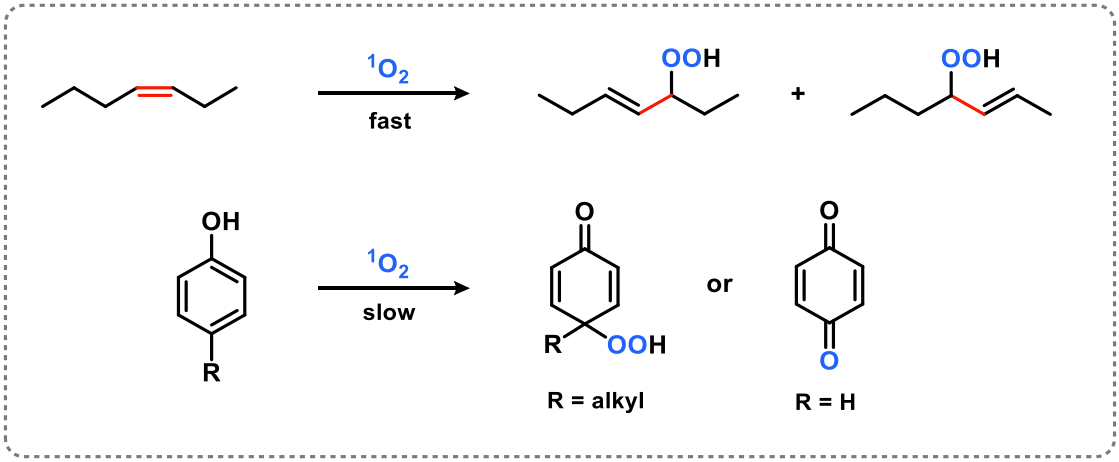

Scheme 47. Reactivity of $^1O_2$ with multiple oxidation sites of the cardanol molecule.

In addition, a phenol can by oxidized to 1,4-benzoquinone by singlet oxygen (Scheme 47),[6] and $Ti(O^iPr)_4$ is known to catalyze the ring-opening of an epoxide by a phenol[7] which may lead to a polymerization of the reaction mixture.

2 Results and Discussion

We obtained cardanol from the Cardolite® company which provided us with free samples of their commercial NC-700 CNSL mixture. To purify the industrial mixture from remaining cardol (a compound similar to cardanol with an additional hydroxyl group at the phenol moiety) and tiny red stain particles, it was subjected a column chromatography with subsequent HPLC analysis (Figure 11).

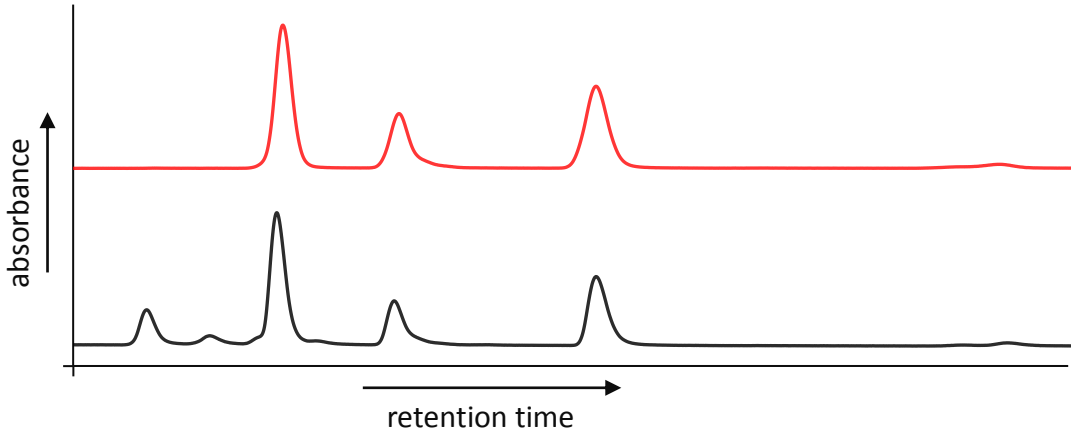

Figure 11. HPLC/UV-VIS spectra of NC-700 before (black) and after (red) column chromatography. Detector wavelength 220 nm, reversed-phase column.

By integration of the HPLC spectra recorded at 280 nm (absorption only by the phenol moiety) and analysis by NMR and MS, the composition of the mixture (in the red chromatogram: from left to right) was determined to 40 % (cardanol, one double bond), 20 % (cardanol, two double bonds), 38 % (cardanol, three double bonds), and 2 % (saturated cardanol). From literature-reported relative reaction rates of olefins, we concluded cardanol is about half as reactive as phenylcyclohexene in a singlet oxygen photooxygenation (see scheme 6 and scheme 40).

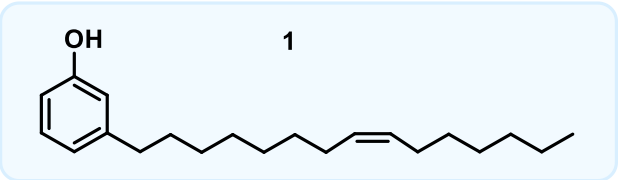

Scheme 48. Monoene cardanol (**1**).

We could isolate the monoene cardanol (Scheme 48) by semi-preparative RP-HPLC in sufficient amounts (about 2 g per day) to investigate the reactivity of this compound class towards Schenck ene oxygenation with singlet oxygen in our micro-flow reactor. The reaction mixture after oxygenation of a mixture of multiple-unsaturated cardanols is too complex for identification of single compounds and determination of complete by ^{1}H-NMR; thus, preliminary mechanistic investigations were conducted with the monoene.

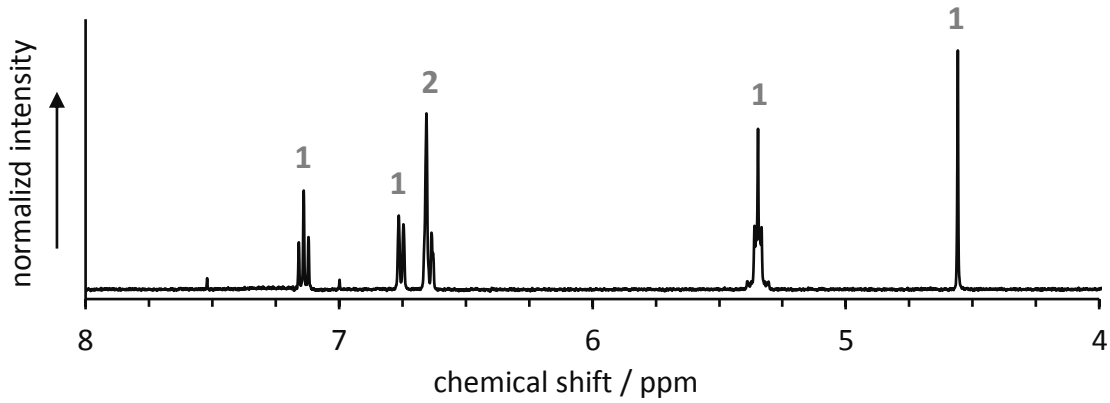

Figure 12. ^{1}H-NMR of **1** in $CDCl_3$. Integration results are denoted in gray.

The phenolic O*H* proton is visible between 4 and 5 ppm when dry and acid-free $CDCl_3$ is used for NMR measurements. The aromatic region above 6.5 ppm shows a triplet, two doublets, and a singlet overlaying one of the doublets. After photooxygenation of **1** (0.05 M in MeCN, 1 mM MB, 12 bar O_2, 12.8 m reactor tubing length, 0 °C, 0.5 mL/min liquid flow rate, 8 min irradiation time) in the micro-flow reactor, the substrate was completely consumed.

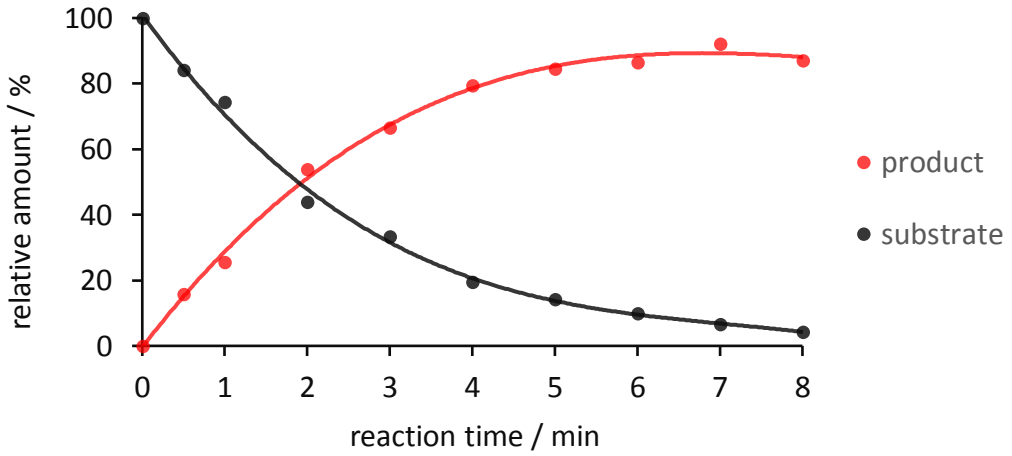

Figure 13. Yield of hydroperoxide over time. Determined by ^{1}H-NMR, Me_2SO_2 as standard.

By addition of the oxidation-stable standard dimethylsulfone (Me_2SO_2), substrate and products can be quantified over time (Figure 13). Measuring chemical kinetics in flow is different from taking a sample in a batch reaction as samples can only be taken at the outlet of the capillary; in any section of the flow reactor, the conversion is different. Thus, the continuous flow reaction was first started without the light source. When a steady and continuous slug flow was established, the light source was turned on and small samples were collected at the outlet. By addition of $CDCl_3$ and measuring ^{1}H-NMR with 512 scans, quantitation with these small volumes was successful.

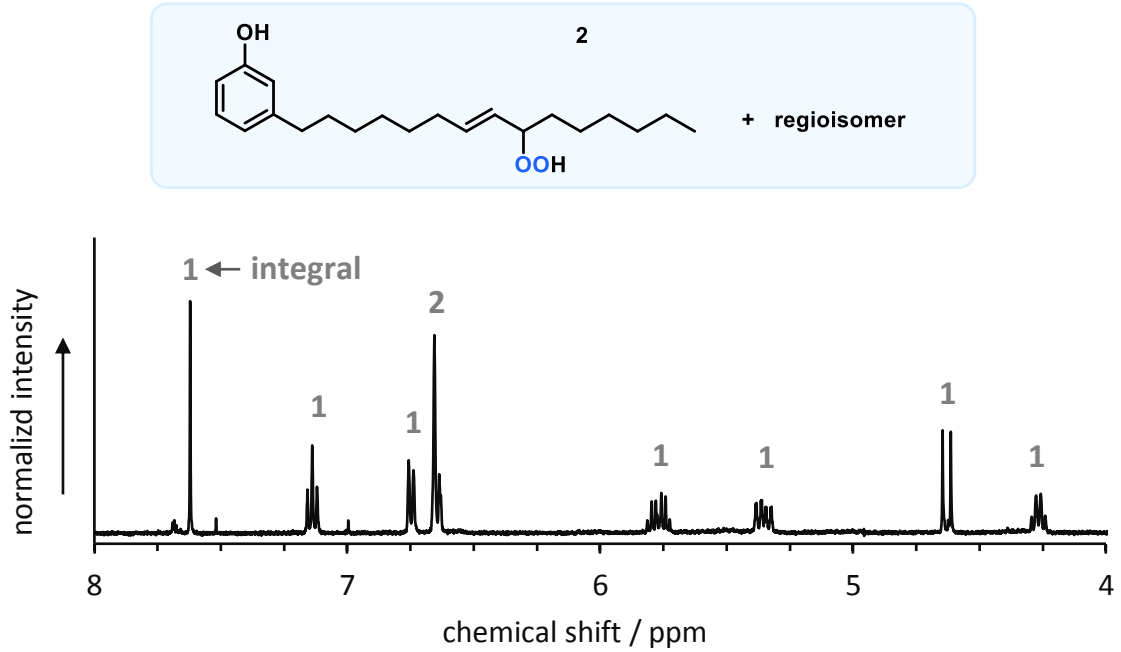

Figure 14. Structure and ^{1}H-NMR of **2** in $CDCl_3$ after photooxygenation of **1**. Integration results are denoted in gray.

The conversion of the cardanol monoene can also be calculated by comparison of integrals at a chemical shift of 5.3 and 5.8 ppm (complete conversion when equal). Two regioisomeric products are formed, which is also apparent from the ^{1}H-NMR spectrum: distinct peaks of phenolic O*H* protons are visible at a chemical shift of 4.6 ppm, each one with an integral of 0.5. The corresponding ^{13}C-NMR spectrum shows two products with chemicals shifts of related carbon atoms differing between 0.0 and 0.2 ppm. Thus, a 1:1 mixture of regioisomers was formed.

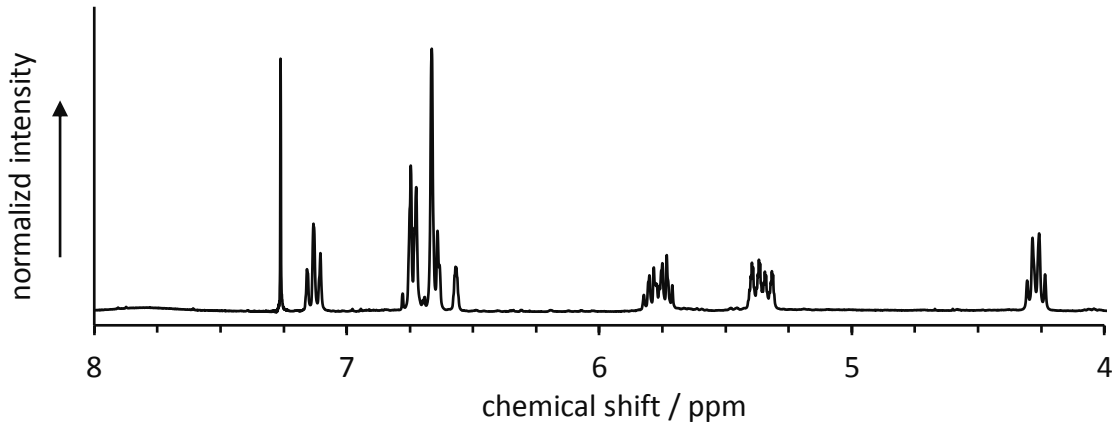

Figure 15. ^{1}H-NMR spectrum ($CDCl_3$) after extended oxygenation of **1** with singlet oxygen.

When the reaction solution was oxygenated for 30 more minutes, a change in the aromatic region in the ^{1}H-NMR is apparent: the phenol moiety was slowly oxidized, with new peak shifts very similar to the ones of 1,4-toluquinone (Figure 15).

The ^{1}H-NMR spectrum after oxygenation of the diene cardanol is much more complex, revealing many more products are formed. This can be anticipated by consideration of the multiple reaction sites of cardanol compounds with more than one reactive double bond (Scheme 49).

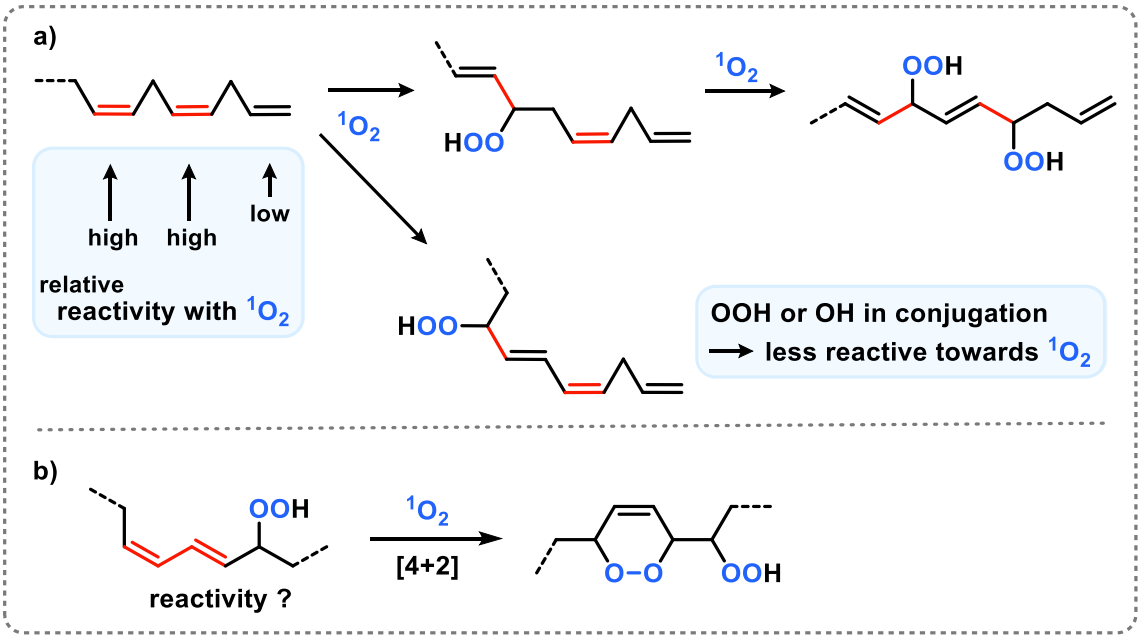

Scheme 49. Reactivity of $^{1}O_2$ with a non-conjugated triene and exemplary reactions (a), determination of rate of endoperoxide formation as part of future investigations (b).

Each disubstituted double bond reacts quickly to an allyl hydroperoxide; depending on the regioisomer formed, a second reaction with singlet oxygen is feasible.

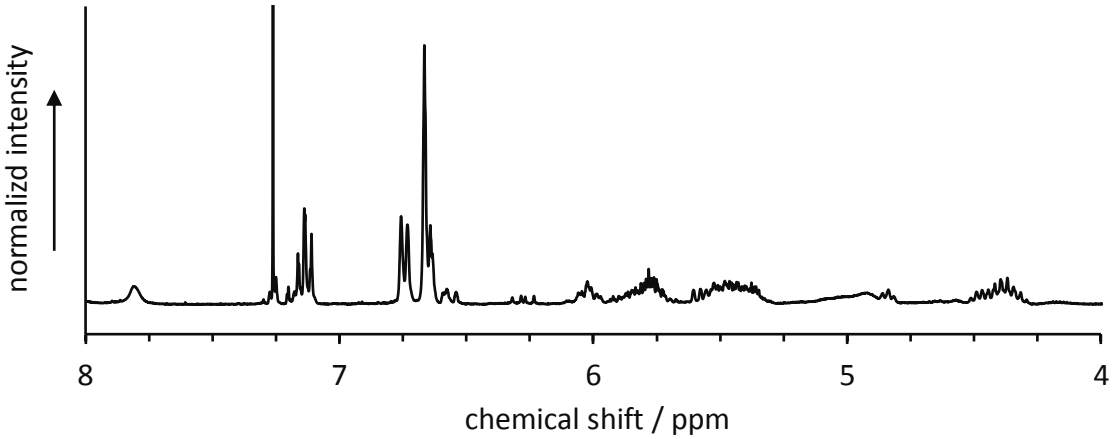

Figure 16. ^{1}H-NMR spectrum ($CDCl_3$) of the complex mixture formed by oxygenation of the cardanol diene substrate.

Attempts to isolate single compounds after oxygenation of the diene (see figure 16 for the ^{1}H-NMR spectrum) by chromatography or analysis by mass spectrometry of the complex mixture were not yet successful. The formed 1,3-dienes can further react with singlet oxygen in a [4+2]-cycloaddition reaction;[8] however, this possible pathway needs to be further investigated by the help of spectroscopic studies.

The formation of stable compounds can be achieved by transformation such as reduction of the allyl hydroperoxides to an allyl alcohol or titanium(IV)-catalyzed transformation to α-epoxy alcohols. By simple addition of 1.1 equiv. (with respect to the amount of alkene moieties in the substrate) of PPh_3 to the reaction mixture after completion of the photooxygenation, complete conversion to the corresponding alcohols could be achieved within minutes. Notably, the raw product mixture could not be analyzed or quantified by thin-layer chromatography or NMR – polarity of the compounds and chemical shift of the phenol moiety differs investigating the products before and after column chromatography.

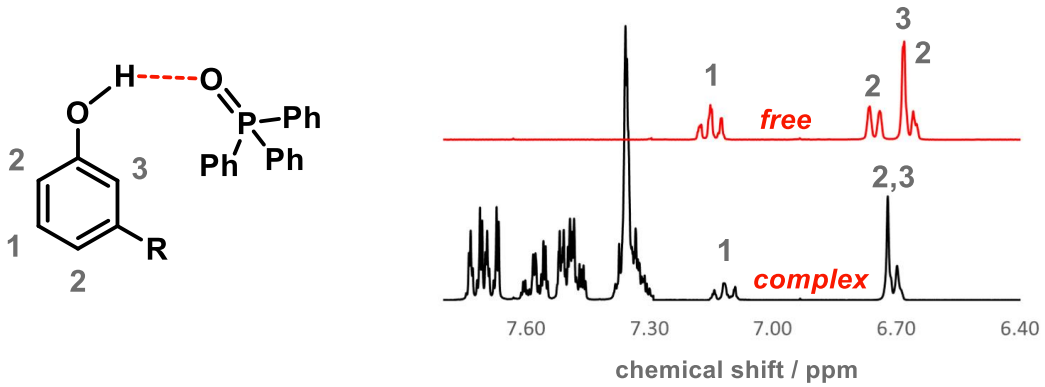

Figure 17. Schematical respresentation of complex formation and corresponding ^{1}H-NMR spectra (black: spectrum after PPh_3O addition). Grey numbers indicate hydrogen positions.

We could reproduce this finding by addition of PPh_3O to a solution of prior isolated cardanol monoene allyl alcohol: a literature-known complex between the phenol and triphenyl phosphine oxide is likely formed in solution (Figure 17).[9] The addition of PPh_3 had no effect.

Acetonitrile or ethanol, in combination with the sensitizer methylene blue, constitute a valuable replacement for the sensitizer system DCM/TPP in the context of green chemistry. The use of titanium(IV) isopropoxide for *in situ* epoxidation, however, is not feasible with hygroscopic solvents such as acetonitrile or ethanol unless dry solvents were used. A solvent-free approach as discussed in chapter V (p. 139) was not successful so far as the monoene substrate is not easily available in large quantities and the substrate is comparatively viscous and unreactive. In a two-step protocol, however, we could convert the previously isolated monoene hydroperoxide with $Ti(O^iPr)_4$ in DCM. We investigated the reaction with different amounts of titanium catalyst (1, 3, 5, 10, and 50 mol%). When 50 mol% catalyst were applied, a red and insoluble polymeric material was formed after 3 h – likely by a literature-known $Ti(O^iPr)_4$-catalyzed epoxide ring opening by phenols in solution.[7] We did not yet investigate this polymerization reaction further, although it may constitute a novel one-step polymerization reaction for cardanol and similar compound classes.

Applying up to 10 mol% $Ti(O^iPr)_4$ in DCM, the hydroperoxides were converted without visible polymerization (Table 3).

Table 3. Conversion of cardanol monoene hydroperoxide with various amounts of [Ti] [a]

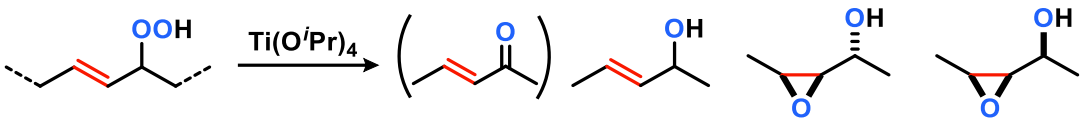

Entry	[Ti] / mol%	rxn time	NMR yield / %			
			st. mat.[b]	all. alc.[c]	*anti*-EPA[d]	*syn*-EPA[e]
1	1	72 h	24	27	19	33
2	3	3 h	37	24	9	25
3	3	72 h	-	27	24	44
4	5	72 h	-	29	23	47
5	10	3 h	15	27	13	40

[a]Conditions: starting material (300 mg), DCM (40 mL), [Ti] = Ti(O^{i}Pr)$_4$, stirred at 0 °C under N_2. Quenched with H_2O and washed with brine after reaction time. [b]starting material (allyl hydroperoxide). [c]allyl alcohol. [d]*anti*-configured α-epoxy alcohol. [e]*syn*-configured α-epoxy alcohol.

1 mol% catalyst was not sufficient to convert the starting material, even in 72 h (entry 1). When 5 mol% titanium(IV) isopropoxide were applied, the substrate was completely converted in 72 h, while shorter reaction times should also be efficient and still must be investigated under these conditions. The formation of the allyl alcohol as side product could not be suppressed with any of the investigated catalyst loadings, with yields of 30% in all cases; other side products like unsaturated ketones were detected in small yields but not quantified. The wished product, an α-epoxy alcohol, was formed preferentially *syn*-configured (*d.r.* 2:1) in up to 70% NMR yield. Notably, the cardanol α-epoxy alcohols were not yet fully characterized; however, we isolated the compounds quantified in table 3 (flash silica chromatography of a small amount of the product mixture, Pe/EA 4/1, TLC R_f-values: 0.44 substrate, 0.37 all. alc., 0.28 *anti*-EPA, 0.20 *syn*-EPA) and compared ^{1}H-NMR spectra with literature-known α-epoxy alcohols, a compound class with characteristic peak shifts (the *syn*-diastereomer features three characteristic peaks with shifts of 2.7, 3.0, and 3.5 ppm, whereas the *anti*-

diastereomer features peak shifts of 2.7, 3.0, and 4.0 ppm).[10] Although these results have to be compared with future investigations of one-step procedures in DCM in continuous flow, yields of 70% for the conversion of this complex substrate with 5 or less mol% titanium(IV) isopropoxide are a promising basis for following studies. Substitution of titanium(IV) isopropoxide by $VO(acac)_2$ or $MoO_2(acac)_2$ may give better results converting substrates such as cardanol; however, these catalysts absorb visible light alike the applied singlet oxygen sensitizers.[11] Applicability of the obtained product mixture for subsequent epoxide ring opening reactions (see scheme 46) is part of ongoing research in our group.

Subsequently, large-scale photooxygenation of the technical cardanol mixture (NC-700) without prior workup or separation of substrates was investigated. The mixture was oxygenated in an enlarged reactor (see figure 20; 40 m capillary, instead of up to 12.8 m used in prior oxygenation reactions in our group) to allow for high productivity, and different oxygen and solvent flow rates were studied (Table 4). A solvent-free approach as discussed in chapter V yielded a maximum of only 40% conversion of the monoene so far, with reasons like catalyst degradation by the technical cardanol mixture and a high viscosity of the substrates generating a high pressure in the capillary (Figure 18; catalyst has a pink color).

Figure 18. Catalyst degradation during solvent-free cardanol oxygenation (reactor inlet at bottom; left) and FEP capillary bursting above a combination of 45 °C and 60 bar (right).

We decided to use a solution flow rate of 2.0 mL/min which allowed for a conversion of the substrates of more than 85% (Table 4, entry 4). It is important to note that 2 % of saturated cardanol (see scheme 45, p. 100) remain in solution

after oxygenation and thus can be used to quantify the conversion of unsaturated cardanols. Peak areas before and after oxygenation were compared *via* HPLC/UV-VIS chromatograms at 220 nm; as acetonitrile is a common solvent for reversed-phase HPLC, the reaction mixture could be directly injected.

Table 4. Photooxygenation of technical cashew nut shell liquid (NC-700 from Cardolite®) [a]

Entry	substrate conc. in mol L^{-1}	solution FR in mL min^{-1}	dye conc. in mol%	conversion of		
				monoene	diene	triene
1	neat [b]	0.1	5 [c]	40	63	55
2	0.3	1.0	1	complete conversion		
3	0.3	3.5	1	80	90	85
4	0.3	2.0	1	85	95	90

[a]Conditions: Reactor length 40 m, 45 °C, solvent MeCN, dye methylene blue, oxygen flow rate adjusted to solution flow rate (FR). Conversion calculated by the help of HPLC/UV-VIS. [b]reaction conducted without solvent, see chapter V. [c]Methylene blue and PrTPP (see chapter V), 2.5 mM each, were applied; the sensitizers were completely quenched (solution no more intensely colored) after the reaction.

With these reactor settings (see also left picture in figure 19; conversion of 11 g min^{-1}), 1 kg of NC-700 was converted in the photo-flow reactor system and subsequently reduced by Na_2SO_3 (70 °C, 12 h).

Figure 19. Large-scale continuous photooxygenation of technical CNSL (left) and subsequent reduction by sodium sulfite (right).

We again applied acetonitrile as solvent for high productivity, whereby substitution by the more environmentally friendly ethanol or methanol will be part of future investigations.

While the resultant polyol mixture is under current investigation for applicability as networking agent for polyurethane polymer synthesis (Scheme 50), results on the hydroxyl (or OH) number are already available.

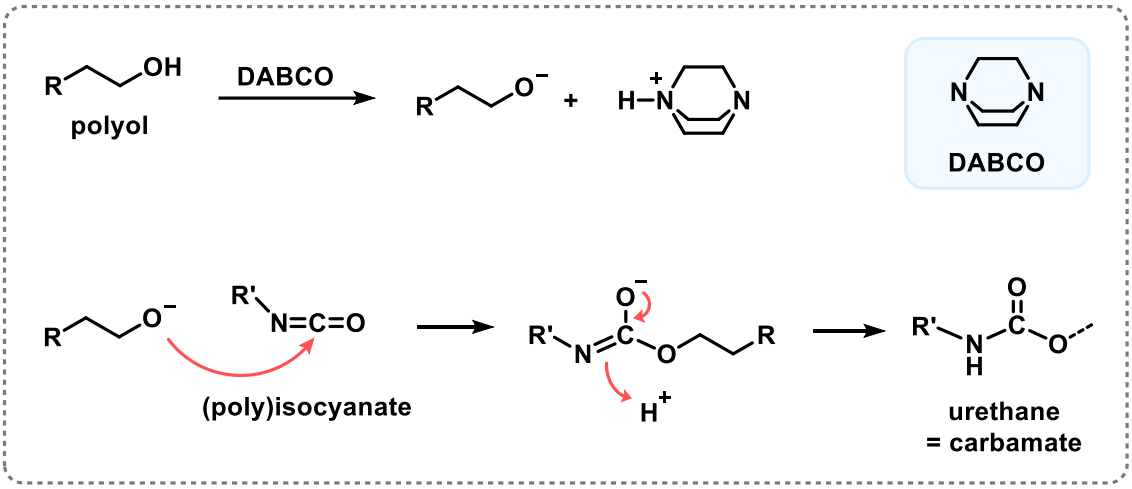

Scheme 50. Polyurethane formation using polyols as networking agents. DABCO = 1,4-diazabicyclo[2.2.2]octane.

This value is defined as the amount of potassium hydroxide (in mg) required to neutralize the acetic acid taken up on acetylation of one gram of the investigated substance that contains hydroxyl groups; special care must be taken to obtain accurate values when a phenol moiety is present.[12] Analysis of our resultant product mixture by an external research group revealed an OH number of 360 – a value we could reproduce by studying the reduction of the formed hydroperoxides with triphenyl phosphine instead of Na_2SO_3. By calibrating PPh_3 against the internal standard dodecanenitrile *via* GC-FID, the consumed PPh_3 and thus the amount of OOH groups present in the converted product mixture could be determined. An OH number of 360 is tantamount to 1.1 hydroxyl groups per product in addition to the phenol moiety at the determined mean conversion rate of 90%.

3 Conclusion

Cashew nut shell liquid obtained by the technical hot oil process was investigated regarding its composition and suitability for photooxygenation reactions with subsequent transformation to stable products. The substrate mixture mainly contained cardanols with a varying degree of unsaturation with high amounts of monoene and triene (40% each). High conversion rates of 11 g min^{-1} were achieved with an especially long flow pathway of 40 meters in a photo-flow microreactor. The obtained allyl hydroperoxide mixture was analyzed by ^{1}H-NMR, HPLC/UV-VIS and GC-FID, and converted to allyl alcohols as well as α-epoxy alcohols. An OH number of 360 of the resultant product mixture after reduction with Na_2SO_3 already revealed an applicability as networking agent for polyurethane polymerization reations. Treating the allyl hydroperoxides with 5 mol% of titanium(IV) isopropoxide in DCM, a product mixture containing 70% α-epoxy alcohols resulted after a reaction time of 72 h. Higher amounts of 50 mol% Ti(IV) led to polymerization of the mixture, possibly by ring-opening of the epoxides by the phenol moiety of the substrates/products.

Future studies will include the substitution of the solvent acetonitrile by the more environmentally friendly ethanol, and optimization of a solvent-free approach which did not allow for more than 50% conversion yet. Investigation of reaction conditions during [Ti] or different metal-catalyzed epoxidation reactions will show if yields of more than 70% of epoxy alcohols can be achieved, with subsequent studies on flow-assisted oxidative ring-opening to triols. Comparison of reaction rates of cardanols with a varying degree of unsaturation and characterization of products after conversion of dienes or trienes will lead to a better understanding of the behaviour of the substrate mixture towards photooxygenation.

4 Experimental Part

Commercial chemicals (≥98% purity) were used as obtained without further purification; Methylene blue (MB) was obtained and applied as the hydrate (CAS 122965-43-9); the technical NC-700 cardanol oil was obtained as free sample from the *Cardolite* company. O_2 gas (99.995%) was applied with a *Brooks Instrument* mass-flow control unit, the system pressure was adjusted by an *IDEX* back-pressure cartridge. TLC was performed using commercial silica gel coated aluminum plates (DC Kieselgel 60 F_{254}, *Merck*); visualization was done using UV light. Staining was realized with a solution of phosphomolybdic acid in ethanol (7 wt%). To distinguish between cardanols with various degree of unsaturation, silver nitrate impregnated silica (SNIS) was used (TLC preparation: 2 g $AgNO_3$ in 10 mL H_2O, added onto normal TLC plates, and dried for 2 min with a heat gun to get rid of water from the plate; the fluorescent marker does no more working afterwards, and phosphomolybdic acid stain was applied). HPLC analyses were carried out on a *Bischoff* HPLC system featuring a DAD 4L UV-VIS detector, 3350 HPLC pump, 0.1-20.0 mL/min pump head, ProntoSIL EUROBOND C18 5 µm (analytical 150x4.6 mm, semi-preparative 150x20 mm) columns. Product yields were determined from isolated materials after normal or flash column chromatography on silica gel (mesh 230-400) or for optimization and screening purposes by quantitative GC-FID measurements, with dodecanenitrile as internal standard on an *Agilent* 7820A GC-System with N_2 as carrier gas. Low-resolution mass spectrometry (LRMS) was carried out on an *Agilent* 6890N GC-System coupled to a 5975 MSD unit and H_2 as carrier gas. NMR spectral data were collected on a *Bruker* Avance 300 (300 MHz for ^1H; 75 MHz for ^{13}C) and a *Bruker* Avance 400 (400 MHz for ^1H; 100 MHz for ^{13}C) spectrometer at 25 °C, typically in $CDCl_3$. Solvent residual peaks or TMS from TMS-containing deuterated solvents were used as internal standard for NMR measurements. The quantification of ^1H cores was obtained by integration of resonance signals. Abbreviations used in ^{13}C-NMR spectra: C_p – primary carbon, C_s – secondary carbon, C_t – tertiary carbon, C_q – quaternary carbon, C_{sp2} – sp^2 hybridization at this atom, C_{sp3} – sp^3 hybridization at this atom. Abbreviations used in ^1H-NMR spectra: s – singlet, bs – broad singlet, d – doublet, t – triplet, q – quartet, m – multiplet, R – organic rest, not hydrogen.

For details on the photo-flow reactor and reactor pictures or schemes, refer to chapter V, especially figure 21 and figure 22 (p. 133), and its experimental section (p. 141 and following).

Cardolite Corporation NC-700 CNSL mixture

The cardanol was obtained as a dark red liquid.

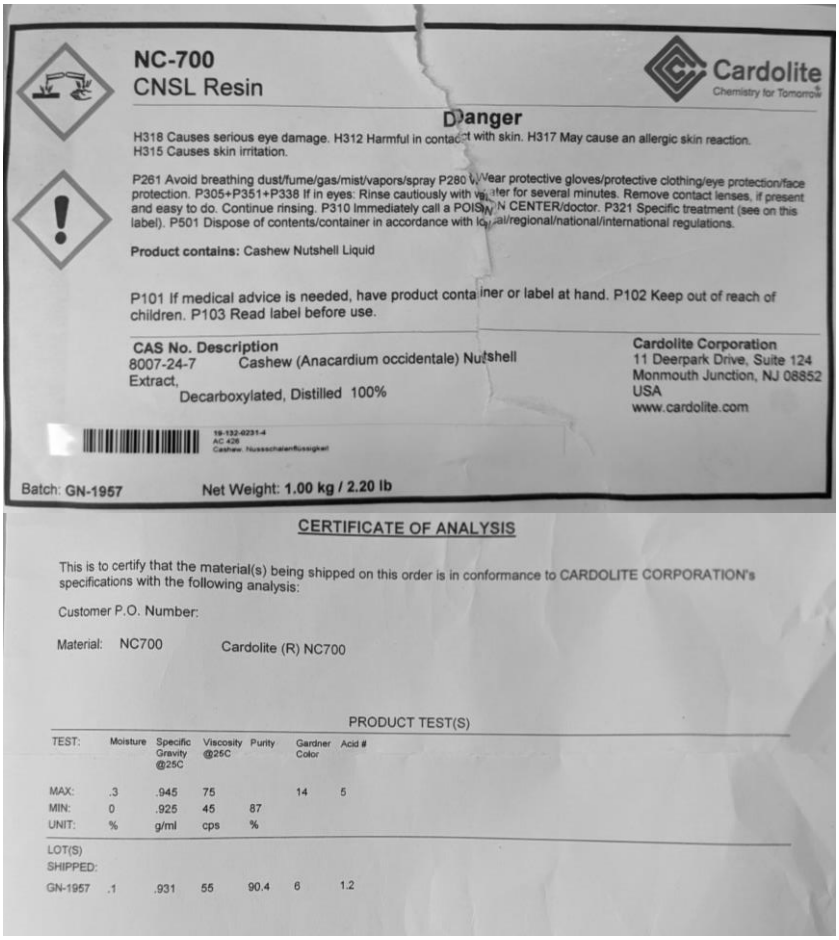

NC-700
CNSL Resin

Cardolite
Chemistry for Tomorrow

Danger

H318 Causes serious eye damage. H312 Harmful in contact with skin. H317 May cause an allergic skin reaction. H315 Causes skin irritation.

P261 Avoid breathing dust/fume/gas/mist/vapors/spray P280 Wear protective gloves/protective clothing/eye protection/face protection. P305+P351+P338 If in eyes: Rinse cautiously with water for several minutes. Remove contact lenses, if present and easy to do. Continue rinsing. P310 Immediately call a POISON CENTER/doctor. P321 Specific treatment (see on this label). P501 Dispose of contents/container in accordance with local/regional/national/international regulations.

Product contains: Cashew Nutshell Liquid

P101 If medical advice is needed, have product container or label at hand. P102 Keep out of reach of children. P103 Read label before use.

CAS No. Description
8007-24-7 Cashew (Anacardium occidentale) Nutshell Extract, Decarboxylated, Distilled 100%

Cardolite Corporation
11 Deerpark Drive, Suite 124
Monmouth Junction, NJ 08852
USA
www.cardolite.com

Batch: GN-1957 Net Weight: **1.00 kg / 2.20 lb**

CERTIFICATE OF ANALYSIS

This is to certify that the material(s) being shipped on this order is in conformance to CARDOLITE CORPORATION's specifications with the following analysis:

Customer P.O. Number:

Material: NC700 Cardolite (R) NC700

PRODUCT TEST(S)

TEST:	Moisture	Specific Gravity @25C	Viscosity @25C	Purity	Gardner Color	Acid #
MAX:	.3	.945	75		14	5
MIN:	0	.925	45	87		
UNIT:	%	g/ml	cps	%		
LOT(S) SHIPPED:						
GN-1957	.1	.931	55	90.4	6	1.2

HPLC separation of the NC-700 mixture:

HPLC separation was conducted with the Bischoff HPLC system in combination with the semi-preparative column (ID 20 mm). Direct injection and a separation flow rate of 19 mL min^{-1} MeCN allowed for separation of 500 mg pre-cleaned (by column chromatography, 40% EA in Pe) NC-700 CNSL per separation. The peak with number 3 depicts the monoene cardanol in the chromatogram:

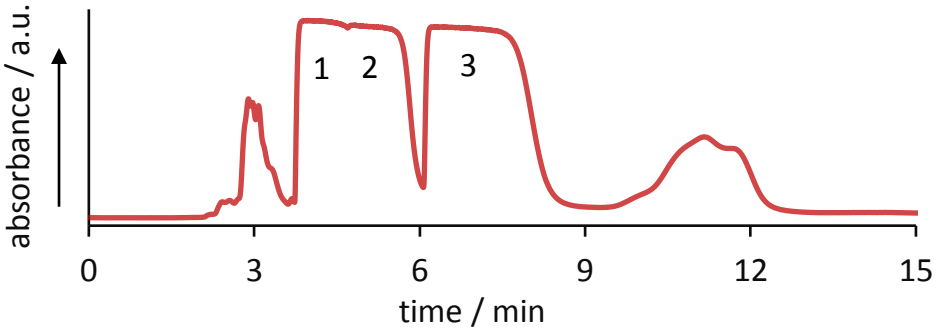

R_f (Pe/EA 4/1) = 0.9. ^{1}H-NMR (300 MHz, $CDCl_3$): δ [ppm] = 7.14 (t, ^3J = 7.7 Hz, 1H), 6.75 (d, ^3J = 7.7 Hz, 1H), 6.65 (d, ^3J = 7.7 Hz, 2H), 5.38 – 5.31 (m, 2H), 4.55 (s, 1H), 2.55 (t, ^3J = 7.4 Hz, 2H), 2.10 – 1.94 (m, 4H), 1.69 – 1.55 (m, 2H), 1.45 – 1.25 (m, 16H), 0.87 (t, ^3J = 6.45 Hz, 3H).

General procedure for solvent-free photooxygenation:

The sensitizer was dissolved in the solvent (ultrasonication) at room temperature. Subsequent filtration in case of methylene blue as sensitizer assured no particles are left in solution. After the substrate was added to the sensitizer solution, it was pumped through commercial FEP or PFA capillary tubing (1/16" OD, 1/32" ID, from Bohlender; irradiated tubing length 12.8 or 39.9 m, tubing wrapped around a glass cylinder with an OD of 65 mm) by an HPLC pump (typical flow rate between 0.5 and 2.0 mL/min). O_2 gas (99.995 %) was applied with a Brooks Instruments mass-flow control, the system end pressure was adjusted by an IDEX back-pressure cartridge. The oxygen flow rate was adjusted so that a laminar slug flow resulted and O_2 was not completely consumed when the solution left the back-pressure cartridge at the end of the reactor tubing. Temperature control was applied from the outside of the reactor coil by a temperature-controlled silicon oil bath. The reactor coil was irradiated from the inside by 24 water-cooled Cree MK-R white LEDs (190 W); typical irradiation time: 7 to 20 min. For more details on the reactor and reactor pictures and schemes, refer to chapter V, especially figure 21 and figure 22 (p. 133).

Photooxygenation of monoene cardanol:

The monoene was oxygenated and purified via column chromatography with EA in pentane (20 % EA) as eluent to give the monoene hydroperoxide regioisomeric mixture in a yield of 86% as orange oil. The regioisomers cannot be separated by normal silica chromatography. Silver nitrate impregnated silica (SNIS) TLC was used for quick estimation of conversion.

R_f values on SNIS TLC (Pe/EA 2/1):
0.91 (monoene)
0.79 (dienene)
0.23 (triene)

Left: Conversion of mono-ene in solvent-free procedure (SF) not complete.

R_f (Pe/EA 4/1) = 0.44. ^{1}H-NMR (300 MHz, $CDCl_3$): δ [ppm] = 7.65 (s, 1H), 7.14 (t, ^3J = 7.7 Hz, 1H), 6.74 (d, ^3J = 7.7 Hz, 1H), 6.64 (d, ^3J = 7.7 Hz, 2H), 5.81 – 5.73 (m, 1H), 5.40 – 5.32 (m, 1H), 4.69 (d, 1H), 4.27 (q, ^3J = 6.7 Hz, 14.7 Hz, 1H), 2.55 (m, 2H), 2.10 – 2.04 (m, 2H), 1.71 – 1.24 (m, 18H), 0.91 – 0.85 (m, 3H).

Reduction of the monoene hydroperoxide to allyl alcohol in small scale:

The allyl hydroperoxide (0.397 g, 1.0 eq.) and triphenyl phosphine (0.528 g, 1.7 eq.) were dissolved in MeCN (15 mL) and stirred for 30 min. The solvent was removed under reduced pressure and the product was isolated from the crude mixture *via* column chromatography with EA in pentane (20 % EA) as eluent. The title compound was gained as yellow oil (0.322 g, 85 %).

R_f (Pe/EA 4/1) = 0.37. ^{1}H-NMR (300 MHz, $CDCl_3$): δ [ppm] = 7.12 (t, ^3J = 7.7 Hz, 1H), 6.72 (d, ^3J = 7.7 Hz, 1H), 6.65 (d, ^3J = 7.7 Hz, 2H), 5.68 – 5.57 (m, 1H), 5.47 – 5.40 (m, 1H), 4.06 – 4.02 (m, 1H), 2.57 (t, ^3J = 7.1 Hz, 2H), 2.05 – 1.98 (m, 2H), 1.61 – 1.20 (m, 18H), 0.91 – 0.85 (m, 3H). ^{13}C-NMR (75 MHz, $CDCl_3$): δ [ppm] = 155.8, 155.7 (C), 144.7, 144.6 (C), 132.8, 132.7 (CH), 132.6, 132.4 (CH), 129.3, 129.3 (CH), 120.7, 120.6 (CH), 115.4, 115.4 (CH), 112.6, 112.56 (CH), 73.6, 73.5 (CH), 37.3, 37.2 (CH_2), 35.7, 35.6 (CH_2), 32.2, 32.0 (CH_2), 31.8, 31.4 (CH_2), 31.2, 31.1 (CH_2), 29.4, 29.3 (CH_2), 29.2, 29.0 (CH_2), 28.9, 28.8 (CH_2), 28.8, 28.7 (CH_2), 25.5, 25.34 (CH_2), 22.6, 22.5 (CH_2), 14.1, 14.1 (CH_3).

Reduction of the monoene hydroperoxide to allyl alcohol in large scale:

Na_2SO_3 (1.0 equiv. with respect to calcd. number of double binds in the substrate mixture) was directly added to the resultant product mixture (allyl hydroperoxide mixture in MeCN together with small amounts of starting material). The mixture was stirred and heated to 70 °C for 12 h. TLC control (Pe/EA 4/1) showed no allyl hydroperoxides left after 8 h.

Kinetic studies on photooxygenation (conversion vs time):

The kinetic study was conducted with a substrate concentration of 0.2 M. The cardanol monoene (0.482 g) and the standard dimethyl sulfone (0.383 g) were dissolved in the sensitizer solution (1 mM MB, 8.0 mL). The microreactor was filled with the reaction mixture with the LED lamp switched off. Afterwards, the lamp was switched on. Samples (0.2 mL) were taken from after the assigned illumination or rather reaction times of 0, 0.5, 1, 2, 3 , 4, 5, 6, 7 and 8 minutes. 0.4 mL $CDCl_3$ was added to the samples which were subsequently analyzed ^{1}H-NMR (512 scans).

Epoxidation of the allyl hydroperoxides:

The allyl hydroperoxides were dissolved in dry dichloromethane (40 mL) at 0 °C. Titanium(IV) isopropoxide was added under nitrogen while stirring. The reaction course was followed by TLC. After the given reaction time, the mixture was quenched with water. The organic phase was washed twice with water (40 mL each) and brine (sat. aq., 35 mL). After drying over $MgSO_4$, the solvent was removed under reduced pressure yielding a brown oil.

anti-configured epoxy alcohol: R_f (Pe/EA 4/1) = 0.28. ^{1}H-NMR (300 MHz, $CDCl_3$): δ [ppm] = 7.14 (t, ^{3}J = 7.7 Hz, 1H), 6.74 (d, ^{3}J = 7.7 Hz, 1H), 6.65 (d, ^{3}J = 7.7 Hz, 1H), 4.93 (s, 1H), 3.79 (s, 1H), 3.01 – 2.99 (m, 1H), 2.78 – 2.76 (m, 1H), 2.58 – 2.54 (m, 1H), 1.86 (s, 1H), 1.61 – 1.29 (m, 20H), 0.90 – 0.88 (m, 3H).

syn-configured epoxy alcohol: R_f (Pe/EA 4/1) = 0.20. ^{1}H-NMR (300 MHz, $CDCl_3$): δ [ppm] = 7.14 (t, ^{3}J = 7.7 Hz, 1H), 6.74 (d, ^{3}J = 7.7 Hz, 1H), 6.65 (d, ^{3}J = 7.7 Hz, 2H), 4.99 – 4.95 (m, 1H), 3.50 – 3.44 (m, 1H), 2.94 – 2.90 (m, 1H), 2.75-2.72 (m, 1H), 2.57 – 2.53 (m, 2H), 1.89 (s, 1H), 1.61 – 1.26 (m, 20H), 0.91 – 0.87 (m, 3H).

NMR spectra:

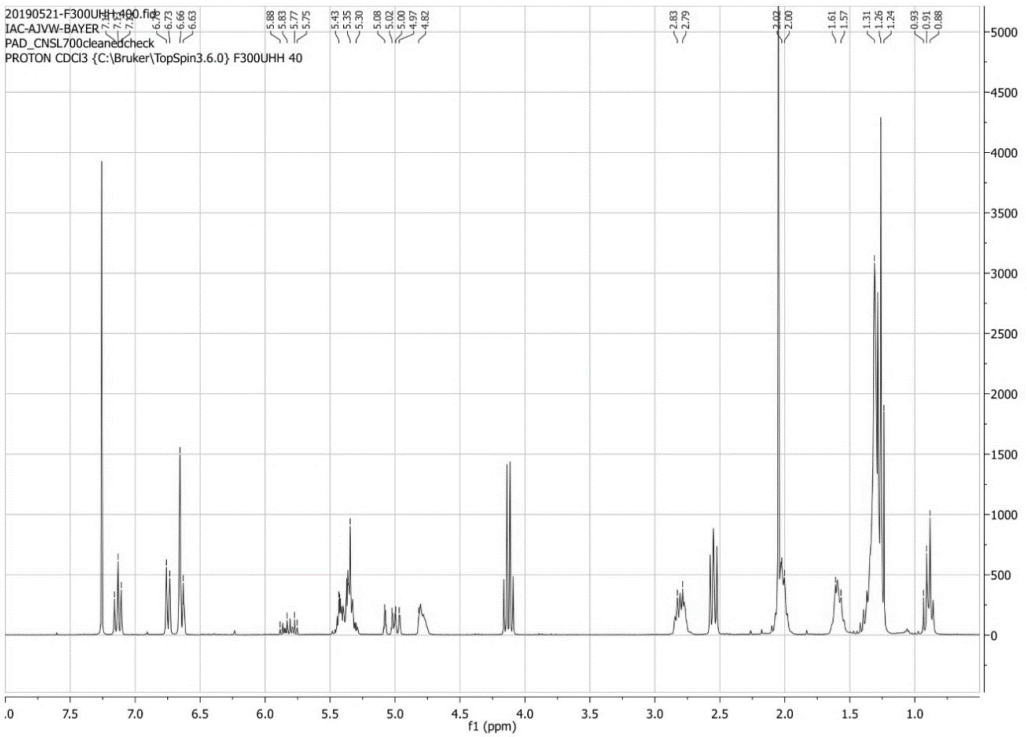

^{1}H-NMR spectrum of the cardanol mixture.

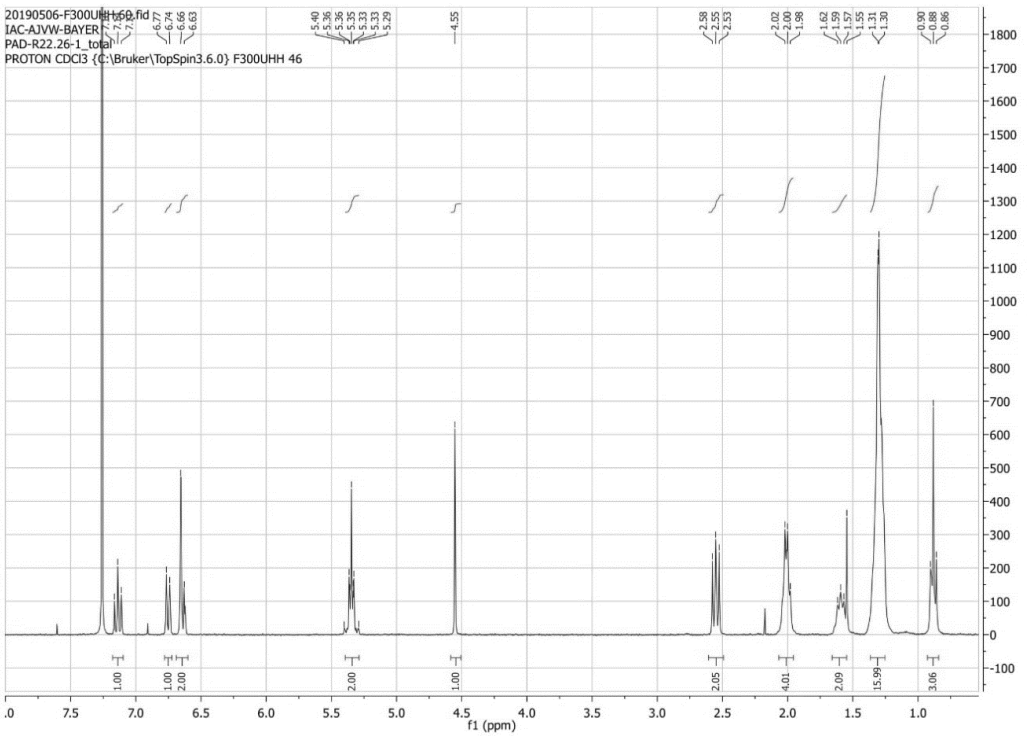

^{1}H-NMR spectrum of cardanol monoene.

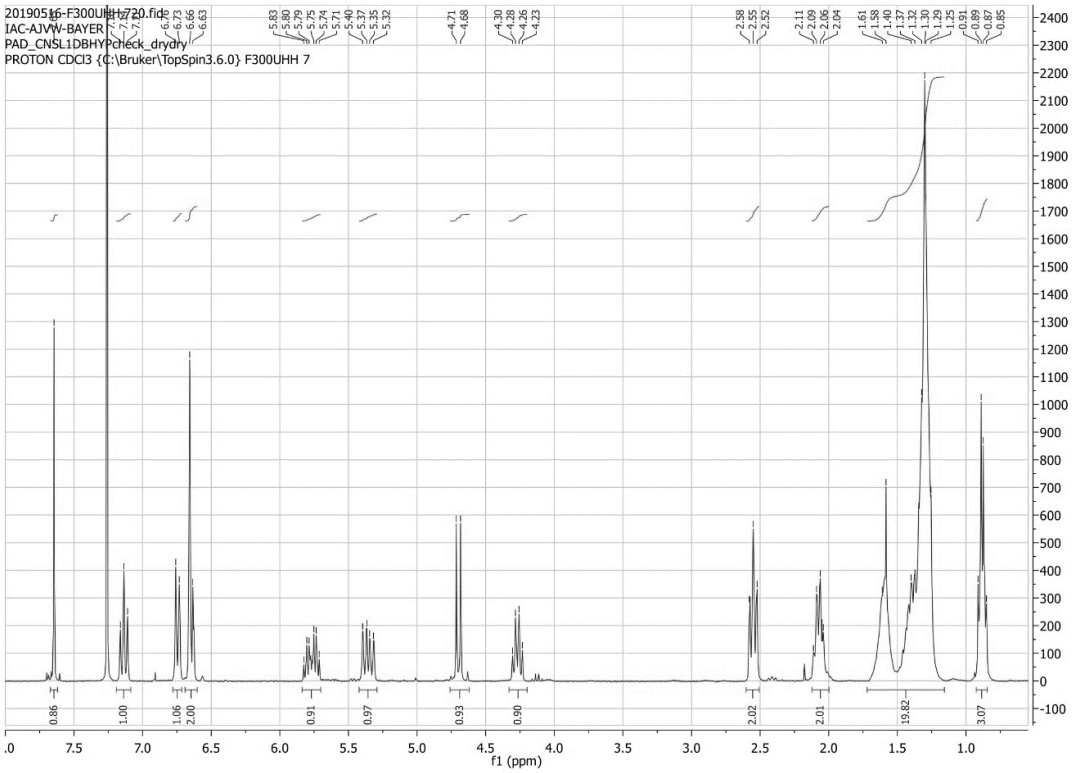

^{1}H-NMR spectrum of the monoene hydroperoxide (+ regioisomer)

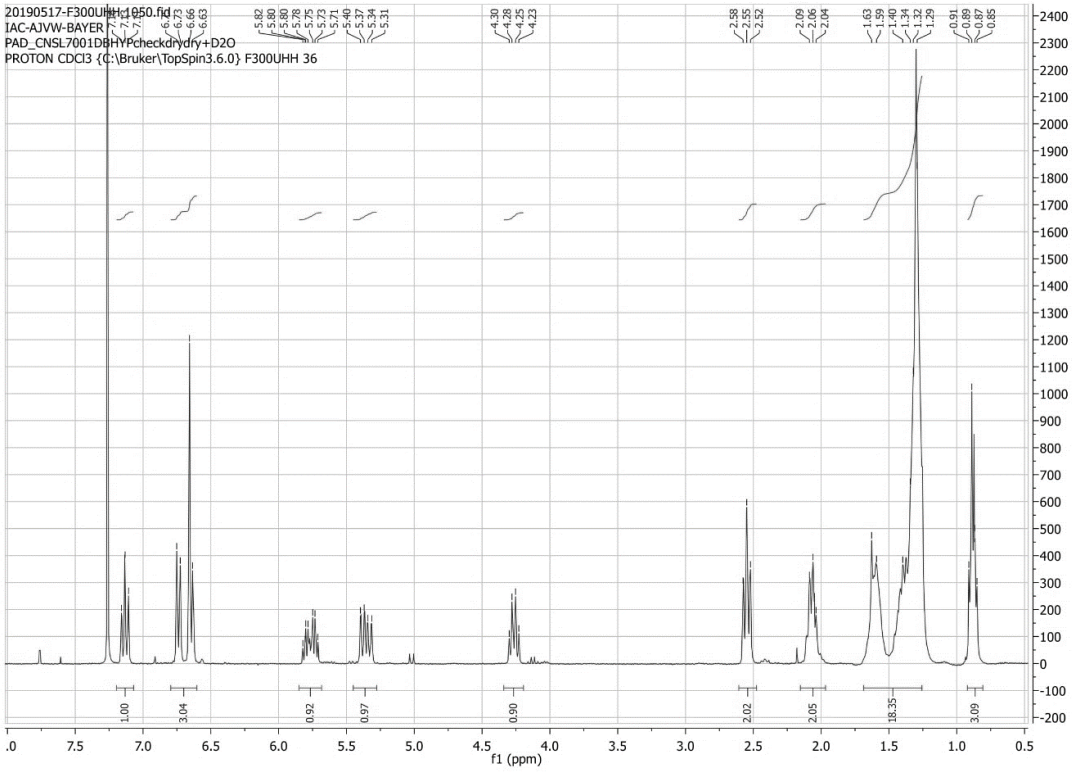

^{1}H-NMR spectrum of the monoene allyl hydroperoxide with added D_2O

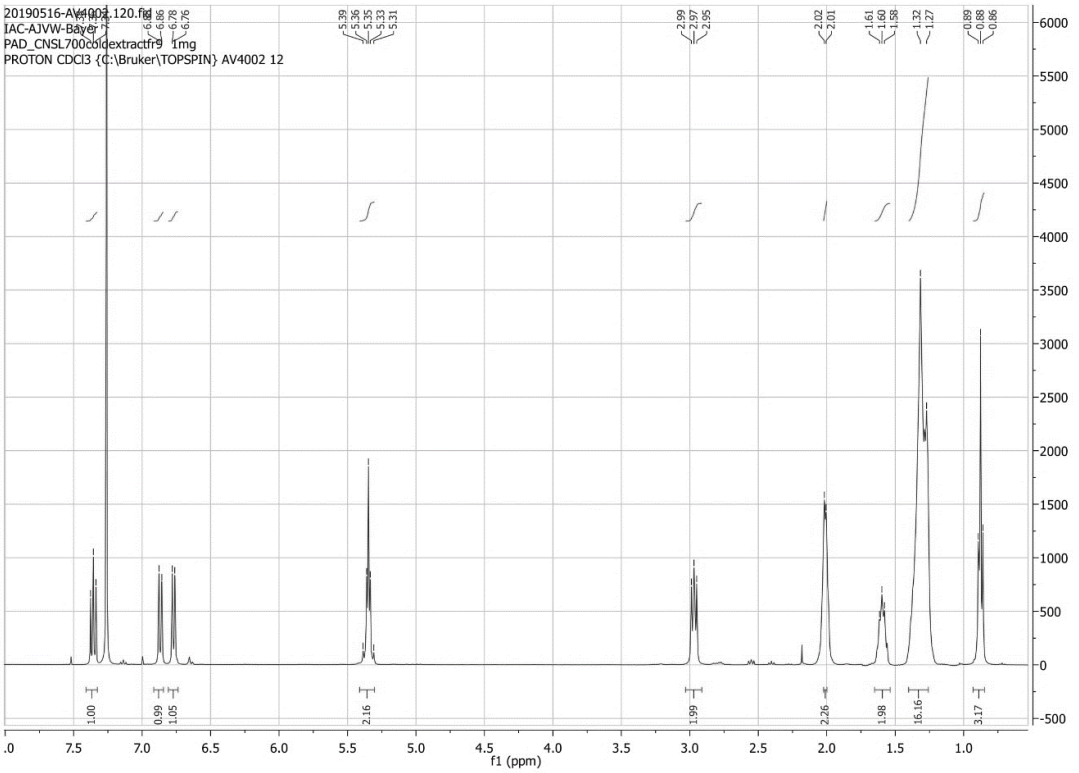

^{1}H-NMR spectrum of anarcadic acid

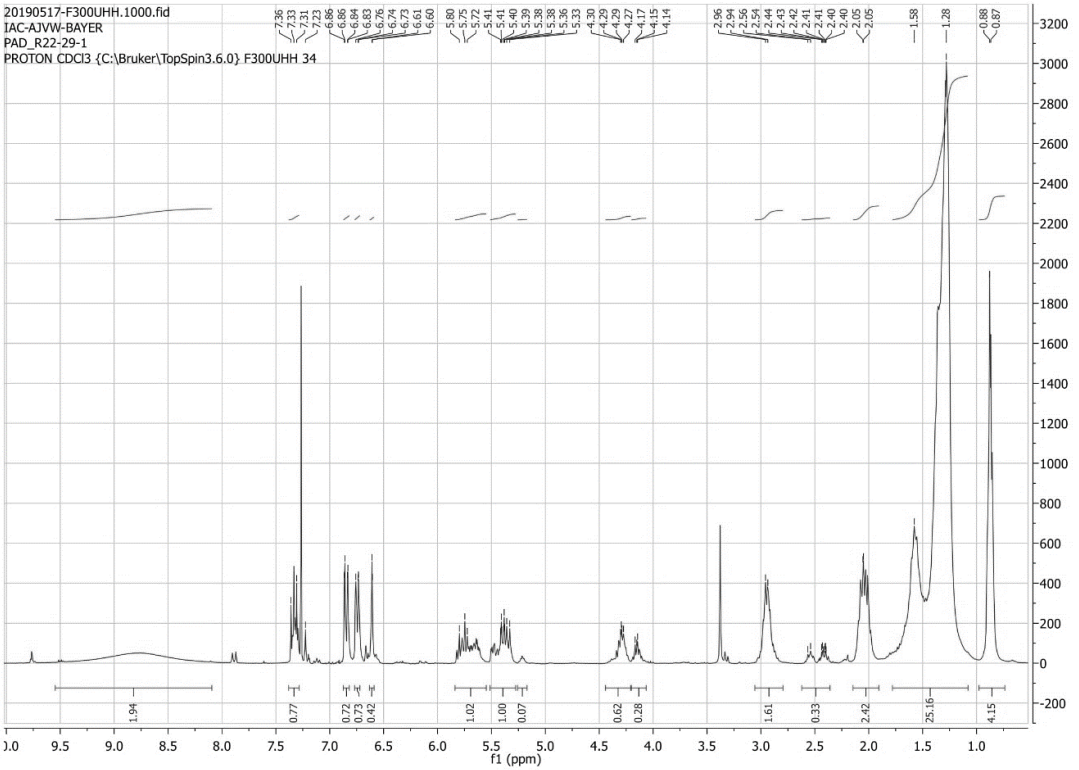

^{1}H-NMR spectrum of product mixture after oxidation of anarcadic acid

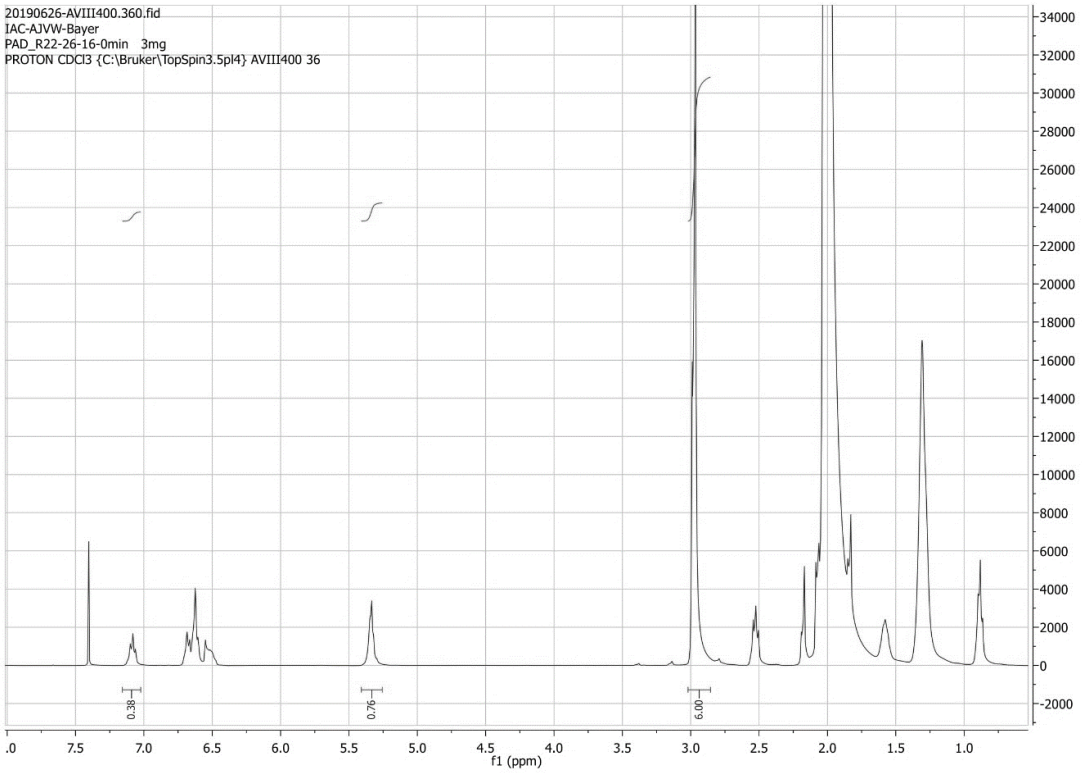

Kinetics: ^{1}H-NMR spectrum of reaction mixture after 0 min

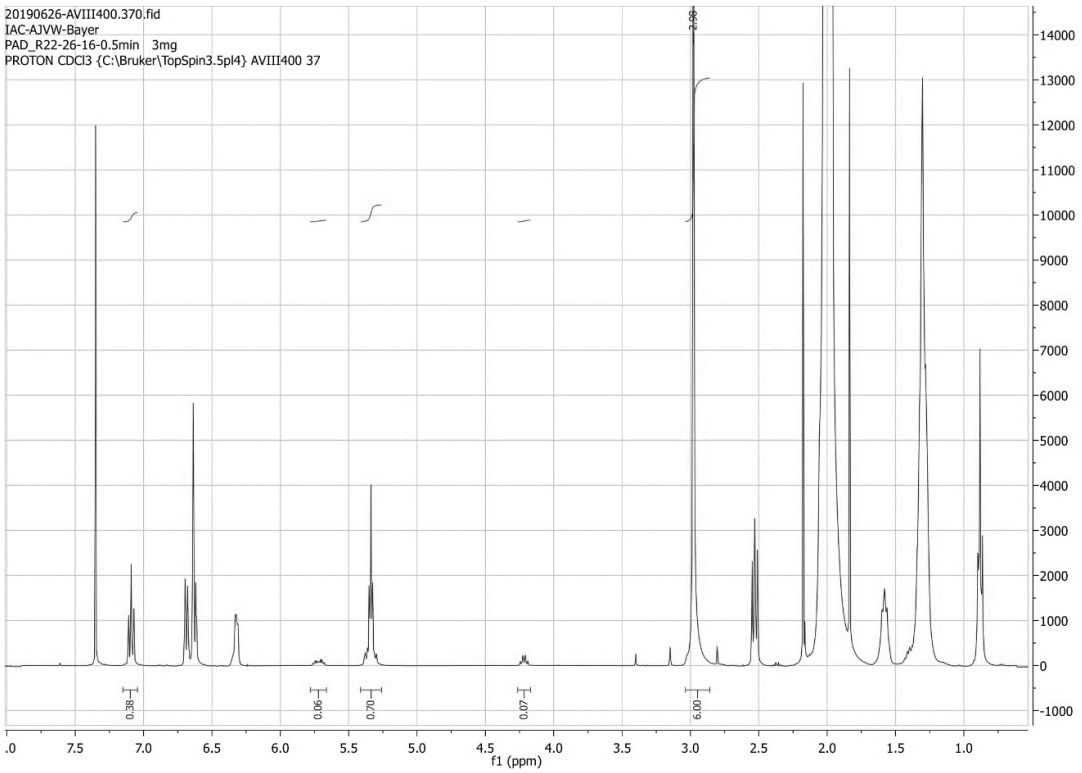

Kinetics: ^{1}H-NMR spectrum of reaction mixture after 0.5 min

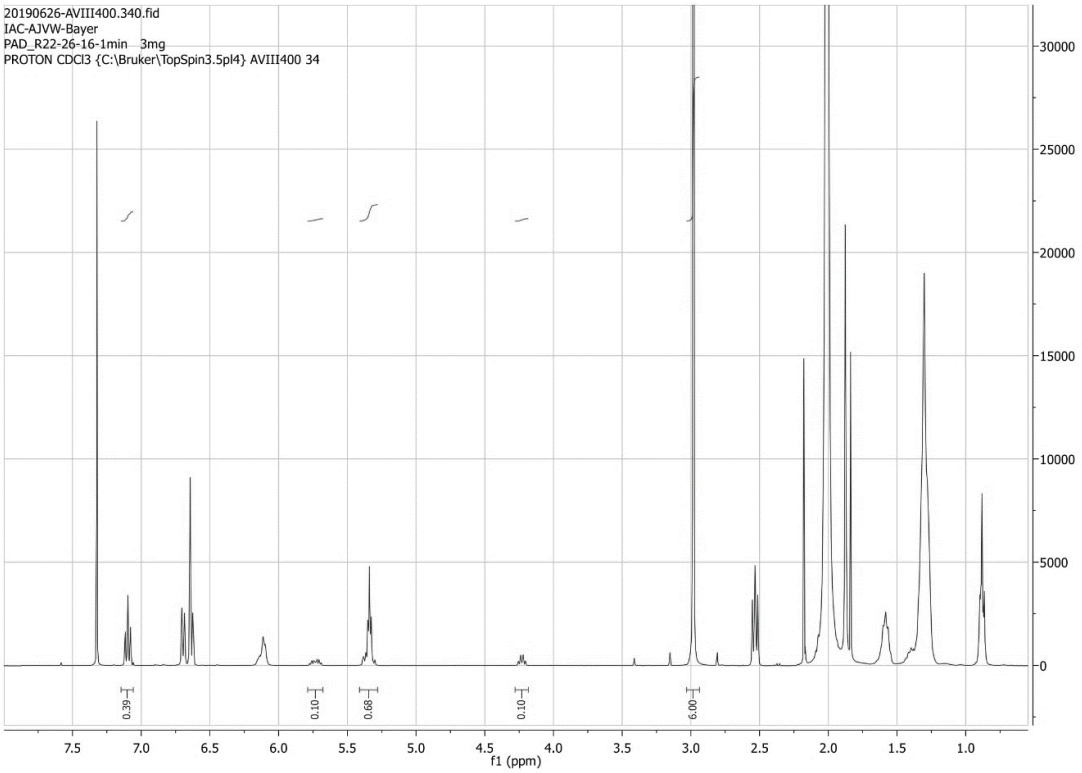

Kinetics: ^{1}H-NMR spectrum of reaction mixture after 1 min

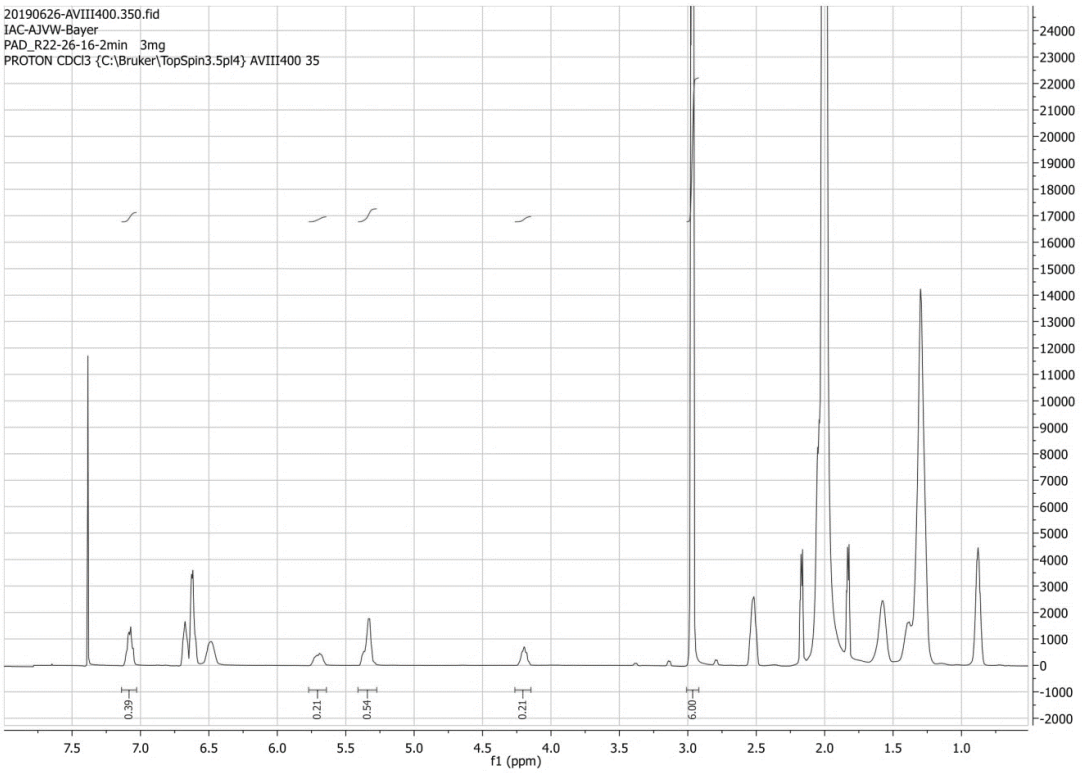

Kinetics: ^{1}H-NMR spectrum of reaction mixture after 2 min

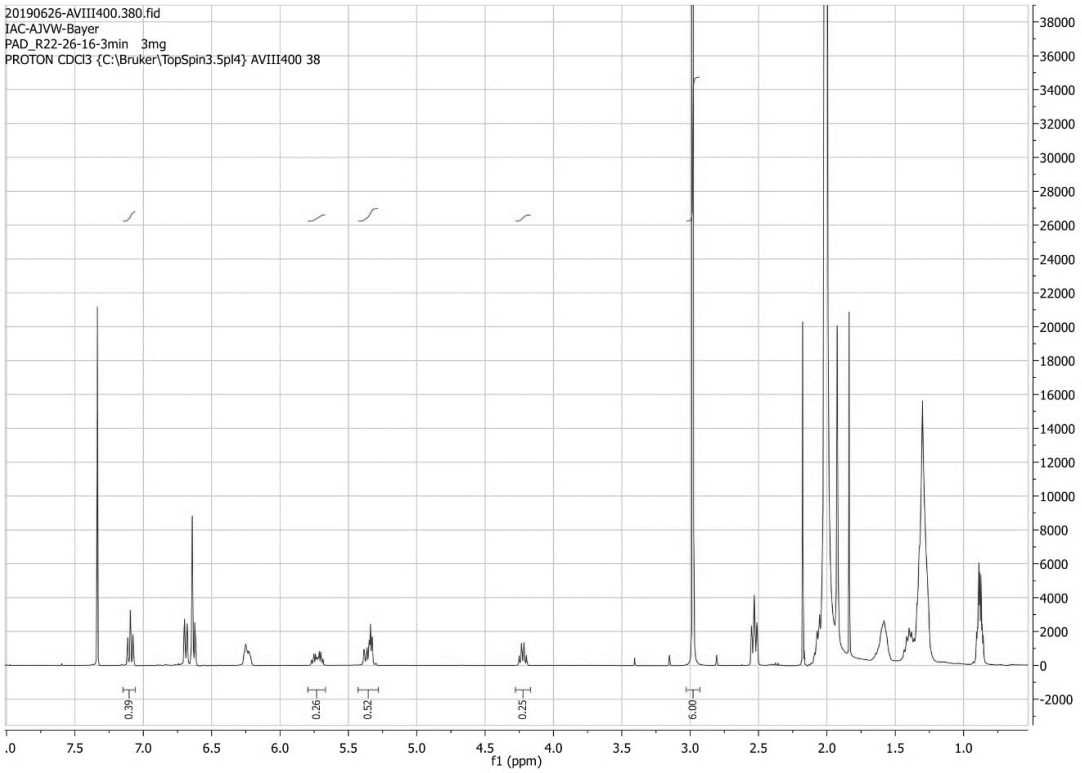

Kinetics: ^{1}H-NMR spectrum of reaction mixture after 3 min

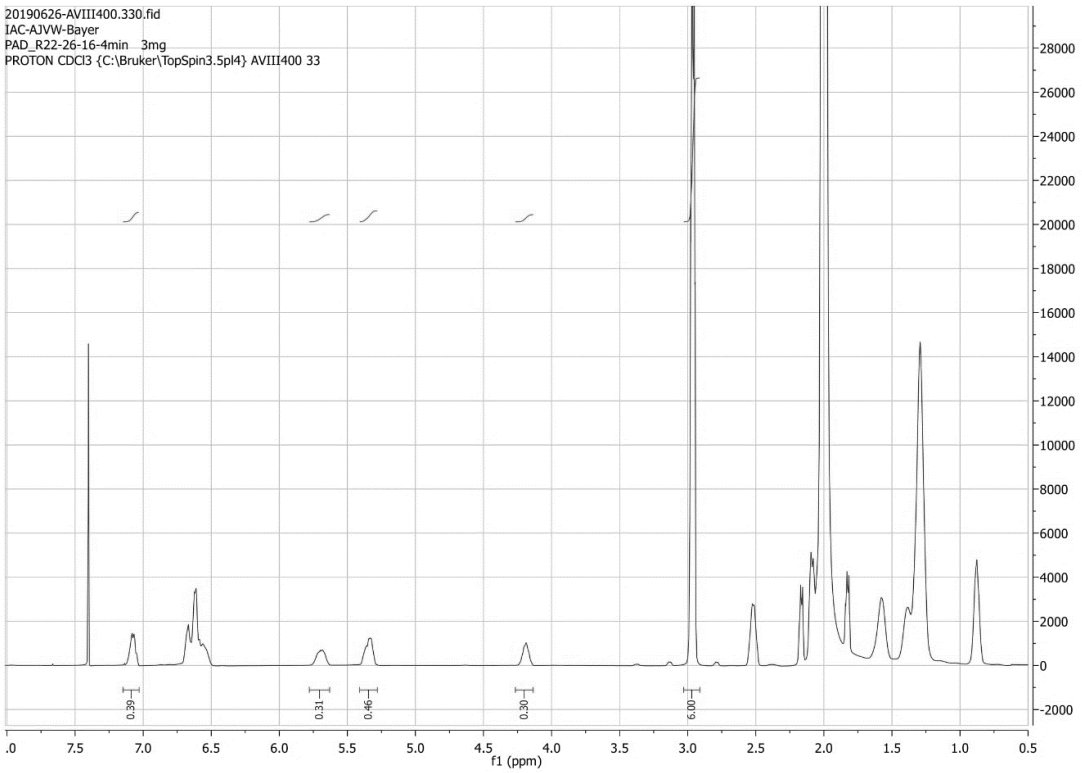

Kinetics: ^{1}H-NMR spectrum of reaction mixture after 4 min

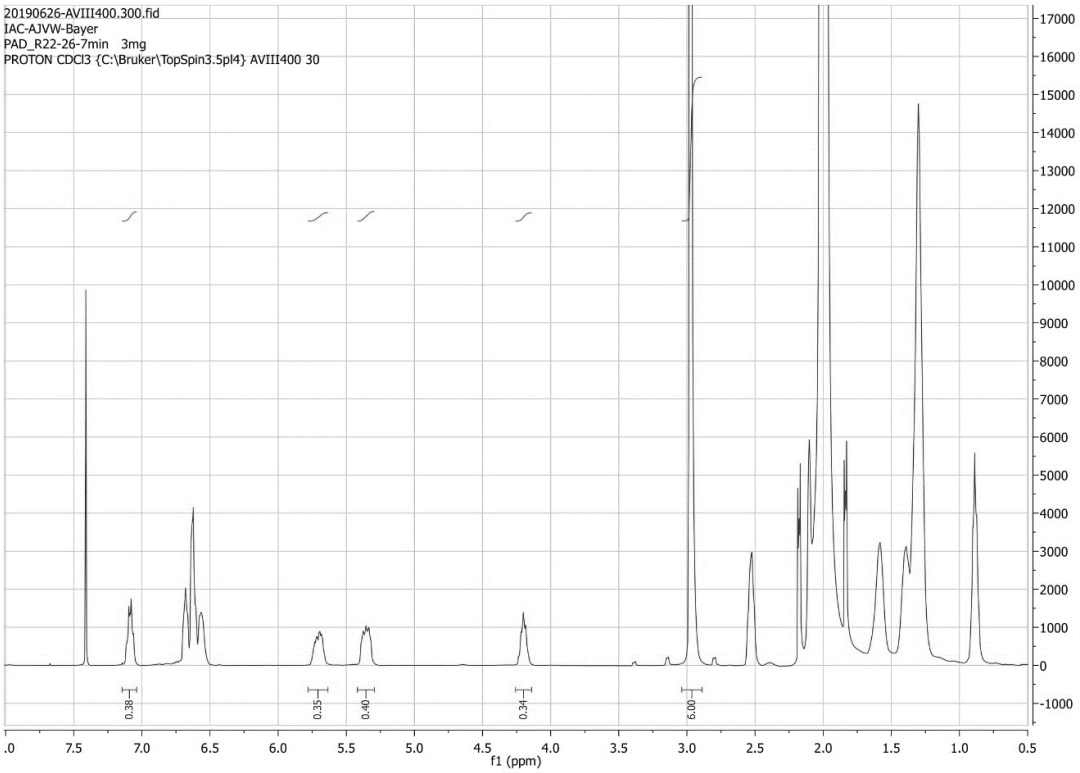

Kinetics: ^{1}H-NMR spectrum of reaction mixture after 7 min

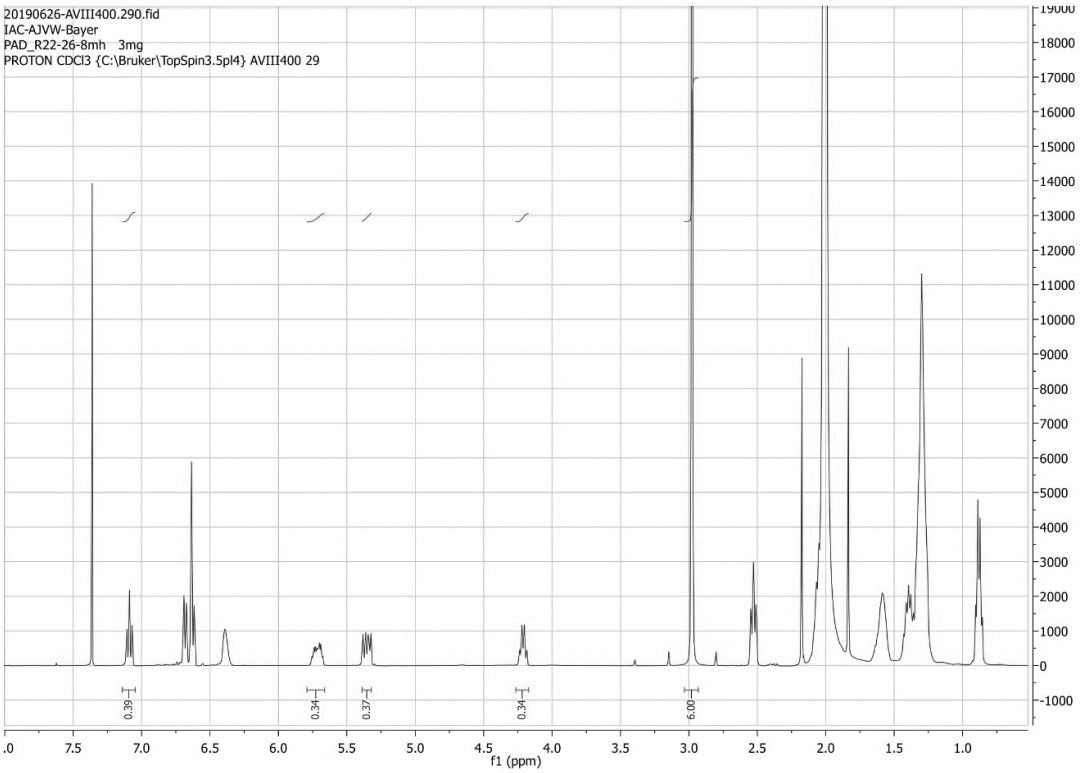

Kinetics: ^{1}H-NMR spectrum of reaction mixture after 8 min

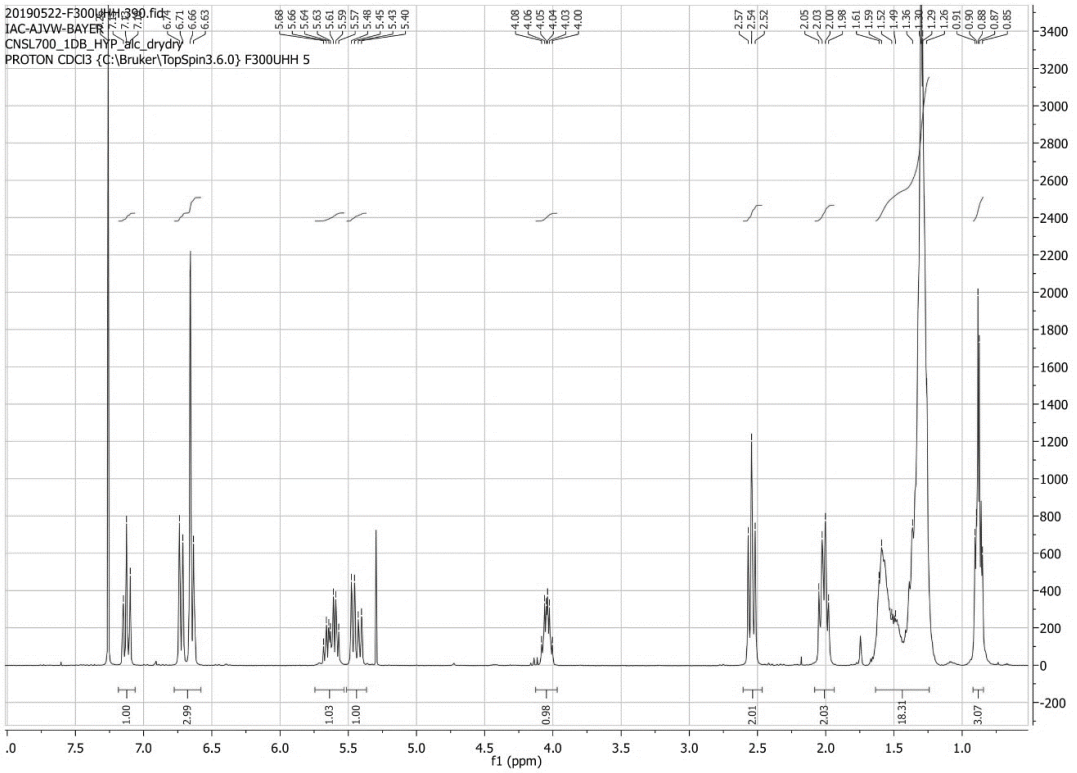

^{1}H-NMR spectrum of the monoene allyl alcohol

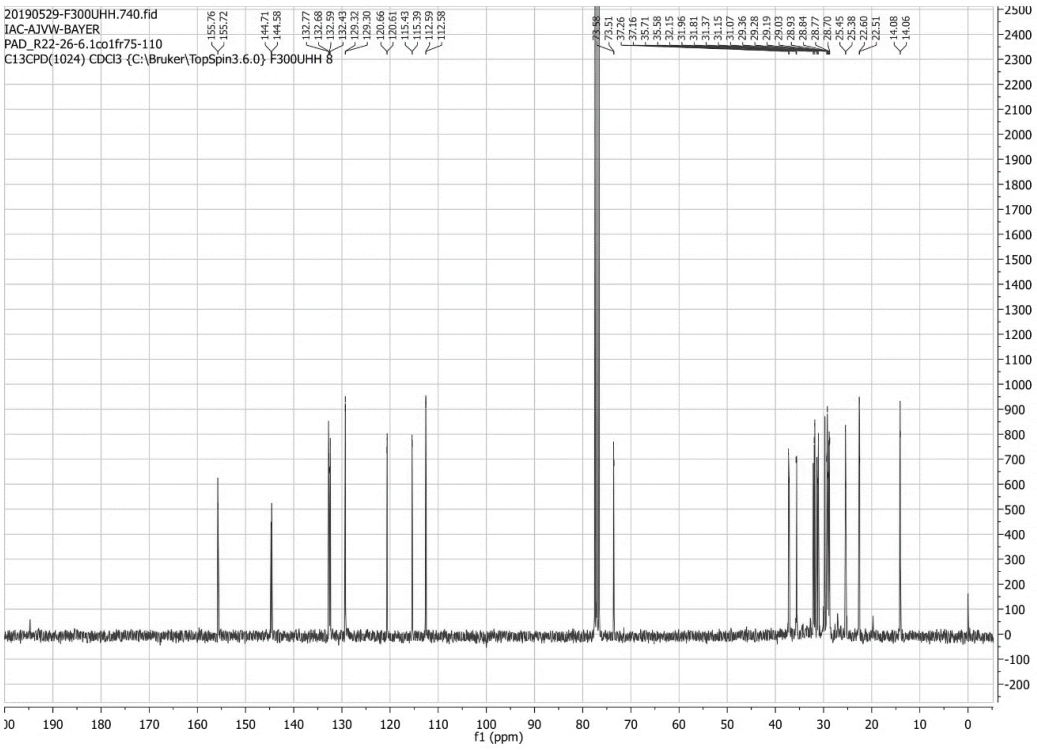

^{13}C-NMR spectrum of the monoene allyl alcohol

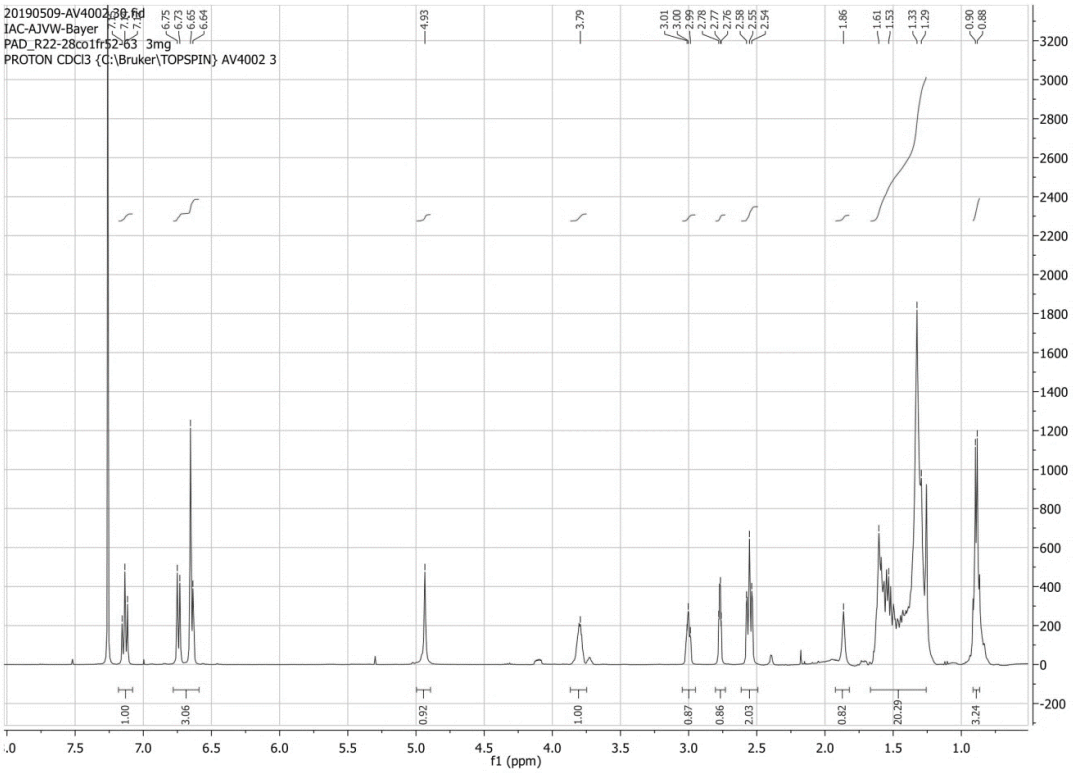

^{1}H-NMR spectrum of *anti*-configured epoxy alcohol

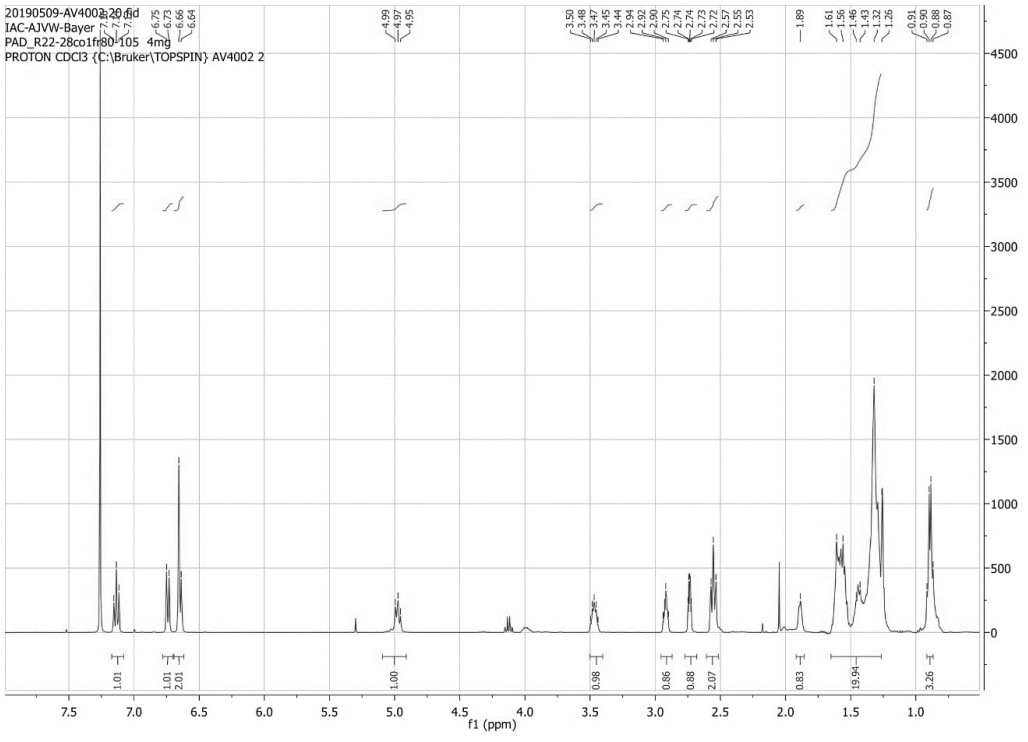

^{1}H-NMR spectrum of *syn*-configured epoxy alcohol

5 References

[1] P. Anilkumar, *Cashew Nut Shell Liquid*, Springer International Publishing, Cham, **2017**.
[2] H. Mutlu, M. A. R. Meier, *Eur. J. Lipid Sci. Technol.* **2010**, *112*, 10–30.
[3] V. S. Balachandran, S. R. Jadhav, P. K. Vemula, G. John, *Chem. Soc. Rev.* **2013**, *42*, 427–438.
[4] W. Adam, A. Griesbeck, E. Staab, *Angew. Chem. Int. Ed.* **1986**, *25*, 269–270.
[5] M. Unverferth, M. A. R. Meier, *Eur. J. Lipid Sci. Technol.* **2018**, *120*, 1800015.
[6] M. J. Thomas, C. S. Foote, *Photochem. Photobiol.* **1978**, *27*, 683–693.
[7] Y. Fukuchi, T. Takahashi, H. Noguchi, M. Saburi, Y. Uchida, *J. Polym. Sci. Polym. Lett.* **1988**, *26*, 401–403.
[8] A. G. Griesbeck, A. De Kiff, M. Kleczka, *Adv. Synth. Catal.* **2014**, *356*, 2839–2845.
[9] R. K. R. Jetti, H.-C. Weiss, V. R. Thalladi, R. Boese, A. Nangia, G. R. Desiraju, *Acta Crystallogr. Sect. C Cryst. Struct. Commun.* **1999**, *55*, 1530–1533.
[10] H. Kilic, W. Adam, P. L. Alsters, *J. Org. Chem.* **2009**, *74*, 1135–1140.
[11] W. Adam, M. Braun, A. Griesbeck, V. Lucchini, E. Staab, B. Will, *J. Am. Chem. Soc.* **1989**, *111*, 203–212.
[12] H. Brunner, H. R. Thomas, *J. Appl. Chem.* **2007**, *3*, 49–54.

V Solvent-Free Continuous Flow Photooxygenation

published with minor modifications as

"An Entirely Solvent-Free Photooxygenation of Olefins under Continuous Flow Conditions"

in *Green Chem.* **2020**, *22*, 2359-2364.

Author contributions:

Patrick Bayer wrote the manuscript and performed the reactions.
The work was supervised by Prof. Dr. Axel Jacobi von Wangelin.

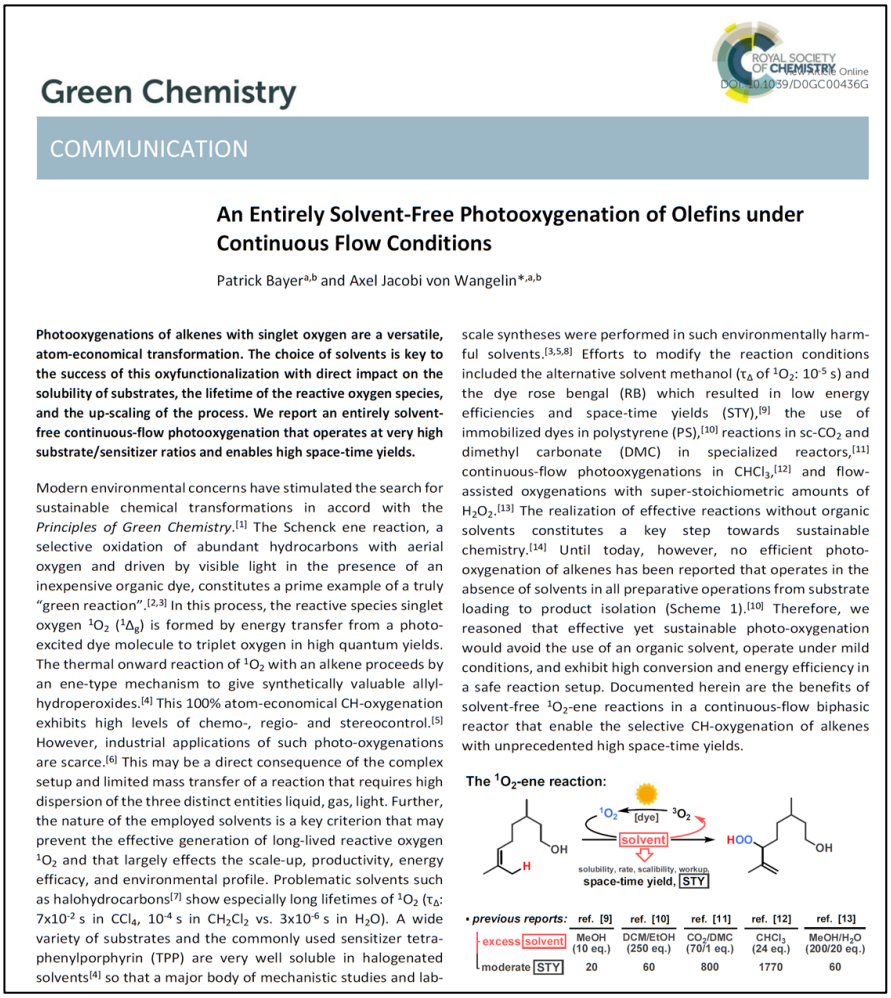

Green Chemistry

COMMUNICATION

ROYAL SOCIETY OF CHEMISTRY Online
DOI: 10.1039/D0GC00436G

An Entirely Solvent-Free Photooxygenation of Olefins under Continuous Flow Conditions

Patrick Bayer[a,b] and Axel Jacobi von Wangelin*[a,b]

Photooxygenations of alkenes with singlet oxygen are a versatile, atom-economical transformation. The choice of solvents is key to the success of this oxyfunctionalization with direct impact on the solubility of substrates, the lifetime of the reactive oxygen species, and the up-scaling of the process. We report an entirely solvent-free continuous-flow photooxygenation that operates at very high substrate/sensitizer ratios and enables high space-time yields.

Modern environmental concerns have stimulated the search for sustainable chemical transformations in accord with the *Principles of Green Chemistry*.[1] The Schenck ene reaction, a selective oxidation of abundant hydrocarbons with aerial oxygen and driven by visible light in the presence of an inexpensive organic dye, constitutes a prime example of a truly "green reaction".[2,3] In this process, the reactive species singlet oxygen $^1O_2$ ($^1\Delta_g$) is formed by energy transfer from a photo-excited dye molecule to triplet oxygen in high quantum yields. The thermal onward reaction of $^1O_2$ with an alkene proceeds by an ene-type mechanism to give synthetically valuable allyl-hydroperoxides.[4] This 100% atom-economical CH-oxygenation exhibits high levels of chemo-, regio- and stereocontrol.[5] However, industrial applications of such photo-oxygenations are scarce.[6] This may be a direct consequence of the complex setup and limited mass transfer of a reaction that requires high dispersion of the three distinct entities liquid, gas, light. Further, the nature of the employed solvents is a key criterion that may prevent the effective generation of long-lived reactive oxygen $^1O_2$ and that largely effects the scale-up, productivity, energy efficacy, and environmental profile. Problematic solvents such as halohydrocarbons[7] show especially long lifetimes of $^1O_2$ (τ_Δ: 7×10^{-2} s in CCl_4, 10^{-4} s in CH_2Cl_2 vs. 3×10^{-6} s in H_2O). A wide variety of substrates and the commonly used sensitizer tetra-phenylporphyrin (TPP) are very well soluble in halogenated solvents[4] so that a major body of mechanistic studies and lab-scale syntheses were performed in such environmentally harmful solvents.[3,5,8] Efforts to modify the reaction conditions included the alternative solvent methanol (τ_Δ of $^1O_2$: 10^{-5} s) and the dye rose bengal (RB) which resulted in low energy efficiencies and space-time yields (STY),[9] the use of immobilized dyes in polystyrene (PS),[10] reactions in sc-CO_2 and dimethyl carbonate (DMC) in specialized reactors,[11] continuous-flow photooxygenations in $CHCl_3$,[12] and flow-assisted oxygenations with super-stoichiometric amounts of H_2O_2.[13] The realization of effective reactions without organic solvents constitutes a key step towards sustainable chemistry.[14] Until today, however, no efficient photo-oxygenation of alkenes has been reported that operates in the absence of solvents in all preparative operations from substrate loading to product isolation (Scheme 1).[10] Therefore, we reasoned that effective yet sustainable photo-oxygenation would avoid the use of an organic solvent, operate under mild conditions, and exhibit high conversion and energy efficiency in a safe reaction setup. Documented herein are the benefits of solvent-free $^1O_2$-ene reactions in a continuous-flow biphasic reactor that enable the selective CH-oxygenation of alkenes with unprecedented high space-time yields.

The $^1O_2$-ene reaction:

• *previous reports:*	ref. [9]	ref. [10]	ref. [11]	ref. [12]	ref. [13]
excess solvent	MeOH (10 eq.)	DCM/EtOH (250 eq.)	CO_2/DMC (70/1 eq.)	$CHCl_3$ (24 eq.)	MeOH/H_2O (200/20 eq.)
moderate STY	20	60	800	1770	60

Reproduced with permission from the Royal Society of Chemistry.

1 Introduction

The photooxygenation of alkenes with singlet oxygen constitutes a versatile, atom-economic transformation. The choice of solvents is key to the success of this oxyfunctionalization reaction as it has direct impact on the solubility of substrates, the lifetime of the reactive oxygen species, and affects the up-scaling of the process. Herein, we report an entirely solvent-free continuous-flow photooxygenation that operates at very high substrate/sensitizer ratios and enables high space-time yields.

Modern environmental concerns have stimulated the search for sustainable chemical transformations in accord with the *Principles of Green Chemistry*.[1] The Schenck ene reaction, a selective oxidation of abundant hydrocarbons with aerial oxygen and driven by visible light in the presence of an inexpensive organic dye, constitutes a prime example of a truly "green reaction".[2,3] In this process, the reactive species singlet oxygen $^1O_2$ ($^1\Delta_g$) is formed by energy transfer from a photo-excited dye molecule to triplet oxygen in high quantum yields. The thermal onward reaction of $^1O_2$ with an alkene proceeds by an ene-type mechanism to give synthetically valuable allyl-hydroperoxides.[4] This 100% atom-economical CH-oxygenation exhibits high levels of chemo-, regio- and stereocontrol.[5] However, industrial applications of such photooxygenations are scarce.[6] This may be a direct consequence of the complex setup and limited mass transfer of a reaction that requires high dispersion of the three distinct entities liquid, gas, light. Further, the nature of the employed solvents is a key criterion that may prevent the effective generation of long-lived reactive oxygen $^1O_2$ and that largely effects the scale-up, productivity, energy efficacy, and environmental profile. Problematic solvents such as halohydrocarbons[7] show especially long lifetimes of $^1O_2$ (τ_Δ: $7x10^{-2}$ s in CCl_4, 10^{-4} s in CH_2Cl_2 vs. $3x10^{-6}$ s in H_2O). A wide variety of substrates and the commonly used sensitizer tetra-phenylporphyrin (TPP) are very well soluble in halogenated solvents[4] so that a major body of mechanistic studies and lab-scale syntheses were performed in such environmentally harmful solvents.[3,5,8]

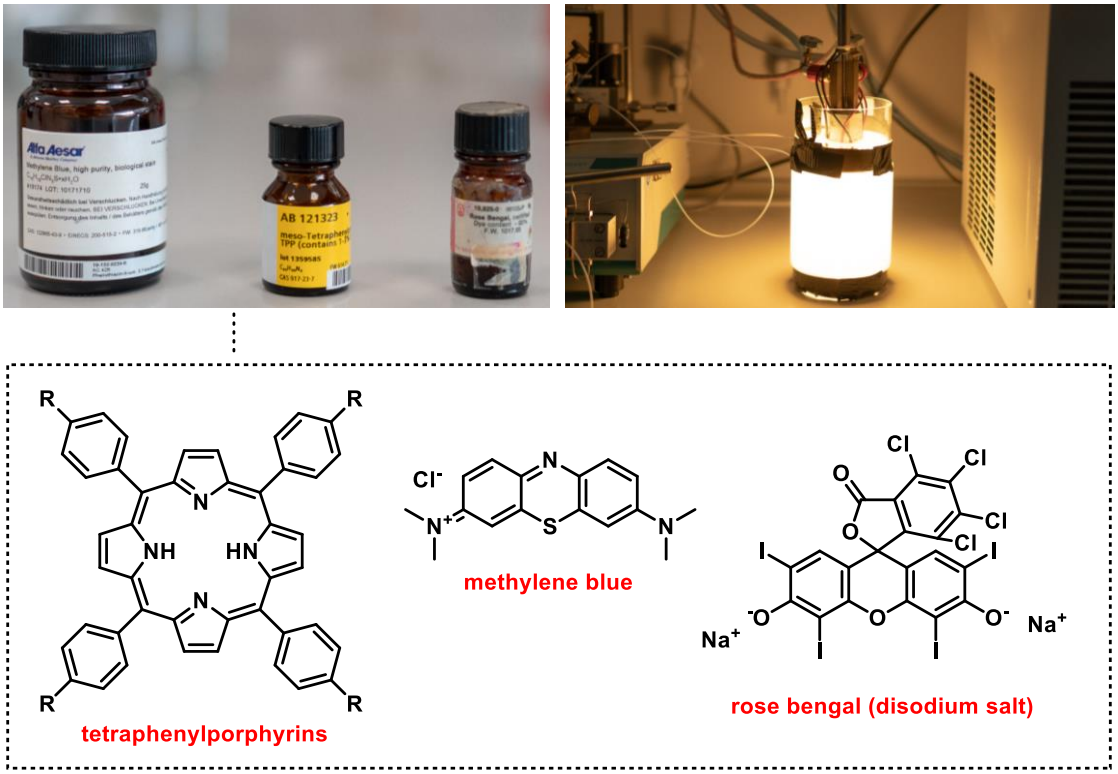

Figure 20. Ideal tools for $^1O_2$ generation: MB, TPP or RB (top left), VIS light irradiation in flow by LEDs (top right), and structures of the three sensitizers (scheme).

Sensitizers like methylene blue (Figure 20) can be dissolved in acetonitrile which, however, features a significantly lower singlet oxygen lifetime than halogenated solvents. Efforts to modify the reaction conditions with the result of less energy consumption or environmental impact include the alternative solvent methanol (τ_Δ of $^1O_2$: 10^{-5} s) and the dye rose bengal (RB) which resulted in low energy efficiencies and space-time yields (STY),[9] the use of immobilized dyes in polystyrene (PS),[10] reactions in sc-CO_2 and dimethyl carbonate (DMC) in specialized reactors,[11] continuous-flow photooxygenations in $CHCl_3$,[12] and flow-assisted oxygenations with super-stoichiometric amounts of H_2O_2.[13] The realization of effective reactions without organic solvents constitutes a key step towards sustainable chemistry.[14]

2 Results and Discussion

Until today no efficient photooxygenation of alkenes has been reported that operates in the absence of solvents in all preparative operations from substrate loading to product isolation (Scheme 51). Existing reports on solvent-free photooxygenations were either conducted in batch with questionable substrate reactivities and product selectivities, or utilize large amounts of solvents for the loading and removal of substrates/products.[10]

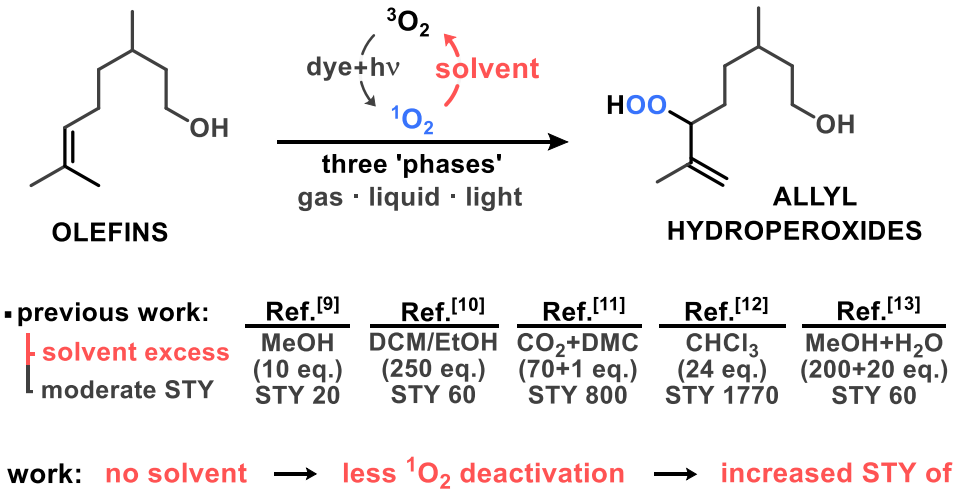

Scheme 51. The $^1O_2$-ene reaction: Key aspects of solvent effects, selected literature protocols, and major achievements of this work. Space-time yields (STY) in g L^{-1} h^{-1}.[15]

Therefore, we reasoned that effective yet sustainable photooxygenation would avoid the use of an organic solvent, operate under mild conditions, and exhibit high conversion and energy efficiency in a safe reaction setup. Documented herein are the benefits of solvent-free $^1O_2$-ene reactions in a continuous-flow biphasic reactor that enable the selective CH-oxygenation of alkenes with unprecedented high space-time yields. The photooxygenations were performed in a home-built, modular flow reactor.[16,17] We initially investigated the compatibility of a series of alkene substrates under photooxygenation conditions in the absence of any solvent in all preparative operations from substrate loading to reaction work-up.[18] Liquid substrates were fed into the flow reactor by a commercial HPLC pump with variable flow rates.

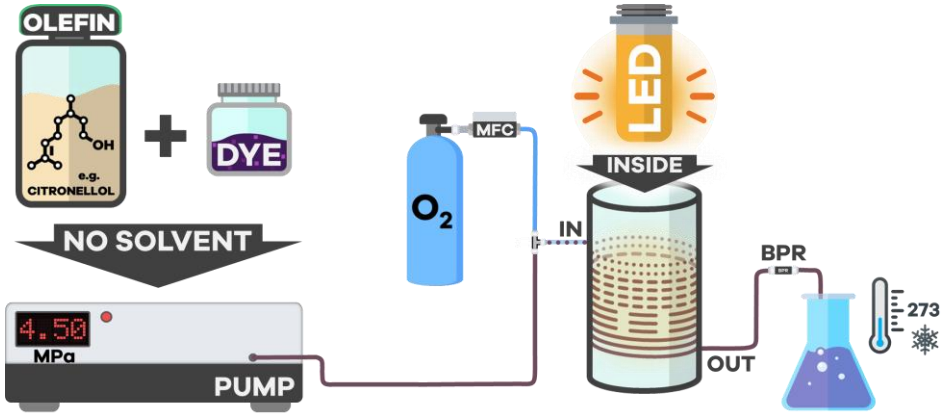

Figure 21. Process setup for the continuous functionalization of liquid olefins.

A parallel inlet of pressurized oxygen was controlled by a thermal mass flow controller (MFC) so that a biphasic slug flow built inside a transparent tubular flow reactor. Flow rates, back-pressure regulator (BPR) settings, reaction temperature, and visible light irradiation by LEDs were easily varied. Nearly complete gas consumption was accomplished by the mutual adjustment of liquid and gas flow rates and pressures (Figure 21, Figure 22).

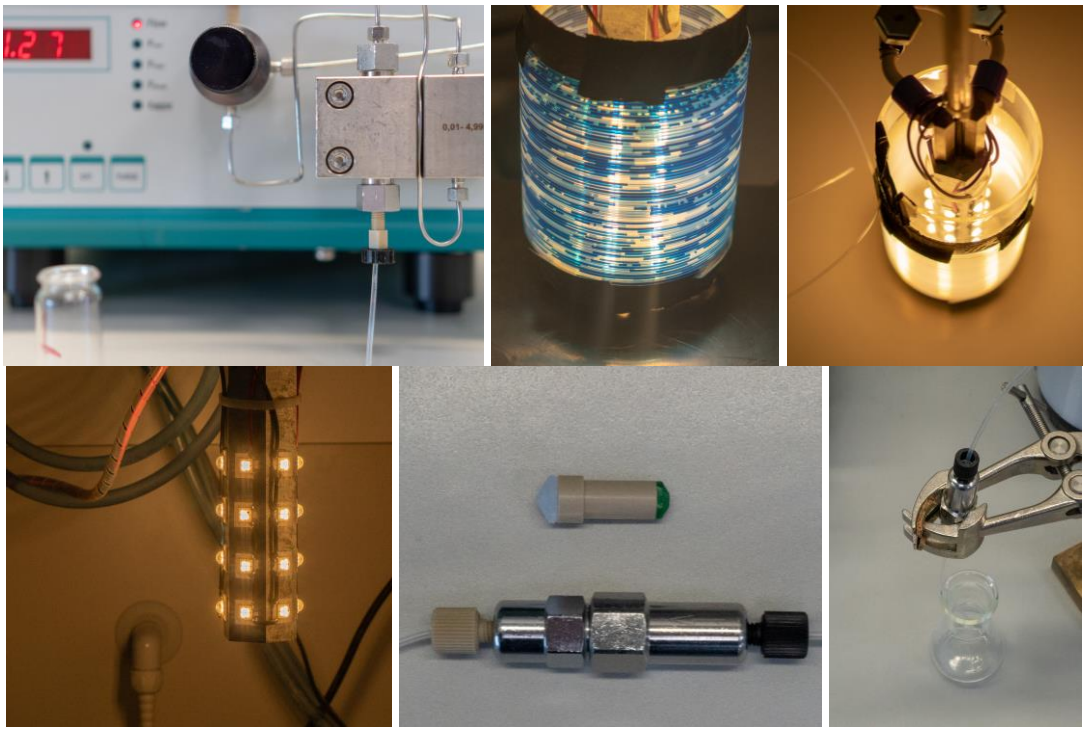

Figure 22. Photographs of the utilized reactor equipment: HPLC pump, flow reactor in action, empty reactor coil and white LED, LED-rod, BPR, sample outlet assembly (from top left).

The photooxygenation of a liquid alkene substrate with aerial oxygen in the presence of visible light behaves as a quasi-three phase reaction (liquid–gas–light).[16] The reaction rates are significantly governed by the mass transfer so that effective dispersion of the three distinct entities is required for rapid conversion. The reaction pressure is a key factor which is directly related to the mass transfer of oxygen to the highly concentrated liquid phase containing a solution of the catalytic sensitizer in the substrate with no added solvent. The use of pressurized oxygen or air and the formation of $^1O_2$ and organic peroxides demand great care. Reactions under (micro)flow conditions provide high levels of safety due to the low reaction volumes, effective heat control, and spatially separated formation and collection of reactive products. Prominent examples of related technical processes with gaseous oxygen include the rose bengal-sensitized oxidation of citronellol in methanol with an annual production on multi-ton scales,[6,9] the oxidation of anthrahydroquinones for hydrogen peroxide production,[19] and the high-pressure oxidation of isobutane to *tert*-butyl hydroperoxide.[20]

A wide range of low-molecular-weight alkenes are liquids under ambient conditions. This also includes several benchmark substrates of $^1O_2$-ene reactions, for example the technical product citronellol (**1**), the cyclic alkene 1-methylcyclohexene (**3**), or chiral allylic alcohols such as **5**. These and related liquid substrates are capable of dissolving common organic dyes such as methylene blue (MB), TPP, or rose bengal (RB) without the need for an additional solvent (Figure 23).

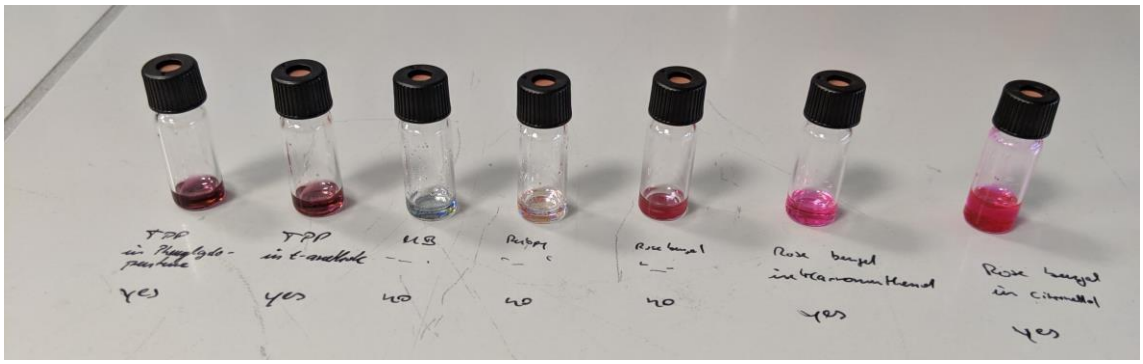

Figure 23. Trial and error (and GC-vials): which sensitizers can be dissolved in the desired substrates in sufficient concentration?

When applying a continuously operated photooxygenation, however, further substrate and product properties such as dynamic viscosity, oxygen solubility,

stability, and reaction rate with $^1O_2$ must be considered. We performed a comparative study of a diverse set of $^1O_2$-ene reactions with a special emphasis on the effect of solvent-free conditions vs. the literature procedures in common organic solvents. The substrate/sensitizer molar ratio was typically 5,000 and could be increased when irradiation times were prolonged. Typically, the sensitizers showed little to no bleaching at normal irradiation times.

Table 5. The effect of variations of reactor parameters on the reaction efficiency.[a]

	Variation of ..		Effect on ..		
	tube length	flow speed	yield	productivity	**STY**
1	× 1	× 1	× 1	× 1	**× 1**
2	× 1	× 2	× 0.5	× 1	**× 1**
3	× 2	× 1	× 1	× 1	**× 0.5**
4	× n	× n	× 1	× n	**× 1**

[a] under the assumption of linear yield-time dependence.

A meaningful evaluation of flow reactor processes that involves reaction efficiency and reactor efficiency is based on the individual space-time yields (STY, given in g L^{-1} h^{-1}) that include product yield, internal reactor volume, and irradiation/residence time (Table 5). A direct comparison of STY values is more insightful than yield or productivity values (yield per time) as long reaction times (entry 3) and up-scaling effects (entry 4) are eliminated. Yield-time-dependences are generally not linear so that comparisons of STY should refer to equal or (even better) complete conversions.[15] We explored a representative set of solvent-free photooxygenations of alkenes (Table 6). The biphasic reactions showed very rapid conversions to the corresponding allyl hydroperoxides under pressurized oxygen with similar yields, mass balances, and selectivities as in the literature reactions in ~0.1-2 M solutions. Nearly identical yields and product ratios as in protocols with medium-polar solvents like acetonitrile were obtained from the solvent-free reactions of the initially investigated citronellol (**1**) and 1-methylcyclohexene (**3**), respectively (entries 1 and 2). While moderate O_2 pressure (7 bar)[16,17] and high sensitizer concentration[21] did not afford full conversions, elevated O_2 pressure (45 bar) enabled rapid reactions and complete conversions after 8 (substrate **1**) or 12 min (substrate **3**).[17,22] Consequently, the photooxygenation of **1** exhibited 4600 g L^{-1} h^{-1} of product formation under

optimized conditions. This productivity of the solvent-free flow reaction significantly outperformed the literature protocol in chloroform solution (maximum STY of 1770 g L^{-1} h^{-1}, no increase at higher O_2 pressure or higher sensitizer concentration)[12].

Table 6. Solvent-free photooxygenation of alkenes.[a]

	Substrate	Sens. [b] STY [c]	Products	Yield Ratio [d]
1	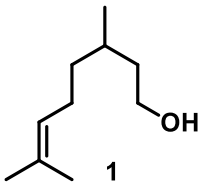 1	 MB 4600	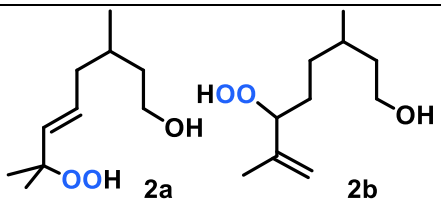 2a 2b	>95% 1:1 (1:1)[e]
2[f]	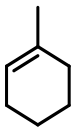 3	 TPP 3200	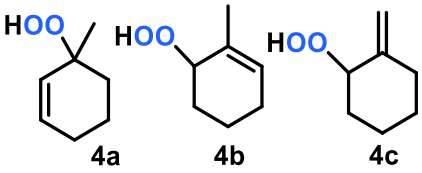 4a 4b 4c	88%[d] 2:1:3 (2:1:3)[e] (3:1:2)[g]
3	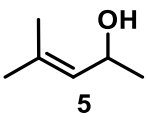 5	 RB 950	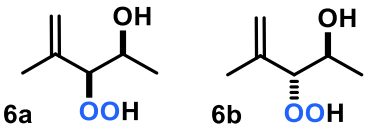 6a 6b	91%[d] 1.8:1 (3:1)[e,h]
4	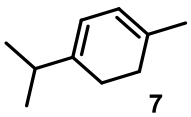 7	 TPP 1900	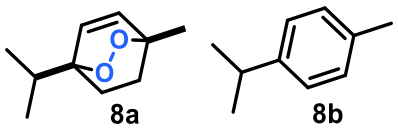 8a 8b	>95%[d] 18:1 (99:1)[e]
5	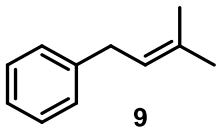 9	 TPP 3900	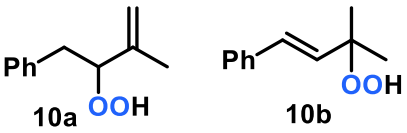 10a 10b	95%[d] 1:1 (1:1)[e]

[a] Conditions: neat reaction in continuous flow reactor, sensitizer dissolved in substrate, 6.3 mL internal reactor volume, irradiation by white LEDs, 45 bar O_2; all reactions gave >95% conversion. [b] Sensitizer used: 2 mM MB or 1.5 mM TPP or 0.9 mM RB. [c] Space-time yields (STY) in g L^{-1} h^{-1}. [d] Product ratios determined by ^{1}H-NMR. [e] Selectivity in solution (substrate 0.1 M in MeCN, 1 mM MB). [f] 0.9 mM TPP, at 92% conversion to prevent over-oxidation of **4b**. [g] Selectivity in CCl_4 or nonpolar PS beads.[2] [h] Selectivity in PS beads.[23]

Notably, the substrates were not completely converted using pressurized air under these conditions. The mass balances of solvent-free and solvent-assisted reactions did not differ considerably when both systems were optimized toward

conditions that prevented product over-oxidation at minimal irradiation times. Generally, higher purities of the desired oxidation products were obtained from solvent-free reactions (by comparison of crude NMR spectra). Extended reaction times not only diminished the space-time yields but typically also led to lower product yields and selectivities due to over-oxidations at different rates for each of the primary allylic hydroperoxides (e.g. rate of $^1O_2$-reactions: **2a**>**2b**, **4b**>**4a**,**4c**). The chiral *s*-alcohol **5** was oxygenated in very good yields with rose bengal (RB) as sensitizer, albeit with slightly lower stereoselectivity (*syn*/*anti* = 1.85) indicating a very polar environment during the reaction.[23] Generally, hydroxyl substituents lower the $^1O_2$-ene reactivity so that full conversions require reduced flow rates and lead to low STY. α-Terpinene **7**, a precursor to the anthelmintic ascaridole **8a**, was converted to the endo-peroxide **8a** with high chemoselectivity.[24]

It is important to note that weakly polar alkenes - such as 2,4,4-trimethyl-2-pentene (**11**), α-pinene (**13**), β-pinene (**15**) - do not dissolve the common commercial photosensitizers MB, TPP or RB (Table 7).[25] Therefore, we prepared the less polar propyl-TPP derivative 5,10,15,20-tetrakis(4-*n*-propylphenyl)porphyrin (PrTPP)[26] which overcomes this limitation as it exhibited sufficient solubility in a series of non-polar alkenes. Consequently, the solvent-free photooxygenation of alkenes in PrTPP involved a homogeneous substrate/sensitizer phase and afforded high yields of the desired allyl hydroperoxides (Table 7). **11** was converted in 30 min yielding **12** without byproducts; the less reactive α- and β-pinene (**13**, **15**) showed slightly lower reactivity.[23] β-Pinene **15** and *cis*-4-octene **17** were completely converted by increasing the internal reactor volume and extended irradiation time which led to lower space-time yields (entries 3, 4). The lower yield during β-pinene oxygenation is due to the reactivity towards singlet oxygen of the resultant hydroperoxide **16**.

Table 7. Solubility of alkenes in TPP dyes (top) and solvent-free photooxygenations of non-polar alkenes.[a]

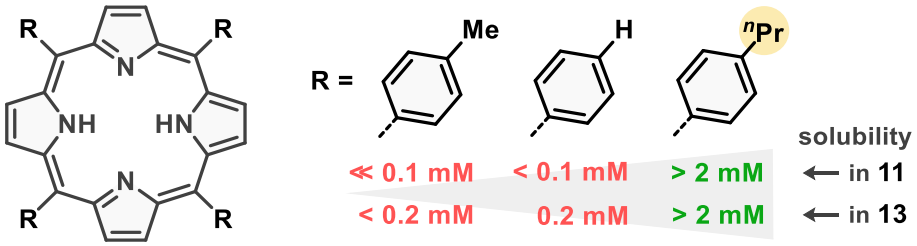

	Substrate	Sensitizer [b] **STY** [c]	Product	Yield [d]
1	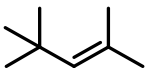 11	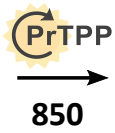 PrTPP **850**	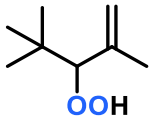 OOH 12	> 95%
2	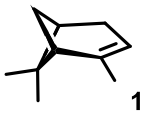 13	 PrTPP **500**	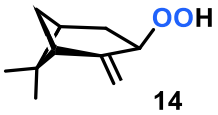 OOH 14	84%
3	 15	 PrTPP **300**	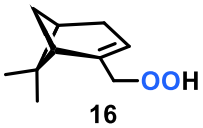 OOH 16	66%
4	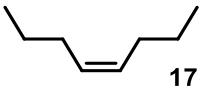 17	 PrTPP **400**	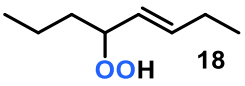 OOH 18	93%

[a] Conditions: Table 6. [b] 1.5 mM PrTPP. [c] STY in g L^{-1} h^{-1}. [d] Determined by ^{1}H-NMR.

While ascaridole (**8a**) is technically applied without further transformation, most allyl hydroperoxide are intrinsically unstable compounds. Several methods of post-synthesis functionalizations and derivatizations have been reported in the literature that utilize the alkene or peroxide groups.[5] The labile peroxide is mostly converted to the more stable alcohol with suitable reductants (e.g. Na_2SO_3, PPh_3) or to α-enones by dehydration (Scheme 52).[5,27]

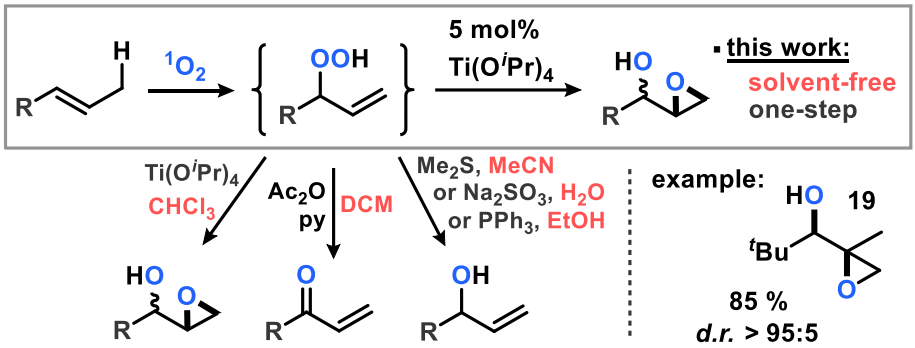

Scheme 52. Selected post-synthesis transformations of $^1O_2$-ene products.[5,28] Solvent-free sequential photooxygenation and Ti-catalyzed self-epoxidation. py = pyridine.

An especially powerful transformation of allyl hydroperoxides that utilizes both functional groups with 100% atom-economy (incl. both O-atoms!) is the Ti-catalyzed self-epoxidation to epoxy alcohols in the absence of any added oxidant.[29] These reactions are typically performed in $CHCl_3$ or CH_2Cl_2 due to precipitation of TiO_2 in hygroscopic solvents (i.e. acetonitrile, alcohols).[5] To our surprise we found that titanium(IV) isopropoxide can be readily dissolved in various alkenes. Therefore, we have performed an overall solvent-free one-step process by simultaneous combination of the solvent-free photooxygenation of **11** to **12** with the solvent-free Ti-catalyzed epoxidation (Scheme 52). The epoxy alcohol **19** was obtained in very high yield and *syn*-diastereoselectivity with 5 mol% Ti(O^{i}Pr)$_4$ after 25 min.

3 Conclusion

We have developed an efficient, solvent-free protocol for photosensitized $^1O_2$-ene oxyfunctionalizations in the presence of low catalytic loadings of organic dyes. This method enabled efficient solubilization of all components, minimized competing deactivation of $^1O_2$, facilitated reaction workup, and minimized the overall energy consumption. Solubility issues of the sensitizer in nonpolar alkenes could be addressed by the employment of a new TPP derivative which generally illustrates that solubilization does not depend on solvent properties but can be equally well addressed by matching combinations of alkenes (liquid under the reaction conditions) and photocatalysts (of various polarity, e.g. TPP derivatives, RB, and MB). However, it should be noted that the absence of a "buffering" solvent may lead to a significant change of reaction polarity and reaction selectivity, so that individual optimization of reactor parameters for each photooxygenation process are advised. The modular reactor setup of this work is applicable to other gas-liquid and gas-liquid-light reactions which are currently being investigated.[30,31] Such solvent-free flow reaction of reagents in high concentrations assures high reaction rates and may be coupled with various in-line analytical tools to monitor reaction conditions and reaction progress.

Figure 24. Zoom on two 1.6 mm (1/16") PFA capillaries containing substrate and PrTPP, surrounded by oxygen at a pressure of 45 bar (650 psi), before (left) and after irradiation.

4 Experimental Part

The experiments involve pressurized oxygen and should be conducted in appropriate equipment with sufficiently high pressure rating and great preparative care due to the formation of potentially explosive oxidation products, especially in contact with metal ion impurities.

Commercial chemicals (≥98% purity) were used as obtained without further purification; exceptions: cis-4-octene (95%), citronellol (97%), α-terpinene (>90%), prenylbenzene (85%). 4-Methyl-3-penten-2-ol was synthesized according to a literature procedure.[32] Methylene blue (MB) was obtained and applied as the hydrate (CAS 122965-43-9); rose bengal (RB) as disodium salt (CAS 632-69-9); tetraphenylporphyrin (TPP; CAS 917-23-7) contained 1-3% chlorin. O_2 gas (99.995%) was applied with a Brooks Instrument mass-flow control unit, the system pressure was adjusted by an IDEX back-pressure cartridge. Commercial FEP and PFA tubings (1/16" OD, 1/32" ID) were purchased from Bohlender. Except for the model substrate citronellol, yields were determined from solution reactions (0.1 M substrate in MeCN, 1 mM MB) by ^{1}H-NMR with dimethyl sulfone as oxidation-stable internal reference. Solvent residual peaks or added tetramethylsilane were used as internal NMR references. The photooxygenations were performed with 24 Cree MK-R white LEDs (190 W total) at 0-45 °C depending on the viscosity and boiling point of the applied olefin. The internal volume of the reactor which contains the substrate during the reaction was used for calculation of the space-time yields.

General procedure for solvent-free photooxygenation:

The sensitizer was dissolved in the substrate (ultrasonication) at room temperature. $Ti(O^iPr)_4$ (5 mol%) was dissolved in this solution in the case of the the one-step photooxygenation-epoxidation (Scheme 52). The obtained solution was pumped through commercial FEP or PFA capillary tubing (1/16" OD, 1/32" ID, from Bohlender; irradiated tubing length 12.8 or 39.9 m) which is wrapped around a glass cylinder (OD 65 mm) at a flow rate of 0.06 to 0.50 mL/min by an HPLC pump. O_2 gas (99.995 %) was applied with a Brooks Instruments mass-flow control, the system pressure was adjusted by an IDEX back-pressure cartridge. The O_2 flow rate was adjusted so that a laminar slug flow resulted and O_2 was not completely consumed when the solution left the back-pressure cartridge at the end of the reactor tubing. Temperature control (0-45 °C depending on viscosity and boiling point of alkene) was applied from the outside of the reactor coil by a temperature-controlled silicon oil bath. The reactor coil was irradiated from the inside by 24 water-cooled Cree MK-R white LEDs (190 W). At the outcome, the products were obtained without further workup (exception: addition of

water and separation of organic phase in the tandem $^1O_2$-ene/Ti-catalysis). See the following illustration:

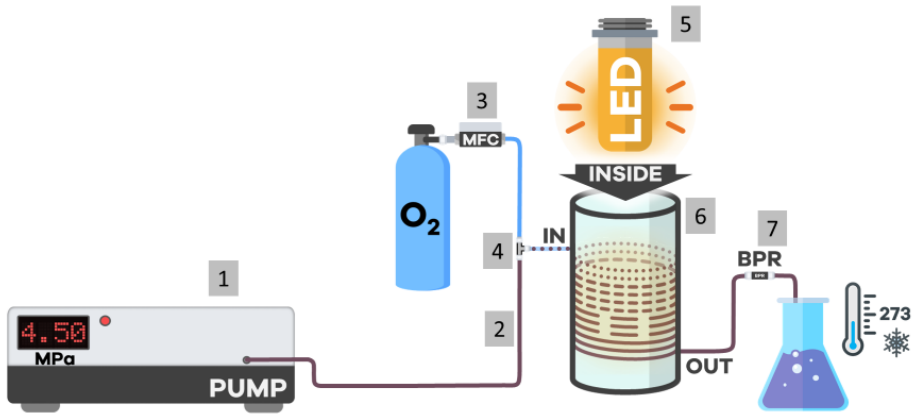

1 HPLC pump: BISCHOFF 2250, 0.01-4.99 mL/min maximum flow speed.
2 Tubing: 1/16 inch outer diameter, 1/32 inch inner diameter: BOLA S1815-04 (FEP) or S1811-02 (PFA)
3 Thermal Gas Mass Flow Controller: BROOKS INSTRUMENTS SLA5850SH1AB1C2A1
4 Tubing connectors: IDEX 1/16 inch connectors. Parts: P-727, F-120
5 LED ring light, 24 Cree MK-R warm-white LEDs, each operating at 11.6 V, 700 mA.
6 Glass Container, 65 mm outer diameter. Tubing wrapped around at the outside.
7 Back Pressure Regulator: IDEX U-609 housing combined with P-765 cartridge, adjusted to 45 bar (650 psi).

Substrate	HPLC flow rate in mL/min	Tubing length in m
1	0.5	12.8
3	0.35	12.8
5	0.1	12.8
7	0.2	12.8

9	0.4	12.8
11	0.1	12.8
13	0.06	12.8
15	0.15	39.9
17	0.15	39.9

5,10,15,20-Tetrakis(4-*n*-propylphenyl)porphyrin (PrTPP):

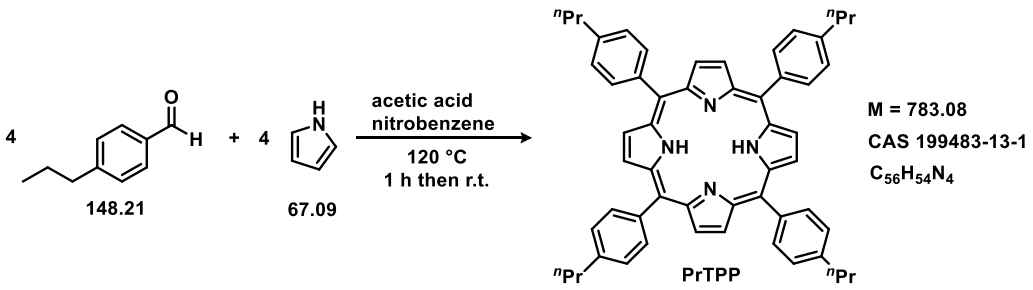

Pyrrole (0.7 mL, 10 mmol) and 4-propylbenzaldehyde (1.48 g, 10 mmol) were added to a hot mixture (heated to 120°C) of acetic acid (75 mL) and nitrobenzene (50 mL). After stirring for 2 h and cooling to 25 °C, DCM (100 mL) was added, and the organic phase was washed with $NaHCO_3$ (sat. aq.). After drying with brine and over Na_2SO_4, the solvents were completely removed *in vacuo*, and MeOH (100 mL) was added to allow

crystallization at -30°C. The precipitate was washed with MeOH and recrystallized from $CHCl_3$/MeOH followed by drying *in vacuo* to give PrTPP as dark pink crystals (195 mg, 0.25 mmol, 10% yield) that are nearly insoluble in MeOH. Purity can be controlled via ^{1}H-NMR by integration of the peak with a shift of -2.63 ppm, which should ideally integrate to a value of two. If below 1.9, the dye should be recrystallized.

PrTPP after washing with methanol, during filtration.

^{1}H-NMR (400 MHz, $CDCl_3$): δ 8.94 (s, 8H; C*H*), 8.18 (d, 8H; C*H*), 7.5 (d, 8H, C*H*), 2.97 (t, 8H, CH_2), 1.98 (m, 8H, CH_2), 1.21 (t, 12H, CH_3), -2.63 (s, 2H, N*H*). ^{13}C-NMR (150 MHz, $CDCl_3$): δ 142.0, 139.5, 134.6, 126.7, 120.1, 38.0, 24.7, 14.1. HRMS (ESI): m/z calcd for $[C_{56}H_{55}N_4]^+$: 783.4421 $[M+H]^+$; found: 783.4412. UV/Vis (in **3**): λ_{max} (ε) 420 (483,000). UV/Vis ($CHCl_3$): λ_{max} (ε) 421 (429,000), 450 nm (63,000 L mol^{-1} cm^{-1}).

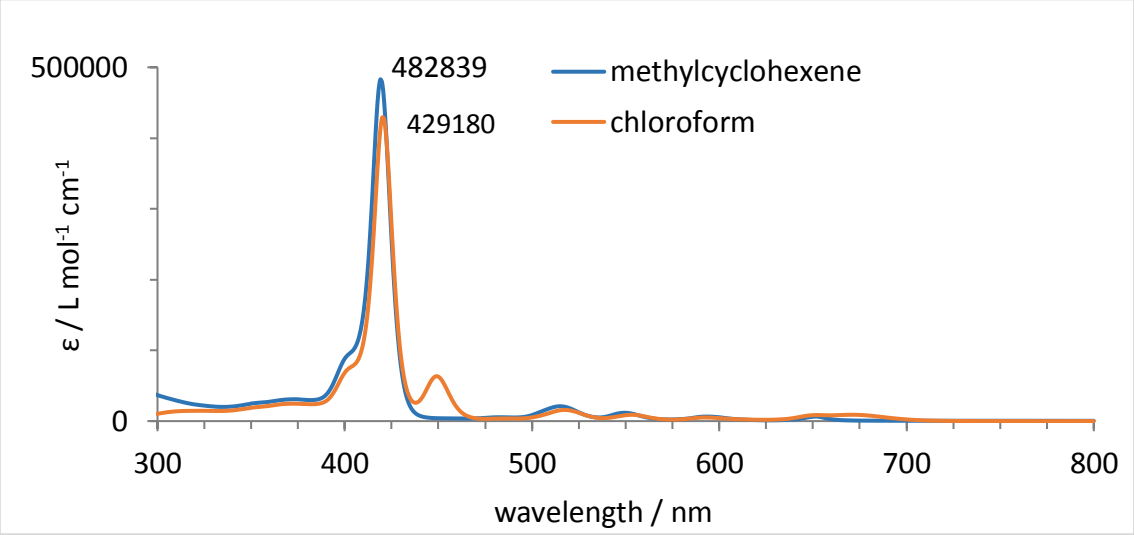

UV-VIS spectra of PrTPP in 1-methylcyclohexene (blue) and chloroform.

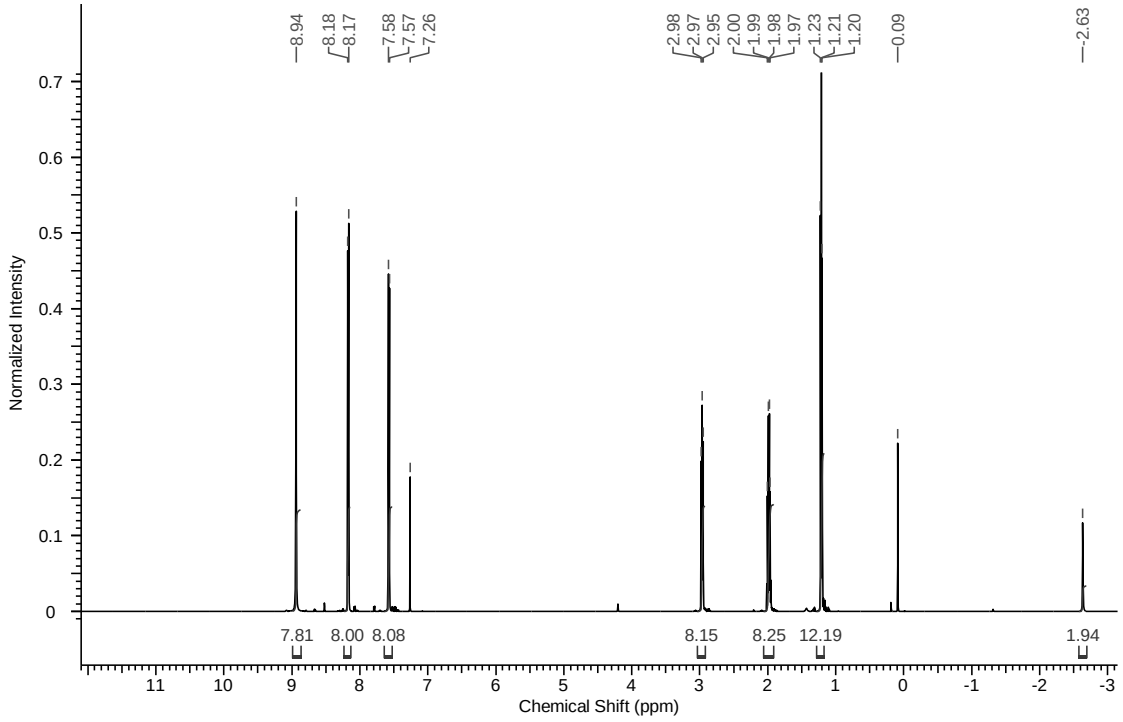

^{1}H- and spectrum of PrTPP, measured in $CDCl_3$.

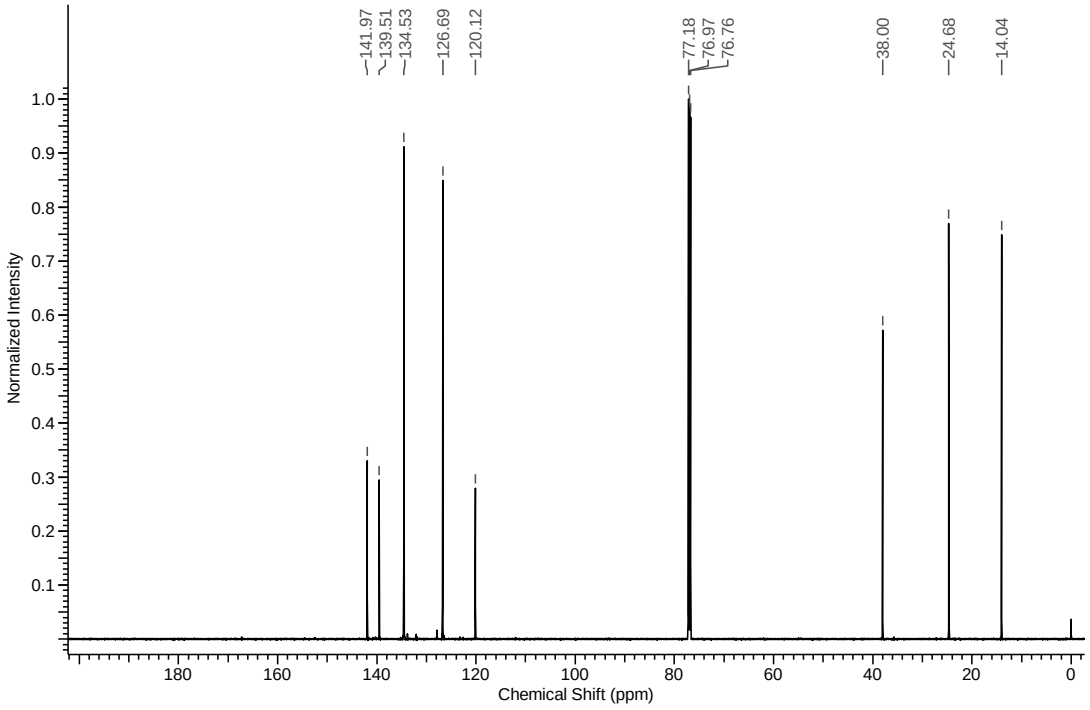

^{13}C-NMR spectrum of PrTPP, measured in $CDCl_3$.

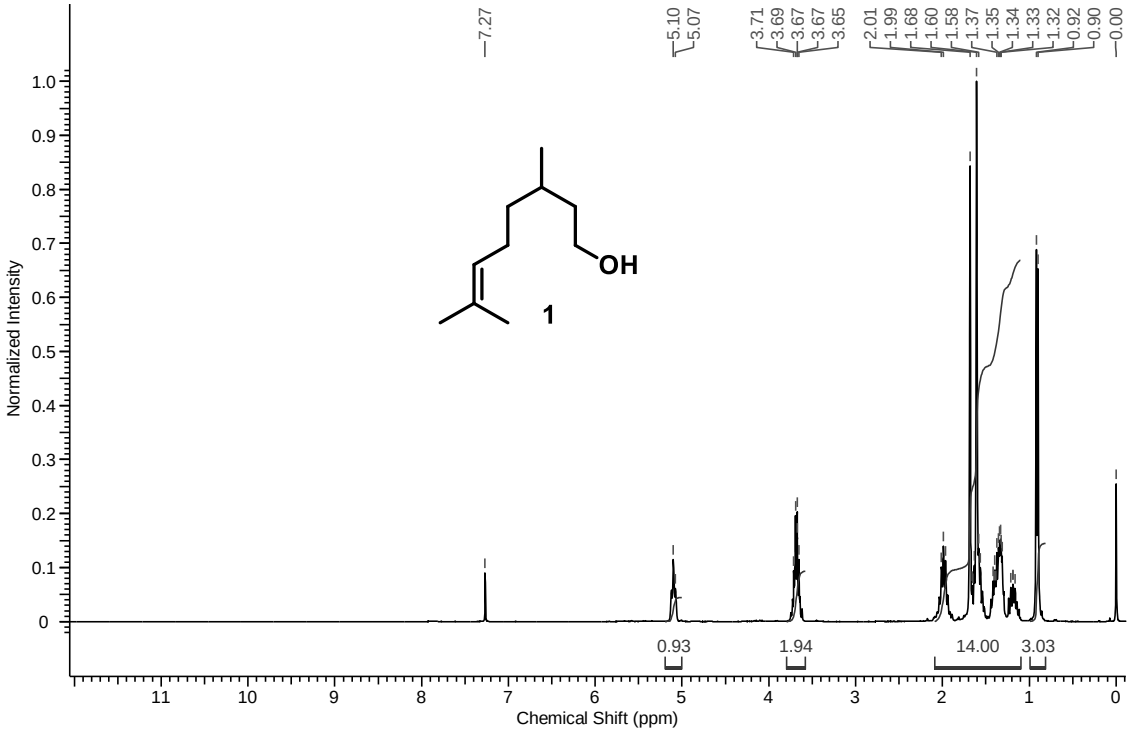

^{1}H-NMR of **1**.

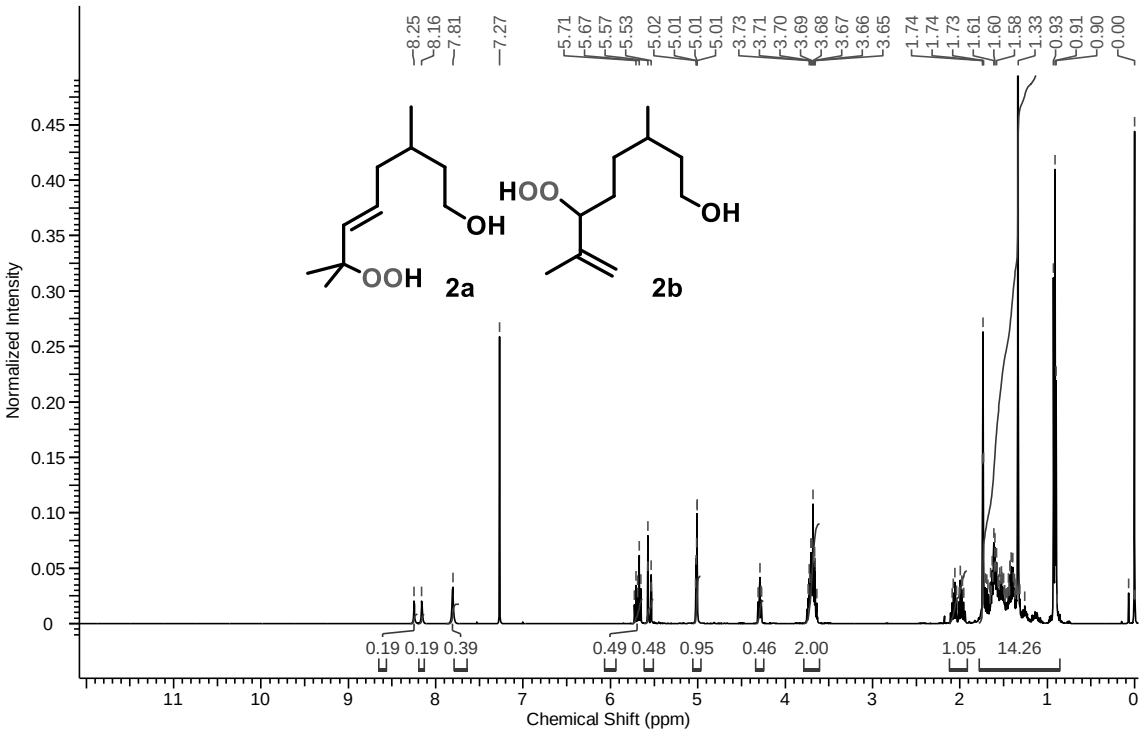

^{1}H-NMR of mixture **2a**, **2b**.

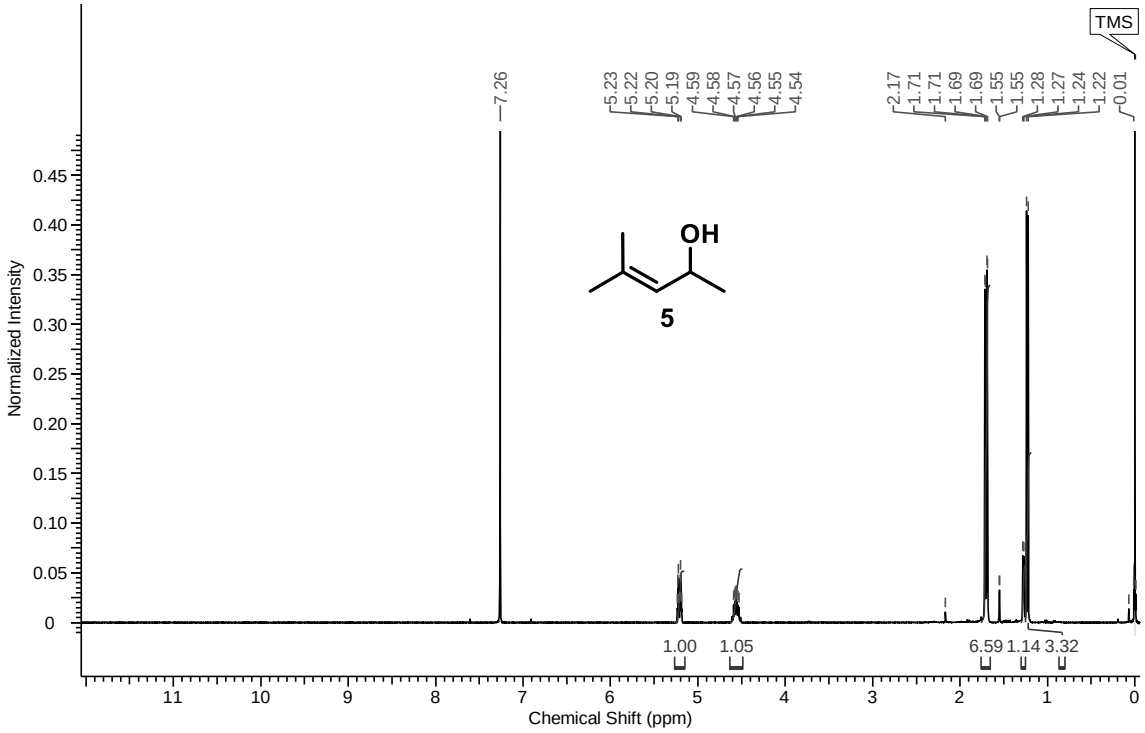

^{1}H-NMR of **5**.

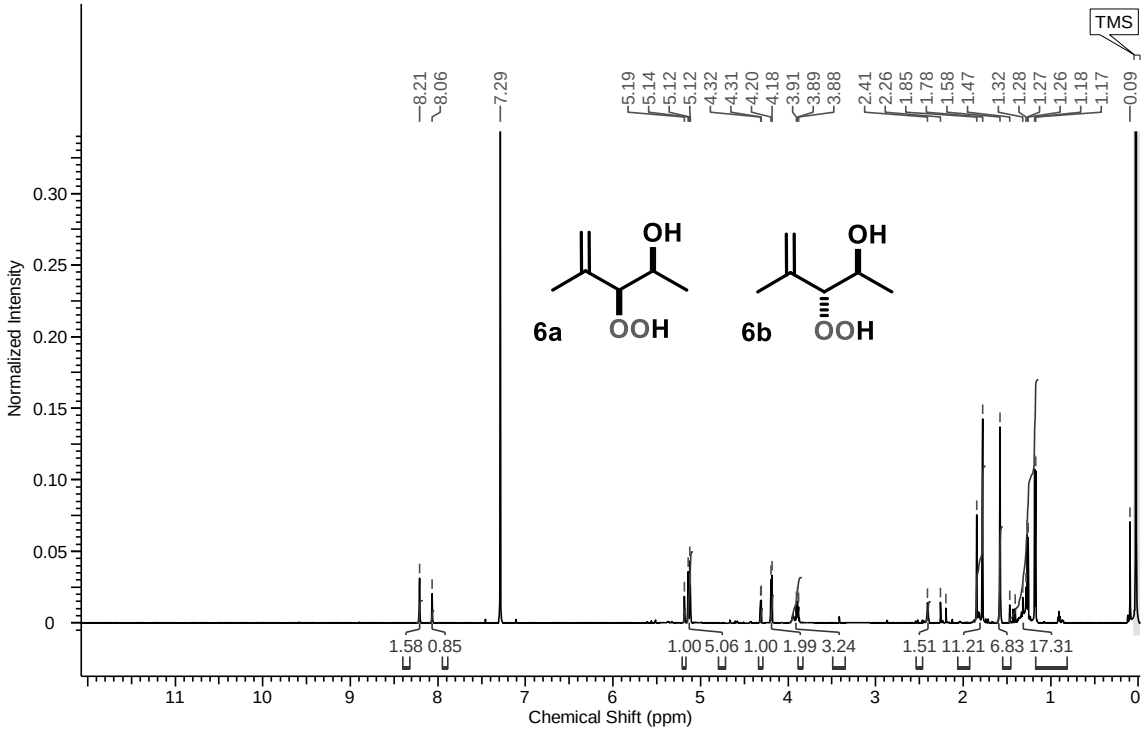

^{1}H-NMR of mixture **6a**, **6b**.

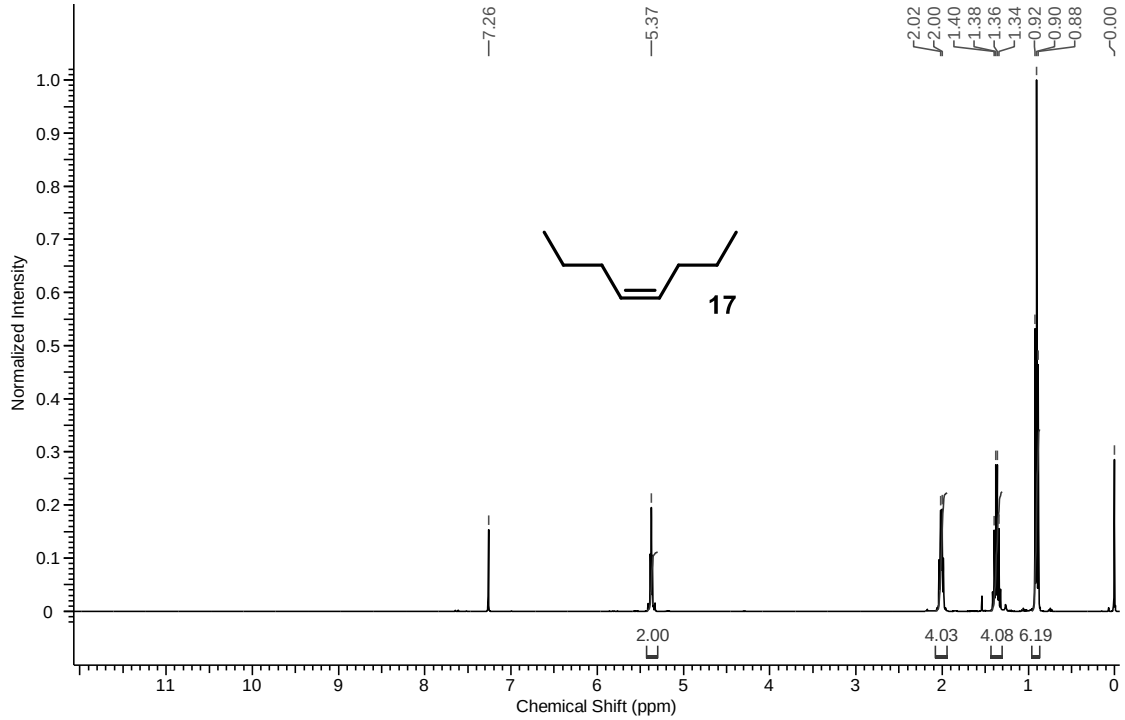

^{1}H-NMR of **17**.

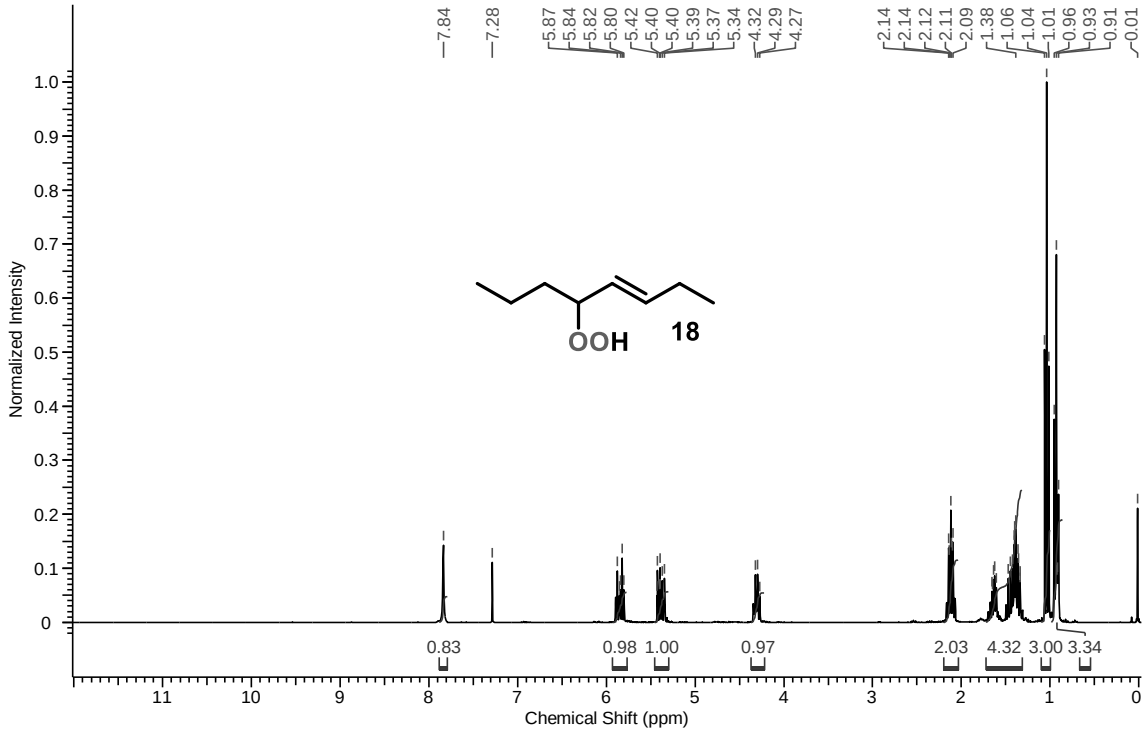

^{1}H-NMR of **18**.

5 References

[1] P. Anastas, N. Eghbali, *Chem. Soc. Rev.* **2010**, *39*, 301–312.
[2] A. G. Griesbeck, A. Bartoschek, *Chem. Commun.* **2002**, *50*, 1594–1595.
[3] P. Bayer, R. Pérez-Ruiz, A. Jacobi von Wangelin, *ChemPhotoChem* **2018**, *2*, 559–570.
[4] S. Nonell, C. Flors, *Singlet Oxygen: Applications in Biosciences and Nanosciences (Volume 1)*, Royal Society Of Chemistry, Cambridge, **2016**.
[5] M. Prein, W. Adam, *Angew. Chem. Int. Ed.* **1996**, *35*, 477–494.
[6] T. Noël, M. Escriba Gelonch, K. Huvaere, in *Photochemical Processes in Continuous-Flow Reactors*, World Scientific Publishing Europe Ltd., London, **2017**, pp. 245–267.
[7] C. Capello, U. Fischer, K. Hungerbühler, *Green Chem.* **2007**, *9*, 927–934.
[8] A. A. Ghogare, A. Greer, *Chem. Rev.* **2016**, *116*, 9994–10034.
[9] W. Pickenhagen, D. Schatowski, Patent DE000019645922A1, **1996**, Title: Verfahren Zur Herstellung von Rosenoxid.
[10] Existing reports on solvent-free photooxygenations are conducted in batch and exhibit high amounts of haloganated solvents for loading and removal of substrates on heterogeneous sensitizers (see A. G. Griesbeck, T. T. El-Idreesy, A. Bartoschek, *Adv. Synth. Catal.* **2004**, *346*, 245–251 or T. Hino, T. Anzai, N. Kuramoto, *Tetrahedron Lett.* **2006**, *47*, 1429–1432).
[11] R. A. Bourne, X. Han, M. Poliakoff, M. W. George, *Angew. Chem. Int. Ed.* **2009**, *48*, 5322–5325.
[12] F. Lévesque, P. H. Seeberger, *Org. Lett.* **2011**, *13*, 5008–5011.
[13] M. Elsherbini, R. K. Allemann, T. Wirth, *Chem. – A Eur. J.* **2019**, *25*, 12486–12490.
[14] M. Obst, B. König, *Eur. J. Org. Chem.* **2018**, 4213–4232.
[15] See the experimental part for details on space-time-yield and definition of reactor volume. The topic is part of critical discussion, see: V. Hessel, S. Hardt, H. Löwe, in Chemical Micro Process Engineering, Wiley-VCH, Weinheim, **2004**, pp. 70–71.
[16] J. Schachtner, P. Bayer, A. Jacobi von Wangelin, *Beilstein J. Org. Chem.* **2016**, *12*, 1798–1811.
[17] P. Bayer, J. Schachtner, M. Májek, A. Jacobi von Wangelin, *Org. Chem. Front.* **2019**, *6*, 2877–2883.
[18] The use of a substrate-soluble catalyst is reported in the field of photocatalysis, for example in the oxidation of benzyl alcohol to benzaldehyde using 9-phenyl-10-methylacridinium, see K. Ohkubo, K. Suga, S. Fukuzumi, *Chem. Commun.* **2006**, 2018-2020.
[19] B. Maurer, Patent US6982072, **2006**, Title: Process for the Production of Hydrogen Peroxide.
[20] R. N. Cochran, S.-C. Lin, Patent US5243084, **1993**, Title: Oxidation of Isobutane to Tertiary Butyl Hydroperoxide.
[21] TPP is known to quench singlet oxygen when concentrations above 2 mM are applied, see F. Lévesque, P. H. Seeberger, *Org. Lett.* **2011**, *13*, 5008–5011 or P. R. Ogilby, C. S. Foote, *J. Am. Chem. Soc.* **1983**, *105*, 3423–3430.
[22] Empirical observations showed that the substrate/oxygen ratio should not exceed a value of 30 in the presented setup for continuous photooxygenation - with and without solvent use. The concentration of oxygen is 0.2 M at 45 bar in pure citronellol compared to 0.3 M in acetonitrile at this pressure. The concentration of an olefin (neat) is roughly 6 mol/L. Oxygen solubility is evaluated by measuring the volume of released oxygen after expansion of an initially pressurized bubble-free gas-saturated

solution downstream of the BPR, see also supplementary information of A. Kouridaki, K. Huvaere, *React. Chem. Eng.* **2017**, *2*, 590–597.
[23] A. G. Griesbeck, T. T. El-Idreesy, A. Bartoschek, *Adv. Synth. Catal.* **2004**, *346*, 245–251.
[24] J. Rudbäck, M. A. Bergström, A. Börje, U. Nilsson, A.-T. Karlberg, *Chem. Res. Toxicol.* **2012**, *25*, 713–721.
[25] Dye concentrations of > 0.5 mM result in efficient oxygenation.
[26] Existing reports on 5,10,15,20-tetrakis(4-n-propylphenyl)porphyrin (N. W. Griffiths, M. F. Wyatt, S. D. Kean, A. E. Graham, B. K. Stein, A. G. Brenton, *Rapid Commun. Mass Spectrom.* **2010**, *24*, 1629–1635) are missing significant information on synthesis and product characterization.
[27] I. A. Yaremenko, V. A. Vil', D. V. Demchuk, A. O. Terent'ev, *Beilstein J. Org. Chem.* **2016**, *12*, 1647–1748.
[28] Displayed are the "greenest" solvents we are aware of which are typically used in such transformations.
[29] W. Adam, M. Braun, A. Griesbeck, V. Lucchini, E. Staab, B. Will, *J. Am. Chem. Soc.* **1989**, *111*, 203–212.
[30] N. J. W. Straathof, Y. Su, V. Hessel, T. Noël, *Nat. Protoc.* **2016**, *11*, 10–21.
[31] D. Cambié, C. Bottecchia, N. J. W. Straathof, V. Hessel, T. Noël, *Chem. Rev.* **2016**, *116*, 10276–10341.
[32] A. H. Gau, G. L. Lin, B. J. Uang, F. L. Liao, S. L. Wang, *J. Org. Chem.* **1999**, *64*, 2194–2201.

VI Thesis Summary

1 Summary

The presented thesis is introduced by a general overview over reactions with oxygen and light, with a focus on singlet oxygen, an energy-enriched and especially reactive form of the naturally occurring triplet oxygen abundant in air. In addition, topics such as reactor technology and information on environmental aspects are covered.

A review about stereoselectivity observations during singlet oxygen ene reactions is following the introduction. Multiple reports on product selectivities are used for the synthesis of natural products and drugs which makes the operationally simple and mild singlet oxygen ene reaction an attractive step in total synthesis.

Subsequently, mechanistic investigations on the photooxygenation of 1-aryl-1-cyclohexenes in a modular micro photo-flow reactor, accompanied by results on synthesis and analysis of the peroxide-containing products, are presented. An unusual zwitterionic intermediate is proposed and supported by synthetic observations as well as DFT calculations. A variety of peroxyl compounds could be isolated and fully characterized demonstrating the somewhat surprising stability of an O-O bond under ambient conditions.

After concluding these half mechanistic, half synthetic studies, results on the oxygenation of cardanol are summarized. This waste product arises in 10^6 tons per year during cashew nut processing and thus constitutes a valuable renewable feedstock; the main part contains information on modification and optimization of the flow reactor and details on NMR as well as HPLC/UV-VIS analysis. The polyol products can be used for polymerization reactions, for example as crosslinking agent during polyurethane synthesis.

The main section is concluded by studies on the possibilities and limits of a novel process for an entirely solvent-free photooxygenation of olefins under continuous-flow conditions applying highly pressurized oxygen. By application of an oxygen pressure of 45 bar in a special pressure and temperature-resistant PFA capillary, an oxygen concentration of 0.2 mol L^{-1} in neat substrates was realized. The reactor setup is illustrated in detail and allows for efficient photooxygenation and high space-time yields applying commercial sensitizers as well as a novel alkylated tetraphenylporphyrin dye.

2 Zusammenfassung

Die vorgestellte Doktorarbeit wird eingeleitet mit einem Überblick über Reaktionen mit Sauerstoff und Licht. Ein Fokus liegt dabei auf Singulett-Sauerstoff, welcher eine energieangereicherte Form des in der Luft vorhandenen Triplet-Sauerstoffs darstellt und besonders reaktiv gegenüber ungesättigten Kohlenwasserstoffen aufweist. Auch Themen wie Flussreaktortechnologie und umweltbezogene Aspekte werden in der Einleitung berücksichtigt.

Es folgt im Anschluss ein Literaturübersichtsartikel über stereoselektive Singulett-Sauerstoff-En Reaktionen. Verschiedene Beispiele für die Synthese von Natur- und Arzneistoffen werden mit Bezug auf vorangegangene Selektivitätsstudien vorgestellt. Singulett-Sauerstoff, welcher im Labormaßstab einfach erzeugbar ist, wird damit als wertvolles Reagens unter anderem in der Totalsynthese deutlich.

Im darauf folgenden Kapitel werden mechanistische Untersuchungen bei der Photo-Oxidation von 1-Aryl-1-cyclohexenen in einem modularen "dreiphasigen" Gas-Flüssig-Licht Flussreaktor vorgestellt. Es wird dabei auf Synthese und Analyse der erhaltenen Produkte eingegangen, ein wahrscheinlicher zwitterionischer Übergangszustand vorgeschlagen, sowie dieser anhand Modellrechnungen und synthetischer Beobachtungen erklärt. Auf den ersten Blick instabile Peroxide mit Sauerstoff-Sauerstoff-Bindungen konnten isoliert, charakterisiert und für Zeiträume von mehreren Tagen bis Monaten aufbewahrt werden.

Auf diesen halb mechanistischen, halb synthetischen Artikel folgen Untersuchungen zur Oxidierbarkeit von Cardanol, einem erneuerbaren Rohstoff, der bei der Verarbeitung von Cashew-Nüssen in einer Menge von 10^6 Tonnen pro Jahr als Abfall anfällt. Informationen zur Modifikation des Flussreaktors zum Umsatz hoher Mengen dieses Rohstoffs sowie detaillierte Ergebnisse von NMR-Untersuchungen und HPLC Analysen sind enthalten. Die nach bisherigen Untersuchungen erhaltenen Polyole können den Analysen zufolge beispielsweise für Polymersynthesen wie der PU-Schaum-Produktion verwendet werden. Die Reaktivität von mehrfach ungesättigten Cardanolen oder Darstellung von Triolen mithilfe eines Titan(IV)-Katalysators sind Gegenstand zukünftiger Untersuchungen auf diesem Themengebiet.

Der Hauptteil wird abgeschlossen durch die Vorstellung eines innovativen Prozesses zur lösungsmittelfreien Photo-Oxidation von Olefinen in einem modularen Flussreaktor unter hohem Druck. Indem ein Sauerstoffdruck von 45 Bar verwendet wird, können Konzentrationen von rund 0,2 Mol pro Liter an Sauerstoff im verwendeten Ausgangsstoff realisiert werden, wodurch eine sehr effiziente Oxidation mit hoher Raum-Zeit-Ausbeute erreicht wird. Dafür wurden außer Sauerstoff und LEDs lediglich kommerziell erhältliche Farbstoffe (oder in manchen Fällen ein speziell synthetisiertes alkyl-substituiertes Tetraphenylporphyrin) verwendet. Funktionsweise, Entwicklung und Anpassung des dafür verwendeten modularen Flussreaktors werden dabei detailliert beschrieben.

VII Appendix

1 List of Abbreviations

"	inch; 1 inch = 25.4 mm
a	year(s)
a.u.	arbitrary units
AJvW	Axel Jacobi von Wangelin
aq	aqueous
Ar	aryl
BPR	back pressure regulator
c	concentration
calcd	calculated
CFL	compact fluorescent lamp
chem	chemistry
CNSL	cashew nut shell liquid
conc	concentration
d	day
d.r.	diastereomeric ratio
DCM	dichloromethane
DOI	digital object identifier
E	energy
e.g.	*exempli gratia*
EA	ethyl acetate
EHS	environmental, health and safety
EI	electron impact
EI	electron impact
EPA	epoxy alcohol
EPO	endoperoxide; -O-O- motif present in a ring
eq	equivalent(s)
equiv	equivalent(s)
ESI	electrospray ionization
esp	especially
Et	ethyl
extr	extracted
FEP	copolymer of hexafluoropropylene and tetrafluoroethylene
FID	flame ionization detector
FR	flow rate
front	frontiers
GC	gas chromatography
h	hour(s)
HPLC	high-performance liquid chromatography
HYP	hydroperoxide; H-O-O- motif present
ID	inner diameter
int	intensity
^{i}Pr	2-propyl
IR	infrared radiation, $720 < \lambda_{IR} < 10^6$ nm
ISC	intersystem crossing
LCA	lifecycle assessment
LED	light-emitting diode

M	molar; mol L^{-1}
MB	methylene blue
Me	methyl
MFC	mass flow controller
min	minute(s)
MO	molecular orbital; theory describing electronic structures using QM
mol%	molar percentage
MR	microstructured reactor; typical lateral dimensions below 1 mm
MS	mass spectrometry
NIR	near-infrared radiation, $720 < \lambda_{NIR} < 1400$ nm
NMR	nuclear magnetic resonance
^{n}Pr	1-propyl
OD	outer diameter
org	organic
ox	oxidative
p	page
Pe	pentane
PFA	copolymers of tetrafluoroethylene and perfluoroalkoxyvinylethers
PLA	polylactic acid
pp	pages
ppm	part(s) per million
prim	primary
PrTPP	5,10,15,20-tetrakis(4-*n*-propylphenyl)porphyrin
PS	polystyrene
QM	quantum mechanics; fundamental theory on the properties of nature
R	organic rest
RB	rose bengal disodium salt
red	reductive
ref	reference
rel	relative
R_f	retention factor
RGB	color model with three additive primary colors: red, green and blue.
ROS	reactive oxygen species
RP	reversed phase
rxn	reaction
s	second(s)
S	sensitizer
sc	supercritical
sec	secondary
SET	single-electron transfer
STY	space-time yield; in g L^{-1} h^{-1}
t	ton(s)
tert	tertiary
TLC	thin-layer chromatography
TPP	tetraphenylporphyrin
TS	transition state
UV	ultraviolet radiation, $10 < \lambda_{UV} < 380$ nm
VIS	radiation visible to humans, $380 < \lambda_{VIS} < 720$ nm
w/	with
w/o	without
ZPE	zero-point energy
ε	molar extinction coefficient (in L mol^{-1} cm^{-1})
λ_{max}	wavelength of an absorption maximum
τ_Δ	average lifetime

2 List of Figures

Information on figures and licensed pictures from third parties:

Figure 1: ASTM (American Society for Testing and Materials) G-173-03 reference spectra. Data obtained from the given citation and https://www.nrel.gov/grid/solar-resource/spectra-am1.5.html (accessed 09 March 2020) and https://www.nrel.gov/grid/solar-resource/spectra-wehrli.html (accessed 10 April 2020, for wavelengths below 280 nm). The original data is smoothed (moving average, 5 data points) for better visibility.

Figure 2: Photograph used with kind permission of the Schenck family, namely Naomi Schenck.

Figure 7: Photograph © Max-Planck-Institut für Kolloid- und Grenzflächenforschung, reprinted with kind permission.

3 Acknowledgements

This section is devoted to all that helped me in the last three and a half years during my PhD studies in Regensburg and Hamburg. Thank you – this thesis would not exist without you!

In the first place I want to thank Axel, for being such a great supervisor. I want to thank you for offering me the large freedom, which I had in the selection of my research projects, while also having the time to discuss my current problems. You always supported me in what I did for what I am very thankful.

I would also like to thank all the members – past or present – of the AJvW group for the nice and friendly atmosphere. Especially I would like to thank Josef, Michael, and Guojiao for their relaxed attitude, and coping with me in the writing rooms, labs, and kitchen. To Dieter, for early breakfasts, numerous hours after 10 p.m. in the University, trying out new recipes, and much more. To Sebastian, who spent the four and a half years in the AJvW group in parallel to me, for sharing ups and downs, thoughts about life and more. To Luana and Andrey, and all the other researchers of the group. Thanks goes also to Thomas, for regular solvent refills, sharing a good mood and being a nice technician. I am also thankful to the members of my thesis committee Prof. Dr. Burkhard König, Prof. Dr. Frank-Michael Matysik, and Apl. Prof. Dr. Rainer Müller – for finding the time to participate in my defense and read this thesis. Special thanks goes to Burkhard König, who – indirectly by financial support as head of the GRK – facilitated numerous great conference trips that I love to look back on.

Zu guter Letzt möchte ich im Speziellen auch meinen Eltern, Anton und Manuela Bayer, meinem Bruder Maximilian Bayer, sowie allen übrigen Familien-mitgliedern für ihre unentwegte Unterstützung und das Vertrauen in mich und auf meinem Weg danken.

The presented research was generously supported by the Deutsche Forschungsgesellschaft Graduate School "Chemical Photocatalysis" at the University of Regensburg (DFG, GRK 1626).

4 CV and List of Publications

PATRICK BAYER

CHEMICAL SCIENTIST

PROFILE

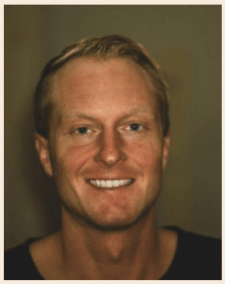

Born Aug 7, 1990 (Germany)
Location Pocking (Germany)
German Citizenship

patrick.bayer@mail.com

LANGUAGES

German. ★★★★
English. ★★★½
French. ★½☆☆
Italian. ★☆☆☆

SIGNATURE

WORK EXPERIENCE

Ph.D. Degree (Dr. rer. nat., in process) 2016 - 2020
University of Regensburg (UR), University of Hamburg
Ph.D. Thesis "High-Pressure Photooxygenation of Olefins in Flow: Mechanism, Reactivity and Reactor Design" under supervision of Prof. Dr. A. Jacobi von Wangelin (UR)
Member of the Graduate School "GRK 1626 - Chemical Photocatalysis" (UR)

Petrol Station Employee 2011
Pocking
During the waiting period for initiation of the chemistry studies

Basic Military Service 2010
Stetten/Cham
In the German Armed Forces

EDUCATION

Master Degree 2014 - 2016
University of Regensburg
Master Thesis "Investigations into the Photooxygenation of 1-Phenyl-1-Cyclohexenes under Continuous Flow Conditions" (1.0) under supervision of Prof. Dr. A. Jacobi von Wangelin. Master degree (M.Sc.) at the University of Regensburg (1.4)

Bachelor Degree 2011 - 2014
University of Regensburg
Bachelor degree (B.Sc.) at the University of Regensburg (2.0)

Higher Education Qualification 2001 - 2010
Academic High School Pocking
General higher education entrance qualification (2.0)

REFERENCES

Prof. Dr. Axel Jacobi von Wangelin
University of Hamburg
E-mail: axel.jacobi@chemie.uni-hamburg.de

A Flow Reactor Setup for Photochemistry of Biphasic Gas/Liquid Reactions

J. Schachtner, P. Bayer, A. Jacobi von Wangelin

Beilstein J. Org. Chem. **2016**, *12*, 1798–1811.

DOI: 10.3762/bjoc.12.170

Stereoselective Photooxidations by the Schenck Ene Reaction

P. Bayer, R. Pérez-Ruiz, A. Jacobi von Wangelin

ChemPhotoChem **2018**, *2*, 559–570.

DOI: 10.1002/cptc.201800058

Visible Light-Mediated Photo-Oxygenation of Arylcyclohexenes

P. Bayer, J. Schachtner, M. Májek, A. Jacobi von Wangelin

Org. Chem. Front. **2019**, *6*, 2877–2883.

DOI: 10.1039/C9QO00493A

An Entirely Solvent-Free Photooxygenation of Olefins Under Continuous Flow Conditions

P. Bayer, A. Jacobi von Wangelin

Green Chem. **2020**, *22*, 2359-2364.

DOI: 10.1039/D0GC00436G.

Conference Contributions:

7 conferences, 2 talks, 6 posters (1 poster prize)

Patrick Bayer

12 May 2020